

"Best Available Copy"

ARO 26466.7-EG-CF

②

DTIC FILE COPY

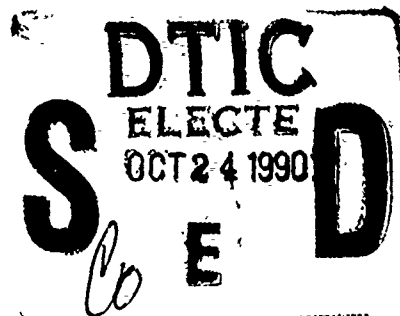
The Third Workshop

on

**DYNAMICS AND AEROELASTIC  
STABILITY MODELING OF  
ROTORCRAFT SYSTEMS**

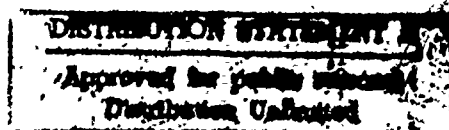
March 12-14, 1990  
Duke University  
Durham, North Carolina

AD-A227 930



Sponsored by

The United States  
Army Research Office  
and  
Duke University  
School of Engineering



90 10 23 200

# REPORT DOCUMENTATION PAGE

Form Approved  
OMB No. 0704-0188

Public reporting burden for this collection of information is estimated to average 1 hour per response, including the time for reviewing instructions, searching existing data sources, gathering and maintaining the data needed, and completing and reviewing the collection of information. Send comments regarding this burden estimate or any other aspect of this collection of information, including suggestions for reducing this burden, to Washington Headquarters Services, Directorate for Information Operations and Reports, 1215 Jefferson Davis Highway, Suite 1204, Arlington, VA 22202-4302, and to the Office of Management and Budget, Paperwork Reduction Project (0704-0188), Washington, DC 20503.

1. AGENCY USE ONLY (Leave blank)		2. REPORT DATE	3. REPORT TYPE AND DATES COVERED Final 1 May 1989 - 30 June 1990	
4. TITLE AND SUBTITLE The Third Workshop on Dynamics and Aeroelastic Stability Modeling of Rotorcraft Systems			5. FUNDING NUMBERS DAAL03-89-G-0023	
6. AUTHOR(S) Earl H. Dowell				
7. PERFORMING ORGANIZATION NAME(S) AND ADDRESS(ES) Duke University School of Engineering Durham, NC 27706			8. PERFORMING ORGANIZATION REPORT NUMBER	
9. SPONSORING/MONITORING AGENCY NAME(S) AND ADDRESS(ES) U. S. Army Research Office P. O. Box 12211 Research Triangle Park, NC 27709-2211			10. SPONSORING/MONITORING AGENCY REPORT NUMBER ARO 26466.1-EG-CF	
11. SUPPLEMENTARY NOTES The view, opinions and/or findings contained in this report are those of the author(s) and should not be construed as an official Department of the Army position, policy, or decision, unless so designated by other documentation.				
12a. DISTRIBUTION/AVAILABILITY STATEMENT Approved for public release; distribution unlimited.			12b. DISTRIBUTION CODE	
13. ABSTRACT (Maximum 200 words) ➤ The workshop was held as scheduled. Sessions included rotorcraft dynamics research, physical modeling, rotorcraft centers of excellence, aeroelasticity and stability, response dynamics and control, mathematics of modeling, and experimental-theoretical investigations.				
14. SUBJECT TERMS Rotorcraft Systems, Rotorcraft Dynamics, Aeroelasticity, Response Dynamics, Stability Modeling, Workshop (JS)			15. NUMBER OF PAGES 239	
			16. PRICE CODE	
17. SECURITY CLASSIFICATION OF REPORT UNCLASSIFIED	18. SECURITY CLASSIFICATION OF THIS PAGE UNCLASSIFIED	19. SECURITY CLASSIFICATION OF ABSTRACT UNCLASSIFIED	20. LIMITATION OF ABSTRACT UL	

# Formulation and Evaluation of an Analytical Model for Composite Box-Beams

Edward C. Smith  
Minta Martin Fellow

Inderjit Chopra  
Professor

Center for Rotorcraft Education and Research  
Department of Aerospace Engineering  
University of Maryland  
College Park, Maryland

## Abstract

A direct analytical beam formulation is developed for predicting the effective elastic stiffnesses and corresponding load deformation behavior of tailored composite box-beams. Deformation of the beam is described by extension, bending, torsion, transverse shearing, and torsion-related out-of-plane warping. Evaluation and validation of the analysis is conducted by correlation with both experimental results and detailed finite element solutions. The analysis is evaluated for thin-walled composite beams with no elastic coupling designs with varying degrees of extension-torsion and bending-shear couplings, and designs with bending-torsion and extension-shear coupling. The analysis performed well over a wide range of test cases, generally predicting beam deformations within 10% of detailed finite element solutions. The importance of three non-classical structural phenomenon is systematically investigated for coupled composite beams. Torsion-related out-of-plane warping can substantially influence torsion and coupled torsion deformations; twist of a symmetric layup box-beam under a tip bending load can increase up to 200% due to warping. Couplings associated with transverse shear deformations can significantly alter the elastic response of tailored composite box-beams; effective bending stiffness of highly coupled anti-symmetric layup beams can be reduced more than 30%. Two-dimensional in-plane elastic behavior of the plies is also very important to the accuracy of composite box-beam analysis; load deflection results for anti-symmetric layup beams can be altered by 30-100% by not accounting for this elastic behavior.

NOTE: This abstract is being substituted for the paper by R. Barrett. It will be presented Tuesday, March 13, 1990 from 4:00-4:30 p.m. by Edward C. Smith.

The Third Workshop

on

**DYNAMICS AND AEROELASTIC  
STABILITY MODELING OF  
ROTORCRAFT SYSTEMS**

March 12-14, 1990  
Duke University  
Durham, North Carolina



**Duke University**  
**School of Engineering**  
DURHAM, NORTH CAROLINA 27706

OFFICE OF THE DEAN

TELEPHONE (919) 684-2214

March 12, 1990

Dear Colleague:

Welcome to the Army Research Office/Duke University School of Engineering Workshop on Dynamics and Aeroelastic Stability Modeling of Rotorcraft Systems. We are delighted to have you join the other distinguished workshop participants and hope that you will find your time at Duke both enjoyable and productive.

The School of Engineering occupies a unique position at Duke providing both a modern liberal arts education centered on science and technology for our undergraduates and a professional program for our graduate students. In addition to the standard fields of civil, mechanical and electrical engineering, we also provide programs in biochemical engineering, biomedical engineering, environmental engineering and materials science. The quality of our students is unsurpassed.

It is our pleasure to co-host your visit and we hope that you will call on us for any help that you may require. We look forward to your returning again to Duke University.

*Earl Dowell*

Earl H. Dowell  
Dean, School of Engineering  
Duke University



Accession For	
NTIS GRA&I	<input checked="checked" type="checkbox"/>
DTIC TAB	<input type="checkbox"/>
Unannounced	<input type="checkbox"/>
Justification	
By _____	
Distribution/	
Availability Codes	
Dist	Avail and/or Special
A-1	

UNITED STATES ARMY RESEARCH OFFICE/  
DUKE UNIVERSITY SCHOOL OF ENGINEERING

WORKSHOP ON DYNAMICS AND AEROELASTIC  
STABILITY MODELING OF ROTORCRAFT SYSTEMS

PROGRAM SCHEDULE

. MONDAY, MARCH 12, 1990

SESSION CHAIRMAN: G. Anderson

8:30 - 8:45	WELCOME AND ANNOUNCEMENTS E. Dowell, Duke
8:45 - 9:45	SOME REFLECTIONS ON OPPORTUNITIES FOR ROTORCRAFT DYNAMICS RESEARCH R. Ormiston, Army, Ames Research Center
9:45 - 10:45	HELICOPTER DYNAMICS AND AEROELASTICITY: KEY IDEAS AND INSIGHTS P. Friedmann, UCLA
11:00 - 12:00	PANEL DISCUSSION ON FUTURE DIRECTIONS FOR ROTORCRAFT RESEARCH J. Yen, Bell, Panel Coordinator
12:30 - 2:00	LUNCH THE ROLE OF HELICOPTERS IN EMERGENCY MEDICINE J. Moylan, M.D., Trauma Unit Chief and Surgeon, Duke

SESSION CHAIRMAN: A. Gessow

<u>2:00 - 5:00</u>	<u>PHYSICAL MODELING</u>
2:00 - 2:30	PHYSICAL ASPECTS OF ROTOR BODY COUPLING H. Curtiss, Jr., Princeton University
2:30 - 3:00	ANALYSIS OF SECTIONAL PROPERTIES OF CURVED, TWISTED, NONHOMOGENVOUS, ANISOTROPIC BEAMS D. Hodges, M. Borri, V. Berdichevsky, Georgia Tech
3:00 - 3:30	NONLINEAR ANALYSIS OF CURVED, TWISTED, NONHOMOGENVOUS, ANISOTROPIC BEAMS D. Hodges, A. Atilgan, Georgia Tech.

. MONDAY, MARCH 12, 1990 cont.

- 3:30 - 4:00 INVESTIGATION OF THE USE OF EXTENSION - TWIST  
COUPLING IN COMPOSITE ROTOR BLADES FOR APPLICATION  
TO TILTROTOR AIRCRAFT  
R. Lake, NASA Langley Research Center
- 4:00 - 4:30 COMBINED USE OF FINITE-STATE LIFT AND INFLOW  
MODELS FOR ROTORCRAFT MODELING  
D. Peters, W. Stumpf, C. He, Georgia Tech
- 4:30 - 5:00 SPACE/TIME - DOMAIN FINITE ELEMENTS FOR  
STRUCTURES, DYNAMICS, AND CONTROL  
D. Hodges, D. Peters, M. Borri, Georgia Tech

. TUESDAY, MARCH 13, 1990

SESSION CHAIRMAN: J. Wu

8:30 - 9:00 THE ROTORCRAFT CENTER OF EXCELLENCE AT MARYLAND  
A. Gessow, Maryland

9:00 - 9:30 THE ROTORCRAFT CENTER OF EXCELLENCE AT RPI  
R. Loewy, RPI

9:45 - 12:15 AEROELASTICITY AND STABILITY

9:45 - 10:15 DYNAMIC ANALYSIS OF UNCONVENTIONAL HIGH-SPEED  
ROTORCRAFT  
K. Sangha, McDonnell Douglas

10:15 - 10:45 ROTOR BLADE STABILITY VALIDATION UTILIZING A  
COUPLED AEROROELASTIC ANALYSIS WITH REFINED  
AERODYNAMIC MODELING  
M. Torok, Maryland

10:45 - 11:15 AEROELASTIC ANALYSIS OF ROTOR BLADES  
V. Dhar, VPI & SU

11:15 - 11:45 AEROELASTIC STABILITY ANALYSIS IN MANEUVERING  
FLIGHT  
R. Celi, Maryland

11:45 - 12:15 AEROELASTIC STABILITY OF MULTIPLE LOAD PATH ROTOR  
BLADES  
V. Murthy, Syracuse

12:30 - 2:00 LUNCH

SESSION CHAIRMAN: R. Loewy

2:00 - 5:00 RESPONSE DYNAMICS AND CONTROL

2:00 - 2:30 COUPLED LONGITUDINAL, BENDING, AND TORSIONAL  
VIBRATIONS OF A CRACKED, ROTATING, TIMOSHENKO  
SHAFT  
R. Plaut, K. Collins, J. Wauer, VPI & SU

2:30 - 3:00 NONLINEAR VIBRATIONS OF A CANTILEVER COMPOSITE  
BEAM UNDER PLANAR HARMONIC BASE EXCITATION  
A. Nayfeh and P.- J. F. Pai, VPI & SU

. TUESDAY, MARCH 13, 1990 cont.

3:00	-	3:30	EFFECTS OF ROTATING FRAME TURBULENCE (RFT) ON HELICOPTER BODY RESPONSE J. Prasad, Georgia Tech
3:30	-	4:00	DYNAMICS OF ROTOR BLADES IN CURVED STEADY FLIGHT M. Crespo da Silva, RPI
4:00	-	4:30	INTELLIGENT ROTOR BLADE ACTUATION METHODOLOGY R. Barrett, I. Chopra, Maryland
4:30	-	5:00	ACTIVE CONTROL OF HELICOPTER GROUND AND AIR RESONANCE G. Reichert, Braunschweig
6:30			WORKSHOP DINNER

. WEDNESDAY, MARCH 14, 1990

SESSION CHAIRMAN: R. Ormiston

9:00 - 9:30 THE ROTORCRAFT CENTER OF EXCELLENCE AT GEORGIA  
TECH  
D. Schrage, Georgia Tech

9:45 - 12:15 MATHEMATICS OF MODELING

9:45 - 10:15 FLAP-LAG-TORSIONAL DYNAMICS OF ROTOR BLADES BY A  
DIRECT, "TRANSFER MATRIX" METHOD  
M. Crespo da Silva, RPI

10:15 - 10:45 A DIRECT NUMERICAL EVALUATION OF FLOQUET  
TRANSITION MATRICES FOR PERIODIC SYSTEMS  
S.C. Sinha, Auburn

10:45 - 11:15 LYAPUNOV EXPONENTS FOR STOCHASTIC SYSTEMS WITH  
APPLICATIONS TO HELICOPTER DYNAMICS  
N. Sri Namachchivaya, Illinois

11:15 - 11:45 RECENT EFFORTS IN INTEGRATED AERODYNAMIC  
LOAD/DYNAMIC OPTIMIZATION OF HELICOPTER ROTOR  
BLADES  
A. Chattopadhyay, NASA Langley Research Center

11:45 - 12:15 APPLICATION OF DYNOPT OPTIMIZATION PROGRAM FOR  
TUNING FREQUENCIES OF HELICOPTER AIRFRAME  
STRUCTURES  
T. Murthy, Lockheed

12:30 - 2:00 LUNCH

SESSION CHAIRMAN: D. Schrage

2:00 - 4:30 EXPERIMENTAL-THEORETICAL INVESTIGATIONS

2:00 - 2:30 AN EXPERIMENTAL AND ANALYTICAL INVESTIGATION OF  
DYNAMIC STALL EFFECTS ON ISOLATED ROTOR FLAP-LAG  
STABILITY  
G. Gaonkar, Florida Atlantic

2:30 - 3:00 MEASUREMENTS AND PREDICTIONS CONCERNING ROTOR  
STABILITY  
I. Carfarelli, ONERA

. WEDNESDAY, MARCH 14, 1990 cont.

- 3:00 - 3:30      EXPERIMENTAL INVESTIGATIONS OF HELICOPTER  
STRUCTURAL DYNAMICS AND THE INTERACTION WITH  
VIBRATION REDUCTION SYSTEMS  
M. Degener, DLR Gottingen
- 3:30 - 4:00      EXPERIMENTAL IDENTIFICATION OF HELICOPTER ROTOR  
DYNAMICS USING KINEMATIC OBSERVERS  
R. McKillip, Jr., Princeton
- 4:00 - 4:30      VALIDATION OF ROTOR VIBRATORY AIRLOADS AND  
APPLICATIONS TO HELICOPTER RESPONSE  
J. Yen, Bell

Some Reflections on Opportunities for  
Rotorcraft Dynamics Research

Robert A. Ormiston  
US Army Aeroflightdynamics Directorate

Abstract  
for

ARO/Duke Workshop on Dynamics and Aeroelastic Stability  
Modeling of Rotorcraft Systems, March 12-14, 1990

The establishment of the US Army Aviation Research and Technology Activity, the ARO Rotorcraft Centers of Excellence Program, the NASA Rotorcraft Program, and the expansion of rotorcraft applications in the military and civil fields have all contributed to tremendous expansion in rotorcraft basic research over the last twenty years. In view of the challenging technical complexity of rotorcraft, it is not surprising that many areas of research still need considerable attention. Nevertheless, some topics inevitably receive substantial attention, while other topics could benefit from more emphasis. The purpose of this presentation is to present observations gained from the government research perspective with the hope of stimulating more attention for selected topics and suggesting alternative methods or approaches to achieving the end goals of rotorcraft research. The goals themselves warrant some discussion as well.

The presentation will include specific examples to address these topics in the context of rotorcraft aeroelastic stability, rotor loads, experimental investigations and analysis validation, and the role of comprehensive analysis in rotorcraft R&D.



**HELICOPTER ROTOR DYNAMICS AND AEROELASTICITY:  
SOME KEY IDEAS AND INSIGHTS**

**BY**

**PERETZ P. FRIEDMANN**

**MECHANICAL, AEROSPACE AND NUCLEAR ENGINEERING DEPARTMENT  
UNIVERSITY OF CALIFORNIA, LOS ANGELES, CA 90024, U.S.A.**

**Presented at the Third Workshop on  
DYNAMICS AND AEROELASTIC STABILITY MODELING OF  
ROTORCRAFT SYSTEMS  
12-14 March 1990  
Duke University  
Durham, North Carolina**

# HELICOPTER ROTOR DYNAMICS AND AEROELASTICITY: SOME KEY IDEAS AND INSIGHTS

Peretz P. Friedmann\*

*Mechanical, Aerospace and Nuclear Engineering Department  
University of California, Los Angeles, CA 90024, U.S.A.*

**Abstract** - The purpose of this paper is to provide a detailed discussion of four important current topics in helicopter rotor dynamics and aeroelasticity. These topics are: (1) the role of geometric nonlinearities in rotary-wing aeroelasticity; (2) structural modeling, free vibration and aeroelastic analysis of composite rotor blades; (3) modeling of coupled rotor/fuselage aeromechanical problems and their active control; and (4) use of higher harmonic control (HHC) for vibration reduction in helicopter rotors in forward flight. Hopefully this discussion will provide an improved fundamental understanding of the current state of the art. Thus future research can be focused on problems which remain to be solved instead of producing marginal improvements on problems which are already understood.

## NOTATION

$a$	= two-dimensional lift curve slope
$b$	= semi-chord
$A, B$	= first order system and control matrices
$C_{d0}$	= profile drag coefficient
$\hat{e}_x, \hat{e}_y, \hat{e}_z$	= unit vector associated with the undeformed blade, Fig. 1.
$\hat{e}_x, \hat{e}_y, \hat{e}_z$	= triad $\hat{e}_x, \hat{e}_y, \hat{e}_z$ after deformation, Fig. 1
$e$	= blade root offset
$i, j, k$	= unit vector in the direction $x, y$ , and $z$ respectively, Fig. 1
$J$	= cost functional
$K_x, K_y, K_z$	= flap, lag and torsion springs
$l$	= length of flexible portion of blade
$M_F$	= nondimensional fuselage mass
$R$	= blade radius
$[S]$	= transformation matrix between deformed and undeformed triads of unit vectors, Eq. (1)
$S_{ij}$	= elements of matrix $[S]$
$t$	= time
$T$	= $n \times m$ HHC transfer matrix
$u, v, w$	= components of the displacement of a point on the elastic axis of the blade, Fig. 1
$W_z$	= diagonal weighting matrix on vibrations
$W_\theta$	= diagonal weighting matrix on control amplitudes
$W_{\dot{\theta}}$	= diagonal weighting on control rate of change
$x_A$	= offset between blade aerodynamic center (A.C) and elastic axis (E.A)
$x_l$	= offset between blade center of mass (C.G) and elastic axis
$x, y, z$	= coordinates shown in Fig. 1
$x, u$	= system state and control vectors
$Z$	= $n \times 1$ vector of vibration amplitudes
$Z_0$	= $n \times 1$ vector of baseline vibrations
$\beta_p$	= precone angle
$\epsilon$	= basis for order of magnitude, associated with typical elastic blade slope
$\theta_{HH}$	= HHC control angle
$\Delta\theta(i)$	= $\theta(i) - \theta(i-1)$
$\theta$	= total pitch angle
$\theta_0$	= collective pitch
$\theta_{1s}, \theta_{1c}$	= cyclic pitch components
$\theta_{pk}$	= pitch of the $k$ th blade
$\theta_{0s}, \theta_{0c}, \theta_{0s}$	= amplitudes of HHC sine input in collective, longitudinal, and lateral control degrees of freedom
$\theta_{0c}, \theta_{0c}, \theta_{0s}$	= amplitudes of HHC cosine input in collective, longitudinal, and lateral control degrees of freedom
$\lambda, \lambda_{1c}, \lambda_{1s}$	= inflow ratio, and its cyclic components
$\mu$	= advance ratio

\* Professor and Chairman

$\phi$	= rotation of cross section of blade around the elastic axis
$\psi$	= azimuth angle of blade, $\psi = \Omega t$
$\Omega$	= speed of rotation
$\omega_{HH}$	= HH frequency
$\omega_{H1}, \omega_{F1}, \omega_F$	= inplane, torsional and flapwise nondimensional fundamental frequency
$( )$	= nondimensionalized, quantity, frequencies by $\Omega$ , length by $l$
$( )$	= $\partial/\partial\psi$

## 1. INTRODUCTION

During the last two decades, since Loewy's [1] comprehensive review of rotary-wing dynamic and aeroelastic problems was published a vast body of published research, on these topics has appeared in the literature. This substantial body of research has also been discussed in a considerable number of survey papers which have emphasized various aspects of the rotary-wing aeroelastic stability and response problem together with the related vibration problems and their control by active and passive means. For convenience these survey papers [1-13] are cited in chronological order. Loewy's survey [1] was followed by a more restrictive survey by Dat [2] which discussed unsteady aerodynamic and vibration problems in forward flight. Hohenemser [3] discussed some aeromechanical stability problems as part of the broader field of flight mechanics. Friedmann [4,5] presented a detailed chronological discussion of rotary-wing aeroelasticity emphasizing the role of geometrical nonlinearities, due to moderate blade deflections, unsteady aerodynamics and forward flight. A similar discussion which was restricted to the case of hover and hingeless and bearingless rotors was also provided by Ormiston [6]. In addition to these papers which have emphasized primarily aeroelastic stability, two other surveys [7,8] have dealt exclusively with the vibration problem and its active and passive control in rotorcraft.

More recently Johnson [9,10] has published a comprehensive review paper which described both the aeroelastic stability and rotorcraft vibration problems in the context of dynamics of advanced rotor systems. Friedmann [11] has described the main developments between 1983-87 emphasizing new methods for formulating aeroelastic problems, treatment of the forward flight problem, coupled rotor/fuselage analyses, structural modeling and structural optimization, and the use of active controls for vibration reduction and stability augmentation. A more restrictive review emphasizing some practical design aspects capable of alleviating aeromechanical problems was presented by Miao [12]. Finally it should be noted that a very comprehensive research report [13] has been published recently which contains a detailed review of research carried out under Army/NASA sponsorship, between 1967 and 1987.

The purpose of this paper is not to present another review of the literature in this field. Instead the main objective here is to discuss four specific and important topics in rotor dynamics and aeroelasticity where the body of available research has reached a sufficient level of maturity for key ideas to emerge. The emergence of these key concepts provides good insight on the course of research which needs to be conducted on these topics in the future.

The four topics which will be discussed in this paper are briefly described below:

1. *The role of geometric nonlinearities in rotary-wing aeroelasticity.* Methods for the effective formulation of the equations governing the rotary-wing aeroelastic problem are described and the importance of third and higher order geometrically nonlinear terms is discussed.
2. *Structural modeling, free vibration and aeroelastic analysis of composite rotor blades.* Available structural and structural dynamic models for composite rotor blades are discussed including geometrically nonlinear terms and general cross-sectional geometries.
3. *Modeling of coupled rotor/fuselage aeromechanical problems and their active control.* Various approaches for formulating such equations in forward flight are discussed. Various control approaches for stabilizing air resonance in hover and forward flight are considered. The active control of the flap-lag problem and coupled flap-lag-torsional problem are also briefly discussed.
4. *Use of higher harmonic control for vibration reduction in helicopter rotors in forward flight.* Available active control techniques for vibration reduction in forward flight are discussed. A new aeroelastic simulation capability for higher harmonic control is presented together with some important conclusions obtained from this research.

It is expected that the discussion of the four topics described above will provide an improved understanding of the state of the art. Thus future research can be focused on problems which remain to be solved.

## 2. THE ROLE OF GEOMETRIC NONLINEARITIES IN ROTARY-WING AEROELASTICITY

During the last twenty years it has been firmly established that geometrical nonlinearities, due to moderate blade deflections, play an important role in the aeroelastic stability analysis of hingeless and bearingless rotor blades [4-6,9-11,13]. The role of these terms for articulated blades is slightly less important but still significant [1,2,12-13].

As described in Refs. 5, 9, 11, and 13 a number of beam theories accounting for moderate as well as large deflections of blades have been developed and are available. These theories can be divided into two basic categories: (a) those which are based on ordering schemes and are valid for moderate deflections, and (b) those which are valid for large deflections, and are not based on ordering schemes. The moderate deflection theories have been developed primarily between 1970-80 and the large deflection theories have been developed since 1980. It is therefore quite relevant to try and determine the significance of higher order geometrical nonlinearities, such as third order and higher order nonlinear terms, on the aeroelastic stability of hingeless and bearingless rotor blades in hover and forward flight.

The source and structure of the geometrically nonlinear terms associated with *moderate blade deflections*, is conveniently illustrated by the transformation between the triad of unit vectors describing the deformed and undeformed state of a hingeless rotor blade, see Figs. 1a and 1b. Such a transformation, based on the assumption of small strains and finite rotations (slopes) has the following mathematical form [5]

$$\begin{Bmatrix} c'_x \\ c'_y \\ c'_z \end{Bmatrix} = [S] \begin{Bmatrix} \hat{c}_x \\ \hat{c}_y \\ \hat{c}_z \end{Bmatrix} \quad (1)$$

where the elements of the transformation matrix  $[S]$  determine the accuracy or order of the theory. For example for a second order type theory  $S_{ij}$ 's are given by:

$$\begin{aligned} S_{11} &= 1; \quad S_{12} = v_{,x}; \quad S_{13} = w_{,x} \\ S_{21} &= -(v_{,x} + \phi w_{,x}); \quad S_{22} = 1; \quad S_{23} = \phi \\ S_{31} &= -(w_{,xx} - \phi v_{,x}); \quad S_{32} = -(\phi + v_{,x} w_{,x}); \quad S_{33} = 1 \end{aligned} \quad (2)$$

Transformations of this type combined with the Euler Bernoulli assumption have been used as the basis for moderate deflection beam theories which are suitable for the aeroelastic stability and response analysis of isotropic hingeless and bearingless rotor blades [5,11,13].

When such transformations are incorporated in the derivation of the inertia and aerodynamic operators associated with the rotary wing aeroelastic problem many, relatively small, nonlinear terms emerge. Such terms clearly represent considerable complication in the equations of motion from an algebraic point of view. The final equations of motion can be obtained using two different approaches [11].

One approach is based on generating the equations of motion in explicit form. The explicit approach is frequently combined with an ordering scheme [5] to "manage" the large number of terms associated with geometric nonlinearities. The purpose of the ordering scheme is to provide a rational basis for neglecting higher order terms in a consistent manner. A suitable *example* for an ordering scheme used in deriving the equations of motion for a hingeless rotor blade in forward flight is given below. Orders of magnitude are assigned to the various parameters of the problem in terms of elastic blade slopes which are assumed to be moderate, i.e., slopes are of order  $\epsilon$ , with  $0.10 \leq \epsilon \leq 0.20$ , and the assumption

$$O(1) + O(\epsilon^2) = O(1) \quad (3)$$

is used when deriving the equations.

For the coupled flap-lag-torsional problem in forward flight the orders of magnitude for the relevant quantities are listed below:

$$\begin{aligned} w_{,x} = v_{,x} = \phi = O(\epsilon); \quad \lambda = \lambda_{1s} = \lambda_{1c} = \frac{w}{R} = \frac{v}{R} = O(\epsilon) \\ \frac{c}{R} = \frac{b}{R} = \beta_p = O(\epsilon); \quad \mu = O(1); \quad \theta = \theta_{1s} = \theta_{1c} = O(\epsilon^{1/4}) \\ \frac{u}{R} = \bar{x}_1 = \bar{x}_A = O(\epsilon^2); \quad c_{do/s} = O(\epsilon^{3/2}); \quad \frac{x}{l} = \frac{\partial}{\partial \bar{x}} = \frac{\partial}{\partial \psi} = O(1) \end{aligned} \quad (4)$$

It is important to note that ordering schemes are not unique, a somewhat different combination of parameters [14] can be also used as the basis of an ordering scheme for the same coupled flap-lag-torsional problem of a hingeless rotor blade in forward flight. Furthermore ordering schemes are based on common sense and experience with practical blade configuration thus their application requires both care and a certain degree of flexibility.

Ordering schemes are also convenient when using general purpose algebraic manipulators, such as MACSYMA [15] to derive equations of motion in explicit form. Since algebraic tasks are relegated to a computer, it is fairly easy to retain additional higher order terms. For example by changing the basic assumption in the ordering scheme to

$$O(1) + O(\epsilon^3) = O(1) \quad (5)$$

one can include the next group of higher order terms. For this case the various elements of the transformation matrix  $S_{ij}$ , Eq (1), can be rewritten as [20]

$$\begin{aligned} S_{11} &= 1 - \frac{1}{2}(v_{,x}^2 + w_{,x}^2); \quad S_{12} = v_{,x}; \quad S_{13} = w_{,x} \\ S_{21} &= -(v_{,x} + \phi w_{,x} + \frac{1}{2}v_{,x}w_{,x}^2); \quad S_{22} = 1 - \frac{1}{2}v_{,x}^2 - \phi v_{,x}w_{,x}; \\ S_{23} &= \phi - \frac{1}{2}w_{,x}^2\phi; \quad S_{31} = -(w_{,xx} - \phi v_{,x} - \frac{1}{2}v_{,x}^2w_{,x}); \\ S_{32} &= -(\phi + v_{,x}w_{,x} - \frac{1}{2}v_{,x}^2\phi); \quad S_{33} = 1 - \frac{1}{2}w_{,x}^2 \end{aligned} \quad (6)$$

For this case explicit derivation of the equations of motion is feasible only when using symbolic algebraic manipulation on a computer.

Such explicit derivations of the equation of motion have a number of advantages. First it enables one to write out the equations of motion with considerable detail. Thus one can inspect the equations and identify the coupling terms introduced by retaining the geometrically nonlinear terms. Physical interpretation of such coupling terms facilitates the understanding of equations. Furthermore equations derived by various researchers can be compared with each other and differences between various formulations can be clarified. Another advantage is associated with the computational efficiency inherent in such formulations. Numerical implementation of blade stability and response calculations based on such equations are more efficient and computer storage requirements are reduced. This represents an advantage in structural optimization studies of rotor blades with aeroelastic constraints [16-18] which require repetitive evaluation of the objective functions and the constraints.

A second, and more recent, approach to generating rotary-wing equations of motion is based on the implicit approach [11]. In this approach the equations of motion are never explicitly written down and they are generated numerically by the computer during the solution process. This approach is particularly effective when combined with the finite element approach, for the spatial discretization of the equation. This approach allows the treatment of complicated configurations, provides considerable flexibility in the representation of the aerodynamic loads [19], and does not require the use of ordering schemes and the inherent approximations associated with such ordering schemes.

More recent studies use small strain and large rotation type of analyses [21-23] which utilize Rodrigues parameters to represent finite rotations. This approach when coupled with an implicit formulation completely eliminates the need for using an ordering scheme. Furthermore it also removes the need to use the torsional quasi-coordinate which was present in a previous formulation [24] and created complexity in the finite element models based on this formulation. Use of Euler angles combined with an implicit formulation is equally effective for representing the large displacement of both isotropic or composite beams [25]. These models are more consistent and mathematically more elegant than blade models based on ordering schemes. At the same time the incorporation of such models into a general analysis is more complicated. Thus to date the only aeroelastic analysis capability based on such general formulation is the GRASP program [26].

Based on the discussion presented above one can now assess the importance of third and higher order terms in rotordynamic models. For the case of aeroelastic stability of hingeless rotor blades in hover a recent study [27,28] has investigated the influence of third order nonlinear terms, similar to those in Eq. (6) when compared to second order nonlinear terms, similar to those in Eq. (2). It was concluded that for torsionally soft blades ( $\omega_{T1} = 2.5$ ) and high collective pitch settings ( $\theta_0 > 0.20$ ) the effect of these higher order terms on the stability boundaries was fairly small (less than 10%). Thus the effect of third order, and higher order nonlinear terms, on blade aeroelastic stability appears to be limited. The retention of higher order nonlinear terms can be useful in the study of mathematical properties of the transformations which relate the position vectors of the deformed and undeformed states of a blade undergoing nonlinear deformation [29].

Another interesting question which can be asked is whether dynamic models of rotor blades which are based on nonlinear beam kinematics with finite large rotations are superior to previous moderate rotations theories, based on ordering schemes? There is no unique answer to this intriguing question. When one uses criteria based on mathematical elegance, consistency and accuracy large deflection theories have a slight advantage because the structural and inertia operators obtained when using these theories are slightly more accurate. However, it is essential to note that in order to complete the formulation of aeroelastic problem the unsteady aerodynamic loads have to be combined with the inertia and the structural parts. Previous reviews of the unsteady aerodynamics used in aeroelastic problems [2,5,9-11,13] have clearly indicated that the aerodynamic theories used for this purpose are *linear* theories, except when one attempts to model dynamic stall, or transonic effects. Therefore the combination of kinematical model which contains third order nonlinear terms, with a linear incompressible aerodynamic theory such as Greenberg's theory [27,28] does not produce necessarily a consistent aeroelastic model. This point is well illustrated by a recent study by Hodges, Kwon and Shankar [30] where it was shown that by combining three dimensional tip loss and unsteady inflow effects with a conventional moderate deflection theory remarkable agreement between theoretical and experimental results were obtained. In Fig. 2, taken from Ref. 30, the lead-lag damping of a stiff-in-plane hingeless rotor blade, with configuration parameters chosen from the experimental model rotor with soft pitch flexure, zero precone and droop, is shown for various collective pitch angles. Since both theoretical predictions have the same structural model, the differences are due to aerodynamics. Clearly the results with the three dimensional unsteady aerodynamics, denoted as panel method in Fig. 2, give much better agreement with the experimental data than those based on two dimensional quasi-steady aerodynamics, denoted 2-D theory. This example indicates that the key to substantial improvements in the aeroelastic modeling capability of rotor blades is linked to improved unsteady aerodynamic models, and not to the retention of third and higher order geometrically nonlinear terms.

Another basic inconsistency in the formulation of beam models for moderate and large deflections is associated with the fact that frequently excessive preoccupation with geometrically nonlinear terms leads to the neglect of simple structural effects such as those associated with Timoshenko beams, namely shear and rotary inertia.

Using a finite element model capable of capturing Timoshenko beam effects in an accurate manner [31] and calculating the influence of Timoshenko beam effects on the first three flapwise and first three in-plane of rotation frequencies of graphite-epoxy beam having the cross-sectional dimensions shown in Fig. 3, with a length of 15 feet and rotating at  $\Omega = 400$  RPM, yields the results presented in Table 1. It is evident that for this particular case the influence of shear and rotary inertia on the lead-lag or in-plane of rotation modes, and in particular the frequency of the second and third mode can be significant. Thus incorporation of such effects could be of equal importance to third order geometrical nonlinearities. Obviously the incorporation of true anisotropy, present in composite rotor blades is a much more important topic. This topic is the subject matter of the next section.

### 3. STRUCTURAL MODELING, FREE VIBRATION AND AEROELASTIC ANALYSIS OF COMPOSITE ROTOR BLADES

Most of the structural models developed to date have been restricted to isotropic material properties. On the other hand modern helicopter blades are frequently built of composites. To remedy this situation a substantial share of the recent studies in this field has been aimed at the development of models which are suitable for the structural and aeroelastic analysis of composite rotor blades. The important attributes of such a structural model, require the capability to represent transverse shear deformation, cross-sectional warping and elastic coupling, in addition to an adequate representation of geometric nonlinearities. Rotor blades are typically modeled as a beam. In a beam theory, the deformations of the cross-section, both in and out of the plane, are assumed to be either small or neglected. Therefore, an approach commonly used in the available structural models for composite rotor blade analysis is to determine the cross section warping functions, shear center location and cross sectional properties based on a linear theory. The linear, two dimensional analysis for the cross-section is decoupled from the nonlinear, one-dimensional global analysis for the beam and can be done once for each cross section of a non-uniform beam. This decoupling is usually assumed in the literature without rigorous proof. The discussion of composite rotor blade structural modeling can, therefore, be divided into two categories: (1) Modeling approaches which lead to the determination of the stiffness properties of arbitrary blade cross sections. Anisotropic materials and the composite nature of the blade are taken into account in this category. (2) Structural models which use an one-dimensional beam kinematics suitable for composite rotor blade analysis. A typical structural model in this category should include geometric nonlinearities, pretwist, transverse shear deformation and cross section warping. Many of the existing composite rotor blade models in category (1) were reviewed in detail in a recent review paper by Hodges [32]. Our objective here is not to duplicate Hodges' review, but to consider the subject from a slightly different perspective.

Mansfield and Sobey [33] initiated the first pioneering study of this difficult subject. They developed the stiffness properties of a fiber composite tube subjected to coupled bending, torsion, and extension. Transverse shear and warping of the cross section was not included in the model. This model is too primitive to be suitable for composite rotor blade aeroelastic analysis. However, the authors made some attempts to explore the potential of this model for the innovative idea of aeroelastic tailoring.

Rehfield [34] used a similar approach but included out-of-plane warping and transverse shear deformation. This was strictly a static theory for a single cell, thin walled, closed cross section composite, with arbitrary layup, undergoing small displacements. This model was suitable for preliminary design, or frequency tailoring studies, as well as linear free vibration analysis of nonrotating composite beams. Pretwist, dynamic effects and geometric nonlinearities which are known to play a major role in helicopter rotor dynamics are not accounted for. This relatively simple theory was correlated by Nixon [35] with experimental data and by Hodges, Nixon and Rehfield [36] with a NAS-TRAN finite element analysis of a beam model with a single closed cell. Wörmle [37] developed a linear, two-dimensional finite element model to calculate the cross section warping functions of a composite beam under transverse and torsional shear. With these warping functions, the shear center locations and the stiffness properties of the cross section could be calculated. The cross section can have arbitrary shape but the material properties were restricted to monoclinic.

A more general model for calculating the shear center and the stiffness properties of an arbitrarily shaped composite cross section was developed by Kosmatka [38]. He used a two-dimensional isoparametric eight node quadrilateral finite element model to obtain the St. Venant solution of the cross-section warping functions of a tip loaded composite cantilever beam with an arbitrary cross section. The beam was assumed to be prismatic (axially uniform), nonhomogeneous, and anisotropic. The blade material was generally orthotropic, i.e., orthotropic material whose material principal axes are oriented arbitrarily. Therefore, the beam behaves in an anisotropic manner. Subsequently this model was combined with a companion moderate deflection beam theory suitable for the structural dynamic analysis of advanced prop-fan blades and helicopter rotors, which will be discussed later in this section.

Giavotto, et al. [39] also formulated a two-dimensional finite element model for determining cross section warping functions, shear center location and stiffness properties. A special feature of this formulation is that the resulting equations have both extremity solutions and central solutions. The central solutions correspond to the warping displacements due to applied loads without considering end effects, while the extremity solutions correspond to the warping displacements due to end effects. Subsequently this work was extended by Borri and Merlini [40] to include the so-called geometric section stiffness associated with large displacement formulations. Bauchau [41] developed a beam theory for anisotropic materials based on the assumption that the cross section of the beam does not deform in its own plane. The out-of-plane cross section warping was expressed in terms of the so-called eigenwarpings. This theory is valid for thin-walled, closed, multi-celled beams with transversely isotropic material properties. Subsequently it was extended by Bauchau, Coffenberry and Rehfield [42] to allow for general orthotropic material properties.

All the studies described in this section up to this point employed a separate two-dimensional analysis to determine the cross sectional warping functions and stiffness properties. For non-uniform beams, such a two-dimensional analysis is carried out once for each cross section. A new approach developed by Lee and Kim [43] and Stemple and Lee [44] uses a finite element formulation which can represent thin-walled beams with arbitrary cross sections, general spanwise taper and planform distributions and allows arbitrary cross section warping. This was accomplished by distributing warping nodes over the cross section situated at the node of regular beam type finite element. Thus the treatment of the cross section warping is coupled with the treatment of the beam bending, torsion and extension. This formulation considered only the out-of-plane warping and linear problems, or small deflection problems.

Recently, Stemple and Lee [45] have extended this formulation to allow for large deflection static and free vibration analysis of rotating composite beams. The disadvantage of this approach is that the analysis is more expensive than those whose cross section analysis is decoupled from the nonlinear beam analysis. Furthermore the numerical results obtained from this theory were not compared to other available theories, thus the validity of the theory still remains to be determined.

The structural theories discussed so far emphasize the modeling approach associated with category (1), where the emphasis is on determining the shear center, warping and cross-sectional properties of the composite cross section. For category (2) structural modeling, where the emphasis is one-dimensional beam kinematics suitable for the analysis of composite rotor blades, two types of theories are available depending on the level of geometric nonlinearity being retained in the one-dimensional beam kinematics. The first type is based on a moderate deflection type of theory while the second type is capable of modeling large deflections. Moderate deflection theories usually rely on an ordering scheme to limit the magnitude of blade displacements and rotations. While large deflection theories do not utilize an ordering scheme to limit the magnitude of blade displacements and rotations. For such theories the only assumption used to neglect higher order terms is the assumption that the strains are small.

In rotary wing aeroelasticity moderate deflection theories are usually adequate provided that a consistent ordering scheme is used. The first aeroelastic model for a composite rotor blade in hover was presented in a comprehensive study by Hong and Chopra [46]. In this specialized model, the blade was treated as a single-cell, laminated box beam composed of an arbitrary lay-up of composite plies. The strain-displacement relations for moderate deflections were taken from Hodges and Dowell [24], which does not include the effect of transverse shear deformations. Each lamina of the laminate was assumed to have orthotropic material properties. The equations of motion were obtained using Hamilton's principle. A finite element model was used to discretize the equations of motion. Numerical results for the coupled flap-lag-torsional behavior of hingeless rotor blades clearly illustrated the strong coupling effects introduced by the composite nature of the blade. These coupling terms which depend on fiber orientation have a strong influence on blade stability boundaries in hover. Subsequently this analysis was extended to the modeling of composite bearingless rotor blades in hover [47] and a systematic study was carried out to identify the importance of the stiffness coupling terms on blade stability with fiber orientation and for different configurations. In this model the composite flexbeam of the bearingless rotor blade was represented by an I-section consisting of three laminates. Each laminate is composed of an arbitrary lay-up of composite plies. The outboard main blade and the torque tube were assumed to be made of isotropic materials. Thus this model represents a somewhat idealized model for a composite bearingless rotor blade. In addition to aeroelastic stability studies of composite rotor blades in hover, Panda and Chopra [48] also studied the aeroelastic stability and response of hingeless composite rotor blades in forward flight using the structural model presented in Ref. 46. It was found that ply orientation is effective in reducing both blade response and hub shears.

A more comprehensive analysis for the structural dynamic modeling of composite advanced prop-fan blades, which with some modifications, is also suitable for the general modeling of curved, pretwisted composite rotor blades was developed by Kosmatka [38]. The cross section geometry of the blade is arbitrary, and the associated cross section stiffness properties and shear center location can be obtained from the accompanying linear two-dimensional finite element model which has been discussed earlier in this section. In the one-dimensional, nonlinear analysis, the curved pretwisted blade was modeled by a series of straight beam elements which are aligned with the curved line of shear centers of the blade. Each beam finite element was derived using Hamilton's principle and the following basic assumptions: the beam has an arbitrary amount of pretwist, undergoes moderate deflections, is composed of generally orthotropic materials, has an arbitrary cross sectional shape, and rotates about a vector in space. Numerical results for frequencies and mode shapes obtained from this structural dynamic model were in good agreement with modal tests on conventional and advanced propellers [49,50]. Bauchau and Hong [51-53] have developed a series of large deflection composite beam models which are intended for rotor blade structural dynamic and aeroelastic analysis. The first of these models [51] used a finite element approach combined with a general global coordinate system. While the model was general it also proved itself to be computationally inefficient. A second version of this model [52] used a curvilinear coordinate system and the resulting finite element model was found to be computationally more efficient than the first one. However some deficiencies associated with the derivation of the strain displacement relation were noted by Hong in his dissertation [54]. After additional improvements in the model a final version of this theory which is capable of modeling naturally curved and twisted beams undergoing large displacements and rotations and small strains was developed. The kinematics of this theory is an extension of the common approach, using the definition of Green strains, to include effects such as small initial curvature, transverse shear deformations and out-of-plane warpings. The fundamental assumptions in the kinematics are the indefinability of the cross-section in its own plane and a revised small strain assumption. In this revised small strain assumption, both axial and shearing strains are still neglected compared to unity, however, no assumption is made about the relative magnitude between the axial and shearing strains. Therefore, the second order shear strain coupling terms in the axial strain expression are retained under this revised small strain assumption. The commonly used small strain assumption, which include an additional assumption that the axial and shearing strains are of the same order of magnitude, was often successfully used in beam models with isotropic or slightly anisotropic materials. However, Bauchau and Hong [53] showed that it might not be adequate for beams with highly anisotropic material by comparing the analytical and experimental results of a thin-walled kevlar beam. The strain-displacement relations were derived using an implicit formulation with seven unknown functions which depend on the space coordinate, namely three displacement components, three rotation parameters (Euler angles were used), and the amplitude of the torsional warping. The three rotation parameters, which are used to describe the large rotations from the undeformed to the deformed triad of unit vectors, are defined implicitly in the rotation matrix instead of appearing explicitly in the strain-displacement relations. An extension of this model for free vibration analysis can be found in Hong's dissertation [54]. Using this model a number of cases testing the static large deflection capability and the free vibration capability of the model were computed. However an aeroelastic analysis of a rotor blade, based on this model, is not available to date.

Recently Minguet and Dugundji [55,56] have developed a large deflection composite blade model for static [55] and free vibration [56] analysis. Large deflections are accounted for by using the Euler angles to describe the transformation between a global and local coordinate system after deformation. However, transverse shear deformation, and cross section warping were not incorporated in this model. Thus the model is more suitable for the study of flat composite strips than actual rotor blades.

Atilgan and Hodges [57] have recently presented a theory for nonhomogeneous, anisotropic beams undergoing large global rotation, small local rotation and small strain. They used a perturbation procedure to obtain a linear two-dimensional cross section analysis which is decoupled from the nonlinear one-dimensional global analysis. The nonlinear beam kinematics was based on a study by Danielson and Hodges [58]. The nonlinear beam kinematics, which

defines a conjugate stress measure, describes a constitutive relationship and develops the momentum balance conditions, was based on Atluri [59]. The cross section warping, both near the ends (boundary layer solutions) and away from the ends (St. Venant solutions) was obtained in terms of force and moment strains from a linear two-dimensional equation. The three force strains include axial and both transverse shear strains at the reference line, the three moment strains are torsion and curvature quantities [58]. Since the strain components from the nonlinear beam kinematics are expressed in terms of force and moment strains, and cross section warpings, it is possible to obtain a one-dimensional system of equations in terms of force and moment strains only by substituting the solutions for the cross sectional warpings into the strain expressions. However, the authors abandoned this procedure as being too tedious and unnecessary. Instead, they chose to follow the same approach as Giavotto, et al. [39], which solves the cross section warping functions in terms of force and moment stress resultants. A geometric stiffness matrix was also formulated in this model. This matrix and the material stiffness matrix were intended to be used in an incremental updated Lagrangian formulation for large deflections. A general mixed variational principle was used in the formulation of the one-dimensional, geometrically nonlinear global analysis. No numerical results were presented in this paper. This study draws rather heavily on the material presented in Refs. 39 and 59 and its principal contribution seems to be the derivation of a geometric stiffness matrix.

From this review of the literature on available structural models capable of representing composite rotor blades it is evident that this has been an active area of research during the last five years. Yet it is remarkable to note that despite the availability of such models the only published body of research which actually contains aeroelastic stability and response type of results is that published by Chopra and his associates [46-48]. This is somewhat disappointing since the potential for aeroelastic tailoring for composite rotor blades has been demonstrated [46]. A typical result, Fig 4, taken from Ref. 48, shows that for a four bladed hingeless soft-in-plane composite rotor, where the composite single cell box has symmetric laminates, the ply orientation angle,  $\Lambda^\circ$ , for the vertical walls of the box has a very significant effect on the peak-to-peak value of nondimensional vertical hub shears. This quantity is indicative of the vibration levels experienced at the hub. It is interesting to note that both positive and negative ply angles reduce the oscillatory hub shear, however positive angles of  $30^\circ$  are more effective in reducing vibration levels. In view of the positive nature of coupling effects present in composite blades one would expect to see more studies of this type which take advantage of the vibratory load reduction potential present in composite blades.

Instead of the excessive preoccupation with arbitrarily large deflection theories for composite beams it appears to be more sensible to derive realistic composite blade models, based on moderate deflection theories, and use them to explore the potential for designing composite rotor blades which have low vibration levels and good aeroelastic stability margins. Based on the present state-of-the-art it appears that a moderate deflection type of beam theory combined with a cross-sectional analysis of the composite blade presented in Refs. 38 or 39 would be both suitable and adequate for this purpose.

#### 4. MODELING OF COUPLED ROTOR/FUSELAGE AEROMECHANICAL PROBLEMS AND THEIR ACTIVE CONTROL

The aeromechanical instability of a helicopter, on the ground or in flight, is caused by coupling between the rotor and body degrees of freedom. This instability is commonly denoted air resonance when the helicopter is in flight and ground resonance when the helicopter is on the ground. The physical phenomenon associated with this instability is quite complex. The rotor lead-lag regressing mode usually couples with the body pitch or roll to cause an instability. The nature of the coupling which is both aerodynamic and inertial is introduced in the rotor by body or support motion. The importance of developing a mathematically consistent model capable of representing the coupled rotor/fuselage dynamic system has already been discussed in previous reviews [5,6,9-11,13]. With the use of algebraic symbolic manipulative programs or implicit formulations [26,60] sophisticated mathematical models for coupled rotor/fuselage aeromechanical problems can be formulated and solved.

The primary purpose of this section is to discuss a number of modeling aspects for this class of problems which have been shown to be important by recent research. Subsequently research on the use of active controls to stabilize this class of aeromechanical problems is also described.

Many previous air resonance studies [6,9-11,13] were limited by simplifying assumptions such as hover, blades which were assumed to be torsionally rigid or aerodynamic loads based on quasisteady assumptions. Recent studies [61,62] have clarified the role of unsteady aerodynamics, forward flight and torsional flexibility on air resonance. Furthermore the mathematical model derived for this coupled rotor/fuselage system had also a provision for including an active controller capable of suppressing air-resonance.

The mathematical model of the rotor/fuselage system of Ref. 61 and 62, and its salient features are described next. The fuselage is represented as a rigid body with five degrees of freedom, where three of these are linear translations and two are angular positions of pitch and roll (Fig. 5). Yaw is ignored since its effect in the air resonance problem is known to be small. A simple offset hinged spring restrained rigid blade model is used to represent a hingeless rotor blade (Fig. 6). This assumption simplifies the equations of motion, while retaining the essential features of the air resonance problem. In this model, the blade elasticity is concentrated at a single point called the hinge offset point, and torsional springs are used to represent this flexibility. The dynamic behavior of the rotor blade is represented by three degrees of freedom for each blade, which are flap, lag, and torsion motions. The aerodynamic loads of the rotor blades are based on quasi-steady Greenberg's theory, which is a two dimensional potential flow strip theory. Compressibility and dynamic stall effects are neglected, though they could be important at high advance ratios. Unsteady aerodynamic effects, which are created by the time dependent wake shed by the airfoil as it undergoes arbitrary time dependent motion, are accounted for by using a dynamic inflow model. This simple model uses a third order set of linear differential equations driven by perturbations in the aerodynamic thrust, roll moment, and pitch moment at the rotor hub. The three states of these equations describe the behavior of perturbations in the induced inflow through the rotor plane. The dynamic inflow model coefficients used are those of Ref. 63.



The equations of motion of the coupled rotor/fuselage system are very large and contain geometrically nonlinear terms due to moderate blade deflections in the aerodynamic, inertial, and structural forces. Furthermore, the coupled rotor/fuselage equations have additional complexity due to the presence of the fuselage degrees of freedom. To reduce the equations to a manageable size, an ordering scheme is used in the derivation of the equations of motion to systematically remove the higher order nonlinear terms. The ordering scheme is based on Eq. (3). For this class of problems  $\epsilon$  represents the slopes of the deflections of the blades, which usually are of an order of magnitude which is less than .15. The blade degrees of freedom are assigned an order of  $\epsilon$ , while the fuselage degrees of freedom are of order  $\epsilon^{3/2}$ , the various other parameters have the order of magnitude given in Eqs. (4). A symbolic manipulation program is then used to generate the nonlinear set of equations of the rotor/fuselage system using the ordering scheme. Five fuselage equations result of which three enforce the fuselage translational equilibrium and two enforce the roll and pitch equilibrium. The three resulting rotor blade equations are associated with flap, lag, and torsional motions of each blade. Also, the aerodynamic thrust and roll moments at the hub center are determined for the perturbation aerodynamics in the dynamic inflow equation. All of these equations can be found in detail in Ref. 62.

An active control device to suppress the air resonance instability through a conventional swashplate is also incorporated in this mathematical model. The pitch of the k-th rotor blade is given by the expression

$$\theta_{pk} = (\theta_0 + \Delta\theta_0) + (\theta_{1c} + \Delta\theta_{1c})\cos(\psi_k) + (\theta_{1s} + \Delta\theta_{1s})\sin(\psi_k) \quad (7)$$

The various pitch terms with the symbol  $\Delta$  are small and these represent the active control inputs, while those without  $\Delta$  are the inputs necessary to trim the vehicle.

The stability of the system is determined through the linearization of the equations of motion about a blade equilibrium solution and the helicopter trim solution. The helicopter trim and equilibrium solution are extracted simultaneously using harmonic balance for a straight and level flight condition [61]. After linearization, a multi-blade coordinate transformation is applied, which transforms the set of rotating blade degrees of freedom to a set of hub fixed non-rotating coordinates. This transformation is introduced to take advantage of the favorable properties of the non-rotating coordinate representation. The original representation has periodic coefficients with a fundamental frequency of unity, however, the transformed system has coefficients with a higher fundamental frequency. These higher frequency periodic terms have a reduced influence on the behavior of the system and can be ignored in some analyses at low advance ratios [5]. In hover, the original system has period coefficients with a frequency of unity, but the transformed system has constant coefficients.

Once the transformation is carried out, the system is rewritten in first order form.

$$\dot{x} = A(\psi)x + B(\psi)u \quad (8)$$

The fundamental frequency of the coefficient matrices depends on the number of rotor blades. For an odd bladed system the fundamental frequency is  $N_b$  per revolution, while for an even bladed system the fundamental frequency is  $N_b/2$  per revolution. Stability can now be determined using either an eigenvalue analysis or Floquet theory for the periodic problem in forward flight. An approximate stability analysis in forward flight is also possible by performing an eigen-analysis on the constant coefficient portion of the system matrices in Eq. (8).

The mathematical model was carefully tested by comparing results to other investigator's analytical and experimental results. The correlation with these results was good and verified that the effects of torsion, unsteady aerodynamics, and forward flight were accurately represented in the model [61,63].

This mathematical model was used to analyze the behavior of a four bladed hingeless helicopter somewhat similar to the MBB 105 helicopter. The nominal configuration differs from the MBB 105 in that it has an *unstable air resonance mode*. The system has 37 states. The five body degrees of freedom and the twelve rotor degrees of freedom (three degrees of freedom for each blade) produce 34 position and rate states. The dynamic inflow model augments the system with three more states giving a total system order of 37. Thus even this relatively simple model requires a considerable number of states (or degrees of freedom).

As mentioned before the lead lag regressing mode is the critical degree of freedom associated with air resonance therefore the essential features of this instability are described by damping plots for this particular degree of freedom.

Figure 7 illustrates the influence of unsteady aerodynamics as well as the effect of periodic coefficients (or forward flight) on the lead-lag regressing mode damping of the open loop configuration. The two sets of curves represent air resonance damping of the configuration with quasi-steady aerodynamics and with dynamic inflow at various advance ratios. Dynamic inflow captures primarily the low frequency unsteady aerodynamic effect which is important for rotor/fuselage aeromechanical problems such as air resonance. The stabilizing effect in forward flight, which is evident in the figure, is consistent with behavior observed in previous studies [5,11]. For hover, the system has constant coefficients and thus the constant coefficient approximation and the periodic system produce the same results, as is clearly evident in the figure. It is also shown in the figure that the effect of periodic coefficients is relatively minor. The quasisteady aerodynamic model produces a more stable system than the model which includes the unsteady aerodynamic effects as represented by the dynamic inflow model. It is also worthwhile mentioning that considerable differences between the two models exist particularly in low advance ratios.

Figure 8 shows that neglecting the torsional degree of freedom on the nominal configuration increases the instability of the lead-lag regressing mode. The trend of the two curves also tends to diverge at high advance ratios. The addition of torsion also tends to amplify the effect of the periodic terms. At high values of advance ratio, the flap-lag-torsion model shows a much greater difference between the constant and periodic stability analysis than does the flap-lag analysis.

Coupled rotor/fuselage analyses based on an implicit formulation developed by Done et al. [60] have modeled the effect of swashplate flexibility and control system stiffness on this class of problems. The limited number of numerical results presented [60] do not convey a clear picture of the influence of these additional parameters on the air resonance problem.

Another recent study by Loewy and Zotto [64] studied the effect of rotor shaft flexibility and associated rotor control coupling on the ground/air resonance of helicopters. This is of particular interest for certain types of advanced helicopters which have a relatively flexible shaft. The analysis was formulated using a Lagrangian approach and the equations were derived using symbolic manipulation based on the MACSYMA package. The equations are based initially on large Euler angles however subsequently the equations were simplified using an ordering scheme. The blades were offset hinged spring restrained with flap and lag degrees of freedom for each blade, and a four bladed rotor was considered. The model included a total of 12 degrees of freedom. Two cyclic flap modes, two cyclic lag modes, fuselage pitch and roll, fuselage center of mass translation in two directions, hub translation due to shaft flexibility in two directions, and shaft bending slope in two directions. The blades were assumed to be torsionally stiff. Only hover was considered, the aerodynamic loads were based on simple strip theory, and the periodic coefficients were eliminated using multiblade coordinates. Numerical results were obtained for a configuration similar to the OH-58D helicopter with a four bladed articulated rotor. The effect of shaft flexibility and associated coupling terms, together with the influence of a mass simulating a mast mounted sight on air and ground resonance stability boundaries was studied with considerable detail. It was found that flexibility/control coupling adds new modes of instability for ground resonance, however this was found to be a weak instability which was eliminated by small amounts of structural damping. Air resonance type of instabilities are more susceptible to shaft flexibility/control coupling effects and small amount of structural damping fails to stabilize the coupled rotor/fuselage system. Therefore for certain combinations of parameters shaft/blade pitch coupling effects have to be designed carefully to insure the stability of the air resonance mode.

The air resonance stability of hingeless rotors in forward flight was also studied in Ref. 76. The body of research available on coupled rotor/fuselage aeromechanical problems has reached a remarkable level of maturity in a fairly short period of time. It is also evident that reliable models for this class of problem should contain coupled flap-lag-torsional blades models combined with a fuselage which has pitch and roll as well as two translational degrees of freedom. For certain configurations coupling effects introduced by swashplate flexibility, shaft bending and pitch link flexibility should be also incorporated in the model so as to obtain reliable stability boundaries. The aerodynamic representation which is most suitable for this class of problem is the dynamic inflow model [63]. Up to advance ratios of  $\mu = 0.40$  the role of periodic coefficients is fairly small, and usually the most unstable cases for air resonance occur for the case of hover. For soft-in plane hingeless helicopter configurations and articulated blade configurations forward flight usually introduces a stabilizing effect.

The derivation of coupled rotor/fuselage analyses or models has become fairly routine when using computer algebra or implicit formulations. Therefore studies based on very simple models which contain fewer degrees of freedom than those retained in Refs. 61-62 and 64 will rarely serve a useful purpose, since the validity of such models is questionable.

Improved understanding of aeromechanical phenomena such as air and ground resonance has also raised the possibility of eliminating or suppressing such instabilities using active controls. One possible means of stabilizing or augmenting stability of air resonance is through an active controller operating with a conventional swashplate. This approach is feasible from a practical point of view only if it is simple to implement since it must compete against the straightforward mechanical solution to this problem based on lag dampers. Such an active controller would need sensing and actuating devices leading to an expensive system. However, with the inevitable introduction of other active control devices such as higher harmonic control (HHC) for vibration suppression [65-67] this argument is considerably weakened. Vibration control requires sensors and actuators with bandwidths well above the 1/rev frequency. Since the air resonance instability results in an unstable lead-lag regressing mode (i.e., the mode associated with the  $[1 - \omega_{L1}]$  frequency) these devices would also be sufficient for air resonance control. Thus, sensing and actuator hardware, which may be already available, could be used for additional purposes below the frequency range intended for the available vibration control objective.

Research in the active control of air and ground resonance has been limited to a few studies [68-70], where various theoretical active control studies were presented. The helicopter models used in these studies were quite limited since important effects such as torsional flexibility of the rotor blades, forward flight, and unsteady aerodynamics were all neglected. Furthermore, the studies dealing with the active control of air resonance did not adequately demonstrate the ability of the control schemes to operate through the wide range of operating conditions which can normally be encountered.

A comprehensive study which demonstrated the feasibility of designing a simple active controller capable of suppressing air resonance throughout the flight envelope representative of a wide range of operating conditions which may be encountered by a helicopter, with hingeless blades, has been completed recently [61,62,71]. The coupled rotor/fuselage model representing this system was briefly described at the beginning of this section. The equations of motion describing this system are represented by Eq. (8), and the pitch of the  $k$ -th blade, determined by the controller is expressed by Eq. (7).

The control studies undertaken consisted of two stages. In the first stage [61] the coupled rotor/fuselage system was combined with linear quadratic optimal control theory to design *full state feedback* controllers. These controllers were then used to evaluate the importance of various modeling effects on the closed loop damping of the unstable air resonance mode. It was found that periodic terms in the model seem to play only a small role at advance ratios less than,  $\mu = 0.40$ . With this in mind and considering the cost of extracting periodic optimal gains, it seems reasonable to neglect the periodic terms in the initial stage of controller development. Knowing that the constant model is a reasonable approximation also allows the use of many other control design techniques. The results also indicate that unsteady aerodynamics and blade torsional flexibility seem to be important modeling effects that should be included in a controller design model. Significant errors of between 25 and 50 percent in closed loop lead-lag damping could result in these effects are not included. The collective control input seems to have little influence in controlling air resonance at

high advance ratios, so it was felt to be unnecessary for the complete control task. Finally, partial state feedback of the body states does not seem to be a reasonable approach to controlling air resonance. Poor lead-lag damping results and lead lag progressive mode excitation is a possible consequence. This particular conclusion contradicts the behavior observed for articulated rotors in Ref. 69.

Since full state feedback is not practical and the first stage of the research showed that partial state feedback is not reliable, the second stage of this research [62,71] was based on more advanced control system synthesis techniques to design a suitable controller.

The controller aimed at suppressing air resonance in the flight envelope of the helicopter is based on an optimal state estimator in conjunction with optimal feedback gains [72]. A constant coefficient model is assumed since the results obtained in the first stage indicated that a periodic model was unnecessary. The objective in this portion of the study was to design a controller at an operating condition and require it to function adequately at off design conditions, corresponding to the entire flight envelop of the helicopter. Furthermore in all applications, the design model and the actual plant to be controlled will have unavoidable differences due to the limitations associated with formulating models of physical systems. To overcome these difficulties, the multivariable frequency domain design methods of Refs 73,74 and 75 were used. This allows interpretation of the design process using frequency domain concepts and accounts for the possibility of high frequency modeling error. All this can be accomplished while retaining the structure of the state space approach. The technique, which is based on transfer function singular values, proved to be particularly effective in resolving problems that would not be obvious if only the covariance and weight matrices were used in the design process. To select the design loop shapes, Loop Transfer Recovery was used, which can be interpreted as an optimization balancing system performance requirements and the requirement of stability in presence of modeling errors.

The controller used a single roll rate measurement and both the sine and cosine swashplate inputs. This configuration is particularly simple since the measurement is taken from a non-rotating frame of (the fuselage) reference avoiding the need to send signals across the rotor head. Using sine and cosine inputs is also simple and can be accomplished through a conventional swashplate mechanism. A constant four mode design model consisting of the body roll and pitch modes and the lead-lag regressing and progressing modes was found to be quite practical for control design. The controller was shown to stabilize the system throughout a wide range of loading conditions and forward flight speeds and it required small inputs of the order of three degrees or less.

Some typical results obtained in this study, for the same four bladed hingeless rotor configuration for which results were presented in Figs. 7 and 8, are presented next. The open loop lead-lag regressing mode damping of the helicopter configuration throughout its flight regime is presented in Fig. 9. The horizontal axis is the advance ratio, while the vertical axis is the fuselage mass  $M_F$  nondimensionalized by the blade mass of 52 kg. A nondimensional fuselage mass of 32 plus four blades corresponds to the nominal total mass of 1872 kg. The figure indicates that the system experiences an air resonance instability throughout most of the flight regime. Marginal stability exists at an advance ratio greater than  $\mu = 0.35$  and the point of deepest instability is at  $M_F = 30$  and in the vicinity of hover. Figure 10 shows the same system after the controller designed according to the methodology [71] discussed above, has been applied on the helicopter. From the figure it is clear that the lead lag regressing mode is stable throughout the whole flight regime, and its stability is lowest in the neighborhood of  $M_F = 23$  and  $\mu = 0.11$ .

The body of research described above indicates that during the last five years considerable progress has been made in understanding the role of active controls as a potential means for stabilizing air and ground resonance. It should be noted that air resonance is a relatively mild instability, while ground resonance is substantially stronger thus the former is easier to control. It is interesting to note that partial state feedback of the body states does not seem to be a reasonable approach to controlling air resonance in four bladed hingeless rotors [61]. This is probably due to the fact that for hingeless rotors the coupling between the blade and fuselage degrees of freedom is much stronger. A relatively simple controller using only a single body roll rate measurement and two swashplate control inputs (sine and cosine) was shown to stabilize the air resonance *throughout the whole flight envelope* when using modern state of the art control system design techniques [62,71]. It is precisely this robustness of the modern control system synthesis techniques employed which make them attractive when compared to more classical control techniques employed by Ham and his associates in their research on the use of individual-blade-control for stability augmentation [77].

Finally it should be noted that while the air resonance instability proved itself to be fairly easy to control, the active control of more powerful instabilities such as the fuselage induced flap-lag instability, and the coupled flap-lag-torsional instability of stiff-in-plane hingeless rotor blades in forward flight, which was also studied in Ref. 62, proved itself to be much more difficult to control.

## 5. THE USE OF HIGHER HARMONIC CONTROLS FOR VIBRATION REDUCTION OF HELICOPTER ROTORS IN FORWARD FLIGHT

The use of high frequency blade pitch inputs, referred to as higher harmonic control (HHC), to reduce helicopter vibrations has been investigated in a number of studies. Aircraft flight tests [67,78,79], wind tunnel tests [80-83], and analytical simulations [84-91] have shown that HHC is capable of substantial reduction in helicopter vibration levels encountered in forward flight.

Furthermore the literature in this field has been surveyed in a number of review articles [92,11]. Particularly noteworthy is Johnson's review article [92], which described the state of the art up to 1982 and a recent paper by Shaw et al [82] which provides an excellent perspective on this important topic. Currently it is well understood that HHC produces vibration reduction by modifying the unsteady aerodynamic loads on the rotor blades.

It is quite remarkable that a significant portion of the research in this area involved wind tunnel testing [80-83] and flight testing [67,78,79]. While a number of analytical studies were carried out [84-91] they were less comprehensive than the tests. Previous analytical studies have generally relied on simple analog [87] or frequency domain [87] models of the helicopter response. Other studies [84-86,90,91] were based on using a fairly old aeroelastic response

code, the G400 [93,94] for simulation purposes. The model used in these studies did not have a consistent representation of the geometrical nonlinearities due to moderate deflections. Other shortcomings of this simulation capacity were the lack of time domain aerodynamics needed for capturing high frequency unsteady aerodynamic effects as well as a step by step time integration method which precluded the calculation of direct stability information in forward flight, such as provided by Floquet theory.

Recently a comprehensive aeroelastic simulating capability has been developed [95-97] and used to study a number of fundamental issues in higher harmonic control. The principal topics studied using this new aeroelastic simulation capability are listed below:

- 1 Comparison of the effectiveness of deterministic and cautious controllers based on local and global HHC models in reducing vibratory hub shears.
- 2 Comparison of the response of HHC of roughly equivalent articulated and hingeless rotors.
- 3 Evaluation of changes in hub moments when hub shears are minimized using HHC. Similar calculations are done when HHC is used to try to reduce both hub moments and hub shears simultaneously. These studies are done for both articulated and hingeless blades.
- 4 Determination of the influence of HHC on the aeroelastic stability margins of the blade in forward flight.
- 5 Comparison of the relative additional power requirements experienced when HHC is applied to two similar rotor configurations, one with articulated and one with hingeless blades.

A brief description of the aeroelastic simulation capability, the implementation of HHC and few important conclusions obtained in the course of these studies [95-97] are presented next.

The coupled flap-lag-torsional equations of motion which serve as the basis of this analysis are similar to those derived in Ref. 98. They contain geometrically nonlinear terms due to moderate blade deflections as illustrated in Fig. 1. These equations form the basis of an implicit flap-lag-torsional undergoing small strains and moderate deflections. Thus the equations contain geometrically nonlinear terms in the structural, inertia, and aerodynamic operators associated with this aeroelastic problem. The partial dependence in the equations is eliminated by using a Galerkin type finite element method [19]. A modal coordinate transformation, using six rotating coupled modes, is performed to reduce the number of degrees of freedom. These modes are calculated at a fixed value of collective pitch which depends only on advance ratio. For the configurations considered, the six lowest modes are usually the first three flap, first two lead-lag, and the fundamental torsional modes. The ordinary differential equations are solved using quasilinearization in an iterative manner to obtain the periodic equilibrium position in forward flight, for a propulsive trim type flight condition.

The inertia loads are determined by using D'Alembert's principle. An implicit formulation for the aerodynamic loads is used. At each iteration an approximation to the blade response is produced. This response is then used to generate numerical values of the modeling quantities needed in expressions for the aerodynamic loads to be used in the next iteration. The equations are linearized by writing perturbation equations about the nonlinear equilibrium position. Stability is determined by using Floquet theory.

The unsteady aerodynamics are finite-state time-domain aerodynamics presented in Ref. 99 which are an improved version of the theory developed by Dinyavari and Friedmann [100]. Stall and compressibility effects are neglected. The aeroelastic model is combined with a new trim procedure [95,96] which provides fully coupled simultaneous solution to both the aeroelastic response and the trim problem.

The rotor dynamic model has provisions for inclusion of HHC pitch changes in the structural, inertial, and aerodynamic portions of the model to allow HHC to be input to the model as 4/rev. sine and cosine components in each of the collective, longitudinal, and lateral control degrees of freedom. The general HHC input may be expressed as:

$$\begin{aligned} \theta_{HH} = & [\theta_{0S} \sin \bar{\omega}_{HH} \psi + \theta_{0C} \cos \bar{\omega}_{HH} \psi] \\ & + [\theta_{CS} \sin \bar{\omega}_{HH} \psi + \theta_{CC} \cos \bar{\omega}_{HH} \psi] \cos \psi \\ & + [\theta_{SS} \sin \bar{\omega}_{HH} \psi + \theta_{SC} \cos \bar{\omega}_{HH} \psi] \sin \psi \end{aligned} \quad (9)$$

where  $\theta_{0C}$ ,  $\theta_{0S}$ ,  $\theta_{CS}$ ,  $\theta_{CC}$ ,  $\theta_{SS}$ , and  $\theta_{SC}$  are independent of  $\psi$ . The hub shears to be minimized are calculated by integrating the inertia and aerodynamic loads due to a given blade response over the blade. The loads due to the four blades are then combined and the total loads are transformed to the non-rotating coordinate system. Fourier series representations of these loads are then found and the 4/rev. components extracted. Alternately to calculate blade root loads the Fourier analysis is done in the rotating system at the blade root.

Operating the electro-hydraulic actuators needed to implement HHC will require power from the helicopter powerplant. In addition, the helicopter rotor may require more or less power than at the baseline condition because of the additional aerodynamic loads which are imposed on it by the HHC inputs. The total power used to operate the rotor consists of the power needed to drive the rotor and the power needed to input control pitch at the blade root.

The various contributions to the power required to actuate the blade were calculated with a level of care and detail [96,97] which was not available in previous studies.

The vast majority of all HHC investigations to date have used linear optimal control solutions based on a quadratic cost functional. Therefore this approach was also used in Refs. 95-97. Minimum variance control is based on the minimization of a cost functional which is the expected value of a weighted sum of the mean squares of the control and vibration variables.

Minimum variance controllers are obtained by minimization of the cost functional:

$$J = E \left\{ Z^T(i) W_z Z(i) + \theta^T(i) W_\theta \theta(i) + \Delta \theta^T(i) W_{\Delta \theta} \Delta \theta(i) \right\} \quad (10)$$

Typically  $Z$ ,  $\theta$ , and  $\Delta \theta$  consist of the sine and cosine components of the  $N/\text{rev.}$  vibrations and HHC inputs. The weightings of each of these parameters may be changed to make it more or less important than the other components.

The minimum variance controllers are obtained by taking the partial derivative of  $J$  with respect to  $\theta(i)$  and setting this equal to zero:

$$\frac{\partial J}{\partial \theta(i)} = 0 \quad (11)$$

The resulting set of equations may be solved for the optimal HHC input  $\theta(i)$ .

The form of the resulting algorithm will depend on whether the global or local system model is used and on whether a deterministic or cautious controller is desired.

The global model of the helicopter response to HHC assumes linearity over the entire range of control application.

$$Z(i+1) = Z_0 + T\theta(i) \quad (12)$$

The vibration vector  $Z$  at step  $i+1$  is equal to the baseline vibration  $Z_0$  plus the product of the transfer matrix  $T$  and the control vector  $\theta$  at step  $i$ . This implies that  $T$ , the transfer matrix relating HHC inputs to vibration outputs, is independent of  $\theta(i)$ .

The local model of the helicopter response to HHC is a linearization of the response about the response to the current value of the controller vector:

$$Z(i+1) = Z(i) + T[\theta(i+1) - \theta(i)] \quad (13)$$

or:

$$\Delta Z(i+1) = T\Delta \theta(i+1) \quad (14)$$

The vibration vector  $Z$  at step  $i+1$  is equal to the vibration vector at step  $i$  plus the product of the transfer matrix and the difference in the control vector from step  $i$  to step  $i+1$ . This allows for variation of the transfer matrix  $T$  with input  $\theta$ .

A deterministic and cautious minimum variance controller can be programmed into two algorithms, one for the local and one for the global HHC model [90,92].

A few selected results together with a summary of the most important conclusions obtained in the course of this study [95,97] are presented below.

An interesting test of the ability of the controllers to adapt to changing flight conditions was performed by introducing a step change in advance ratio from  $\mu = 0.30$  to  $\mu = 0.35$ . This was done by starting with a converged optimal solution and its response at  $\mu = 0.30$ , changing the propulsive trim values to those for  $\mu = 0.35$ , and proceeding with iterative control calculations and quasilinearization solution. Results for a four-bladed soft-in-plane hingeless rotor are shown in Figs. 11 and 12.

The iteration history of 4/rev. hub shears for the deterministic and cautious local control are shown in Fig. 11 and the iteration history for the global control are shown in Fig. 12. Application of HHC eliminated essentially all the 4/rev. hub shears within five iterations. With the local controller, the vertical shears rise slowly after the second iteration indicating that the transfer matrix identification has not been ideal. For lack of space the control inputs are not shown here. However examination of these inputs [95] reveals that when the step change in advance ratio was applied to the local controller there were large oscillations in the calculated control inputs and the resultant hub shears. On the other hand when a step change in  $\mu$  was applied to the global controller, the oscillatory behavior in the required control input was reduced substantially and the controller moved fairly smoothly from an initial large increase in shears toward a minimum. A comparison of the three shear components and their baseline values for the local and global controllers is given in Fig. 13. It is evident that the global controller has been more successful in reducing shears.

Another interesting result is associated with the instantaneous control power as a function of azimuth which was evaluated for both the hingeless rotor and a comparable articulated rotor, at an advance ratio of  $\mu = 0.30$ . Figures 14 and 15 show the variation in instantaneous trim power, HHC power, and total control power respectively for the articulated and hingeless blades.

For the hingeless blade the HHC power contributes relatively much more to the total control power as can be observed from the nature of these curves which tend to follow one another closely in Fig. 15. As is evident from comparing the vertical scales, the maximum power excursions are on the order of five times larger for the hingeless blade than for the articulated blade and in addition are much sharper. The peaks are biased toward positive power values so that the total control power over one revolution is much higher for the hingeless than the articulated blade.

The most important conclusions obtained from these studies were:

- 1 Overall blade response was compared for a baseline no HHC condition and the optimal reduced vibration condition. Principal differences were in the torsional and flap response. Overall response magnitudes changed little but large 4/rev. components were introduced to modify the airloads and cancel out vibrations.

- 2 A global controller was used in comparison of the effects of HHC on roughly equivalent articulated and hingeless rotors. Shears were successfully reduced for both rotors by a HHC algorithm which minimized just hub shears. As shears were reduced there were large increases in hub moments for the hingeless rotor but only moderate increases for the articulated rotor. Much larger HHC angles were required to reduce shears for the hingeless rotor.
- 3 Attempts to reduce both hub shears and moments were not very successful for either blade. With the articulated blade moments were already low and were only decreased slightly while shears increased slightly. For the hingeless blade the large moments decreased greatly but only at the expense of poor shear reduction. These results indicate that vibration reductions with HHC may be more difficult in hingeless rotor configurations than for articulated configurations.
- 4 Application of HHC to the hingeless rotor lead to an increase in required power of 1.44% while for the articulated rotor this increase was only 0.18%. The required power increase for the hingeless rotor was somewhat mitigated by a 0.2% increase in rotor thrust.
- 5 Overall blade aeroelastic stability margins were not significantly degraded by application of HHC for either the articulated or hingeless blade.

It is interesting to note that two, somewhat similar studies, on the application of higher harmonic control to hingeless rotor systems were also recently completed by Nguyen and Chopra [101,102]. These studies were based on an advanced HHC aeroelastic simulation capability. The analysis utilizes finite element in both space and time. A nonlinear time domain unsteady aerodynamic model is used to obtain the air loads, and the rotor induced inflow is calculated using a free wake model. The vehicle trim is also obtained from a fully coupled trim/rotor aeroelastic analysis. Thus this simulation capability has many common features with Refs. 95-97, except that the aerodynamic model is more refined when compared to that used by Robinson and Friedmann [95-97]. The higher harmonic control algorithm is also very similar to that employed in Refs. 95-97. This aeroelastic simulation capability was validated by comparing it with the wind tunnel tests conducted on a one-sixth dynamically scaled three-bladed articulated rotor model tested by Boeing Helicopter Co. [82] up to high advance ratios,  $\mu = 0.40$ , and fairly good correlation with the experimental data was obtained.

The conclusions obtained from this study are in agreement with the majority of the conclusions noted in Refs. 95-97. Thus the performance of the global controller was superior to the local controller. When applying HHC on hingeless rotors larger control angles were required than for articulated rotor and a substantial increase in the HHC power requirements was also noted. Furthermore HHC effects on rotor performance were found to be small. An interesting effect noted was the increase in stall areas over the rotor disk, when the local HHC controller was at the edge of the flight boundary.

Fairly extensive tests on a four bladed hingeless rotor, with a minimum variance controller were also described in detail in a recent paper by Lehmann and Kube [103]. An adaptive local controller was found to perform quite well over the whole envelope tested. Considerable detail on the actual hardware, and digital control implementation of HHC for the test configuration is presented in the paper. Effective vibration reduction for the hingeless rotor was obtained with a gain adjustment (adaptation) algorithm. The power requirement for HHC during the test was not discussed in this study.

A very comprehensive wind tunnel test program on a three bladed articulated model rotor (CH-47D) was also conducted by Shaw et al. [82]. It was found that HHC is highly effective on articulated three bladed rotors. Harmonic hub load response to HHC was found to be linear up to 3 degrees and it was insensitive to flight condition. Furthermore a fixed-parameter control law was found to be fully effective for vibration reduction. Figure 16, taken from Ref. 82, shows that closed loop HHC was extremely effective in suppressing vibratory hub forces. The fixed-gain controller, when configured to regulate 3/rev vertical force and 2/rev and 4/rev inplane shears, suppressed all three of these components simultaneously by 90 percent in almost all of the trimmed and quasi-steady maneuvering test envelope.

From the discussion presented in this section it is evident that comprehensive aeroelastic simulations of HHC have a very useful role in this field. In addition to being much more cost effective than wind tunnel tests and flight tests, they provide one with an ideal basis for planning such tests. Furthermore experience with flight tests [67] indicates that scale model tests do not always correlate well with wind tunnel tests. Thus correlation between aeroelastic simulation programs of HHC which correlate well with wind tunnel tests provide one with a tool suitable for simulating flight tests.

The evidence available from recent studies seems to imply that the practical implementation of HHC on hingeless rotor systems could be more difficult, and less effective, than similar implementation of HHC on articulated rotors. Control angles needed for HHC on hingeless rotors are significantly larger and power requirements could be also between 2-5 times larger. Simultaneous reduction of both hub shears and moments on hingeless rotors is also more difficult, and rotating blade root loads can be also substantially larger. One possible explanation for these observations is the strong physical coupling between the bending and torsional degrees of freedom which exists in most hingeless rotor blades. This can also cause the increase in the power required for implementing HHC on such rotors. Since the higher harmonic movement of the complete blade during its HHC, introduces more complex motion due to the coupling effect and thus requires more power.

Finally, it appears that adaptive controller may not be always required in order to implement an effective HHC vibration reduction.

## 6. CONCLUDING REMARKS

This paper provides a detailed discussion of four important topics in helicopter rotor dynamics and aeroelasticity. Hopefully this discussion will provide an improved fundamental understanding of the current state of the art. Thus future research on these topics can be focused on problems which remain to be solved instead of producing marginal improvements on problems which are already well understood.

For aeroelastic and aeromechanical stability problems incorporation of geometrically nonlinear terms due to moderate deflections has become fairly routine. Both moderate deflection beam theories and large deflection theories are available, and both can serve as a basis for aeroelastic stability and response analysis. It is noted that improvement of the unsteady aerodynamics in rotary wing aeroelastic analyses is much more important than the incorporation of higher order geometrically nonlinear terms. Excessive preoccupation with such higher order terms provides only diminishing benefits.

A number of recent composite beam theories, suitable for modeling composite blades have been developed however these have yet to be implemented in a comprehensive aeroelastic stability or response analysis. The significant potential for aeroelastic tailoring inherent in composite rotor blades remains to be exploited.

The body of research available on coupled rotor/fuselage aeromechanical problems has reached a remarkable level of maturity in a fairly short period of time. Reliable models for this class of problems should contain coupled flap lag-torsional blade models combined with a fuselage which has pitch and roll as well as two translational degrees of freedom. Simpler models can easily lead to inaccurate results. Air resonance in hingeless rotors can be actively controlled throughout the entire flight envelope using a simple control system designed using modern control system synthesis techniques.

The state of the art in applying HHC to articulated rotors appears to be quite promising. The application of HHC to hingeless rotors could have practical implementation problem. Aeroelastic simulations of HHC have a very useful role in providing an improved fundamental understanding on the implementation of HHC on different types of rotor systems. A substantial amount of additional research in this topic is required so as to guarantee its implementation on the next generation of rotorcraft.

#### ACKNOWLEDGMENT

This research was funded in part by NASA Ames Research Center, Moffett Field, CA, under Grants NAG2-209 and NAG2-477. Modest funding by McDonnell Douglas Helicopter Company is also acknowledged. The useful comments and discussions with Dr. S. Jackling from NASA Ames are gratefully acknowledged. I wish to express my appreciation to my students, Dr. L. Robinson and K. Yuan for their help in preparing portions of this paper.

#### REFERENCES

1. Loewy, R.G., "Review of Rotary-Wing V/STOL Dynamic and Aeroelastic Problems," *J. Am. Helicopter Soc.*, Vol. 14, pp. 3-23, 1969.
2. Dat, R., "Aeroelasticity of Rotary Wing Aircraft," *Helicopter Aerodynamics and Dynamics*, Agard Lecture Series, No. 63, Chapter 4, 1973.
3. Hohenemser, K.H., "Hingeless Rotorcraft Flight Dynamics," Agardograph No. 197, 1974.
4. Friedmann, P.P., "Recent Development in Rotary-Wing Aeroelasticity," *J. Aircraft*, Vol. 14, pp. 1027-1041, 1977.
5. Friedmann, P.P., "Formulation and Solution of Rotary-Wing Aeroelastic Stability and Response Problems," *Vertica*, Vol. 7, pp. 101-141, 1983.
6. Ormiston, R.A., "Investigation of Hingeless Rotor Stability," *Vertica*, Vol. 7, pp. 143-181, 1983.
7. Reichert, G., "Helicopter Vibration Control - A Survey," *Vertica*, Vol. 5, pp. 1-20, 1981.
8. Loewy, R.G., "Helicopter Vibrations: A Technological Perspective," *J. Am. Helicopter Soc.*, Vol. 29, pp. 4-30, 1984.
9. Johnson, W., "Recent Developments in Dynamics of Advanced Rotor Systems - Part I," *Vertica*, Vol. 10, pp. 73-107, 1986.
10. Johnson, W., "Recent Developments in Dynamics of Advanced Rotor Systems - Part II," *Vertica*, Vol. 10, pp. 109-150, 1986.
11. Friedmann, P.P., "Recent Trends in Rotary-Wing Aeroelasticity," *Vertica*, Vol. 11, No. 1/2, pp. 139-170, 1987.
12. Miao, W., "Influence of Pitch Axis Location and Orientation on Rotor Aeroelastic Stability," *Vertica*, Vol. 11, No. 1/2, pp. 171-185, 1987.
13. Ormiston, R.A., Warmbrodt, W.G., Hodges, D.H. and Peters, D.A., "Survey of Army/NASA Rotorcraft Aeroelastic Stability Research," NASA TM-101026, Oct. 1988.
14. Karunamoorthy, S.N. and Peters, D.A., "Use of Hierarchical Elastic Blade Equations and Automatic Trim for Rotor Response," *Vertica*, Vol. 11, No. 1/2, pp. 233-248, 1987.
15. Crespo DaSilva, M.R.M. and Hodges, D.H., "The Role of Computerized Symbolic Manipulations in Rotorcraft Dynamic Analysis," *Cmptrs. and Math. with Appls.*, Vol. 12A, pp. 161-172, 1986.
16. Friedmann, P.P., "Application of Modern Structural Optimization to Vibration Reduction in Rotorcraft," *Vertica*, Vol. 9, pp. 363-373, 1985.
17. Celi, R. and Friedmann, P.P., "Structural Optimization with Aeroelastic Constraints of Rotor Blades with Straight and Swept Tips," AIAA Paper 88-2297, *Proc. AIAA/ASME/ASCE/AHS 29th Structures Structural Dynamics and Materials Conf.*, Williamsburg, VA, April 18-20, 1988, Part 2, pp. 668-680.
18. Lim, J.W. and Chopra, I., "Aeroelastic Optimization of a Helicopter Rotor," *J. Am. Helicopter Soc.*, Vol. 34, No. 1, pp. 52-62, 1989.
19. Celi, R. and Friedmann, P.P., "Rotor Blade Aeroelasticity in Forward Flight with an Implicit Aerodynamic Formulation," *AIAA J.*, Vol. 26, No. 12, pp. 1425-1433, 1988.
20. Rosen, A., Loewy, R.G. and Mathew, M.B., "Nonlinear Analysis of Pretwisted Rods Using Principal Curvature Transformation - Part I: Theoretical Derivation," *AIAA J.*, Vol. 25, No. 3, pp. 470-478.
21. Hodges, D.H., "Nonlinear Equations for the Dynamics of Pretwisted Beams Undergoing Small Strains and Large Rotations," NASA TP-2470, 1985.
22. Hodges, D.H., "Nonlinear Beam Kinematics for Small Strains and Finite Rotations," *Vertica*, Vol. 11, No. 3, pp. 573-589, 1987.
23. Danielson, D.A. and Hodges, D.H., "A Beam Theory for Large Global Rotation, Moderate Local Rotation, and Small Strain," *J. Appl. Mech.*, Vol. 55, pp. 179-184.

24. Hodges, D.H. and Dowell, E.H., "Nonlinear Equations of Motion for the Elastic Bending and Torsion of Twisted Non-Uniform Blades," NASA TN D-7818, 1974.
25. Bauchau, O.A. and Hong, C.H., "Large Displacement Analysis of Naturally Curved and Twisted Composite Beams," *AIAA Journal*, Vol. 25, No. 11, pp. 1469-1475, 1987.
26. Hodges, D.H., Hopkins, A.K., Kunz, D.L. and Hinnant, H.E., "Introduction to GRASP - General Rotorcraft Aeromechanical Stability Program - A Modern Approach to Rotorcraft Modeling," *Proc. 42nd Ann. Forum Am. Helicopter Soc.*, Washington, DC, pp. 739-756, 1986.
27. Crespo DaSilva, M.R.M. and Hodges, D.H., "Nonlinear Flexure and Torsion of Rotating Beams, with Application to Helicopter Blades - I. Formulation," *Vertica*, Vol. 10, pp. 151-169, 1986.
28. Crespo DaSilva, M.R.M. and Hodges, D.H., "Nonlinear Flexure and Torsion of Rotating Beams, with Application to Helicopter Blades - II. Results for Hover," *Vertica*, Vol. 10, pp. 171-186, 1986.
29. Hodges, D.H., Ormiston, R.A. and Peters, D.A., "On the Nonlinear Deformation Geometry of Euler Bernoulli Beams," NASA TP-1566, 1980.
30. Hodges, D.H., Kwon, O.J. and Sankar, L.N., "Stability of Hingeless Rotors in Hover Using Three-Dimensional Unsteady Aerodynamics," *Proc. 45th Ann. Forum of the Am. Helicopter Soc.*, Boston, MA, May 22-24, 1989, pp. 989-998.
31. Tessler, A. and Dong, S.B., "On a Hierarchy of Conforming Timoshenko Beam Elements," *Computers and Structures*, Vol. 14, No. 3-4, pp. 335-344, 1981.
32. Hodges, D.H., "Review of Composite Rotor Blade Modeling," AIAA Paper 88-2249, *Proc. AIAA/ASME/ASCE/AHS 29th Structures, Structural Dynamics, and Materials Conf.*, Williamsburg, VA, April 18-20, 1988, pp. 305-312.
33. Mansfield, E.H. and Sobey, A.J., "The Fiber Composite Helicopter Blade - Part I: Stiffness Properties - Part 2: Prospects for Aeroelastic Tailoring," *Aeronautical Quarterly*, Vol. 30, pp. 413-449, 1979.
34. Rehfield, L.W., "Design Analysis Methodology for Composite Rotor Blades," Presented at the 7th DoD/NASA Conf. on Fibrous Composites in Structural Design, Denver CO, June 17-20, 1985, AFVAL-TR-85-3094, pp. (V(a)-1)-(V(a)-15).
35. Nixon, M.W., "Extension-Twist Coupling of Composite Circular Tubes with Application to Tilt Rotor Blade Design," *Proc. 28th Structures, Structural Dynamics and Materials Conf.*, April 6-8, 1987, Monterey, CA, AIAA Paper No. 87-0772, pp. 295-303.
36. Hodges, R.V., Nixon, M.W. and Rehfield, L.W., "Comparison of Composite Rotor Blade Models. A Coupled-Beam Analysis and An MSC/NASTRAN Finite Element Model," NASA TM 89024, 1987.
37. Wörmle, R., "Calculation of the Cross Section Properties and the Shear Stresses of Composite Rotor Blades," *Vertica*, Vol. 6, pp. 111-129, 1982.
38. Kosmatka, J.B., "Structural Dynamic Modeling of Advanced Composite Propellers by the Finite Element Method," Ph.D. Dissertation, Mechanical, Aerospace and Nuclear Engineering Department, Univ. of Calif., Los Angeles, 1986.
39. Giavotto, V., Borri, M., Mantegazza, P. and Ghiringhelli, G., Carmashi, V., Maffioli, G.C. and Massi, F., "Anisotropic Beam Theory and Applications," *Computers and Structures*, Vol. 16, pp. 403-413, 1983.
40. Borri, M. and Merlini, T., "A Large Displacement Formulation for Anisotropic Beam Analysis," *Meccanica*, Vol. 21, pp. 30-37, 1986.
41. Bauchau, O.A., "A Beam Theory for Anisotropic Materials," *J. Appl. Mech.*, Vol. 52, pp. 416-422, 1985.
42. Bauchau, O.A., Coffenberry, B.S. and Rehfield, L.W., "Composite Box Beam Analysis: Theory and Experiments," *J. Reinforced Plastics and Composites*, Vol. 6, pp. 25-35, 1987.
43. Lee, S.W. and Kim, Y.H., "A New Approach to the Finite Element Modeling of Beams," *Int'l. J. for Num. Methods in Engr.*, Vol. 24, pp. 2327-2341, 1987.
44. Stemple, A.D. and Lee, S.W., "Finite Element Model for Composite Beams with Arbitrary Cross-Sectional Warping," *AIAA Journal*, Vol. 26, No. 12, pp. 1512-1520, Dec. 1988.
45. Stemple, A.D. and Lee, S.W., "Large Deflection Static and Dynamic Finite Element Analysis of Composite Beams with Arbitrary Cross-Sectional Warping," AIAA Paper 89-1363-CP, *Proc. of the AIAA/ASME/ASCE/AHS/ACS 30th Structures, Structural Dynamics and Materials Conf.*, Mobile, AL, April 1989, pp. 1788-1798.
46. Hong, C.H. and Chopra, I., "Aeroelastic Stability Analysis of a Composite Rotor Blade," *J. Am. Helicopter Soc.*, Vol. 30, No. 2, pp. 57-67, 1985.
47. Hong, C.H. and Chopra, I., "Aeroelastic Stability of a Composite Bearingless Rotor Blade," *J. Am. Helicopter Soc.*, Vol. 31, No. 4, pp. 29-35, 1986.
48. Panda, B. and Chopra, I., "Dynamics of Composite Rotor Blades in Forward Flight," *Vertica*, Vol. 11, No. 1/2, pp. 187-209, 1987.
49. Kosmatka, J.B. and Friedmann, P.P., "Structural Dynamic Modeling of Advanced Composite Propellers by the Finite Element Method," *Proc. AIAA/ASME/ASCE/AHS 28th Structures, Structural Dynamics and Materials Conf.*, Monterey, CA, Vol. II, 1987, pp. 111-124.
50. Kosmatka, J.B. and Friedmann, P.P., "Vibration Analysis of Composite Turbopropellers Using a Nonlinear Beam-Type Finite Element Approach," *AIAA Journal*, Vol. 27, No. 11, November 1989, pp. 1606-1614.
51. Bauchau, O.A. and Hong, C.H., "Finite Element Approach to Rotor Blade Modeling," *J. Am. Helicopter Soc.*, Vol. 32, No. 1, pp. 60-67, Jan. 1987.
52. Bauchau, O.A. and Hong, C.H., "Large Displacement Analysis of Naturally Curved and Twisted Composite Beams," *AIAA Journal*, Vol. 25, No. 11, pp. 1469-1475, Nov. 1987.
53. Bauchau, O.A. and Hong, C.H., "Nonlinear Composite Beam Theory," *J. Appl. Mech.*, Vol. 55, pp. 156-163, March 1988.
54. Hong, C.H., "Finite Element Approach to the Dynamic Analysis of Composite Helicopter Blades," Ph.D. Dissertation, Rensselaer Polytechnic Institute, Troy, NY, 1987.
55. Minguet, P. and Dugundji, J., "Experiments and Analysis for Structurally Coupled Composite Blades Under Large Deflections: Part I - Static Behavior," AIAA Paper No. 89-1366-CP, *Proc. 30th AIAA/ASME/ASCE/AHS/ACS Structures, Structural Dynamics and Materials Conf.*, Mobile, AL, April 1989, pp. 1807-1816.



- 56 Minguet, P. and Dugundji, J., "Experiments and Analysis for Structurally Coupled Composite Blades Under Large Deflections: Part 2 - Dynamic Behavior," AIAA Paper No. 89-1366-CP, *Proc. 30th AIAA/ASME/ASCE/AHS/ACS Structures, Structural Dynamics and Materials Conf.*, Mobile, AL, April 1989, pp. 1817-1827.
- 57 Atilgan, A.R. and Hodges, D.H., "A Geometrically Nonlinear Analysis for Nonhomogeneous, Anisotropic Beams," AIAA Paper No. 89-1264-CP, *Proc. 30th AIAA/ASME/ASCE/AHS/ACS Structures, Structural Dynamics and Materials Conf.*, Mobile, AL, April 1989, pp. 895-908.
- 58 Danielson, D.A. and Hodges, D.H., "Nonlinear Beam Kinematics by Decomposition of the Rotation Tensor," *J. Appl. Mech.*, Vol. 54, No. 2, pp. 258-262, 1987.
- 59 Atluri, S.N., "Alternate Stress and Conjugate Strain Measures, and Mixed Variational Formulations Involving Rigid Rotations for Computational Analyses of Finitely Deformed Solids, with Applications to Plates and Shells: Part I - Theory," *Computers and Structures*, Vol. 18, No. 1, pp. 93-116, 1984.
- 60 Done, G.T.S., Jiggins, P.T.W. and Patel, M.H., "Further Experience with a New Approach to Helicopter Aeroelasticity," *Vertica*, Vol. 12, No. 4, 1988, p00. 357-369.
- 61 Takahashi, M.D. and Friedmann, P.P., "Active Control of Helicopter Air Resonance in Hover and Forward Flight," AIAA Paper No. 88-2407, *Proc. AIAA/ASME/ASCE/AHS 29th Structures, Structural Dynamics and Materials Conf.*, Williamsburg, VA, April 18-20, 1988, pp. 1521-1532.
- 62 Takahashi, M.D., "Active Control of Helicopter Aeromechanical and Aeroelastic Instabilities," Ph.D. Dissertation, Mechanical, Aerospace and Nuclear Engineering Department, University of California, Los Angeles, June 1988.
- 63 Pitt, D.M. and Peters, D.A., "Theoretical Predictions of Dynamic Inflow Derivatives," *Vertica*, Vol. 5, 1981, pp. 21-34.
- 64 Loewy, R.G. and Zotto, M., "Helicopter Ground/Air Resonance Including Rotor Shaft Flexibility and Control Coupling," *Proceedings of 45th Ann. Forum Helicopter Soc.*, Boston, MA, May 22-24, 1989, pp. 19-32.
- 65 Shaw, J. and Albion, N., "Active Control of the Helicopter Rotor for Vibration Reduction," *Proceedings of 36th Ann. Forum Helicopter Soc.*, Washington, DC, May 1980.
- 66 Wood, E.R. and Powers, R.W., "Practical Design Considerations for the Flightworthy Higher Harmonic Control System," *Proceedings of 36th Ann. Forum Helicopter Soc.*, Washington, DC, May 1980.
- 67 Wood, R.E., Powers, R.W., Cline, J.H. and Hammond, C.E., "On Developing and Flight Testing a Higher Harmonic Control System," *J. Am. Helicopter Soc.*, Vol. 30, No. 1, pp. 3-20, Jan. 1985.
- 68 Straub, F.K. and Warmbrodt, W., "The Use of Active Controls to Augment Rotor/Fuselage Stability," *J. Am. Helicopter Soc.*, Vol. 30, No. 3, pp. 13-22, July 1985.
- 69 Straub, F.K., "Optimal Control of Helicopter Aeromechanical Stability," *Vertica*, Vol. 11, No. 3, 1987, pp. 12-22.
- 70 Young, M.I., Bailey, D.J. and Hirschbein, M.S., "Open and Closed Loop Stability of Hingeless Rotor Helicopter and Air Ground Resonance," Paper No. 20, NASA-SP 352, 1974.
- 71 Takahashi, M.D. and Friedmann, P.P., "Design of a Simple Active Controller to Suppress Helicopter Air Resonance," *Proceedings 44th Ann. Forum Am. Helicopter Soc.*, Washington, DC, June 1988, pp. 305-316.
- 72 Kwakernaak, H. and Sivan, R., *Linear Optimal Control Systems*, John Wiley & Sons, Inc., New York, 1972, Chaps. 3,5.
- 73 Doyle, J.C. and Stein, G., "Multivariable Feedback Design: Concepts for a Classical/Modern Synthesis," *IEEE Trans. Automatic Control*, Vol. AC-26, No. 1, Feb. 1981, pp. 4-16.
- 74 Safonov, M.G., Laub, A.J. and Hartmann, G.L., "Feedback Properties of Multivariable Systems. The Role and Use of the Return Difference Matrix," *IEEE Trans. Automatic Control*, Vol. AC-26, No. 1, Feb. 1981, pp. 47-65.
- 75 Stein, G., "The LQG/LTR Procedure for Multivariable Feedback Control Design," *IEEE Trans. Automatic Control*, Vol. AC-32, No. 2, Feb. 1987, pp. 105-114.
- 76 Wang, J.M., Jang, J. and Chopra, I., "Air Resonance Stability of Hingeless Rotors in Forward Flight," Paper No. 18, *Proc. 14th European Rotorcraft Forum*, Milano, Italy, Sept. 20-23, 1988, pp. 18.1-18.18. DC, June 1986.
- 77 Ham, N.D., "Helicopter Individual-Blade-Control Research at MIT 1977-1985," *Vertica*, Vol. 11, pp. 109-122, 1986.
- 78 Miao, W. and Frye, H.M., "Flight Demonstration of Higher Harmonic Control (HHC) on S-76," 42nd Annual Forum of the AHS, Washington, D.C., June 1986.
- 79 Polychroniadis, M. and Achache, M., "Higher Harmonic Control: Flight Tests of an Experimental System on SA 349 Research Gazelle," 42nd Annual Forum on the AHS, Washington, D.C., June 1986.
- 80 Molusis, J.A., Hammond, C.E. and Cline, J.H., "A Unified Approach to the Optimal Design of Adaptive and Gain Scheduled Controllers to Achieve Minimum Helicopter Vibration," *AHS Journal*, Vol. 28, No. 2, April 1983, pp. 9-18.
- 81 Ham, N., "Helicopter Individual-Blade-Control and its Applications," 39th Annual Forum of the AHS, St. Louis, MO, May 1983.
- 82 Shaw, J., Albion, N., Hanker, E.J. and Teal, R.S., "Higher Harmonic Control. Wind Tunnel Demonstration of Fully Effective Vibratory Hub Force Suppression," *J. of the AHS*, Vol. 34, No. 1, Jan 1989, pp. 14-25.
- 83 Lehmann, G., "The Effect of Higher Harmonic Control (HHC) on a Four-Bladed Hingeless Model Rotor," *Vertica*, Vol. 9, No. 3, 1985, pp. 273-284.
- 84 Davis, M.W., "Development and Evaluation of a Generic Active Helicopter Vibration Controller," *Proc. 40th Ann. Natl. Forum of the AHS*, Arlington, VA, May 1984.
- 85 Taylor, R.B., Farrar, F.A. and Miao, W., "An Active Control System for Helicopter Vibration Reduction by Higher Harmonic Pitch," AIAA paper No. 80-0672, 36th Annual Forum, AHS, Washington, DC, May 1980.
- 86 Molusis, J.A., "The Importance of Nonlinearity on the Higher Harmonic Control of Helicopter Vibration," 39th Annual Forum of the AHS, St. Louis, MO, May 1983.
- 87 Chopra, I. and J.L. McCloud, "A Numerical Simulation Study of Open-Loop, Closed-Loop and Adaptive Multicyclic Control Systems," *AHS Journal*, Vol. 28, No. 1, January 1983.
- 88 Jacob, H.G. and Lehmann, G., "Optimization of Blade Pitch Angle for Higher Harmonic Rotor Control," *Vertica*, Vol. 7, No. 3, 1983, pp. 271-286.
- 89 McKillip, R.M., "Kinematic Observers for Active Control of Helicopter Rotor Vibration," *Proc. 12th European Rotorcraft Forum*, Paper No. 65, Garmisch-Partenkirchen, Fed. Rep. Germany, Sept. 1986.

- 90) Davis, M W, "Refinement and Evaluation of Helicopter Real-Time Self-Adaptive Active Vibration Controller Algorithms, NASA CR-3821, 1983.
- 91) Taylor, R B., Zwicke, P.E., Gold, P. and Miao, W., "Analytical Design and Evaluation of an Active Control System for Helicopter Vibration Reduction and Gust Response Alleviation," NASA CR-152377, 1980.
- 92) Johnson, W., "Self-Tuning Regulators for Multicyclic Control of Helicopter Vibrations," NASA Technical Paper 1996, 1982.
- 93) Bielawa, R L., Cheney, M.C., Jr and Novak, R.C. "Investigation of a Bearingless Rotor Concept Having a Composite Primary Structures," NAFSA CR-2638, 1976.
- 94) Bielawa, R L., "Aeroelastic Analysis for Helicopter Rotor Blades with Time Variable," Nonlinear Structural Twist and Multiple Redundance-Mathematical Derivation and Program User's Manual," NAFSA CR-2638, 1976.
- 95) Robinson, L.H and Friedmann, P.P., "Analytic Simulation of Higher Harmonic Control Using a New Aeroelastic Model," AIAA Paper 89-1321-CP, *Proc. AIAA/ASME/ASCE/AHS 30th Structures, Structural Dynamics and Materials Conference*, Mobile, AL, April 1989, Part III, pp. 1394-1406.
- 96) Robinson, L., "Aeroelastic Simulation of Higher Harmonic Control," Ph.D. Dissertation, Mechanical, Aerospace and Nuclear Engineering Department, University of California, Los Angeles, June 1988.
- 97) Robinson, L. and Friedmann, P.P., "A Study of Fundamental Issues in Higher Harmonic Control Using Aeroelastic Simulation," Proceedings of National Specialist's Meeting on Rotorcraft Dynamics, Fort Worth, TX, Nov. 13-14, 1989.
- 98) Shamie, J. and Friedmann, P., "Effect of Moderate Deflections of the Aeroelastic Stability of a Rotor Blade in Forward Flight," *Proc. Third European Rotorcraft and Powered Lift Aircraft Forum*, Paper No. 24, Aix-en-Provence, France, Sept. 1977.
- 99) Friedmann, P.P. and Robinson, L., "Time Domain Aerodynamic Effects on Coupled Flap-Lag-Torsional Aeroelastic Stability and Response of Rotor Blades," *Proc. 2nd Int'l. Conf. on Basic Rotorcraft Research*, College Park, MD, Feb. 1988.
- 100) Dinyavari, M.A.H. and Friedmann, P.P., "Application of Time-Doman Unsteady Aerodynamics to Rotary-Wing Aeroelasticity," *AIAA Journal*, Vol. 24, No. 9, Sept. 1986, pp. 1424-1432.
- 101) Nguyen, K. and Chopra, I., "Application of Higher Harmonic Control (HHC) to Hingeless Rotor Systems," AIAA Paper 89-1215-CP, *Proc. AIAA/ASME/ASCE/AHS/ACS 30th Structures, Structural Dynamics and Materials Conf.*, Mobile, AL, April 1989, pp. 507-520.
- 102) Nguyen, K. and Chopra, I., "Application of Higher Harmonic Control (HHC) to Rotors Operating at High Speed and Maneuvering Flight," *Proc. Am. Helicopter Soc. 45th Ann. Forum*, Boston, MA, May 1989, pp. 81-96.
- 103) Lehmann, G. and Kube, R., "Automatic Vibration Reduction at a Four Bladed Hingeless Model Rotor - A Wind Tunnel Demonstration," Paper No. 60, *Proc. 14th European Rotorcraft Forum*, Sept. 20-23, 1988, Milan, Italy, pp. 60 1-60.18.

Table I

Frequency Increase due to $\Omega$			Frequency Decrease due to Timoshenko Beam Effects		
Inplane Modes			Inplane Modes		
Mode 1	Mode 2	Mode 3	Mode 1	Mode 2	Mode 3
3.5%	2.6%	1.0%	-1.6%	-9.7%	-19.2%
Out of Plane Modes			Out of Plane Modes		
71.2%	12.8%	4.6%	-0.4%	-2.5%	-5.5%

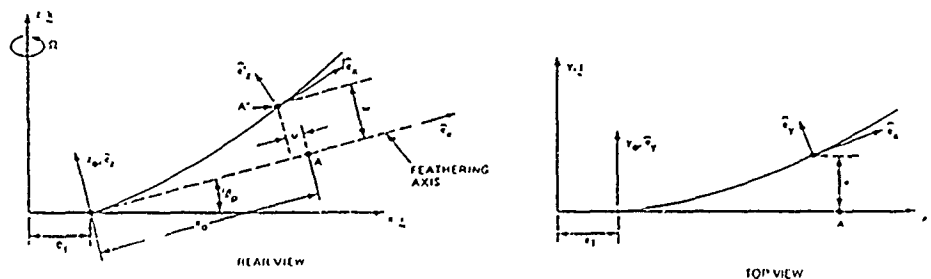


Figure 1a: Geometry of the Blade Elastic Axis Before and After Deformation.

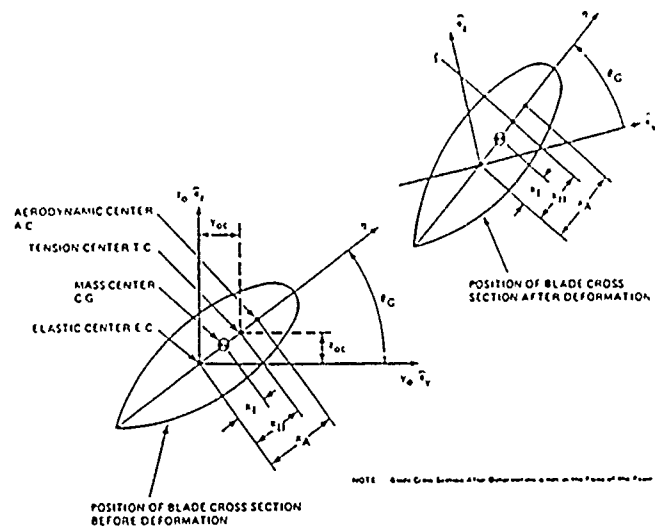


Figure 1b: Blade Cross Sectional Geometry.

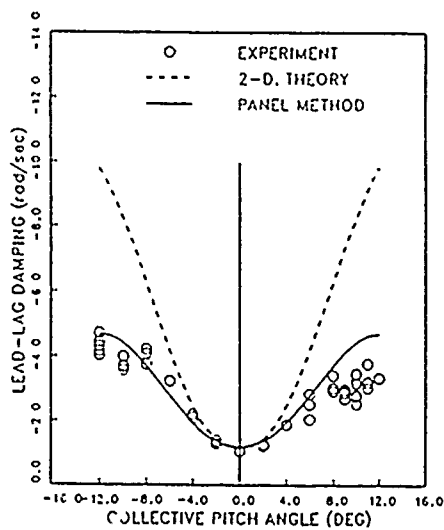


Figure 2: Lead-lag Damping Versus Blade Pitch Angle, Soft Pitch Flexure, Zero Droop, Zero Precone (Ref. 30).

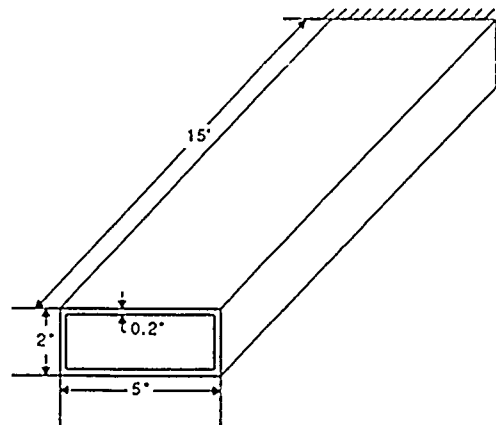


Figure 3: Box Beam for Study of Timoshenko Beam Effects.

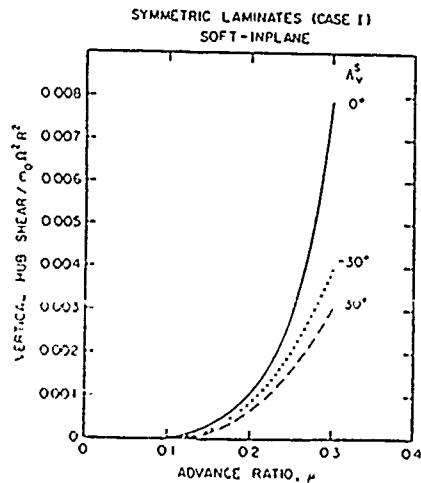


Figure 4: Peak-to-Peak Vertical Hub Shear, Hingeless Composite Blade (Ref. 48).

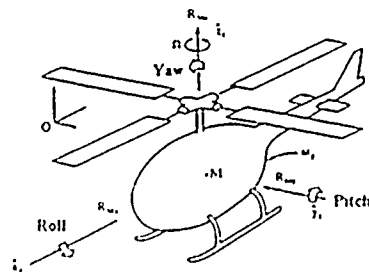


Figure 5: Coupled Rotor/Fuselage Model

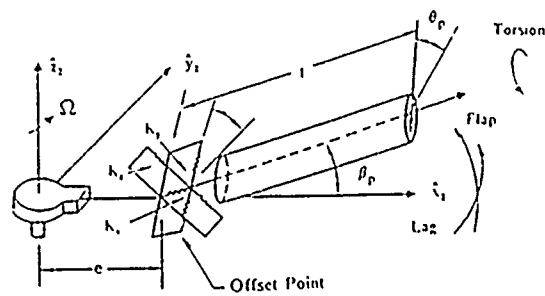


Figure 6: Offset Hinged Spring Restrained Model for Hingeless Blade

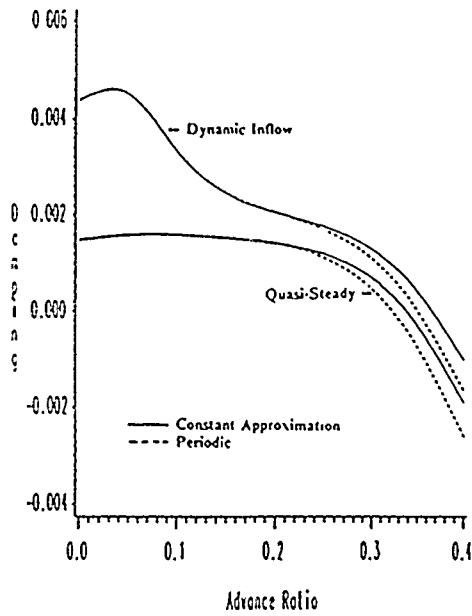


Figure 7: Open Loop Lead-lag Regressing Damping of the Nominal Configuration With and Without Dynamic Inflow.

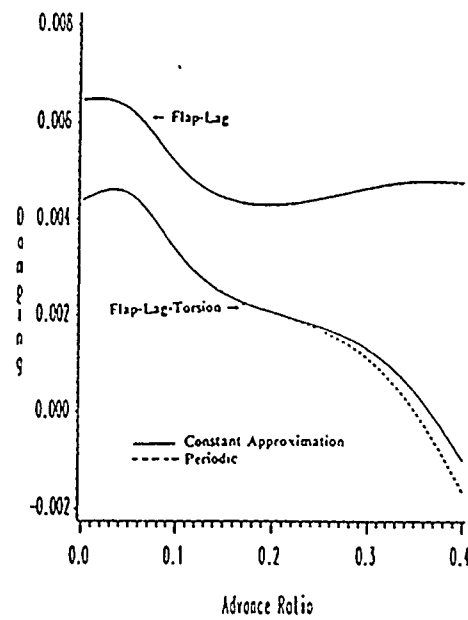


Figure 8: Open Loop Lead-lag Regressing Damping of the Nominal Configuration With and Without Blade Torsional Flexibility.

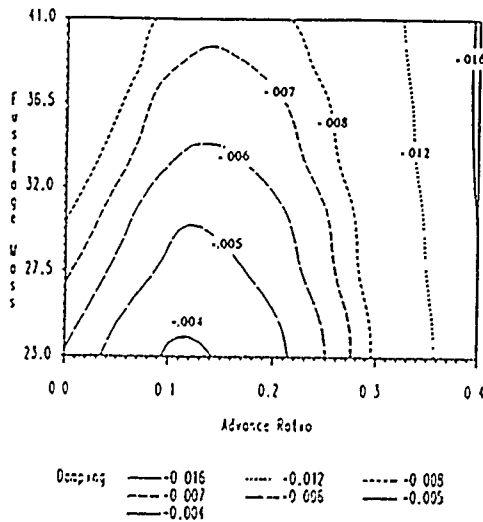


Figure 9: Open Loop Lead-Lag Regressing Mode Damping at Various Fuselage Weights and Advance Ratios.

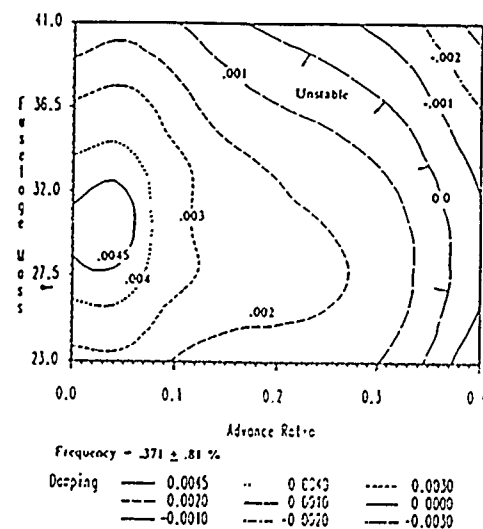


Figure 10: Closed Loop Lead-Lag Regressing Mode Damping Using the Active Controller.

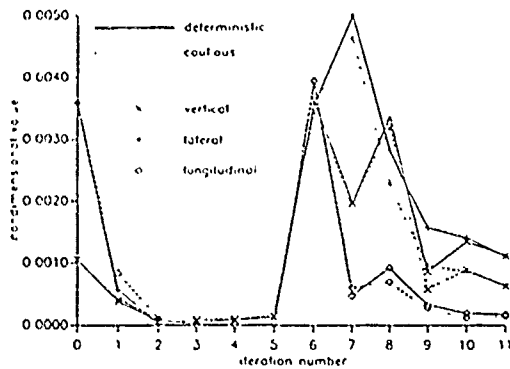


Figure 11: Iteration History of Hub Shears for Deterministic versus Cautious Local Control Optimization at  $\mu = 0.30$ , then Step change from  $\mu = 0.30$  to  $\mu = 0.35$ .

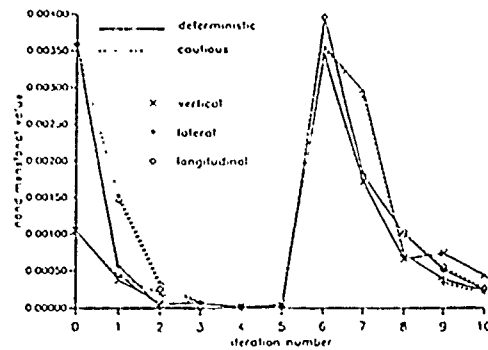


Figure 12: Iteration History of Hub Shears for Deterministic versus Cautious Global Control Optimization at  $\mu = 0.30$ , then Step change from  $\mu = 0.30$  to  $\mu = 0.35$ .

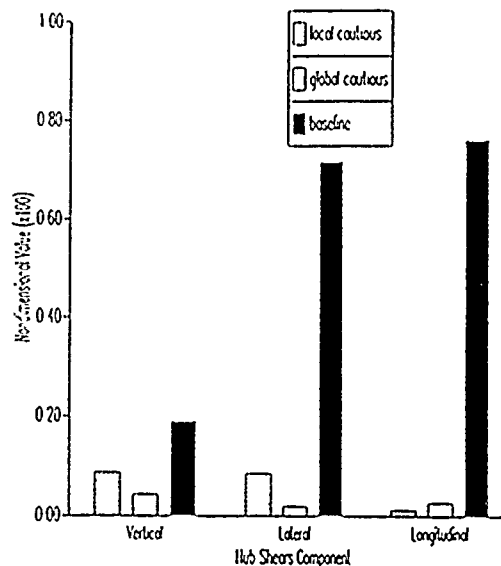


Figure 13: Baseline Shears for  $\mu = 0.35$  and  $\mu = 0.30$  to  $\mu = 0.35$ , Local and Global Shears Five Iterations After Step Change from Controllers.

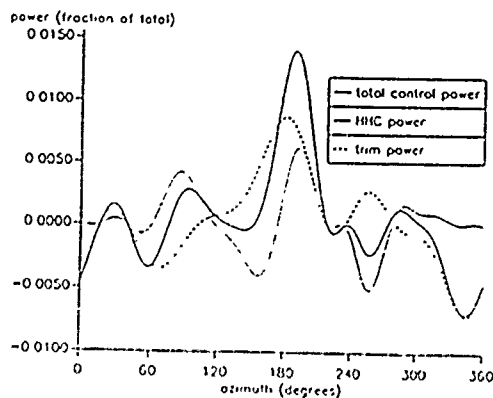


Figure 14: Variation of Trim Power, HHC Power and Total Control Power with Azimuth Articulated Blade, Advance Ratio  $\mu = 0.30$ ; 5% Blade Root Offset, Cautious Global Control.

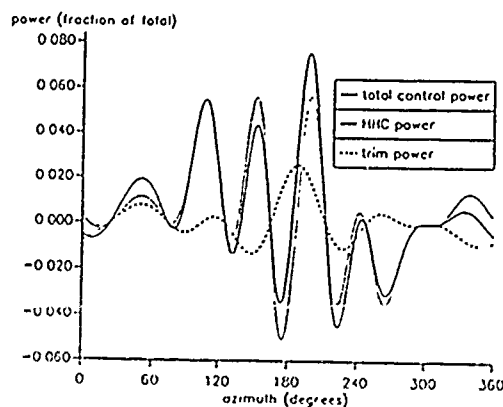


Figure 15: Variation of Trim Power, HHC Power and Total Control Power with Azimuth, Hingeless Blade, Advance Ratio  $\mu = 0.30$ ; 5% Blade Root Offset, Cautious Global Control.

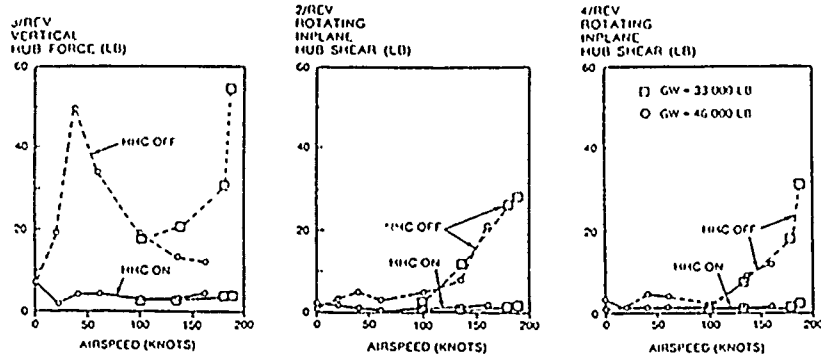


Figure 16: Measured HHC Effectiveness in Trimmed Level Flight, (Ref. 82).

## PHYSICAL ASPECTS OF ROTOR-BODY COUPLING

H. C. Curtiss, Jr.  
Princeton University

The influence of various modelling assumptions on the dynamic stability and response characteristics of helicopters will be discussed using a linearized theory with body and rotor degrees of freedom. Emphasis will be placed on physical interpretation of the primary sources of rotor-body coupling and their influence on the response and stability characteristics. Prediction of the time and frequency domain response characteristic of helicopters to control inputs will be discussed and the effect of various approximations on the correlation of theory with experiment described.

# Analysis of Sectional Properties of Curved, Twisted, Nonhomogeneous, Anisotropic Beams

Marco Borri  
Dipartimento di Ingegneria Aerospaziale  
Politecnico di Milano  
Milano, Italy

Dewey H. Hodges, Ali R. Atilgan, and Victor L. Berdichevsky  
School of Aerospace Engineering  
Georgia Institute of Technology  
Atlanta, Georgia

The nonlinear theories of Borri and Mantegazza (1985) and Hodges (1989) express the strain field in terms of so-called intrinsic strain measures which have the unique property that the derivatives of the strain energy with respect to these measures are the actual section forces and moments in the deformed beam basis. Therefore, the constitutive relations can be expressed in terms of material and geometric stiffness constants for a cross section. An analysis of the sectional properties of nonhomogeneous, anisotropic beams is presented which takes initial curvature and twist into account. All possible types of couplings between extensional, shear, bending, and torsional deformation are included. The analysis is an extension of the earlier work by Giavotto *et al.* (1983) and leads to a two-dimensional finite element formulation over the section under consideration. The method will be compared with other methods in the literature including the work of Soviet mechanicians.



# Nonlinear Analysis of Curved, Twisted, Nonhomogeneous, Anisotropic Beams

Dewey H. Hodges and Ali R. Atilgan  
School of Aerospace Engineering  
Georgia Institute of Technology  
Atlanta, Georgia

Tremendous progress has been made in the last few years toward simplifying the analysis of beams which are undergoing large deformation. In previous years, analysts became accustomed to writing beam equations explicitly in displacement form and to tedious ordering schemes which could not be applied rigorously. For some applications the size and complexity of the equations become overwhelming, leading to the use of symbolic manipulation just to derive the equations. In what will be presented, the exact equations for a beam undergoing arbitrarily large deformation will be written in only a few lines. Moreover, these equations lead to a finite element method which is not only elegant, but very simple to program. The analysis methodology leads to a natural breakdown of the analysis into three parts: (1) exact intrinsic equations of equilibrium in weakest possible form; (2) exact kinematical equations in weakest possible form; (3) approximate constitutive law in terms of sectional elastic constants. An overview of the process is shown below in Figure 1.

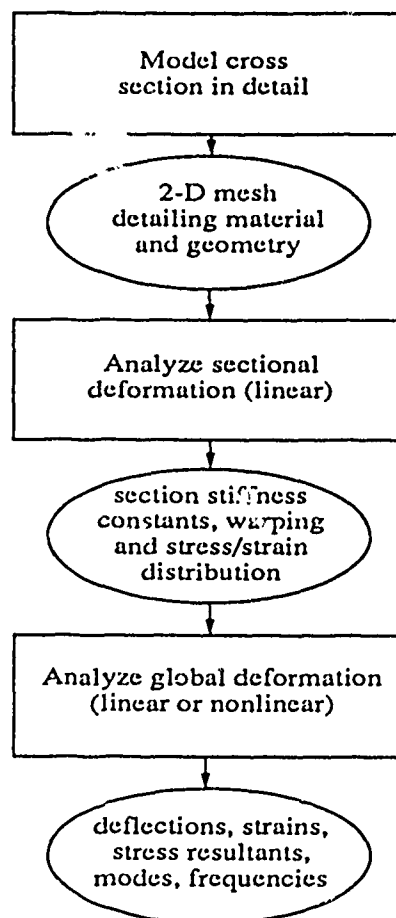


Figure 1: Overview of Anisotropic Beam Analysis

# Investigation of the Use of Extension-Twist Coupling in Composite Rotor Blades for Application to Tiltrotor Aircraft

Renee C. Lake  
U.S. Army Aerostructures Directorate  
NASA Langley Research Center  
Hampton VA 23665

## Abstract

Tiltrotor aircraft are designed to operate in both helicopter and airplane modes of flight. This operational flexibility results in several conflicting design requirements. One such design requirement, which has significant effects on aerodynamic performance, is blade twist. Typically, the twist employed is a compromise between that required in the two different modes of flight. Performance could be improved if it were possible to vary the blade twist between the two flight modes. Tiltrotor aircraft typically vary rotor speed by about 20 percent between the two flight modes. This change in rotor speed induces a rather substantial change in the centrifugal force along the blade, which could be used to passively change the twist of an extension-twist-coupled composite blade. An in-house investigation was initiated several years ago within the Army Aerostructures Directorate at NASA Langley Research Center with the overall objective of demonstrating the increased aerodynamic performance which can be realized in tiltrotor blades that have been elastically-tailored to exhibit extension-twist structural coupling. Analytical and experimental studies have been designed to demonstrate the improvements in tiltrotor blade performance, and ultimately include whirl tests and wind-tunnel tests conducted on a model-scale blade in addition to advanced finite-element analyses. However, the investigation of research areas which are fundamental to the development of elastically-tailored composite tiltrotor blades must first be addressed. For example, the feasibility of producing the desired twist deformation within the operational and material design limits for a tiltrotor blade is a principal driver in the effective development and

evolution of extension-twist-coupled tiltrotor blades. In addition, the structural dynamic characteristics of extension-twist-coupled rotor blades must be assessed, as the elastic couplings can have a significant influence on the dynamic characteristics, such as frequency and mode shape. Also, the bending and twisting deformations of the primary load carrying members of a rotor blade are usually accompanied by additional deformations associated with cross-sectional warping. Therefore, the significance of such warping effects for extension-twist-coupled rotor blades must also be determined. While each of these research areas serves to drive the overall design of a rotor blade and is being addressed, this paper focuses on the investigation of structural dynamic behavior of extension-twist-coupled composite rotor blades.

A study was initiated in which dynamic results from shell-finite-element models were correlated with experimental results obtained from a vibration test of extension-twist coupled composite tubular specimens. The specimens all had non-circular cross sections and were therefore subject to warping deformations. A potentially significant effect on the dynamic behavior of the specimens could occur because the presence of extension-twist coupling in a laminate acts to "magnify" the warping effect. Such "warping-prone" designs are more closely representative of true rotor blade structures and therefore require a thorough investigation of the dynamic characteristics. Three thin-walled cross-sectional geometries were studied: square, D-shape, and flattened ellipse (see figure 1). The test specimens were fabricated utilizing an expandable rubber core and a segmented aluminum female tool configured to the desired final specimen geometry. The overall size and dimensions of each specimen type are also indicated in figure 1. A free-free boundary condition was simulated in the test by suspending the specimens from a test support structure with rubber tubing. A vibration survey was conducted on each specimen to determine structural modes and frequencies. A calibrated impact hammer provided the input excitation for each specimen such that a "roving hammer" concept was employed. Three single-axis accelerometer transducers were block-mounted at an offset on one end of the specimens in a tri-axial configuration.

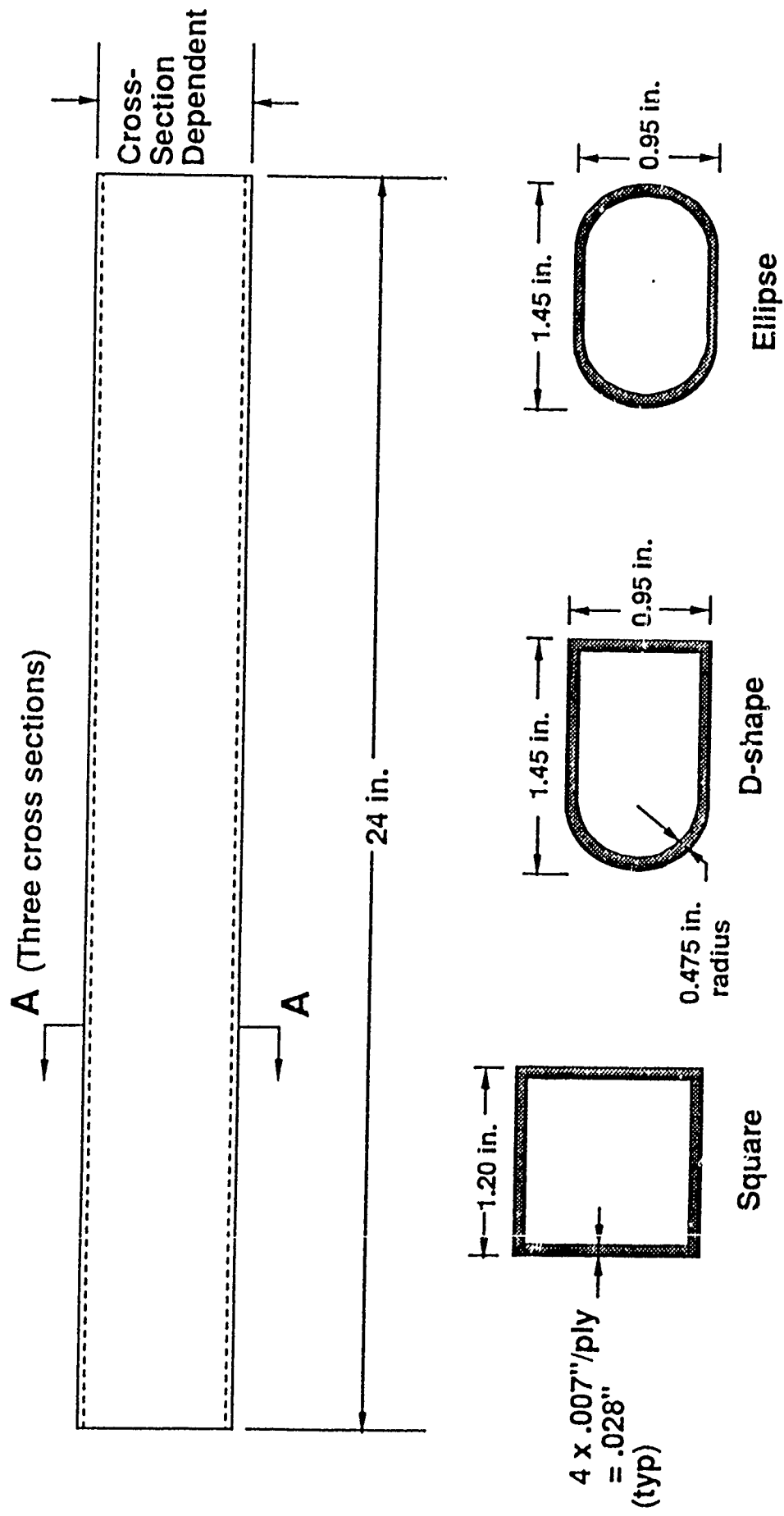
Data acquisition was performed using an HP-3565S computer system using HP-VISTA software. Subsequent curvefitting and parameter extraction was facilitated with the use of SDRC-Tdas software. These results were compared with those obtained from the MSC-NASTRAN shell-finite-element analyses for each specimen type. In addition to the global mode shapes of the shell structures, numerous shell breathing modes were obtained. However, these breathing modes are not of current interest in this study and will not be addressed in the discussion of results.

The preliminary comparison of experimental and analytical data has been conducted and is shown in figures 2 through 4. The data correlation for the elliptical specimens (figure 2) showed the best overall agreement with experiment, yielding results within 5% for the first five global modes (first vertical bending, first lateral bending, second vertical bending, second lateral bending, first torsion), and within 13% for the sixth mode (third vertical bending). The comparison of results for the D-shape specimen (figure 3) produced agreement generally within 6.5% for the five identified modes, with the third global mode (second vertical bending) producing a "worst case" agreement, dropping off to 14%. Frequency and mode shape results for the square cross-section specimen (see figure 4) showed agreement within 10% for the first four global modes. In general, curvefitting of data was performed in the 0-2000 Hz range, as frequencies above this range generally showed diminished phase and coherence characteristics.

In parallel with the aforementioned studies on the tubular specimens, studies have also been initiated on an extension-twist-coupled model rotor blade. The model blade, which was manufactured from existing blade molds for an isotropic rotor blade, was designed with a view towards establishing a preliminary "proof of concept" for extension-twist-coupled rotor blades. Whirl tests of the model blade will provide the basic objective of measuring blade twist as a function of rotor speed. This paper will, however, focus on the investigation of the structural dynamic characteristics of the model blade. The resultant shell-finite-element model of the model rotor blade is shown in figure 5. Results from a normal modes analysis of the rotor blade shell-finite-element model have been

compared with those obtained from a ground vibration test conducted on a fabricated model blade, for both free-free and cantilevered boundary conditions, and are shown in figure 6. In general, the mode shape and frequency correlation shows agreement within 10% for the first five free-free modes. Similar trends are observed for the cantilevered blade, with all identified frequencies generally within this 10% agreement range, with the exception of the first torsion and fourth flap bending modes, which were found to agree within approximately 13%. This comparison of experimental and analytical results serves to establish a foundation for accurately modeling and predicting the structural dynamic behavior of extension-twist-coupled rotor blades.

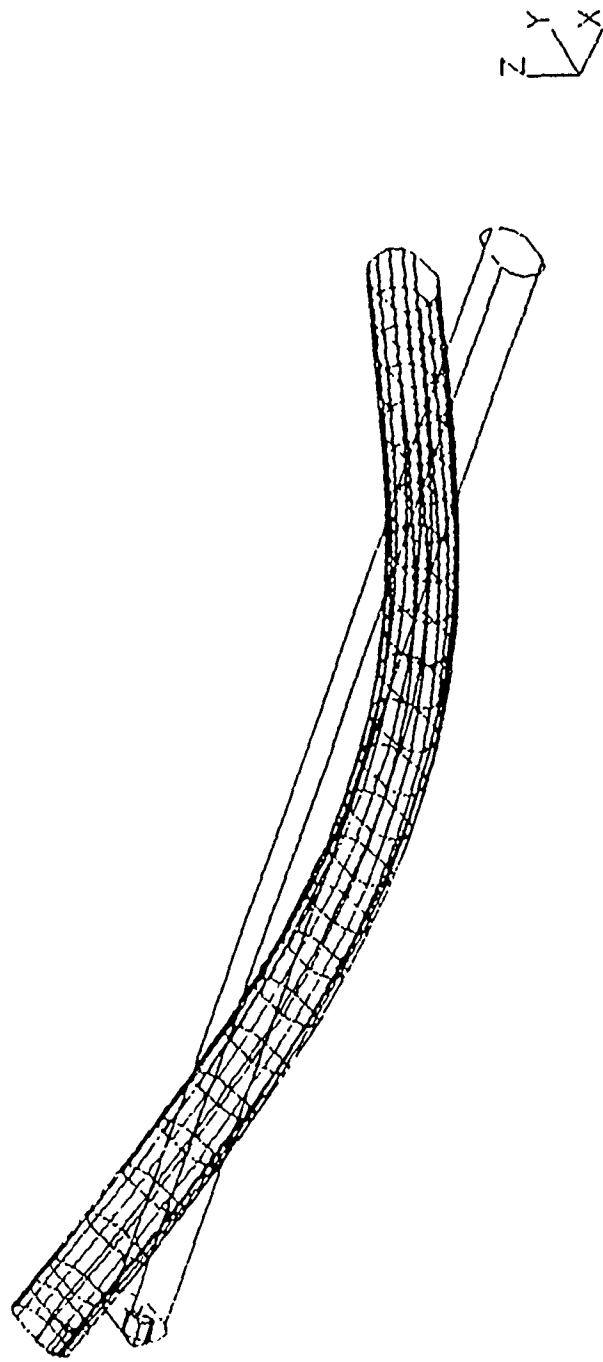
# Warping-Prone Composite Specimens



Sections A-A

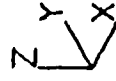
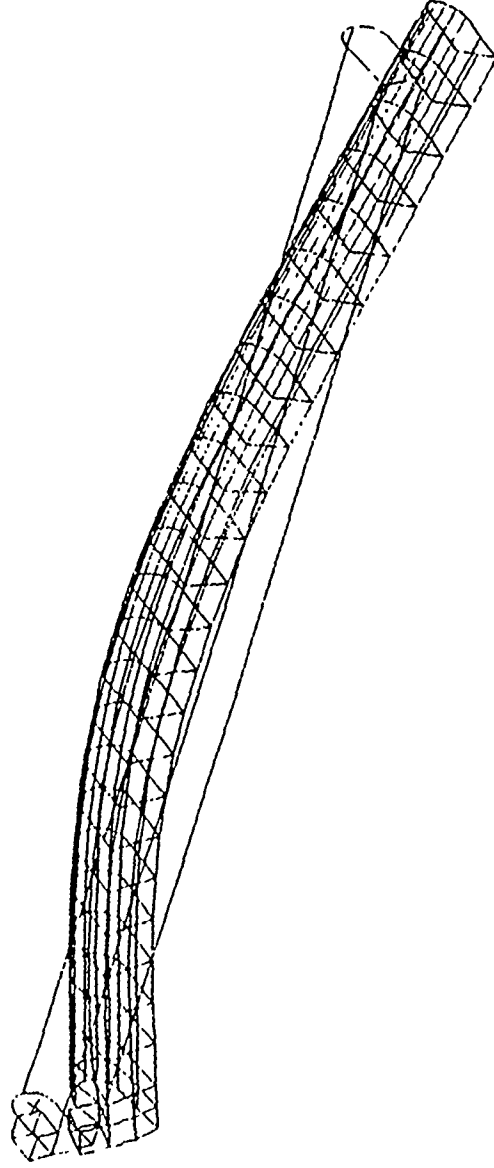
NOTE: Drawing not to scale

# Extension-twist-coupled elliptical specimen



Mode shape	Experimental (Hz)	Analytical (Hz)
First vertical bending	382.6	383.3
First lateral bending	480.6	504.6
Second vertical bending	1033.6	1063.5
Second lateral bending	1279.1	1344.9
First torsion	1613.0	1615.4
Third vertical bending	1864.3	2143.2

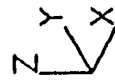
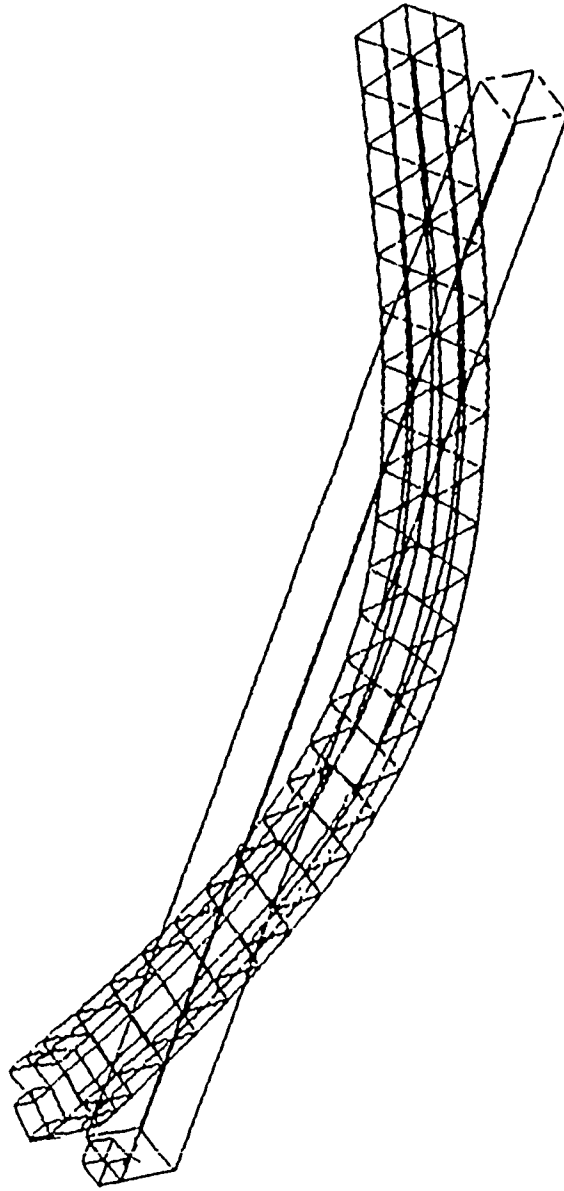
# Extension-twist-coupled D-shape specimen



Mode shape	Experimental (Hz)	Analytical (Hz)
First vertical bending	394.4	402.0
First lateral bending	575.1	596.2
Second vertical bending	904.5	1048.7
First shear	1177.2	1254.9
Second lateral bending	1576.5	1647.7



# Extension-twist-coupled square specimen



Mode shape	Experimental (Hz)	Analytical (Hz)
First vertical bending	464.1	499.8
First lateral bending	486.3	516.0
Second vertical bending/torsion	1261.3	1345.3
Second lateral bending/torsion	1412.2	1559.6

Figure 4

# Extension-Twist-Coupled Model Blade FEM

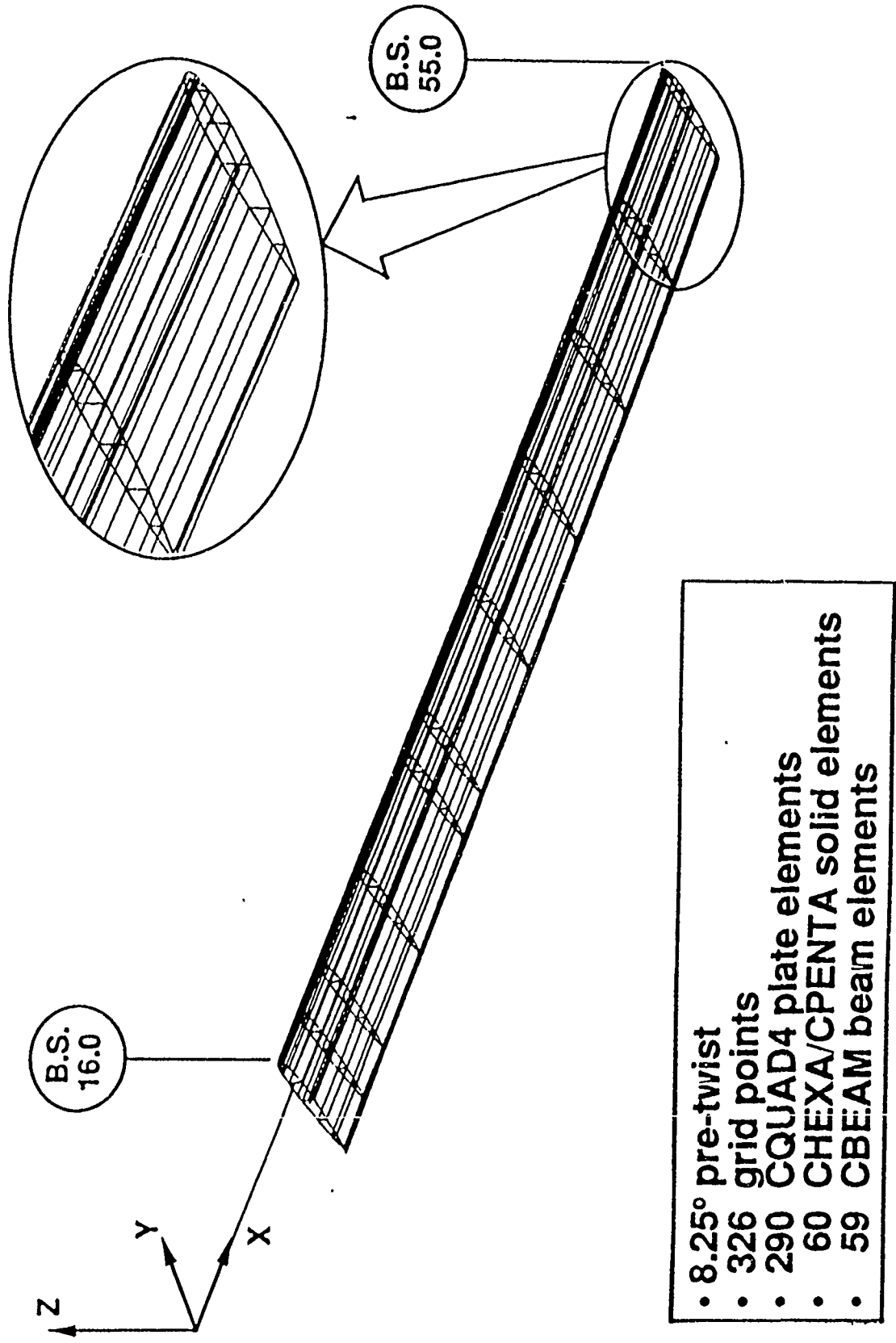


Figure 5

# Extension-twist-coupled model rotor blade

## Vibration Test / Analysis Correlation

Free-Free mode shape	Experimental (Hz)	Analytical (Hz)
First flap bending	33.0	35.35
Second flap bending	94.0	105.07
First lead-lag bending	164.0	153.67
First torsion	190.0	185.76
Third flap bending	211.0	222.83

Cantilevered mode shape	Experimental (Hz)	Analytical (Hz)
First flap bending	6.0	6.75
First lead-lag bending	24.0	26.22
Second flap bending	36.0	39.32
Third flap bending	98.0	103.75
First Torsion	116.0	132.80
Second lead-lag bending	141.0	154.80
Fourth flap bending	180.0	203.00
Second torsion	338.0	305.30

Figure 6

COMBINED USED OF FINITE-STATE LIFT AND  
INFLOW MODELS FOR ROTORCRAFT MODELING

by

David A. Peters  
Walter Stumpf  
Cheng-Jian He

School of Aerospace Engineering  
Georgia Institute of Technology  
Atlanta, Georgia 30332

Submitted to The Third Technical Workshop on  
Dynamics and Aeroelastic Stability Modeling  
of Rotorcraft Systems

Duke University

March 12-14, 1989

Abstract

In the aeroelastic modeling and analysis of rotorcraft, there are several key steps that must be accomplished. First, the various equations for the pieces of the model (i.e., the structure, lift, induced flow, and control system) must be assembled into a set of equations that can be solved by some solution strategy. Second, one must find the trim settings that will result in a periodic solution at a given flight condition. Third, one must perturb this flight condition to obtain perturbation equations. Fourth, these perturbation equations must be solved in order to find frequencies, modes, and stability boundaries; and then control systems can be designed. As it turns out, the determination of trim and the development of perturbation equations can be greatly expedited if the assembled rotorcraft model can be written in terms of a finite number of state variables. Unfortunately, most lift and inflow models do not lend themselves to state representations and, thus, are difficult to use in aeroelasticity analysis beyond simple time-marching.

In this paper, we will review the ARO-sponsored work in which we are attempting to model the entire rotor system with state-variable models. The structure is modeled in terms of generalized Rayleigh-Ritz coordinates, the lift is modeled in terms of the modified ONERA dynamic-stall state variables (circulations and moment coefficients), the wake is modeled in terms of a finite-state induced flow model, and trim is found from a state-space auto-pilot. This combination is also interesting from the point of view that an unsteady wake model implicitly gives some unsteady aerodynamic effects which must then be expunged from the lift model so as not to be counted twice. In our case, this is quite simple to do because the ONERA model is already segregated into the part due to linear, unsteady aerodynamics and the part due to stall. Thus, we simply eliminate the linear state variables from the lift model. Further, we treat the drag in a quasi-steady manner. This leaves four aerodynamic states per aerodynamic control point.

Thus, for a typical computation, we would have 6 structural modes (3 flap, 2 lag, 1 torsion) which is 12 states, 5 aerodynamic modes which is 20 states, four harmonics of inflow which is 15 states, and three controllers which is 6 states. Therefore, there are 53 total states for time-marching and 47 states for stability (the trim controller is turned off for perturbation dynamics). This is a reasonable number of states with which to do meaningful Floquet theory and control system design. We are correlating our results with the SA349 Gazelle measurements and will show some of these at the workshop.

# Space-/Time-Domain Finite Elements for Structures, Dynamics, and Control

Dewey H. Hodges and David A. Peters  
School of Aerospace Engineering  
Georgia Institute of Technology  
Atlanta, Georgia

and

Marco Borri  
Dipartimento di Ingegneria Aerospaziale  
Politecnico di Milano  
Milano, Italy

A variety of applications for spatial and temporal finite elements is described. A weak Hamiltonian formulation is first presented for the dynamics of rigid bodies. With this method, one can either time march or solve periodic two-point-boundary-value problems. All boundary conditions are of the "natural" type, and one can use the crudest possible shape functions and still achieve remarkable accuracy. The method is extended to include formulation and solution of optimal control problems in terms of states, co-states, and control variables. Results are presented for a simple trajectory optimization problem. The method is further extended for determining the nonlinear static response of beams in terms of displacement variables, generalized strain, and section stress resultants. A separate two-dimensional finite element code leads to characterization of the constitutive law in terms of 21 elastic constants for nonhomogeneous, anisotropic beams. For the global deformation of a beam, the entire formulation is so compact that it can be written in a few lines – even for arbitrarily large displacement and rotation. Results are presented that show the convergence properties of this mixed method. The formulation has also been developed for nonlinear statics and dynamics of moving beams although no results are yet available. Future work includes space-time response of moving beams, deployment problems, and disturbance propagation. Development of a similar approach for plate problems appears to be feasible. The potential impact of this methodology on rotorcraft dynamics problems is also discussed.

## The Rotorcraft Center of Excellence at Rensselaer

R. G. Loewy

The U. S. Army Research Office Center of Excellence at Rensselaer, established in 1982 and supported under two five-year contracts, is in its eighth year. This ARO-COE, known as the Rensselaer Rotorcraft Technology Center (RRTC), continues under its originally defined three-part concept: first, to provide advanced and comprehensive educational programs which will attract some of the best and brightest young minds to the study of rotorcraft technology and to up-date professionals in the field, in programs specialized to continuing education; second, to perform research which is at the cutting edge of advances in knowledge and understanding of the phenomena pacing new rotorcraft development and to transfer these advances expeditiously to U. S. developers; and third, to develop new experimental and computational resources in rotorcraft technology for the use and benefit of all appropriate components of the U.S. rotorcraft community.

At this writing, seven faculty/staff and ten graduate students are sponsored in their pursuit of the Center's goals under ARO auspices. Another eight faculty members and twelve graduate students are active, to varying degrees, in the activities of the Center. Some of the latter group are conducting research under industry contracts, others under contracts or grants won from government agencies in addition to the ARO-COE funding, and still others with Rensselaer sponsorship.

Areas of research concentration with ARO-COE support include innovative composite structural design, analysis and fabrication; composite drive shaft system design; non-linear structural dynamics and aeroelasticity - particularly aimed at violent maneuvers; blade-vortex interaction phenomena; rotor shaft flexibility influences on ground/air resonance instabilities; and improving means of mode identification and modification in fuselage ground shake tests. Similar areas of concentration with other than ARO-COE funding include continuing transonic wind tunnel tests of passive wave drag reduction mechanisms in unsteady flow, developing advanced CAD/CAM-FEM linkages using expert systems techniques, conducting shake tests and correlative analyses for the natural modes and frequencies of full scale helicopter fuselage components, completing development of a model rotor impedance testing rig, establishing a major laboratory for symbolic computation, and developing techniques for conducting ground/air resonance stability flight testing using radio-controlled scale models.

Clearly, attempts to make the Center self-supporting, ie independent of ARO-COE continuation beyond July 1992, the end of the present contract, are receiving determined attention. Judging the RRTC by such standard measures as (a) the quality and numbers of graduate students who have and are entering the program, (b) the number and ranking of positions graduates of the program have and are to continuing to enter in the rotorcraft community, and (c) publications in professional journals and presentations at national and international meetings, we believe the ARO-COE program can be pronounced a success of significant proportions.

# DYNAMIC ANALYSIS OF UNCONVENTIONAL HIGH-SPEED ROTORCRAFT<sup>1</sup>

K. B. Sangha and F. K. Straub  
McDonnell Douglas Helicopter Company  
Mesa, Arizona

## ABSTRACT

Rotorcraft designs are evolving rapidly towards the high-speed end. These designs challenge the conventional barriers of rotorcraft capability. The analytical support and evaluation of these concepts poses new challenges to the dynamic analyst. A number of assumptions in traditional analysis are held inviolate, and analyst must define new approaches in order to evaluate designs.

At McDonnell Douglas Helicopter Company, the high-speed rotorcraft challenge is being addressed by the "TrailRotor Convertiplane (TRC)" Concept. The concept calls for a high speed aircraft with hovering capability. The design considered is a twin-rotor configuration (such as in a tiltrotor configuration) that meets the hovering and low-speed forward flight requirement, and jet engines to provide the high-speed forward flight requirements. In the transition from helicopter to cruise conditions, the rotor pylons tilt aft through ninety (90) degrees, simultaneously slowing RPM to near zero, and eventually stop and fold (about the flapping hinge).

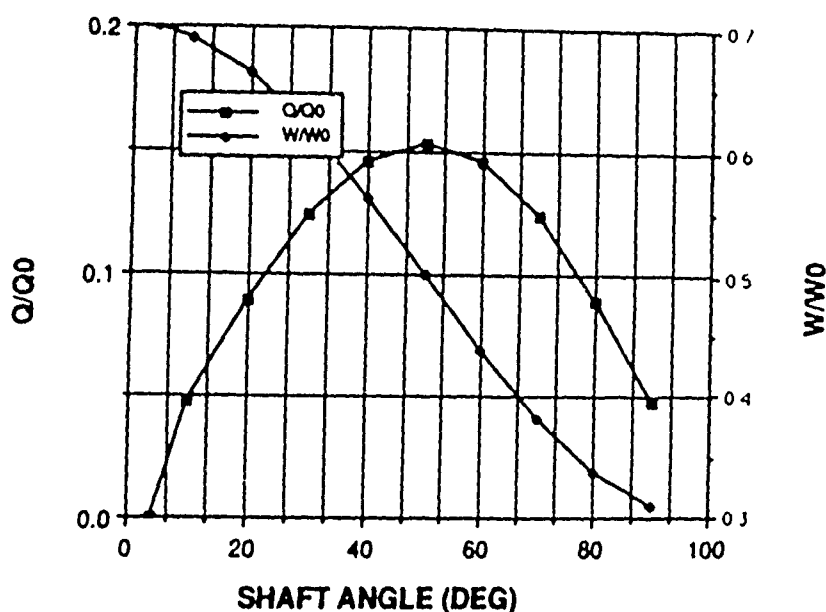
The analytical problem at hand is to (i) examine the feasibility of the concept, (ii) examine the requirements of the rotor and fuselage designs, (iii) suggest designs to promote the doability of the approach.

Existing analytical tools were used in performing the analyses presented in this paper. The key issue to be examined is the feasibility of the conversion from helicopter mode to aircraft (or cruise) mode, and the loads generated during the conversion. Linearized stability and gust response during conversion are additional items to be examined.

The conversion requirements are steady forward flight conditions at 135 Kts, 1G load condition, and nominally 10 seconds for complete conversion. Attendant requirements are small excursions in hub and ship pitching, rolling moments, simplicity of conversion requirements from a design and pilot workload standpoint, and minimal drag forces due to conversion. The term "conversion" includes the shaft rotation through 90 degrees, as well as the RPM bleed from 100 percent to near

<sup>1</sup> Abstract submitted for the 3<sup>rd</sup> Technical Workshop on Dynamics and Aeroelastic Stability Modeling of Rotorcraft Systems, March 12-14 1990, Duke University, Durham, North Carolina





**$Q_0$  = HOVER POWER**  
 **$W_0$  = NOMINAL RPM**

Figure 1: Quasi-steady RPM and Torque Schedules During Conversion

zero. Several approaches to conversion are possible. Two specific approaches are considered in this paper. The analysis was performed using the Comprehensive Analytical Model for Rotorcraft Aerodynamics and Dynamics (CAMRAD/JA).

A quasi-steady equilibrium approach is taken in performing the analysis. By employing the rotor in a windmill brake state, it is possible to simplify the requirements of the transmission system. In a windmill brake state, specific requirements on the rotor torque can be defined during both RPM bleed as well as speed-up. Given these requirements, it is possible to find trim angles that will control the torque and RPM of the rotor. The assumptions made in performing the analysis and the results obtained are outlined in the paper.

Consider the RPM and the corresponding torque schedules versus shaft angle shown in figure 1. The RPM schedule is assumed; and corresponding to it, is the torque requirements that can be fairly easily derived. A trim analysis may now be performed at each intermediate shaft angle, at the desired RPM, and the desired torque requirement. The trim control angles so obtained determine the necessary schedule in order to require the appropriate rotor torque and therefore result in an RPM bleed. The effects of the shaft tilt dynamics are not included in the model. As the rotor tilts back, in near auto-rotation, and a torque limit is specified (derived from a desired RPM rate), there is a non-zero thrust generated by the rotor. In response to this thrust, the blades respond through flapping. The flapping generated must be minimal, in order to keep the rotor controllable and minimize blade and hub loads. Since the rotor tilts aft, the thrust manifests itself as an apparent drag force. Additional requirements on the conversion process are therefore to maintain small thrust as well as small flapping. The net torque on the rotor can be controlled

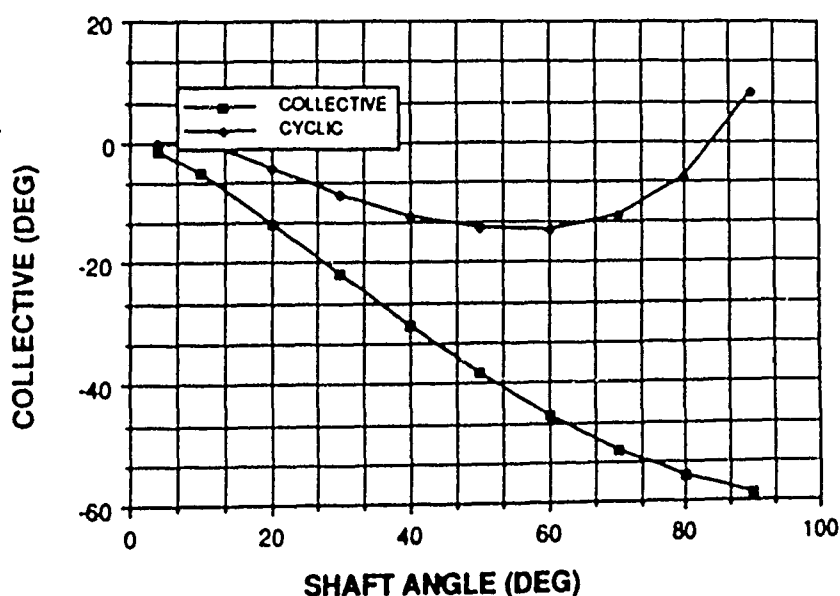


Figure 2: Quasi-steady Control Requirements During Conversion

by prescribing the collective, while the flapping can be controlled by prescribing the cyclic. Since the cyclic flapping is controlled to a small amount (2 degrees), the hub moments are also small. For the RPM and torque schedules shown in figure 1, the required control angles are presented in figure 2. The drag force penalty is presented in figure 3. The only parameters that can reduce the drag penalty are twist, RPM and allowable power. A parametric variation of the effects of twist variation is obvious from figure 3.

The quasi-steady trim conditions obtained at each of the intermediate shaft angles may be used to perform a stability and linearized gust response analysis. These, and other analyses performed to characterize possible approaches to conversion, the limitations imposed on these analyses due to analytical assumptions and requirements of future analytical tools are presented in the paper.

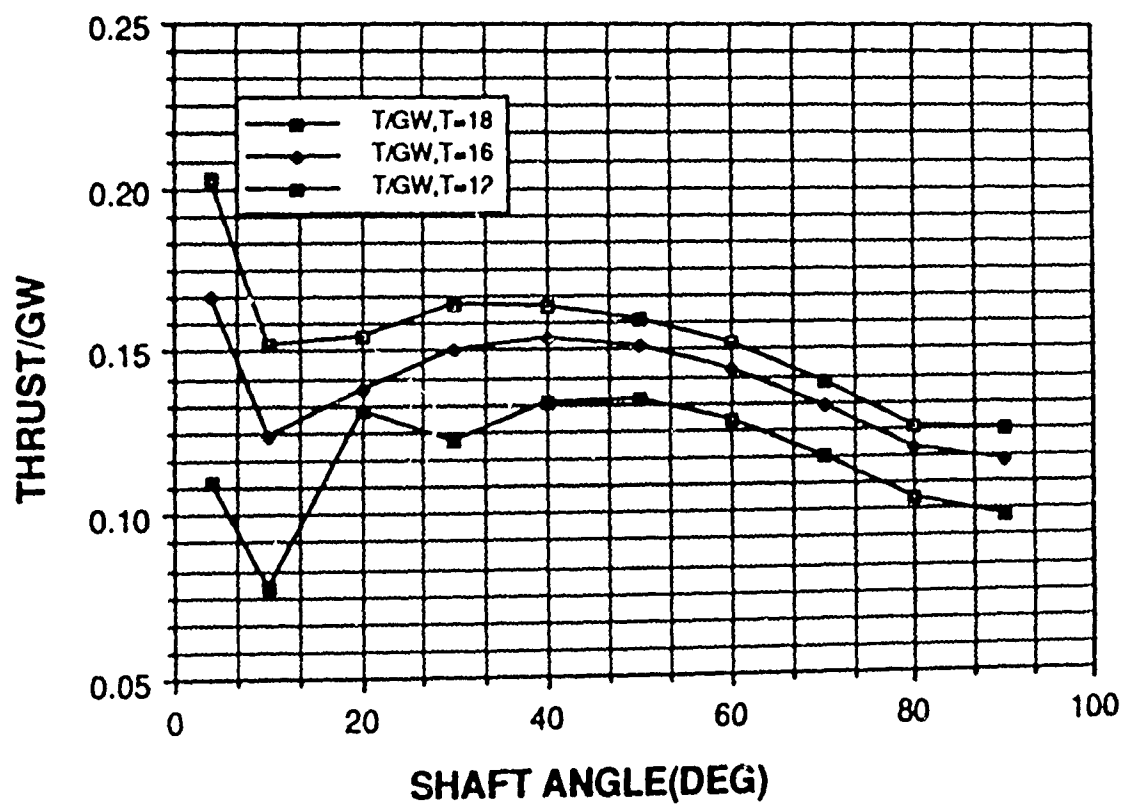


Figure 3: Apparent Drag Penalty During Conversion, as a Function of Twist

# Rotor Blade Stability Validation Utilizing A Coupled Aeroelastic Analysis With Refined Aerodynamic Modeling<sup>1</sup>

Michael S. Torok<sup>2</sup> and Inderjit Chopra<sup>3</sup>

Center for Rotorcraft Education and Research  
Department of Aerospace Engineering  
University of Maryland  
College Park, MD 20742 U.S.A.

## 1 OBJECTIVE

The effects of refined aerodynamic modeling on aeroelastic blade stability are investigated. An advanced non-linear aerodynamic model based on an indicial response method is included into a comprehensive coupled rotorcraft analysis. The aerodynamic analysis accurately predicts blade loadings in attached and separated flow, as well as dynamic stall. Compressibility effects are implicitly included in the formulation. In addition, advanced wake models, both prescribed and free wake analyses, are coupled into the trimmed, rotor response and stability solution. The rotor analysis is formulated using a finite element technique in space and time. Rotor equations of motion and trim equilibrium equations are solved as one coupled solution. Aeroelastic stability is determined utilizing Floquet theory for a linearized system. Blade stability for the complete non-linear system is determined using a modified Sparse Time Domain technique. The rotor analysis is validated in a correlation study with Aerospatiale Gazelle flight test data. The refined aerodynamics significantly affect the blade loads, and at extreme flight conditions, small perturbations in the trim state, substantially alter these loadings. Consequently, the refined aerodynamics play an important role in determination of blade stability. The effects of flow separation, dynamic stall, compressibility and refined wake models, as well as other key parameters, on rotor blade stability are determined. Results are validated in a correlation study with model hingeless rotor experimental data.

## 2 INTRODUCTION

Determination of the aeroelastic stability of a rotor in forward flight presents a chal-

---

<sup>1</sup>Abstract submitted to the Rotorcraft Dynamics Workshop, Duke University

<sup>2</sup>Rotorcraft Fellow

<sup>3</sup>Professor

lenging problem to researchers. This problem is magnified when considering high speed flight conditions near the extremes of a vehicles' flight envelope. Under such conditions, the aerodynamic environment of the rotor is highly non-linear, exhibiting regions of dynamic stall, flow separation and transonic conditions. At low speed, these non-linear effects are reduced, but the complexities of the wake structure also present challenges to the accurate prediction of rotor blade stability.

Due to the complexities of this problem, many simplifications are made to make the analysis more manageable. In recent work [1,2], simplifications include rigid blades, quasi-steady aerodynamics, and uniform or Drees inflow models [3]. Unsteady effects are often approximated with a dynamic inflow model [4]. This method is limited to low frequency effects, and thus cannot predict detailed flow phenomena. Additional investigations are cited in Reference [5]. These approximations yield satisfactory results under moderate flight conditions. At more extreme flight conditions, however, non-linear aerodynamic effects significantly affect blade loadings, and thus simpler models are no longer applicable. At low speeds, the linear Drees inflow model breaks down, and more advanced wake models are required. The present study utilizes a refined non-linear aerodynamic model, as well as prescribed and free wake models, to predict rotor blade stability for several flight conditions. The analysis is validated in a correlation with model hingeless rotor test data.

### 3 ROTOR ANALYSIS

#### 3.1 AERODYNAMIC MODEL

In an effort to capture the complete range of flow characteristics, and still maintain simplicity and efficiency, a recent aerodynamic model, developed by Beddoes and Leishman [6,7] is adopted. This model accurately predicts attached and separated flow, as well as dynamic stall. An important feature of the model is that compressibility effects are implicitly included. The model requires only a few empirical factors, most of which are derived from static airfoil data. The parameters derived from the unsteady data, however, are insensitive to airfoil shape, and thus need not be recalculated for different airfoils. The model has been extensively validated for a series of different airfoil sections over a wide range of flight conditions. This model has been recently incorporated into a comprehensive rotor aeroelastic analysis [8]. This work carried out a parametric study to determine the significance of the refined aerodynamics on the dynamic response of rotors in forward flight. Results showed that at high-speed conditions, the non-linear aerodynamics, or separated and stalled flow, dominate the outboard blade section forces, and significantly affect blade response and blade root loads. These effects were amplified at increased thrust levels. Compressibility effects

were also found to substantially affect the extent of separated flow on the rotor blade.

### 3.2 WAKE MODELS

Refined wake modeling has proven to be very important under certain flight conditions. Recent literature has emphasized the need for further refinements to improve correlations of experimental inflow measurements with predicted values. Current technology provides several models, from classical skewed helices to free wake calculations, and comparisons have been made on their respective ability to predict rotor inflow over a range of flight conditions [9,10,11]. The present analysis incorporates both the prescribed and free wake models from CAMRAD [12].

### 3.3 COUPLED TRIM AND RESPONSE

The trim solution determines rotor pitch controls and vehicle orientation for a propulsive flight condition. The steady response determines the deflected position of the blade for one complete azimuthal cycle. The present investigation utilizes an analysis which solves the coupled, non-linear periodic equations of blade motion and six trim equilibrium equations. The analysis is based on a finite element approximation in both space and time. Each blade is assumed to be an elastic beam undergoing flap bending, lag bending, elastic twist and axial deflection. The blades are discretized into a number of beam elements, each having fifteen degrees of freedom. To reduce computational time, a large number of finite element equations are transformed to the modal space as a few normal mode equations (6-9 modes are normally used). The periodic, non-linear, response solution is determined by using a temporal finite element discretization. Fourth order Lagrangian shape functions are utilized within each time element. The finite element in time formulation is based on Hamilton's weak principle. Resulting normal mode equations are ultimately solved as a set of non-linear algebraic equations. The solution is obtained utilizing an iterative, modified Newton method [1,13].

Concurrent with the solution of the blade equations of motion, is the solution of the vehicle trim equations. The vehicle is trimmed on all axes for both force and moment equilibrium (6 equations). The modified Newton solution method allows the two solutions to be coupled to produce a unique solution that satisfies both blade and vehicle equilibrium equations. The force summation method is used to determine hub forces as a sum of inertial and aerodynamic loadings [14].

### 3.4 AEROELASTIC STABILITY

Linearized blade stability is determined using Floquet transition matrix theory [15]. A normal mode approach is used, utilizing the coupled blade modes determined about the trimmed mean deflections. The perturbation equations of motion are numerically integrated to determine the transition matrix. A complex eigenanalysis is performed on this matrix to assess the stability of each blade mode. Modal decay rates are derived from resulting eigenvalues. A positive decay rate denotes an unstable mode.

Rotor blade stability for a non-linear response is determined using a modified Sparse Time Domain (STD) technique, recently developed [16]. The STD technique is a multi-degree of freedom technique for estimating the modal damping parameters from transient response data. Solutions of system equations are performed utilizing a windowing technique. This method ultimately determines the damping characteristics for each mode, which in turn determine blade stability.

## 4 RESULTS AND CONCLUSIONS

The effects of refined aerodynamic analyses have been studied in depth in a correlation study with flight test data [17]. The data used is from a modified, experimental SA349/2 Modified Gazelle helicopter [18]. The SA349/2 is outfitted with an Aerospatiale advanced geometry rotor. This articulated rotor includes a damped lag articulation hub, and three high speed (Grande Vitesse) research blades. The rotor blade airfoil section is an OA209, 9 percent thickness airfoil, and the blade has a non-linear twist distribution.

The correlation included validation of the analysis for three flight conditions, varying both advance ratio and thrust coefficient; low speed-low thrust, high speed-low thrust, and high speed-high thrust [17]. Aerodynamic blade loads (normal force and pitching moment) and blade bending moments (flap and lag) were investigated. For a moderate flight condition, high speed-low thrust, blade section normal force was well predicted, Figure 1. Non-linear aerodynamic effects were small for this flight condition. Flap bending moments were also satisfactorily predicted, Figure 2. Use of a refined wake analysis proved necessary to predict the harmonics of the bending moments. At high speed, prescribed and free wake models gave similar results. At the low speed flight condition, the free wake model substantially improved the correlation of blade section normal force on the retreating side of the disk, Figure 3. At a high speed-high thrust flight condition, the non-linear aerodynamic effects were quite significant. Pitching moment correlations were improved by including non-linear aerodynamic effects, Figure 4. The effect of small perturbations in the rotor thrust were

also studied. A small increase in thrust significantly altered the blade section pitching moment as dynamic stall occurred on the blade giving rise to a large spike in the resulting moment, Figure 5. The sensitivity of blade loads to such perturbations are quite important in determining blade stability. Additional results depicted good correlation of trimmed vehicle controls and vehicle orientation, and a substantial influence of blade twist and compressibility effects on the extent of separated flow on the rotor.

The validation of the analysis yields confidence in the predictive capabilities of the refined aerodynamics. The current research effort extends these advanced analyses into the determination of rotor blade stability. Results are being correlated with model hingeless rotor test data to validate the analyses and assess the effects of the refined aerodynamics. The test configuration was an isolated, soft in-plane, rotor with discrete flap and lead-lag flexures and relatively rigid blades. Data was acquired for both hover and forward flight [19]. Preliminary results show that a linearized Floquet analysis yields accurate results under moderate flight conditions, Figures 6-7. At more extreme conditions, namely increasing advance ratios, a discrepancy arises in the correlation. Further investigation, utilizing a non-linear modified STD technique, will determine if these discrepancies are attributable to non-linear aerodynamic effects. Ultimately, the effects of flow separation, dynamic stall, compressibility, refined wake modeling and other key parameters on rotor blade stability will be investigated over a range of flight conditions.

## References

- [1] Panda,B., Chopra,I., "Flap-Lag-Torsion Stability in Forward Flight", Journal of the American Helicopter Society, 30, No. 4, Oct. 1985.
- [2] Gaonkar,G.H., McNulty,M.J., and Nagabhushanam,J., "An Experimental and Analytical Investigation of Isolated Rotor Flap-Lag Stability in Forward Flight", Presented at the 11th European Rotorcraft Forum, London, England, September 1985.
- [3] Drees,J.M., "A Theory of Airflow Through Rotors and its Application to Some Helicopter Problems", Journal of the Helicopter Association of Great Britain, Vol. 3, No. 2, July-September 1949.
- [4] Gaonkar,G.H., and Peters,D.A., "Effectiveness of Current Dynamic Inflow Models in Hover and Forward Flight", Journal of the American Helicopter Society, 31, No. 2, April 1986.
- [5] Friedmann,P.P., "Aeroelastic Problems in Helicopters, Propellers, and Turbomachinery", *Recent Trends in Aeroelasticity, Structures, and Structural Dynamics*, University of Florida Press, Gainesville, Florida, 1987.
- [6] Beddoes,T.S., "Representation of Airfoil Behavior", Vertica 7, 1983.



- [7] Leishman, J.G., Beddoes, T.S., "A Generalized Model for Unsteady Aerodynamic Behavior and Dynamic Stall using the Indicial Method", Presented at the 42nd Annual Forum of the American Helicopter Society, Washington D.C., June 1986.
- [8] Torok, M.S., Chopra, I., "A Coupled Rotor Aeroelastic Analysis Utilizing Non-Linear Aerodynamics and Refined Wake Modeling", Presented at the 14th European Rotorcraft Forum, Milano, Italy, September 1988.
- [9] Hoad, D., Althoff, S., Elliott, J., "Rotor Inflow Variability with Advance Ratio", Presented at the 44th Annual Forum of the American Helicopter Society, Washington D.C., June 1988.
- [10] Charles, B., Hassan, A., "A Correlation Study of Rotor Inflow in Forward Flight", Presented at the 44th Annual Forum of the American Helicopter Society, Washington D.C., June 1988.
- [11] Yamauchi, G.K., Heffernan, R., Gaubert, M., "Correlation of SA349/2 Helicopter Flight Test Data with a Comprehensive Rotorcraft Model", Journal of the American Helicopter Society, 33, No. 2, April 1988.
- [12] Johnson, W., "A Comprehensive Analytical Model of Rotorcraft Aerodynamics and Dynamics, Part 1: Analysis Development", NASA TM 81182, June 1980.
- [13] Lim, J., Chopra, I., "Design Sensitivity Analysis for an Aeroelastic Optimization of a Helicopter Blade", Presented at the AIAA Dynamics Specialists Conference, Monterey, California, April 1987.
- [14] Lim, J., Chopra, I., "Aeroelastic Optimization of a Helicopter Rotor", Presented at the 44th Annual Forum of the American Helicopter Society, Washington D.C., June 1988.
- [15] Johnson, W., *Helicopter Theory*, Princeton University Press, 1980.
- [16] Tasker, F.A., Chopra, I., "Nonlinear Damping Estimation from Rotor Stability Data Using Time and Frequency Domain Techniques", Presented at the 30th AIAA Structural Dynamics and Materials Conference, Mobile, Alabama, April 1989.
- [17] Torok, M.S., Chopra, I., "Rotor Loads Validation Utilizing a Coupled Rotor Aeroelastic Analysis with Refined Aerodynamic Modeling", Presented at the 45th Annual Forum of the American Helicopter Society, Boston, Massachusetts, May 1989.
- [18] Heffernan, R.M., Gaubert, M., "Structural and Aerodynamic Loads and Performance Measurements of an SA349/2 Helicopter with an Advanced Geometry Rotor", NASA TM 88370, November 1986.
- [19] McNulty, M.J., "Flap-Lag Stability Data for a Small Scale Isolated Hingeless Rotor in Forward Flight", NASA TM 102189, April 1989.

# BLADE SECTION NORMAL FORCE

$\mu = .344, C_T / \sigma = .066$

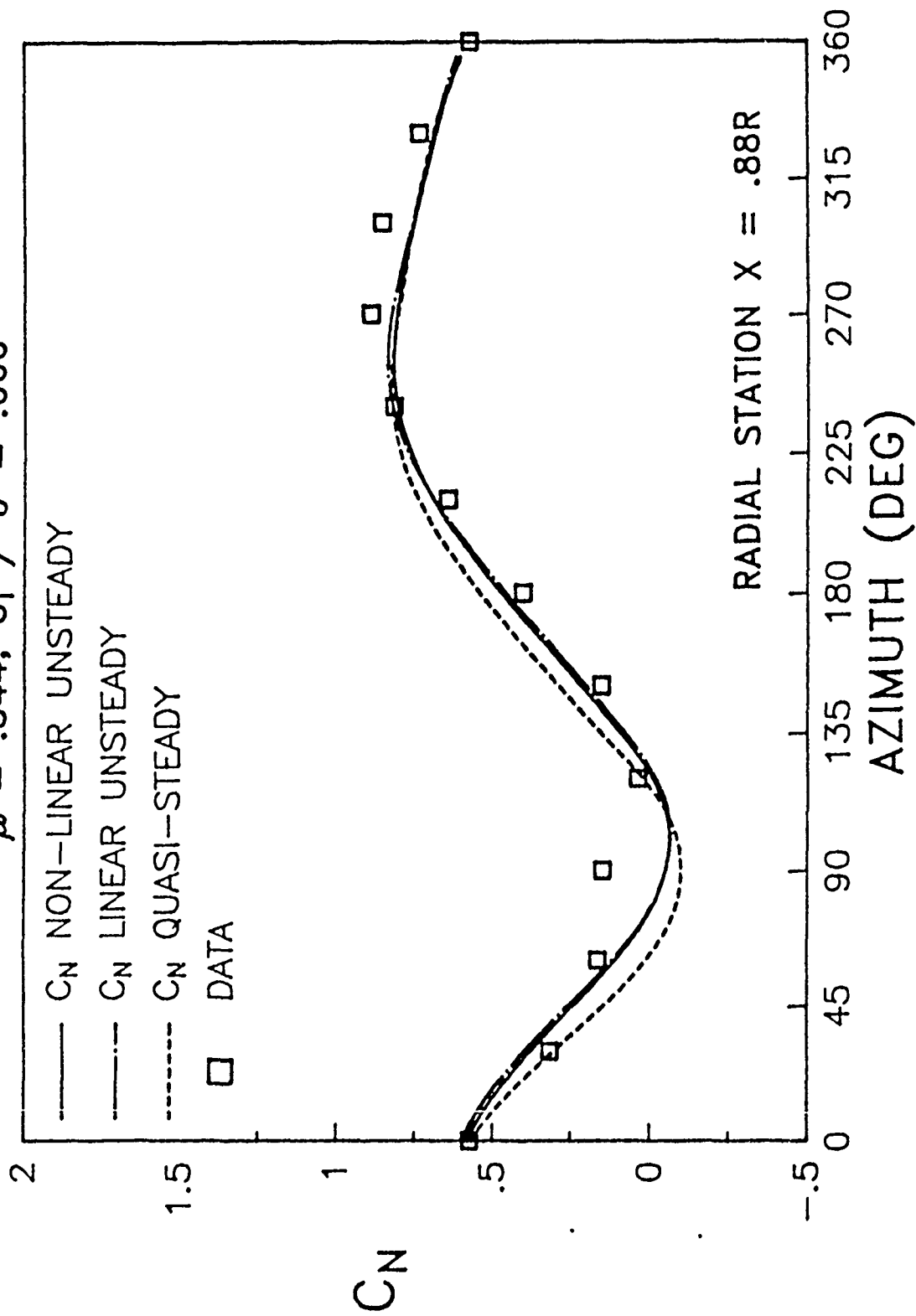


FIGURE 1.

# BLADE SECTION FLAP BENDING MOMENT

$$\mu = .344, C_T / \sigma = .066$$

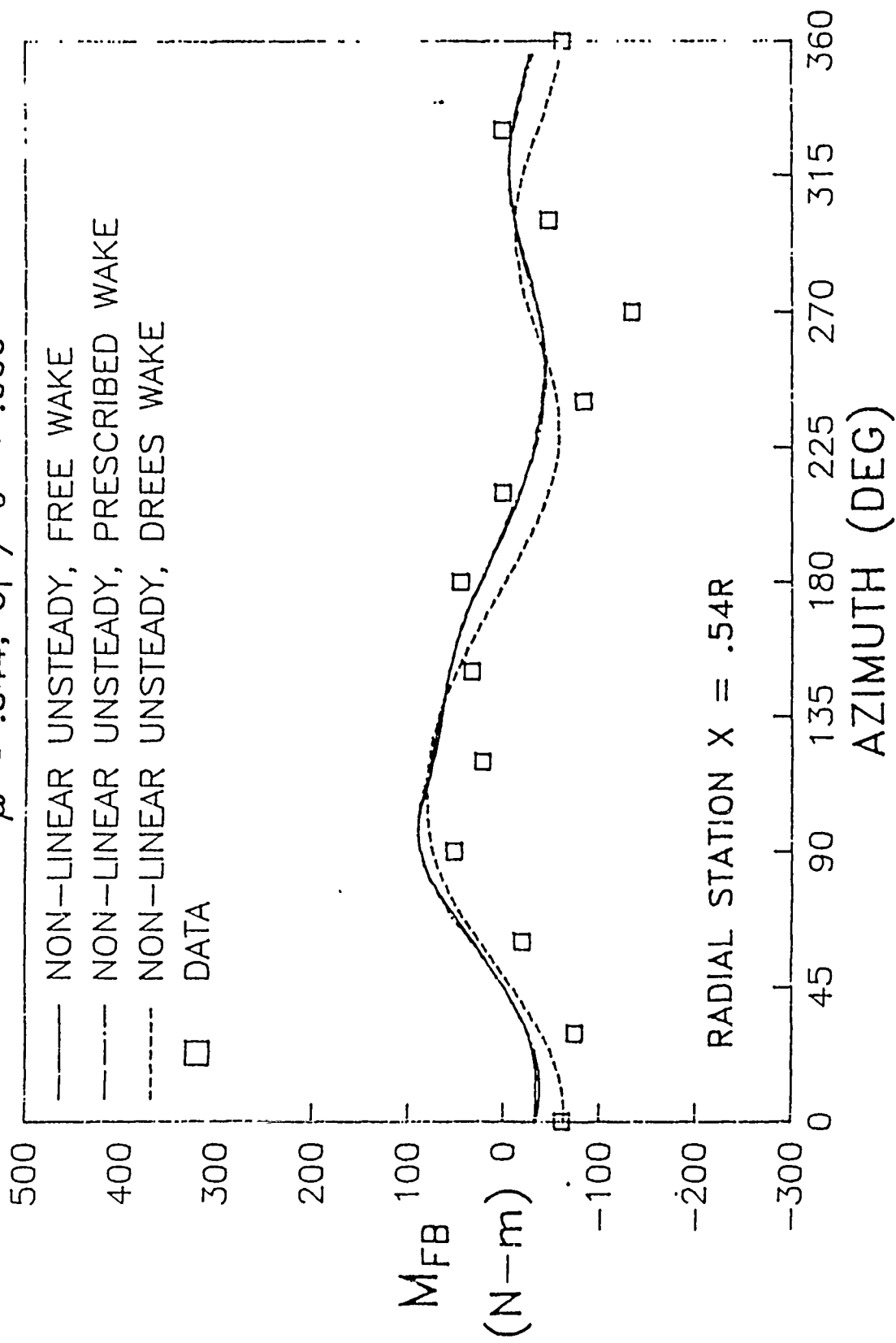
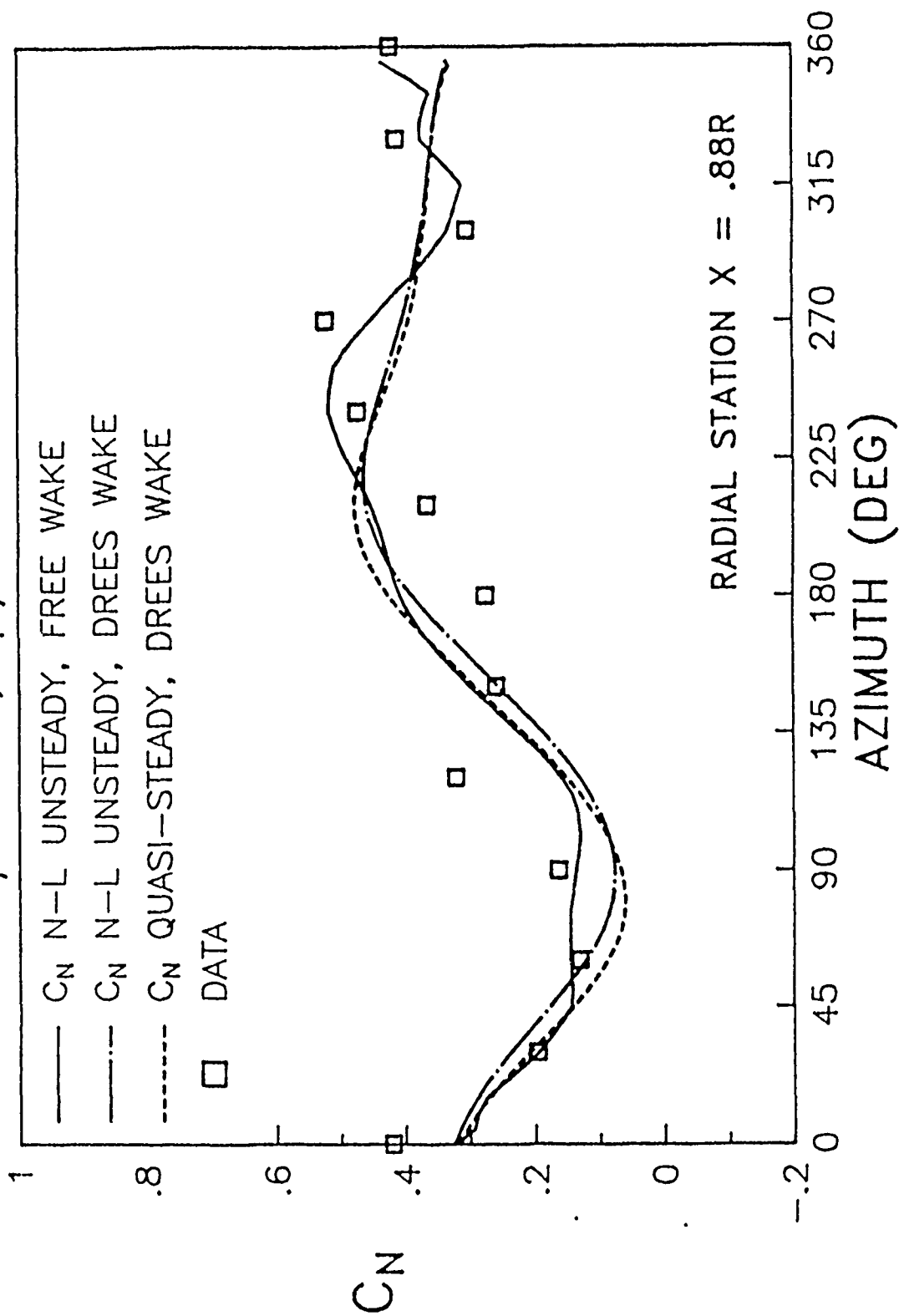


FIGURE 2.

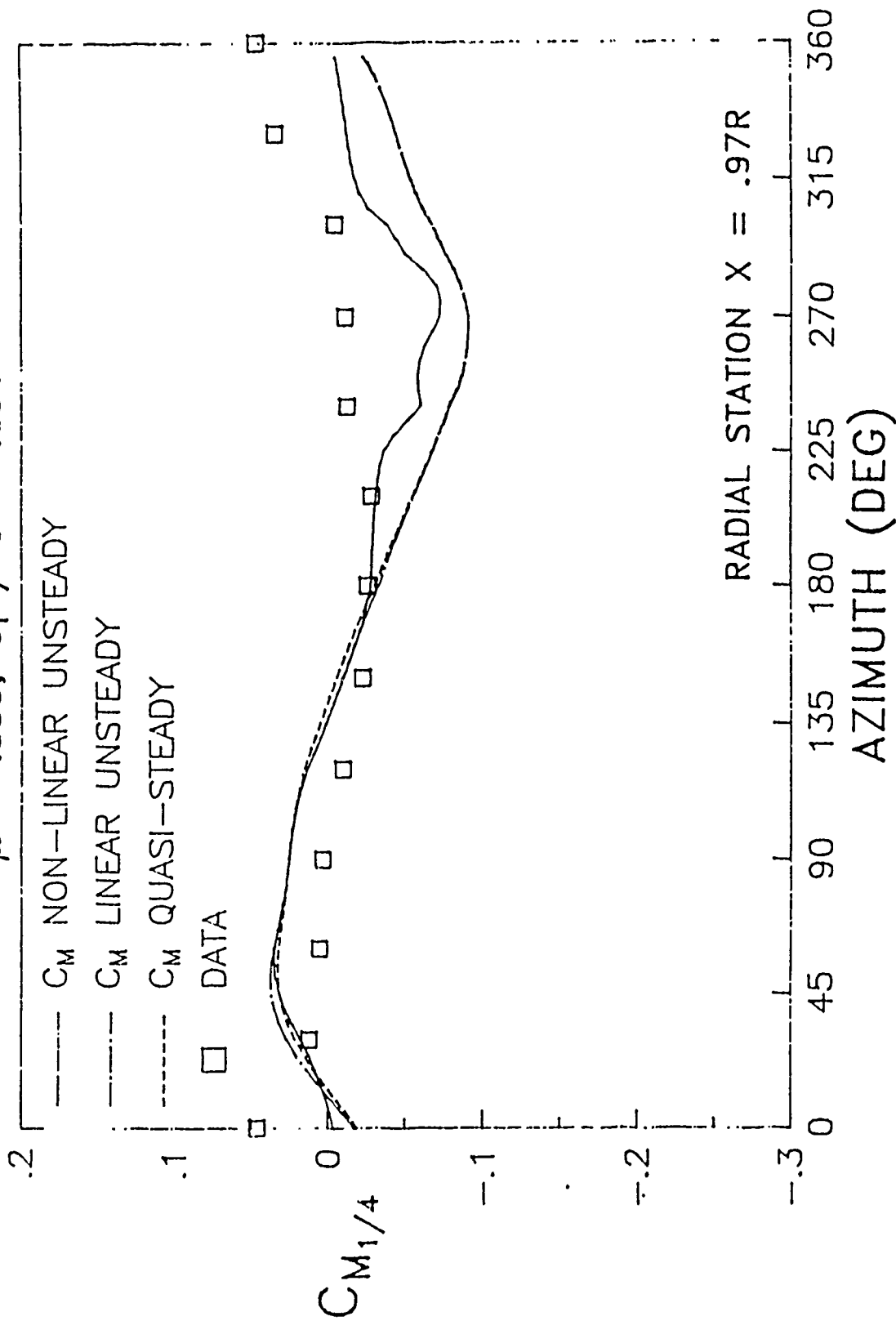
# BLADE SECTION NORMAL FORCE

$\mu = .140, C_T / \sigma = .067$



# BLADE SECTION PITCHING MOMENT

$\mu = .355, C_T / \sigma = .094$



# BLADE SECTION PITCHING MOMENT

$$\mu = .355, C_T / \sigma = .094/.099$$

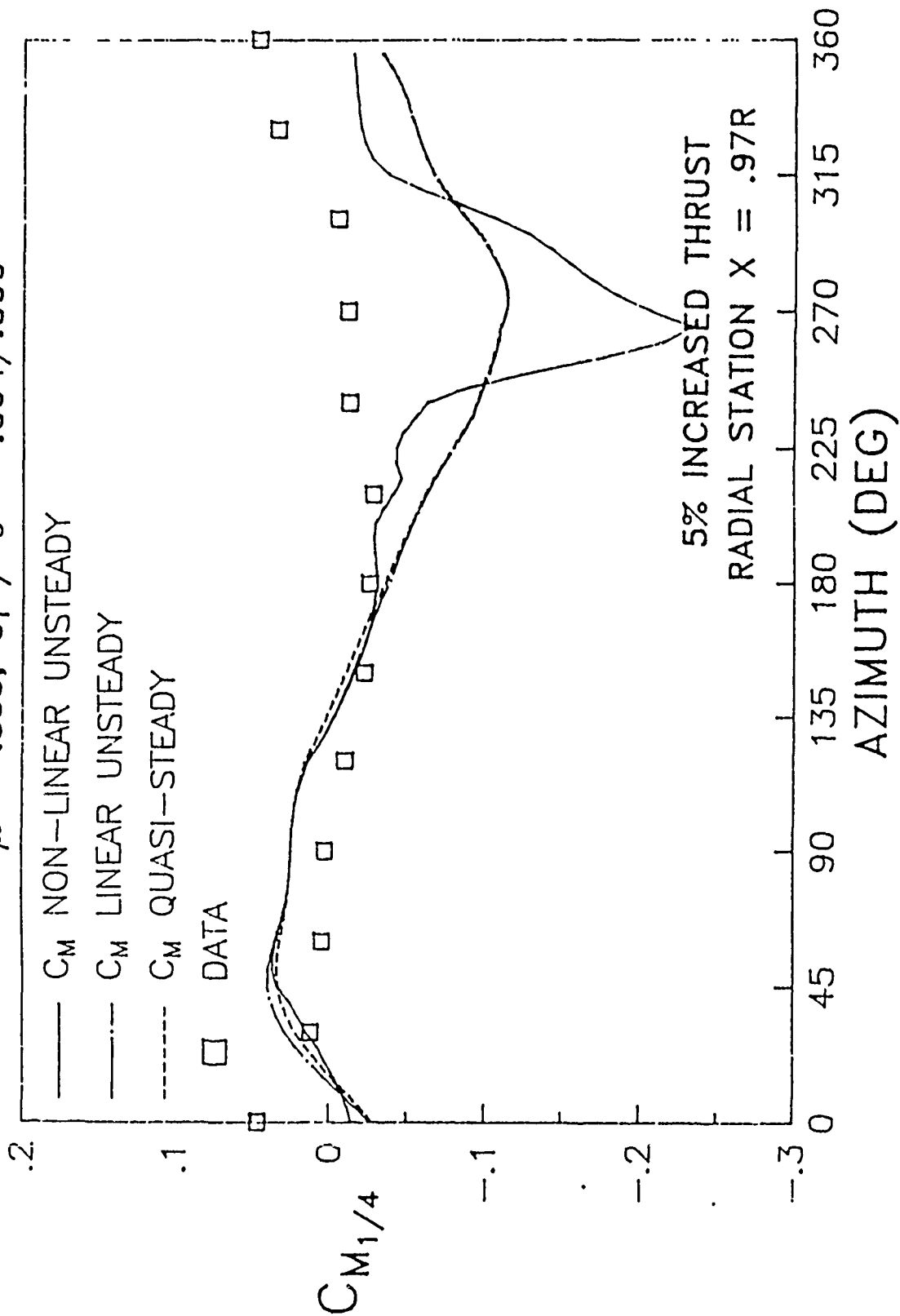


FIGURE 5.

# REGRESSING LAG MODE DAMPING

3° COLLECTIVE, -8° SHAFT TILT, 750 RPM

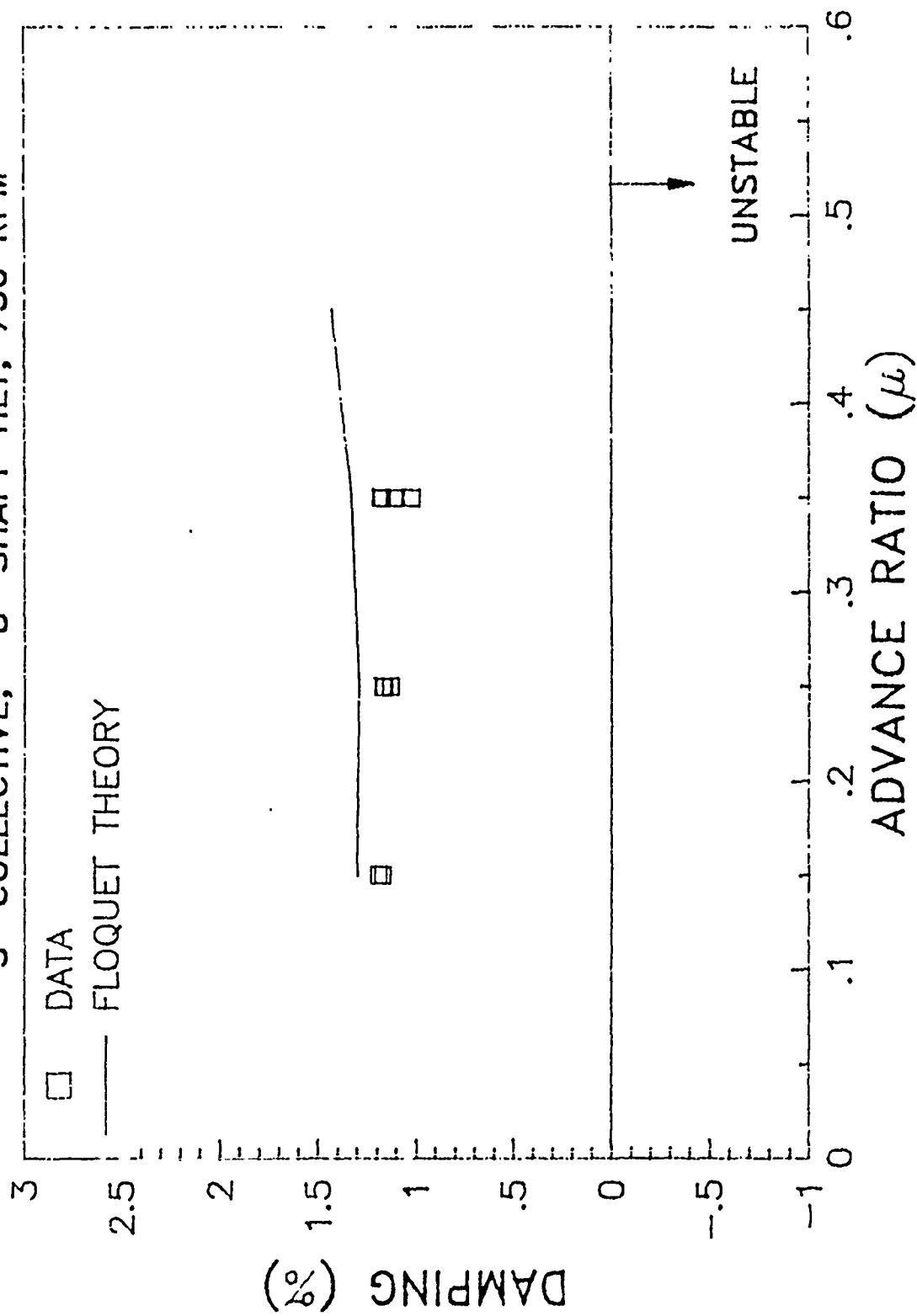
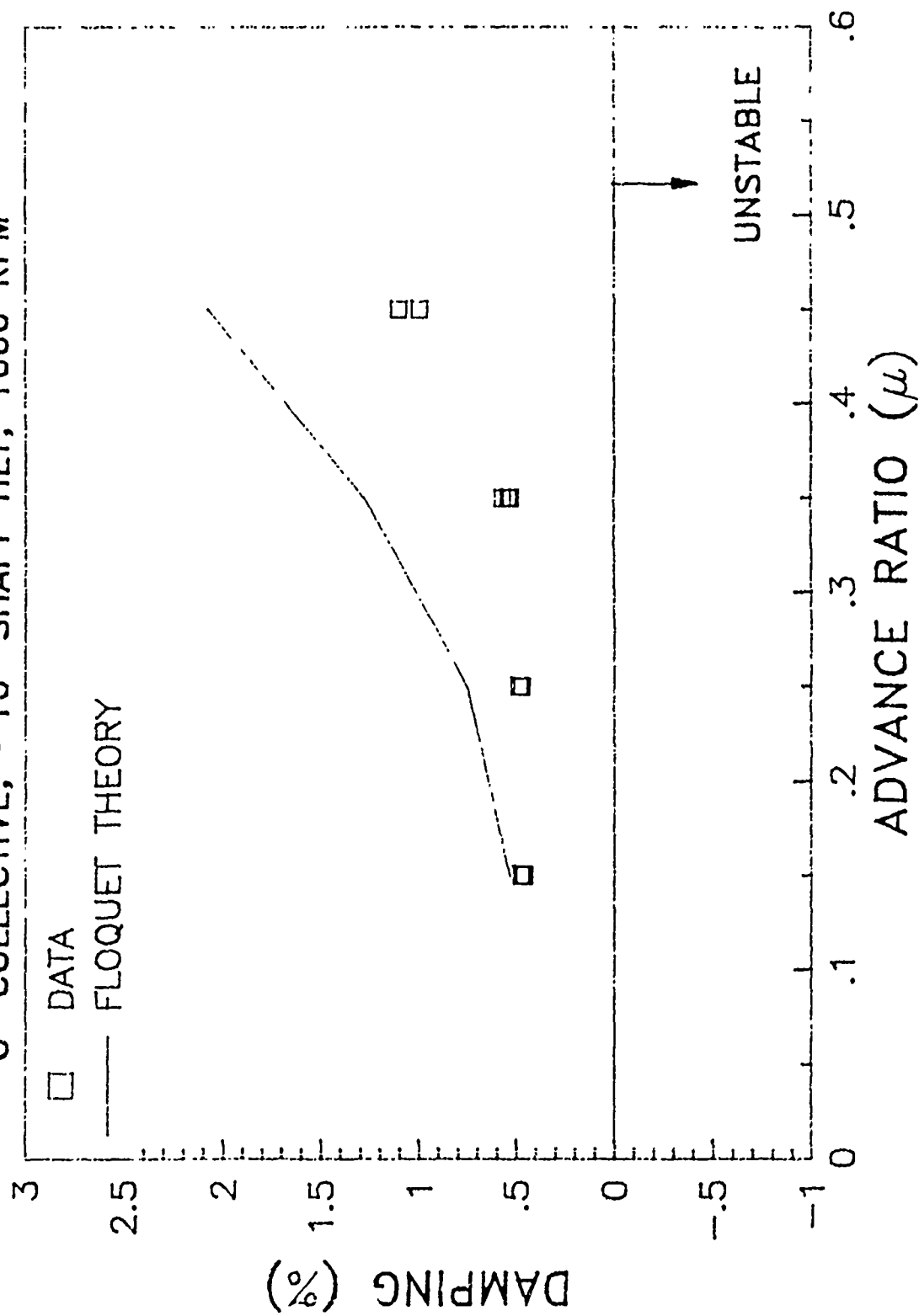


FIGURE 6.

# REGRESSING LAG MODE DAMPING

0° COLLECTIVE, -10° SHAFT TILT, 1000 RPM





# AEROELASTIC ANALYSIS OF ROTOR BLADES

Vikas B. Dhar  
(Graduate Student)

R. K. Kapania  
(Asstt. Professor)

Department of Aerospace & Ocean Engineering  
Virginia Polytechnic & State University  
Blacksburg, VA 24060

## Abstract

Rotary wing aeroelasticity has been an area of considerable activity for the last one decade. A lot of work has gone into developing an accurate and efficient model of rotor blades for analysis purposes, most of which have been referred to in the review by Friedmann [1]. One of the prime areas of research has been structural modelling, with a continued interest shown in geometrically non-linear models for hingeless and bearingless rotor blades. In spite of this spate of research, there is a distinct lack of literature on the analysis of unsymmetrically laminated composite rotor blades.

A simple and efficient element has been developed by Kapania and coworkers [Refs. 2 and 3] for non-linear analysis of unsymmetrically laminated beams and for aeroelastic response of wing boxes with laminated skins. The ongoing research intends to include study of the aeroelastic response of rotor blades. The element can be used to analyse built-up box structures reinforced by stringers. The formulation takes into account the effects of transverse shear, the bending-twist and the bending-stretching coupling inherent in the blades with unsymmetric skins and unsymmetric cross-sections. An important feature of this element is that even though it is a one-dimensional element, it is capable of simulating the structural behaviour of box type structures with the same accuracy as that obtained using WIDOWAC.

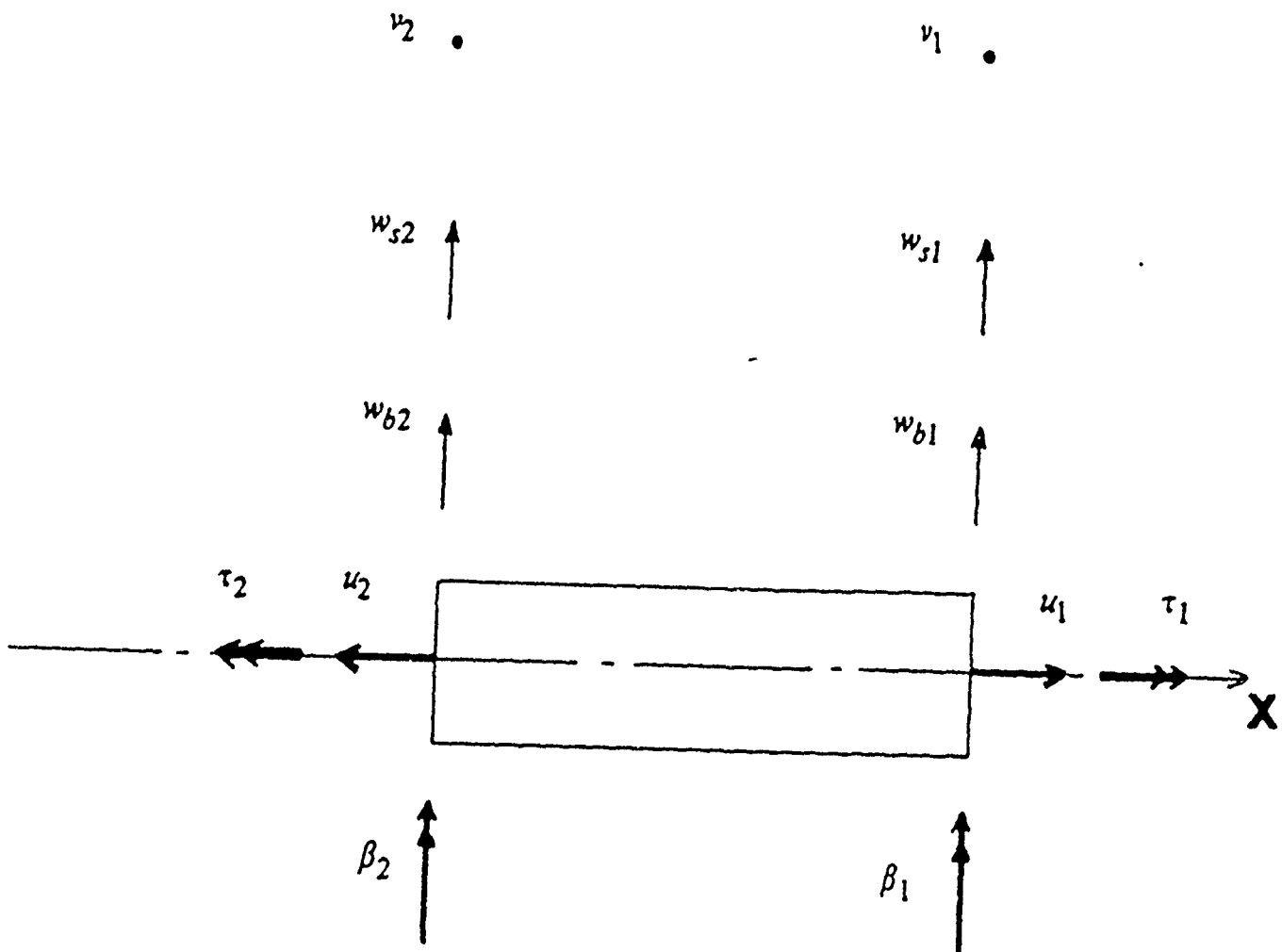
The analysis accounts for, (i) flap-lag coupling due to the unsymmetric nature of the cross-section of the rotor blades; (ii) axial-bending coupling, and the axial-torsion coupling due to either the anisotropic nature of the skin or the presence of sweep as in the case of rotor blades with swept tips.

The effect of axial forces is considered in the incremental stiffness matrix [4] and the non-linear load-displacement path is predicted by a linearized mid-point tangent incremental procedure [Refs. 5 and 6]. The generalised aerodynamic forces are obtained using the principle of virtual work in conjunction with the 2-dimensional quasi-steady aerodynamic theory. The results obtained will be compared with other works to validate the method.

## References.

1. Friedmann, P.P., "Recent trends in Rotary-Wing Aeroelasticity", *Vertica*, Vol. 11, No. 1, 1987, pp. 139-170.

2. Raciti, S., Kapania, R.K., "Non-linear vibrations of unsymmetrically laminated beams", *AIAA Journal*, Vol. 27, No. 2, 1989, pp. 201-210.
3. Castel, F., Kapania, R.K., "A beam element for aeroelastic analysis of damaged and undamaged wings.", a report for CCMS (Virginia Tech) CCMS 88-13.
4. Yang, T.Y., "Finite Element Structural Analysis", Prentice-Hall (1986).
5. Yang, T.Y., "Matrix displacement solution to elastica problems of beams and plates", *International Journal of Solids and Structures*, Vol.9, 1973, pp. 829-842.
6. Yang, T.Y., "Finite displacement plate flexure by the use of matrix incremental approach", *International Journal for Numerical Methods in Engineering*, Vol.4, pp. 415-432.



Element Degrees of Freedom

# AEROELASTIC STABILITY ANALYSIS IN MANEUVERING FLIGHT

Roberto Celi

Assistant Professor

Center for Rotorcraft Education and Research

Department of Aerospace Engineering

University of Maryland, College Park

## EXTENDED ABSTRACT

### Introduction and Problem Statement

The dynamic and aeroelastic problems of hingeless rotor helicopters have been the subject of a considerable amount of research in the past twenty years. Comprehensive reviews of such work have been published by Friedmann [1], Johnson [2], Ormiston [3], and Ormiston *et al.* [4]. One of the advantages of hingeless rotor helicopters over articulated rotor helicopters is greater agility. Therefore it is rather surprising that little or no information has been published on the aeroelastic stability of hingeless rotors in maneuvering flight.

The analytical and experimental studies on hingeless rotor aeroelastic stability have generally focused on steady, straight, 1-g level flight conditions. Maneuvering flight conditions affect the rotor dynamics mainly by changing the load factor, by changing the orientation of the resultant rotor forces and moments, and by introducing pitch and roll angular velocities. Secondary effects are due to the changing of pitch control settings, and the generation of sideslip angles. The effect of these factors on the aeroelastic stability of the rotor has been largely ignored in the published literature.

The objectives of the proposed paper are the following:

1. to present the results of a numerical study of the aeroelastic stability and response of a trimmed hingeless rotor in a steady coordinated turn,
2. to study the effects of steady stall and compressibility airfoil characteristics on the trim conditions of the aircraft, and on the aeroelastic stability of the rotor.

## Mathematical model

The rotor blades are modeled as isotropic, Bernoulli-Euler beams undergoing moderate deflections [5]. The nonlinear, partial differential equations of motion of the blade are discretized using a finite element formulation based on Galerkin method of weighted residuals [6].

The formulation of the rotor aeroelastic problem is based on the "implicit" approach introduced in Ref.[7] for the aerodynamic operator of the equations of motion, and extended in Ref.[8] to the inertia operator. Using this approach, the mathematical expressions for the aerodynamic and inertia loads are not expanded symbolically. Instead, they are built numerically as part of the solution process. This approach all but eliminates the tedious and error prone task of deriving long, explicitly expanded equations describing the complex nonlinear dynamics of the elastic blades attached to a rotating and translating hub.

The equations describing the trim state of the aircraft in the coordinated turn are based on those presented by Chen [9]:

1. Force equilibrium along the  $x$  body axis:

$$X = mg \sin \theta + m(qw - rv)$$

2. Force equilibrium along the  $y$  body axis:

$$Y = -mg \cos \theta \sin \phi + m(ru - pw)$$

3. Force equilibrium along the  $z$  body axis:

$$Z = -mg \cos \theta \cos \phi + m(pv - qu)$$

4. Roll moment equilibrium:

$$L = -I_{yz}(q^2 - r^2) - I_{xz}pq + I_{xy}pr - (I_y - I_z)qr$$

5. Pitch moment equilibrium:

$$M = -I_{xz}(r^2 - p^2) - I_{xy}qr + I_{yz}pq - (I_z - I_x)rp$$

6. Yaw moment equilibrium:

$$N = -I_{xy}(p^2 - q^2) - I_{yz}pr + I_{xz}qr - (I_x - I_y)pq$$

7. Constant portion of main rotor inflow:

$$\lambda = -\mu \tan \alpha_{HP} + \frac{C_T}{2\sqrt{\mu^2 + \lambda^2}}$$

8. Constant portion of tail rotor inflow:

$$\lambda_t = -\mu \tan \alpha_{HPt} + \frac{C_{Tt}}{2\sqrt{\mu_t^2 + \lambda_t^2}}$$

9. Kinematic relationship for bank angle:

$$\sin \phi = \frac{\dot{\psi}V}{g} (\cos \alpha \cos \phi + \sin \alpha \tan \theta) \cos \beta$$

10. Relationship between aerodynamic angle of attack  $\alpha$  and Euler pitch angle  $\theta$ :

$$\cos \alpha \cos \beta \sin \theta - (\sin \beta \sin \phi + \sin \alpha \cos \beta \cos \phi) \cos \theta = \sin \gamma$$

11. Relationship between roll rate and turn rate:

$$p = -\dot{\psi} \sin \theta$$

12. Relationship between pitch rate and turn rate:

$$q = \dot{\psi} \cos \theta \sin \phi$$

13. Relationship between yaw rate and turn rate:

$$r = \dot{\psi} \cos \theta \cos \phi$$

The airspeed components  $u$ ,  $v$ , and  $w$  in the aircraft body axes system  $x$ ,  $y$ ,  $z$  are given by:

$$u = V \cos \alpha \cos \beta \quad (1)$$

$$v = V \sin \beta \quad (2)$$

$$w = V \sin \alpha \cos \beta \quad (3)$$

The 13 unknowns are the collective pitch of the main rotor  $\theta_0$  and of the tail rotor  $\theta_t$ , the longitudinal and lateral cyclic pitch settings  $\theta_{1s}$  and  $\theta_{1c}$ , the steady state roll, pitch, and yaw rates  $p$ ,  $q$ , and  $r$ , the Euler pitch angle  $\theta$ , the aerodynamic angle of attack  $\alpha$ , the sideslip angle  $\beta$ , and the constant portion of the inflow for the main rotor  $\lambda$  and the tail rotor  $\lambda_t$ .

The turn rate  $\dot{\psi}$  ( $> 0$  for a right turn), the magnitude  $V$  of the aircraft velocity vector, and the climb angle  $\gamma$  ( $> 0$  for an ascending turn) define the turning flight condition, and are provided as input.

Detailed expressions for the force components  $X$ ,  $Y$ , and  $Z$ , and for the moment components  $L$ ,  $M$ , and  $N$ , are not presented in this abstract for brevity, but will be provided in the complete version of the paper.

Steady stall and compressibility effects are taken into account through the aerodynamic coefficients of the airfoil. Semi-empirical analytical expressions for the normal force coefficient  $c_n$ , the drag coefficient  $c_d$ , and the moment coefficient  $c_m$ , as a function of angle of attack  $\alpha$  and Mach number  $M$  have been presented by Beddoes for the NACA 0012 airfoil [10]. The values of  $c_n$ ,  $c_m$ , and  $c_d$  generated using these expressions are plotted in Figures 1, 2, and 3 respectively, for a range of values of  $\alpha$  and  $M$ . These expressions are used in the solution of both the coupled trim problem and the aeroelastic stability and response problem.

Three-dimensional tip effects are taken into account in an approximate way, by using Goldstein's circulation correction factor  $k$  [11, pp.103-110], and multiplying the normal force coefficient  $c_n$  and the moment coefficient  $c_m$  at a given blade section by  $k$ .

### Solution Technique

The solution process is divided into two phases, namely:

1. determination of the trim state of the helicopter in the turn, and

## 2. calculation of the aeroelastic response and stability of the rotor.

### *Phase I—Trim in coordinated turn*

The determination of the trim state of the helicopter is coupled with the calculation of the steady state equilibrium position of the rotor. For the trim calculations the system of nonlinear ordinary differential equations (ODE) of motion of the blade is transformed into a set of nonlinear *algebraic* equations using a classical, or global Galerkin method, as described in Ref. [12]. Before Galerkin method is applied, a modal coordinate transformation is performed. If  $m$  modes are used in the coordinate transformation, and each generalized coordinate is approximated with a Fourier series truncated at the  $n$ -th harmonic, then the application of Galerkin method results in the generation of  $m(2n + 1)$  nonlinear algebraic equations. The set of 13 trim equations, Eq. (1) through (13) is appended to those equations, and the combined system is solved simultaneously.

### *Phase II—Rotor aeroelastic stability and response*

For the solution of the rotor aeroelastic problem, the rotor is assumed to be attached to a hub of infinite mass, that rolls, pitches, and yaws at the rates calculated in the trim process. The problem of solving the system of nonlinear ODE of motion of the blades is transformed into that of solving a sequence of linearized ODE, using quasilinearization. Because the equations have periodic coefficients, the stability of the linearized system of ODE is calculated using Floquet theory. The details of the solution procedure, for the case of implicitly formulated aerodynamic and inertia loads, are presented in Refs. [7] and [8].

## Results

The results presented in this section refer to a soft-in-plane blade configuration, with fundamental, rotating, coupled natural frequencies of 0.73/rev, 1.12/rev, and 3.17/rev in lag, flap, and torsion respectively. The blades have uniform mass and stiffness properties along the span. In steady, straight and level flight the rotor is operating at a  $C_T = 0.005$ . The solidity is  $\sigma = 0.07$ . Blade precone, built-in twist, and cross-sectional offsets from the elastic axis are equal to zero.

The first set of results was obtained with a linear, incompressible airfoil model, and neglecting three dimensional aerodynamic effects. Results were

derived for values of the advance ratio  $\mu = 0.1, 0.2$ , and  $0.3$ , and for turn rates  $\dot{\psi} = 0, 0.1, 0.2, 0.4$ , and  $0.6$  rad/sec, corresponding to straight flight, and to one complete 360 degree turn in 63, 31, 16, and 11 seconds respectively. The load factors corresponding to the various combinations of speed and turn rate are summarized in Figure 4. Three coupled modes were used to calculate the trim condition. The modes were the first flap, the first lag, and the first torsion coupled modes. Each generalized modal coordinate was represented as a two harmonics Fourier series. Therefore  $m = 3$  and  $n = 2$ , for a total of 15 equations associated with the rotor elastic deformations. Including the 13 equations associated with the fuselage equations, the trim state of the helicopter is defined by a system of 28 algebraic equations. The quasi-Newton solver HYBRD [13] was used to solve the system. The solution required between 110 and 130 seconds of CPU time on an IBM 3081D mainframe.

The aeroelastic stability calculations were conducted using six coupled modes. Each generalized coordinate was represented as a ten harmonics Fourier series. The calculations were conducted at a fixed advance ratio, for increasing turn rate. The initial approximation to the response at a given turn rate was the solution at the previous turn rate; the initial approximation for the straight flight cases was a rigid blade. Two iterations of quasilinearization were sufficient for all but one of the turning flight conditions; three iterations were required for the straight flight conditions. Each iteration required 180-200 seconds of CPU time.

Figures 5 and 6 show the real part of the characteristic exponent of the first and second lag mode respectively, as a function of the advance ratio and turn rate. The real parts of the characteristic exponents are indicative of the damping, for a system with periodic coefficients. Figures 5 and 6 show that a right turn has a stabilizing effect on these two lowly damped modes, and that this effect becomes larger with increasing advance ratio. The first flap mode and the first torsion mode are essentially unaffected by the turn rate, therefore the appropriate results are not presented here. The second and third flap modes are somewhat destabilized by a right turn. The characteristic exponent of the second flap mode is shown in Figure 7. The damping of the second flap mode is so high that the mode remains well damped even at high load factors.

Additional results were obtained for the same blade configuration, using the nonlinear airfoil characteristics mentioned previously. Figures 8



through 10 show the real parts of the characteristic exponents of the first lag, second lag, and first torsion mode respectively. The advance ratio is  $\mu = 0.2$ , the turn rate is  $\dot{\psi} = 0.25$  rad/sec, and the thrust coefficient is  $C_T/\sigma \approx 0.13$ .

Stall and compressibility affect directly the stability of the blade by modifying the aerodynamic load distribution. Because rotary-wing aeroelastic stability problems are inherently nonlinear, stall and compressibility also affect the stability level of the blade *indirectly* by modifying the trim conditions of the helicopter, including the pitch control settings. In an attempt to separate the two mechanisms, Figures 8 through 10 each show three plots. The first refers to results obtained by neglecting stall and compressibility in both the trim and the aeroelastic stability calculations; in the second, stall and compressibility were modeled in the aeroelastic stability and response calculations but not in the trim calculations; in the third, stall and compressibility are modeled in both the trim and the aeroelastic calculations. Each of the figures shows the characteristic exponents computed at each iteration of quasilinearization. The number of iterations required to achieve convergence, and the size of the changes of the characteristic exponents as the iterations proceed, give an indication on the strength of the nonlinearities in the mathematical model.

Figures 8 through 10 indicate that stall and compressibility have a stabilizing effect on the damping of the first and second lag modes, and a destabilizing effect on the first torsion mode. Stall and compressibility increase the nonlinearity of the problem. This is indicated by the need for an additional iteration of quasilinearization when these effects are present. From a numerical standpoint, quasilinearization converged without problems when stall and compressibility were included, but the computer time required to complete one iteration increased to 450-500 seconds of CPU time. This is probably due to the smaller time steps that the variable-step, variable-order ODE solver [7] selected to deal with faster varying aerodynamic loads.

Additional results are currently being derived, to gain a better understanding of the physical mechanisms that contribute to modify the aeroelastic stability of the rotor. In particular, results are being derived to assess separately the effects of stall and of compressibility. These results will be presented in the final version of the paper.

## Conclusions

The study outlined in this abstract represents a first step toward a basic understanding of an important, yet largely ignored practical problem, namely the aeroelastic behavior of a hingeless rotor in maneuvering flight.

The preliminary results presented in this abstract indicate the following trends:

1. When stall and compressibility effects are neglected, the lag modes appear to be strongly stabilized by a turn. The stabilizing effect increases with increasing turn rate and advance ratio. Some of the higher modes may be destabilized by a turn at very high load factor, but their damping level in rectilinear flight is high, and they remain stable in a turn.
2. Preliminary results on the effect of stall and compressibility suggest that the damping of the lag modes increases when these effects are taken into account. All the remaining modes are destabilized, but not to the extent that they become unstable. Stall and compressibility act directly by modifying the aerodynamic loads, and indirectly by modifying the helicopter trim condition.
3. Stall and compressibility increase the nonlinearity of the aeroelastic problem. Quasilinearization still converges reliably, but the computer time required to complete an iteration increases considerably.

## References

- [1] Friedmann, P.P., "Recent Trends in Rotary-Wing Aeroelasticity," *Vertica*, Vol. 11, (1), 1987.
- [2] Johnson, W., "Recent Developments in the Dynamics of Advanced Rotor Systems," *Vertica*, Vol. 10, (1), 1986, pp. 72-107 (Part I), and Vol.10, (2), 1986, pp. 109-150 (PartII).
- [3] Ormiston, R.A., "Investigation of Hingeless Rotor Stability," *Vertica*, Vol 7, (2), 1983, pp. 143-182.

- [4] Ormiston, R.A., Warmbrodt, W.G., Hodges, D.H., and Peters, D.A., "Rotorcraft Aeroelastic Stability," *Proceedings of the NASA/Army Rotorcraft Technology Conference, Vol.I—Aerodynamics, and Dynamics and Aeroelasticity*, NASA Conference Publication 2495, February 1988, pp.353-529.
- [5] Shamie, J., and Friedmann, P., "Effect of Moderate Deflections on the Aeroelastic Stability of a Rotor Blade in Forward Flight," Paper No.24, *Proceedings of the Third European Rotorcraft Forum*, Aix-en-Provence, France, September 1977.
- [6] Straub, F.K., and Friedmann, P., "Application of the Finite Element Method to Rotary Wing Aeroelasticity," NASA CR-165854, February 1982.
- [7] Celi, R., and Friedmann, P., "Rotor Blade Aeroelasticity in Forward Flight with an Implicit Aerodynamic Formulation," *AIAA Journal*, Vol. 26, December 1988, pp. 1425-1433 .
- [8] Celi, R., "Effect of Hingeless Rotor Aeroelasticity on Helicopter Trim and Longitudinal Stability Using Quasilinearization," Paper AIAA-88-4366-CP, 1988 AIAA Atmospheric Flight Mechanics Conference, Minneapolis, Minnesota, August 1988.
- [9] Chen, R.T.N., and Jeske, J.A., "Kinematic Properties of the Helicopter in Coordinated Turns," NASA Technical Paper 1773, April 1981.
- [10] Beddoes, T.S., "Representation of Airfoil Behavior," *Vertica*, Vol. 7, No. 2, 1983.
- [11] Bramwell, A.R.S., *Helicopter Dynamics*. Edward Arnold, 1976.
- [12] Celi, R., "Aeroelastic Effects on Stability and Control of Hingeless Rotor Helicopters." Paper No.76, *Proceedings of the Fourteenth European Rotorcraft Forum*, Milan, Italy, September 1988.
- [13] More, J.J., Garbow, B.S., and Hillstrom. K.E., "User Guide for MINPACK-1," Argonne National Labs Report ANL-80-74, 1980.

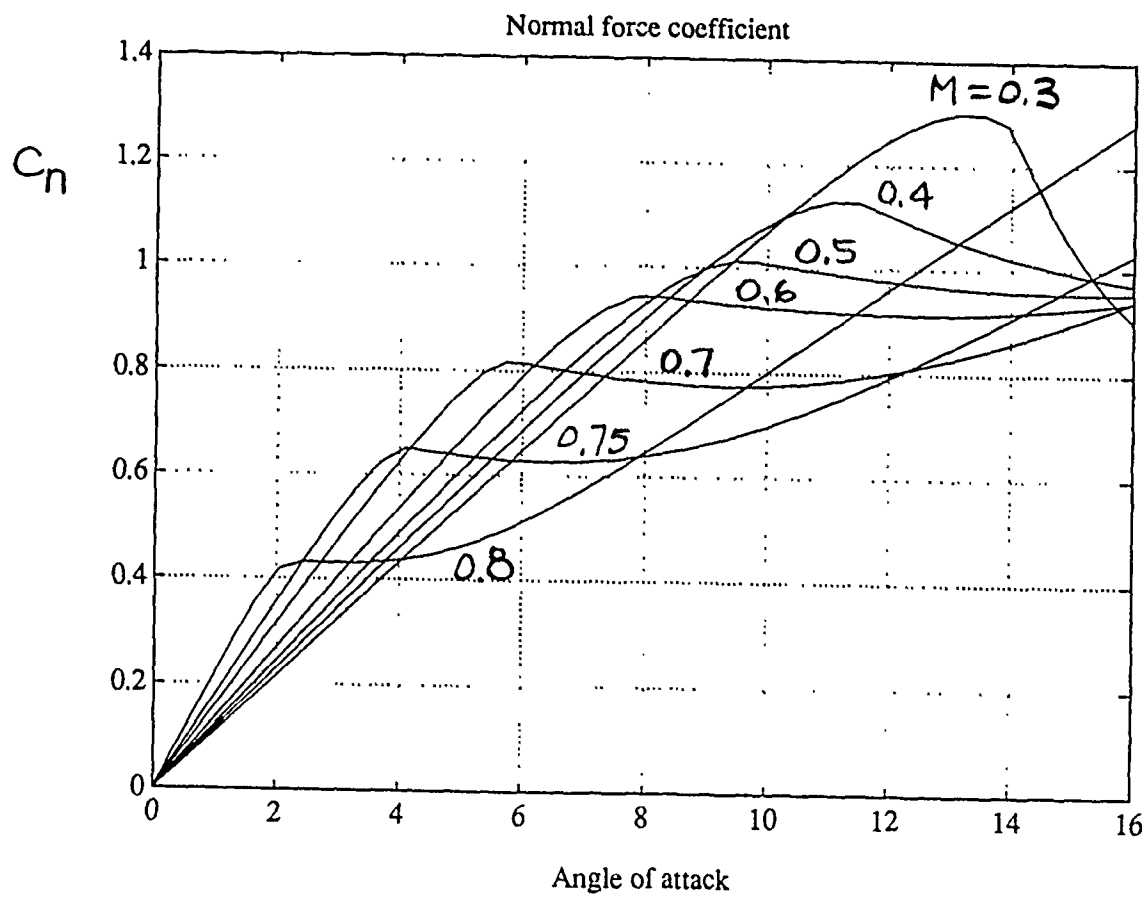


FIGURE 1

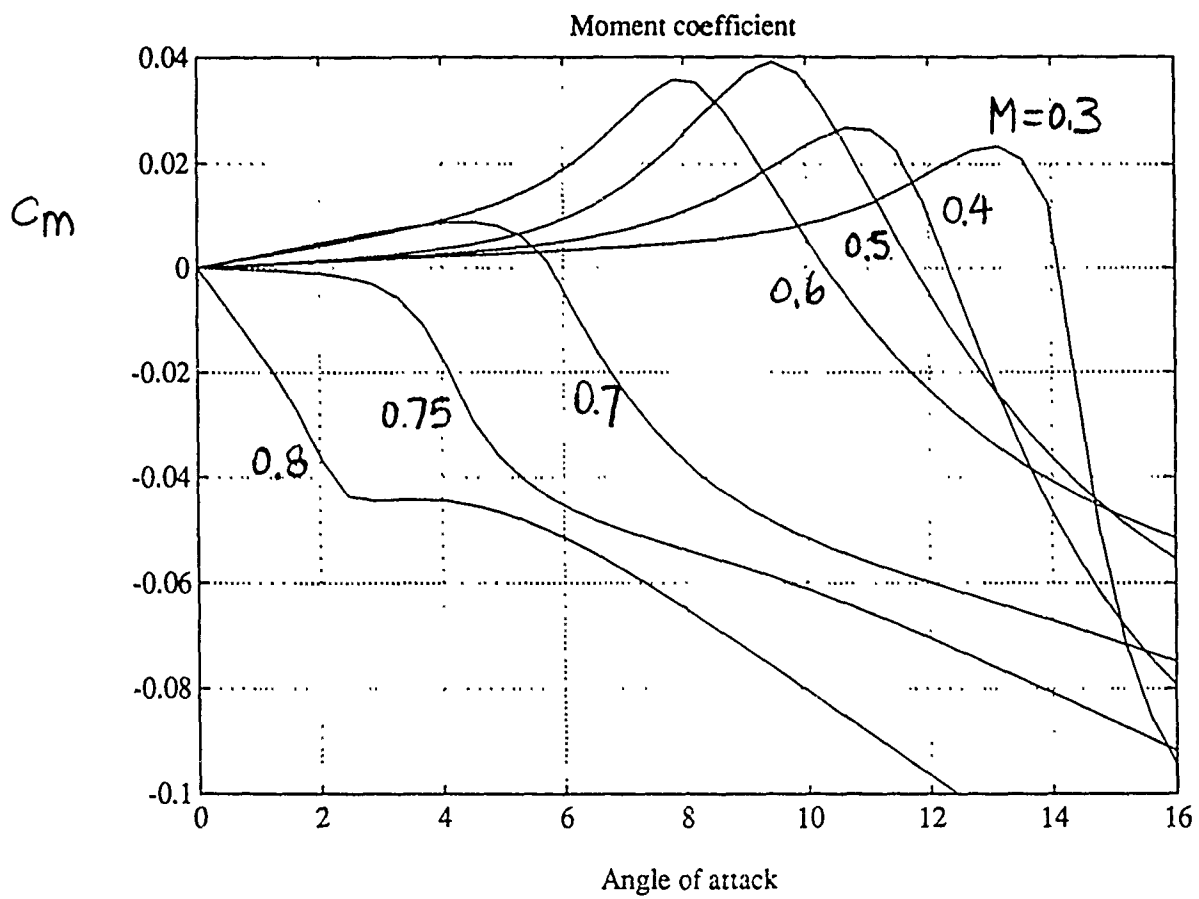


FIGURE 2

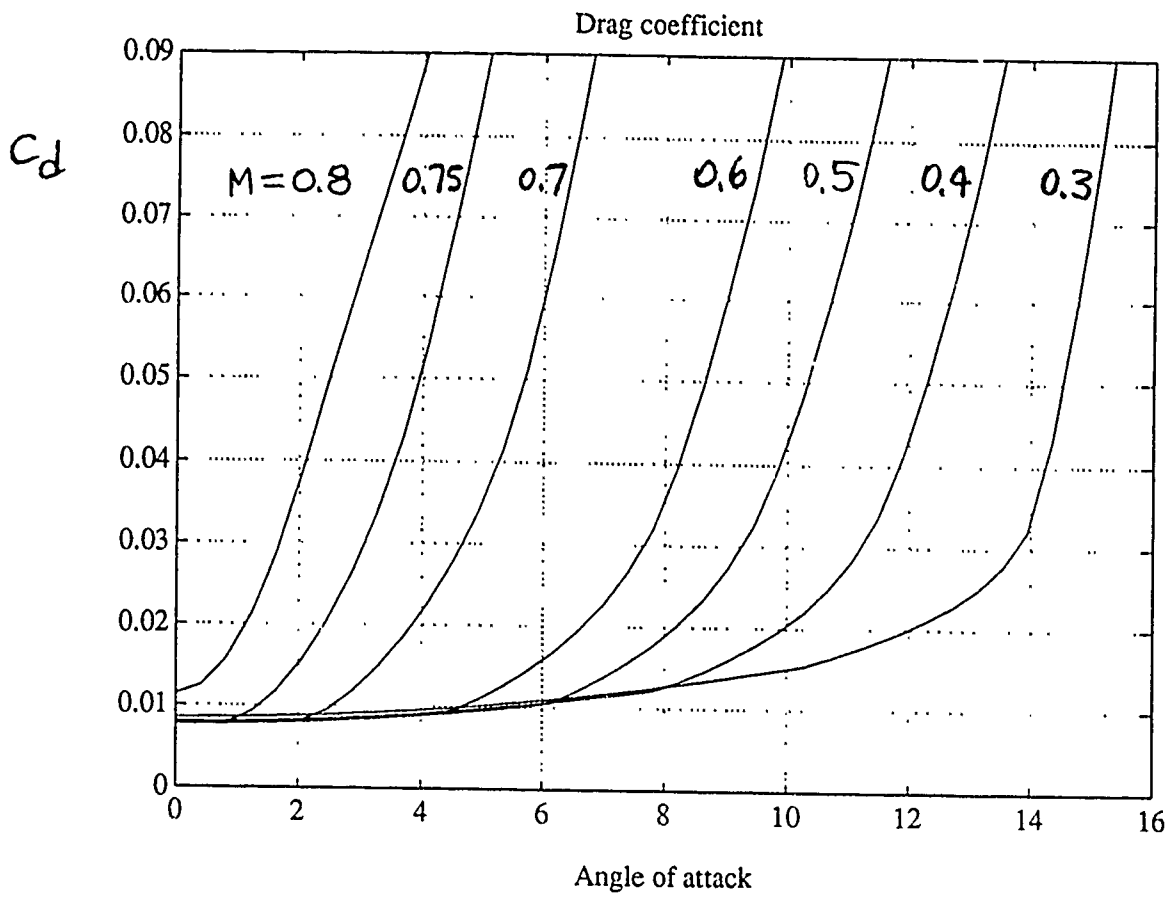


FIGURE 3

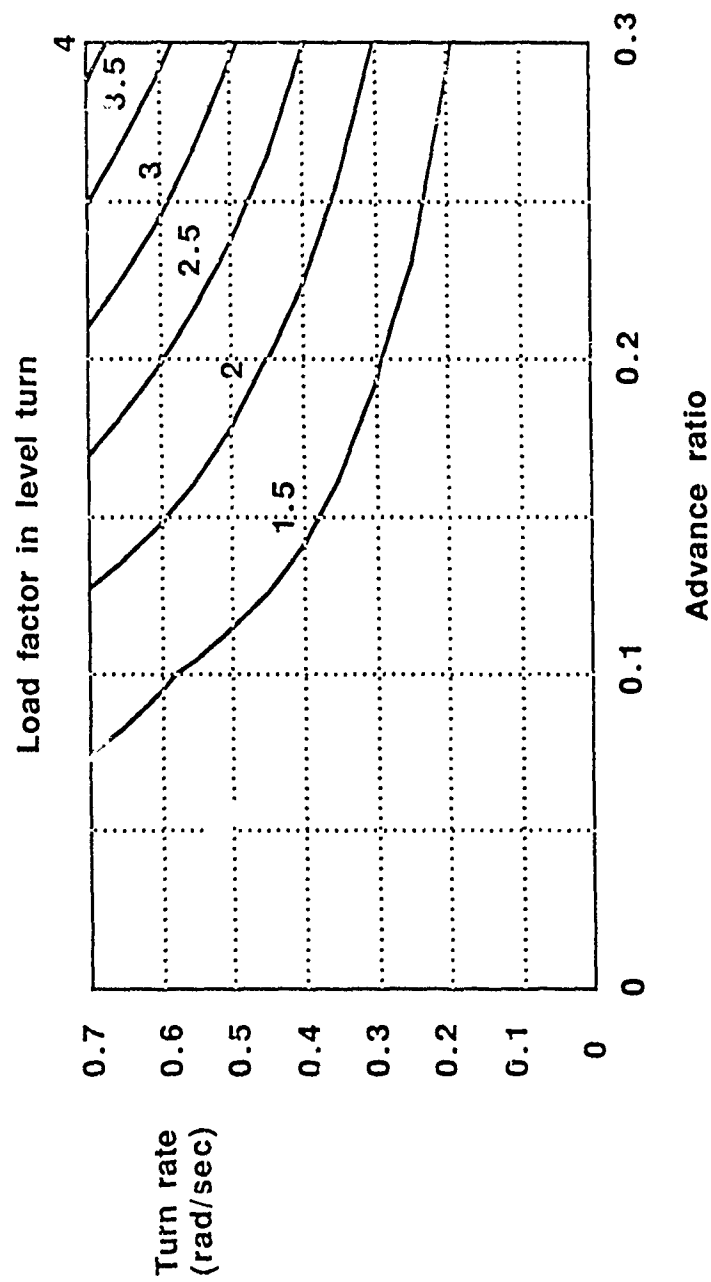


FIGURE 4

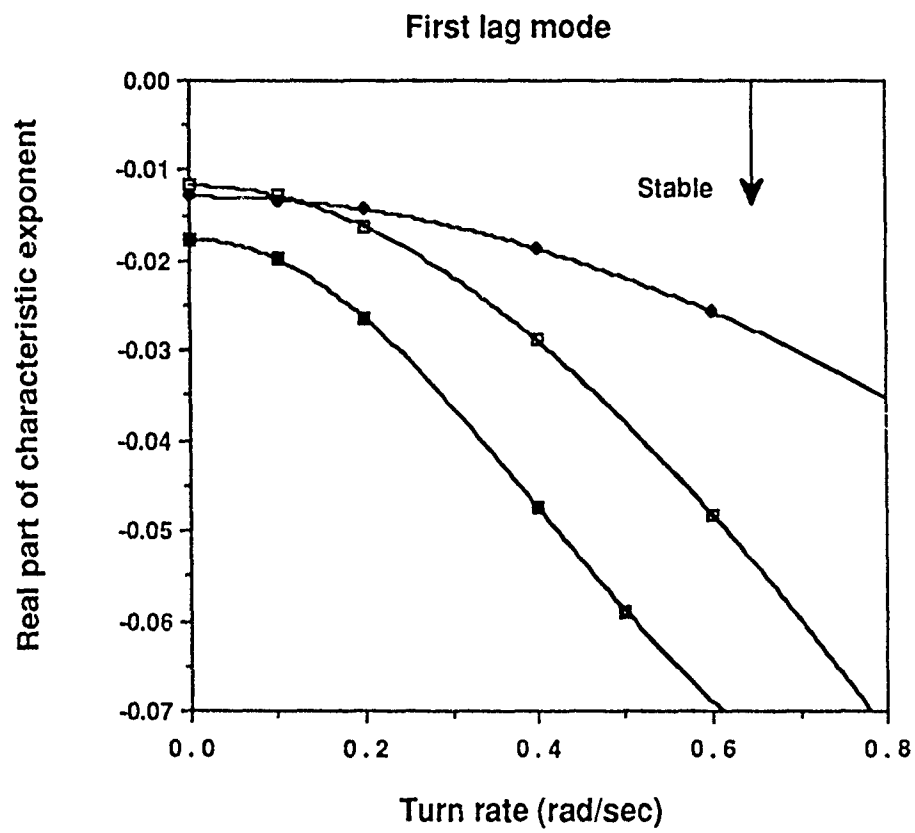


FIGURE 5



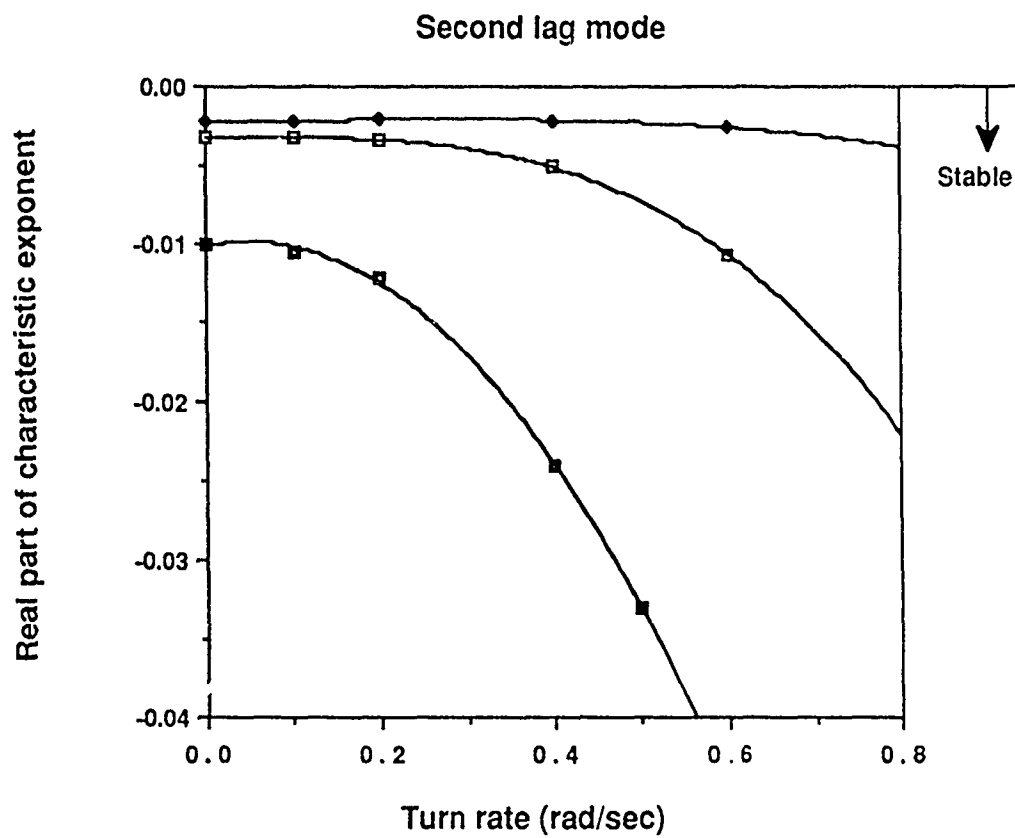


FIGURE 6

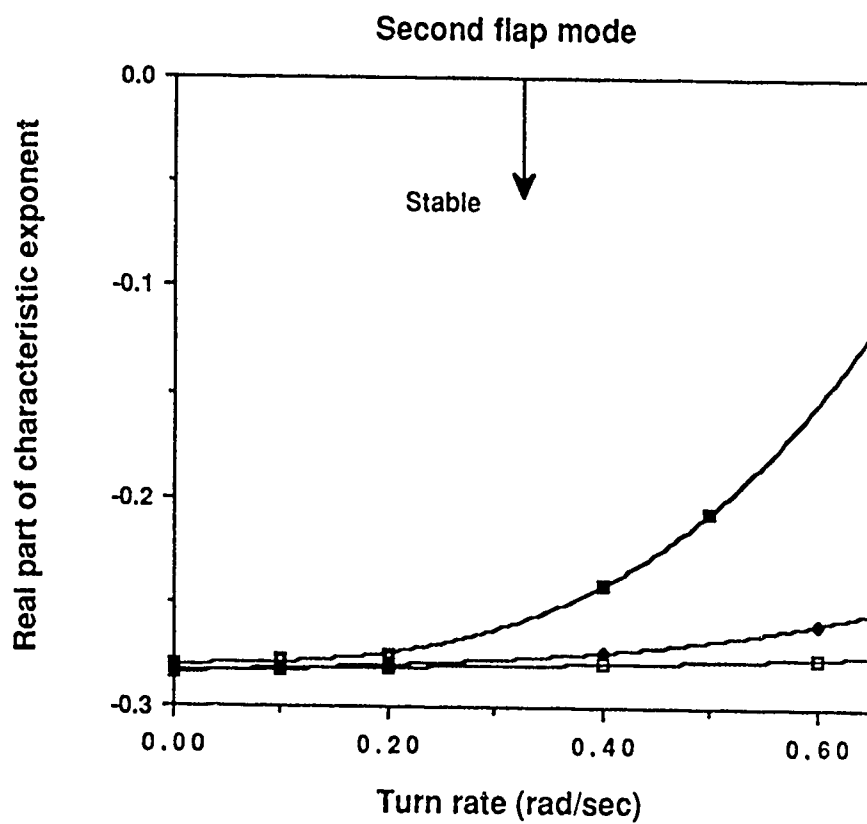
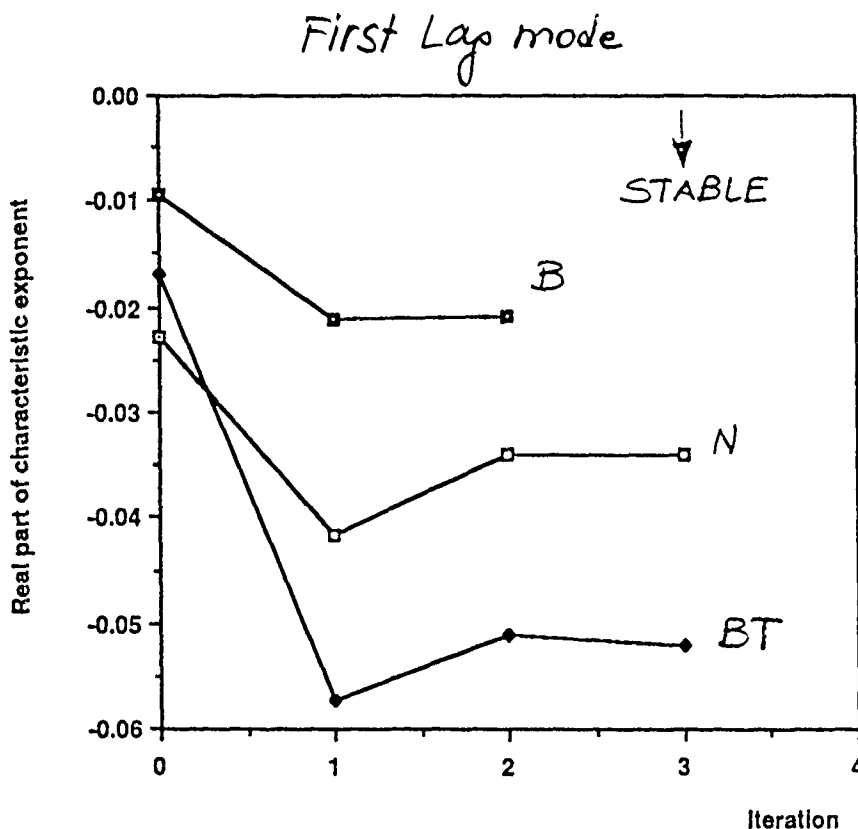


FIGURE 7



Advance ratio  $\mu = 0.2$   
 Turn rate  $\dot{\psi} = 0.25$   
 rad/sec

$$\frac{C_T}{\sigma} \approx 0.13$$

B - Baseline (linear incompressible airfoil characteristics)

BT - Linear incompressible airfoil characteristics for trim only - Nonlinear & compressible for aeroelastic analysis

N - Nonlinear and compressible airfoil characteristics for both trim and aeroelastic analysis

FIGURE 8

# Second Lap Mode

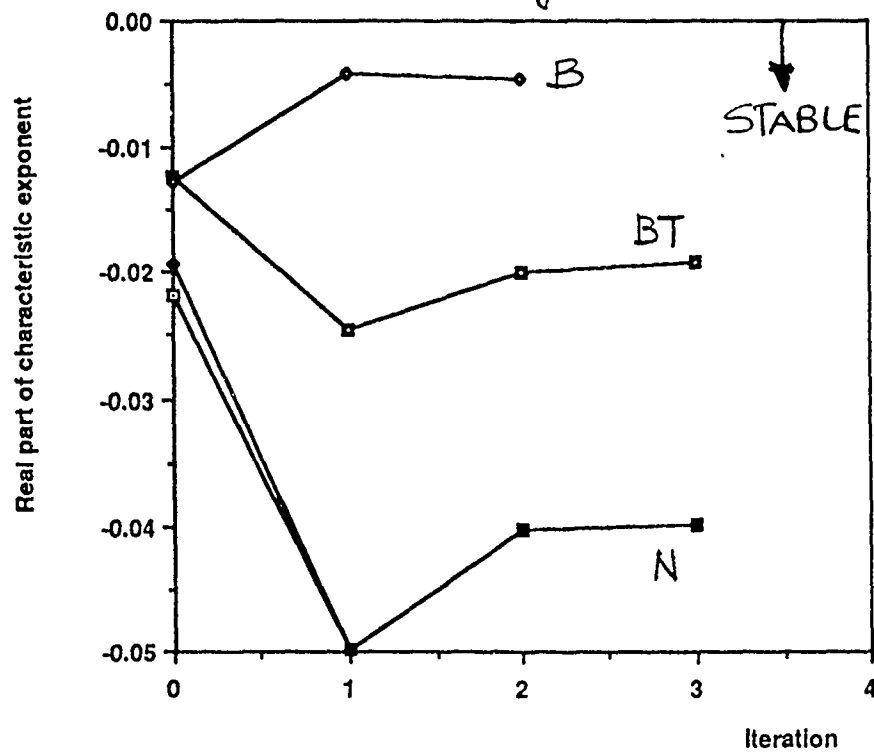


FIGURE 9

First Torsion mode

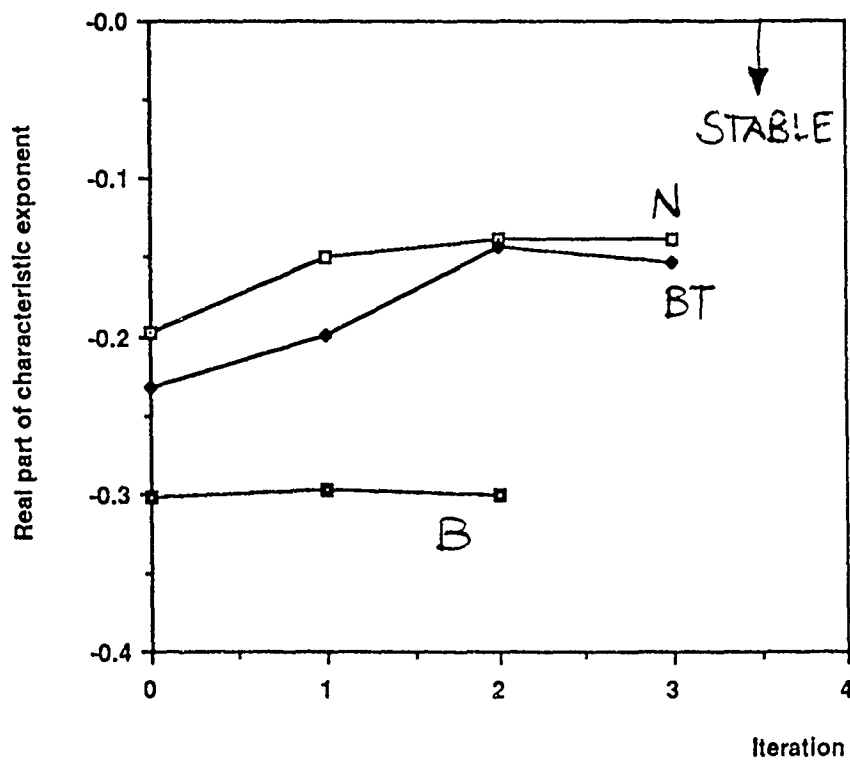


FIGURE 10

Aeroelastic Stability of Multiple  
Load Path Rotor Blades

By

V. R. Murthy

Associate Professor

Department of Mechanical and Aerospace Engineering

139 Link Hall

Syracuse University

Syracuse, N.Y. 13244

and

Daniel M. Lauzon

Presently with McDonnell Douglas Helicopter Company

## Aeroelastic Stability of Multiple Load Path Rotor Blades

The bearingless rotorcraft offers reduced weight, structural simplicity, and superior flying qualities. Bearingless rotor technology has been successfully applied to the tail rotors of the Blackhawk and S-76 helicopters by Sikorsky. Boeing Vertol built the first successful bearingless main rotor and flew it in 1978. Most of the next generation rotorcraft are likely to be designed with bearingless hubs.

All practical designs of bearingless rotors have multiple-load-path hubs. The bearingless rotor tested by Boeing Vertol has three load paths: two fiberglass flexbeams and a filament wound torque tube.

Because of the multiple load paths, the dynamic behavior of bearingless rotors is significantly different than conventional rotors. It is important, therefore, to have the capability to accurately analyze bearingless rotors and how they affect the stability of the entire helicopter.

CAMRAD ( Comprehensive Analytical Model for Rotorcraft Aerodynamics and Dynamics) is a comprehensive rotorcraft analysis program developed at NASA-Ames. The program utilizes new technology to analyze a wide range of rotorcraft problems. This includes the trim solution, performance, loads and noise, stability derivatives and handling qualities, aeroelastic stability, and vibration and gust response.

CAMRAD is limited, however, to single load path modelling. The axial degree of freedom for blade deformation, which is important for multiple load paths, is also not included.

The CAMRAD approach to solving the elastic blade equations is termed the modified Galerkin's method. Exact, nonrotating beam solutions are used in a Galerkin's procedure to solve the rotating beam problem approximately.

Procedures similar to the ones that exist in CAMRAD are being developed for multiple-load-path blades. Once the procedures are developed and validated, it will be possible to extend the CAMRAD procedures to include multiple-load-path bearingless blades. Application of the modified Galerkin's method to multiple-load-path blades has been completed and the results are shown in the next five pages for a model rotor tested by Dawson. Work is in progress for obtaining the trim solution.



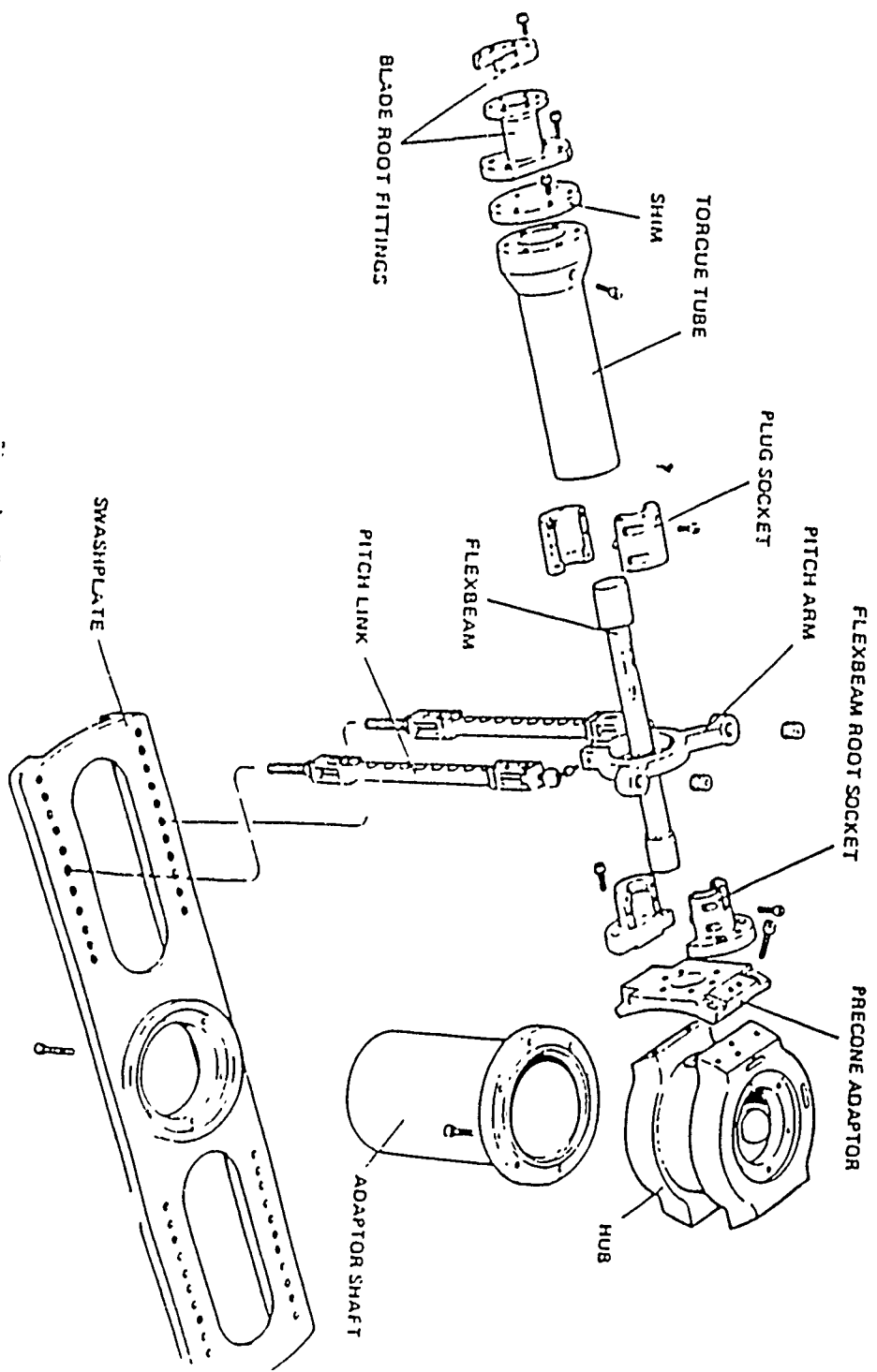


Fig. 1 Dawson Rotor Hub

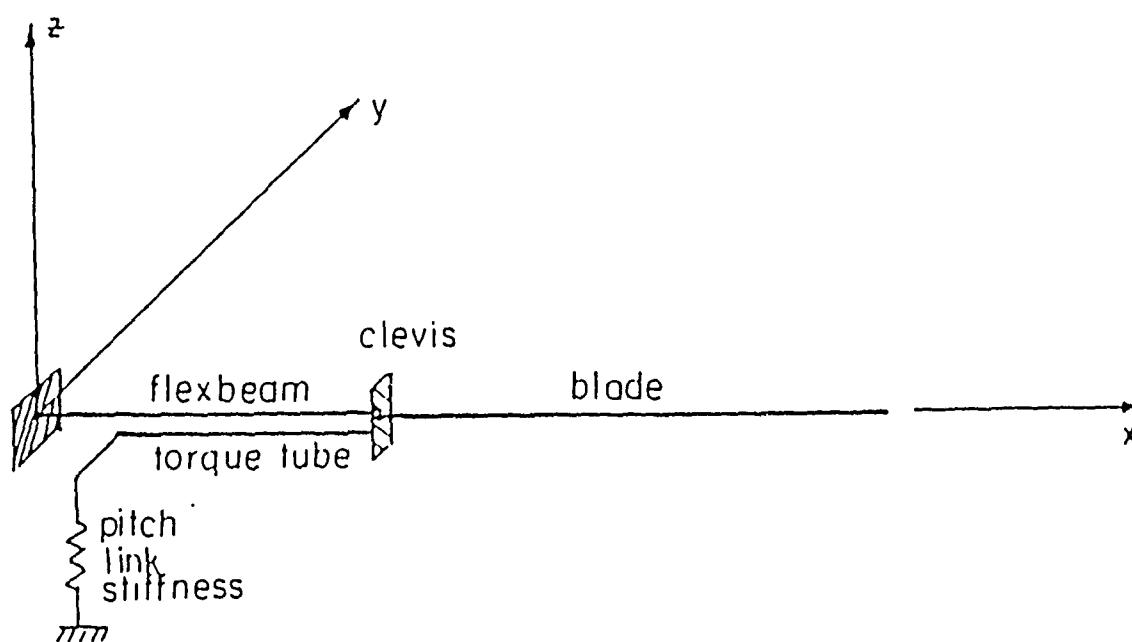


Fig. 2 Dawson rotor model with pitch link

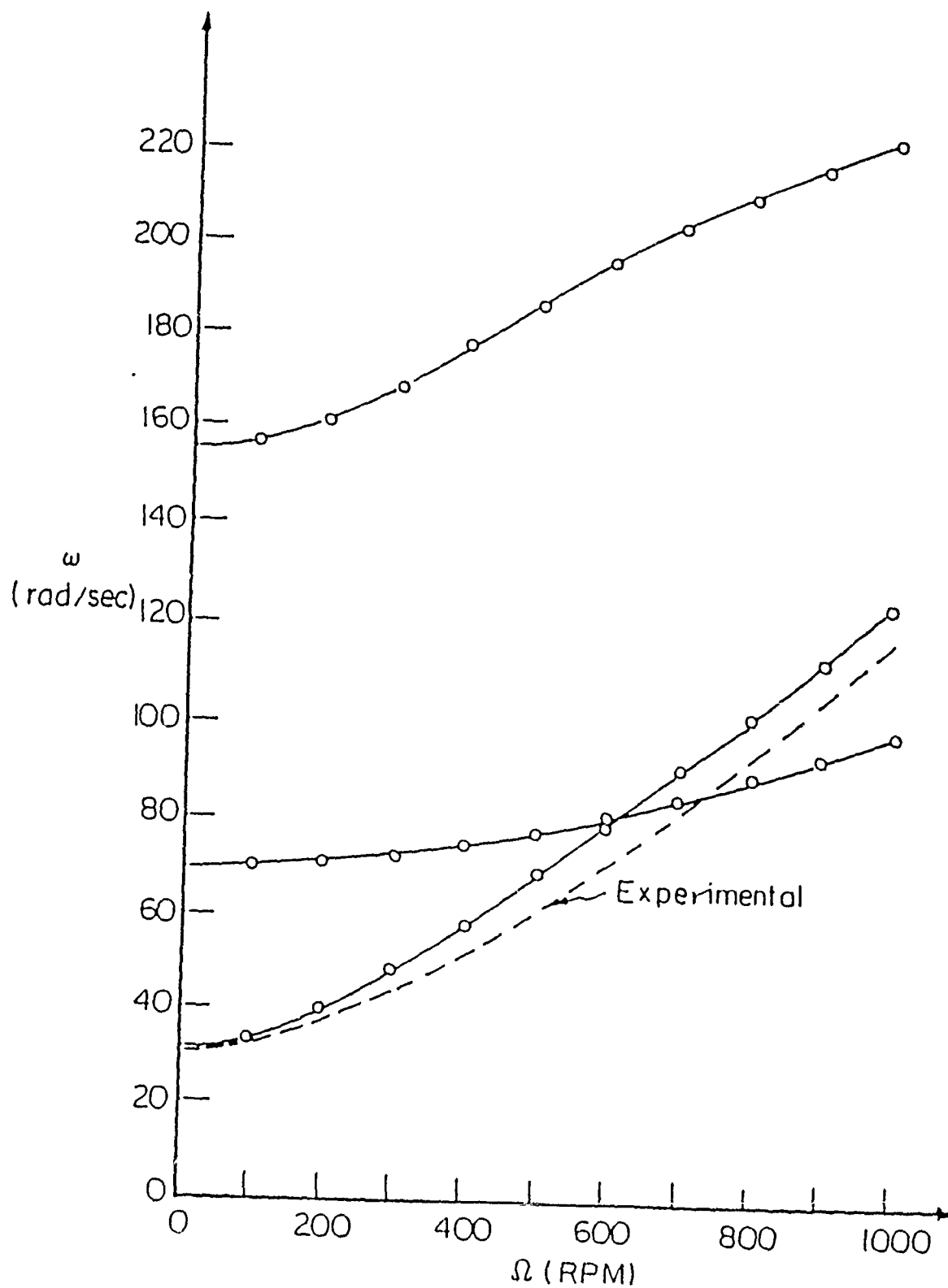


Fig. 3 Fan plot for Dawson rotor with pitch link

Table 1. Dawson Rotor Data

Rotor Property Profile					
Station (in)	mass/length (lbm/in)	El(flap) $10^6(lb - in^2)$	El(chord) $10^6(lb - in^2)$	GJ $10^6(lb - in^2)$	I(polar) (lbm - in <sup>2</sup> /in)
Flexbeam and Root Hardware					
0.0	1.7	44.9	27.3	20.7	704
1.4	1.7	44.9	27.3	20.7	704
1.653	.813	37.2	25.7	17.5	534
1.826	.738	44.7	25.2	10.7	831
2.158	.862	25.4	20.6	30.2	449
2.159	.5	72.1	72.1	10.9	141
2.358	.5	72.1	72.1	10.9	141
2.359	.18	863	863	3.76	0169
3.013	.18	863	863	3.76	0169
3.014	.147	0008	00421	000066	0178
3.158	.147	00084	00127	000066	0178
3.159	.28327	00084	00127	000066	000278
7.014	.24127	00084	00427	000066	000278
Torque Tube					
3.200	.281	12.1	26.7	3.98	.377
3.599	.281	12.1	26.7	3.98	.377
3.600	.0578	1.75	1.75	7.16	0193
6.871	.0578	1.75	1.75	7.16	0193
6.872	.239	2.3	2.3	177	0156
7.014	.239	2.3	2.3	177	0456
Blade and Clevis Hardware					
7.014	.268	3.02	3.02	2.31	120
7.309	.350	5.24	5.24	4.04	209
7.643	.350	5.24	5.24	1.04	209
7.644	.413	8.87	8.87	6.29	324
7.943	.413	8.87	8.87	6.29	324
7.944	.222	1.77	3.66	2.18	055
8.005	.22	1.77	3.66	2.18	055
8.133	.231	1.77	3.66	2.18	055
8.134	.0529	1.24	1.24	0959	00247
8.599	.0510	1.24	1.24	0959	00243
8.781	.191	1.24	1.24	0959	0394
8.930	.191	1.24	1.24	0959	0394
8.931	.0243	0459	0459	0238	000728
8.989	.0296	0538	0538	0288	000867
8.99	.119	0538	0538	0288	0117
9.049	.118	.0991	.0991	0616	0155
9.05	.155	.0991	.0991	0616	0195
9.179	.16	.101	.101	0596	0297
9.18	.0447	.101	.101	0596	00172
9.284	.047	.102	.102	0568	00167
9.285	.0332	0526	0526	0187	000684
9.445	.00763	00228	0617	0012	000711
11.445	.00758	00228	0617	0012	000869
35.445	.00758	00228	0617	0012	000869

Steel:  $\rho = .283 \text{ lbm/in}$ ,  $E = 29.10^6 \text{ lb/in}^2$ ,  $G = 11.10^6 \text{ lb/in}^2$

Titanium:  $\rho = .160 \text{ lbm/in}$ ,  $E = 16.10^6 \text{ lb/in}^2$ ,  $G = 6.2.10^6 \text{ lb/in}^2$

Kevlar:  $\rho = .050 \text{ lbm/in}$ ,  $E = 11.10^6 \text{ lb/in}^2$ ,  $G = 0.3.10^6 \text{ lb/in}^2$

Table 2. Dawson Rotor Natural Frequencies in rad/sec

NO PITCH LINK  $\Omega = 0$  RPMMODIFIED  
GALERKIN'S  
METHOD

TRIG.	POLY.	HASTMAN	(REF. 17) EXPER.
28.94821	28.80157	28.96059	29.4681
72.40210	71.19517	70.94667	68.7380
114.8791	114.5969	114.2242	123.9672
150.2997	148.8603	151.4672	155.9672

WITH PITCH LINK  $\Omega = 1$  RPMMODIFIED  
GALERKIN'S  
METHOD

TRIG.	POLY.	HASTMAN	(REF. 17) EXPER.
31.76623	31.0492	30.12552	30.6619
69.36568	68.6710	70.24667	69.9319
155.4950	152.3382	151.1931	155.8858
216.0065	214.7421	216.9887	240.5293

 $(K_{PL} = 2690 \text{ lb./in.})$

**COUPLED LONGITUDINAL, BENDING, AND  
TORSIONAL VIBRATIONS OF A CRACKED,  
ROTATING, TIMOSHENKO SHAFT**

K. R. Collins<sup>1</sup>, R. H. Plaut<sup>1</sup>, and J. Wauer<sup>2</sup>

---

<sup>1</sup>Charles E. Via, Jr. Department of Civil Engineering, Virginia Polytechnic Institute and State University, Blacksburg, VA 24061, U.S.A.

<sup>2</sup>Institut für Technische Mechanik, Universität Karlsruhe, D-7500 Karlsruhe 1, West Germany.

## ABSTRACT

Many papers have been published which analyze the behavior of cracked rotating shafts [1]. The present investigation is more general than previous work in several respects. The most important are the inclusion of (a) shear deformation and rotatory inertia (Timoshenko model), (b) longitudinal, bending, and torsional motions, and (c) three types of damping.

Except for a single transverse crack, the shaft is assumed to be uniform and to have simply supported ends. Its axis need not be horizontal, and the centroid of its cross-sectional area need not coincide with its center of mass. The material is assumed to be viscoelastic, which models internal damping. External viscous damping is also included. In addition, when the crack is closed, dry friction acts at the crack face.

The crack is assumed to be open when the axial strain at the crack location is positive, and closed when the axial strain there is negative. Following an idea developed by Petroski [2], the discontinuities in stiffness and damping at the crack are represented by concentrated forces. The magnitudes of these forces are determined from the compliance matrix associated with the crack, which was obtained by the use of fracture mechanics in Reference [3].

The governing equations of motion consist of six coupled, partial differential equations involving three deflections and three rotations, which are functions of time and of position along the shaft [4]. The equations are linear during each period of time in which the axial strain has the same sign; when it changes sign (i.e., when the crack opens or closes), some of the stiffness and damping coefficients change. Hence the problem is nonlinear.

Galerkin's method is applied with two terms for each of the deflection and rotation functions. This leads to a system of 12 ordinary differential equations for the time-varying amplitudes of the assumed global shape functions. The system is solved with the use of numerical integration. Time histories of the deflections and rotations are computed and their frequency spectra are obtained.

Attention is focused on the steady-state response of the shaft. The effects of the crack depth and the angular velocity are investigated. Exchanges of energy between the longitudinal, bending, and torsional motions are studied. Both free and forced vibrations are examined.

In conclusion, then, this paper generalizes previous work on cracked rotating shafts in several respects. The results demonstrate the effect of cracks on shaft response. They improve our understanding of the behavior of cracked shafts, and can be utilized in the detection of cracks before the occurrence of failure.

#### REFERENCES

- [1] Wauer, J., "On the Dynamics of Cracked Rotors - A Literature Survey," Applied Mechanics Reviews, to appear.
- [2] Petroski, H. J., "Simple Static and Dynamic Models for the Cracked Elastic Beam," International Journal of Fracture, Vol. 17, 1981, pp. R71-R76.
- [3] Papadopoulos, C. A., and Dimarogonas, A. D., "Coupled Longitudinal and Bending Vibrations of a Rotating Shaft with an Open Crack," Journal of Sound and Vibration, Vol. 117, 1987, pp. 81-93.
- [4] Wauer, J., "Modelling and Formulation of Equations of Motion for Cracked Rotating Shafts," International Journal of Solids and Structures, to appear.



# NONPLANAR VIBRATIONS OF A CANTILEVER COMPOSITE BEAM UNDER PLANAR HARMONIC BASE-EXCITATION

Perng-Jin F. Pai and Ali H. Nayfeh  
Department of Engineering Science and Mechanics  
Virginia Polytechnic Institute and State University  
Blacksburg, Virginia 24061

## ABSTRACT

The dynamic behavior of a long slender beam is of interest in connection with helicopter rotor blades, lengthy robot manipulators, spacecraft antennae, flexible satellites, wind turbine blades, and other systems that perform large and/or complex motions.

In this paper, Newton's second law is used to develop the nonlinear equations of motion and boundary conditions describing the flexural-flexural-torsional vibration of composite beams. The equations contain structural coupling terms and cubic nonlinearities due to curvature and inertia. Three consecutive Euler angles are used to evaluate the transformation matrix between the deformed and undeformed states. Because the twisting-related Euler angle  $\phi$  is not an independent Lagrangian coordinate, the torsional equation is used to define the real twist angle.

The nonplanar responses of a cantilevered, symmetrically laminated graphite-epoxy composite beam subject to lateral harmonic base excitations (see Fig. 1) are investigated using the derived nonlinear coupled integro-differential equations of motion. A powerful technique based on the state space concept and the fundamental matrix method is used to solve for the linear mode shapes. Then a combination of the Galerkin procedure and the method of multiple scales is used to construct a first-order uniform expansion for the case of a primary resonance and a one-to-one internal resonance in which the linear natural frequency of flexural vibrations in one plane is approximately equal to the linear natural frequency of flexural vibrations in the other plane. We determine the ranges of the driving frequency

which result in unstable planar motions and describe quantitatively the ensuing nonplanar motions. We study some of the main characteristics of the nonplanar motions and investigate the possible bifurcations of the response amplitudes when the excitation frequency is varied. We also demonstrate the existence of Hopf bifurcations and the nonexistence of periodic motions for certain excitation parameters. For different range of parameters, the nonplanar motions can be steady whirling motions, whirling motions of the beating type, or chaotic motions.

To the first-order approximation the response of the beam is given by

$$v(s,t) = v_m(s)a_1(t) \cos(\Omega t - \gamma_1) + \dots \quad (1)$$

$$w(s,t) = w_n(s)a_2(t) \cos(\Omega t - \gamma_2) + \dots \quad (2)$$

where  $v_m(s)$  and  $w_n(s)$  are the linear mode shapes of the beam,  $\Omega$  is the excitation frequency, and

$$2\omega_{1m}a_1' + [R_1 + R_2a_2^2 \sin 2(\gamma_1 - \gamma_2)]a_1 = 0 \quad (3)$$

$$[2\omega_{1m}\gamma_1' - R_3 - R_4a_1^2 + R_5a_2^2 + R_2a_2^2 \cos 2(\gamma_1 - \gamma_2)]a_1 = 0 \quad (4)$$

$$2\omega_{2n}a_2' + [E_1 + E_2a_1^2 \sin 2(\gamma_1 - \gamma_2)]a_2 - \beta_8 f \omega_{2n}^2 \sin \gamma_2 = 0 \quad (5)$$

$$[2\omega_{2n}\gamma_2' - E_3 - E_4a_2^2 - E_5a_1^2 - E_2a_1^2 \cos 2(\gamma_1 - \gamma_2)]a_2 - \beta_8 f \omega_{2n}^2 \cos \gamma_2 = 0 \quad (6)$$

Here,  $\omega_{1m}$  and  $\omega_{2n}$  are the linear undamped frequencies of the interacting modes,  $f$  is a measure of the excitation amplitude, and the  $\beta_8$ ,  $R_i$ , and  $E_i$  are constants that are given in quadrature.

Periodic solutions of the beam correspond to the fixed points (i.e., constant solutions) of (3)-(6), which in turn correspond to  $a_1' = a_2' = \gamma_1' = \gamma_2' = 0$ . Thus, (3)-(6) reduce to a set of algebraic equations that can be solved numerically.

Figures 2 and 3 show representative frequency-response curves of the first and second modes. The results show that planar motions in the z-direction may be destabilized by disturbances in the y-direction, resulting in vibrations in both planes. For certain beam and load parameters, nonplanar responses can be either (a) unsteady whirling motions (see Fig. 4(a)-(c)) (lengths and directions of the axes of the elliptical route continuously change and the motion also shows a low-frequency twisting motion), or (b) steady whirling motions (see Fig. 4(d)) (the principal axes of the elliptical route are not parallel to the y- or z-axes), or (c) chaotic motions. The unsteady whirling motions may be periodic if the period of the amplitudes is commensurable with that of the base motion. But this periodicity is not obvious because the twisting frequency is too low. Figure 5 shows the frequency-response curves of a beam with different modes in two principal directions.

### Acknowledgement

This work was supported by the Air Force Office of Scientific Research under Grant No. F49620-87-C-0088 and the National Science Foundation under Grant No. MSM-8521748.

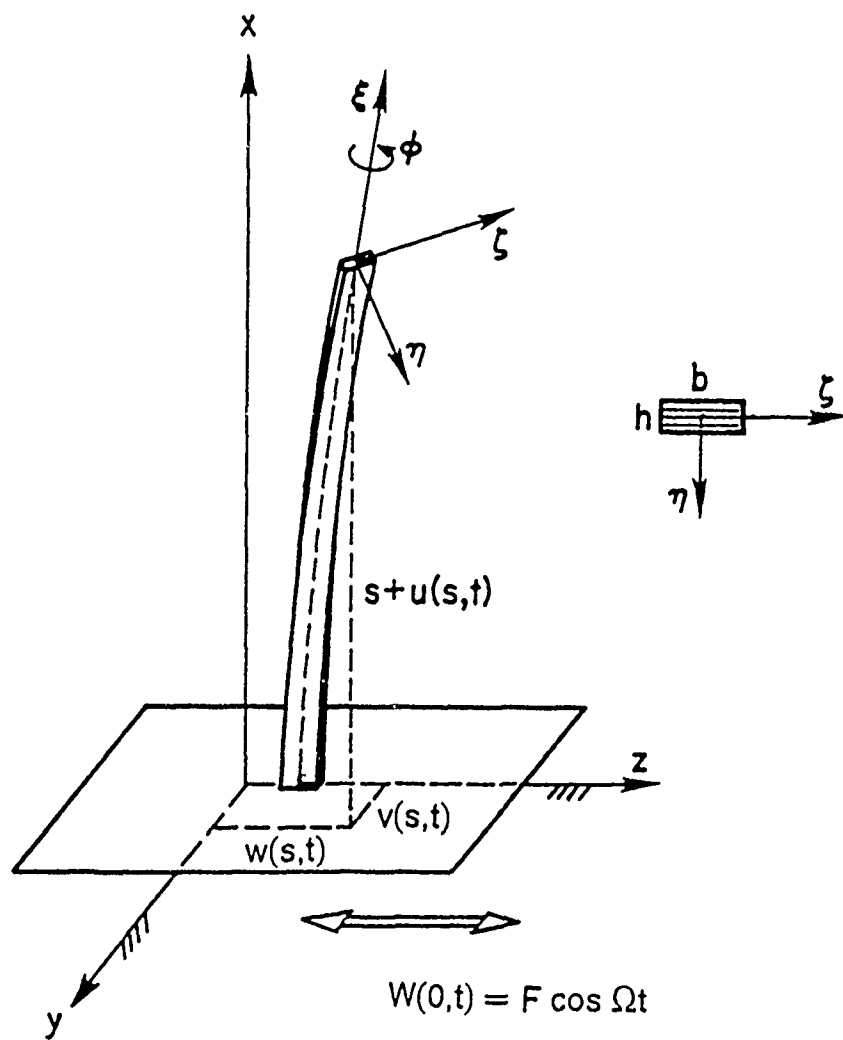


Figure 1. Coordinate systems :  $x$ - $y$ - $z$  = inertial reference frame;  $\xi$  -  $\eta$  -  $\zeta$  = principal axes of the beam's cross section at position  $s$ , which are fixed on the cross section.

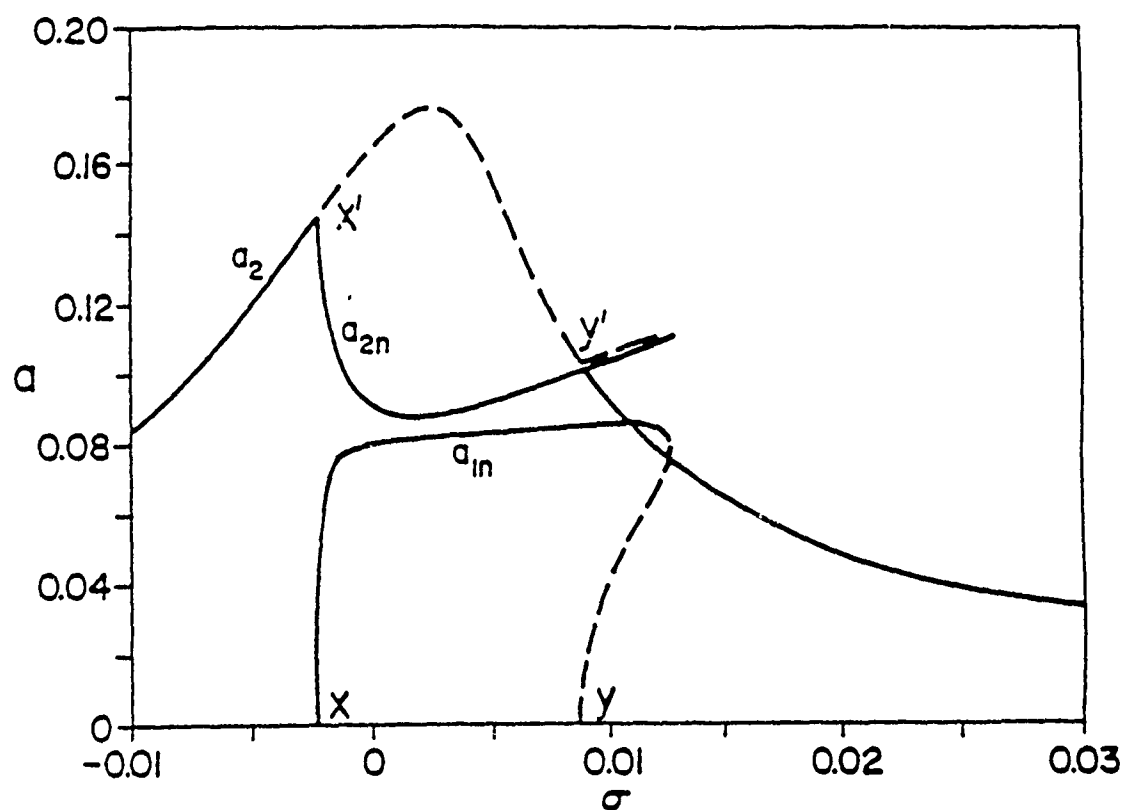


Figure 2. Response curves of the first mode for a beam with an aspect ratio  $b/h \approx 1.0$  : mode (1,1) ,  $\omega_{11} = \omega_{21}$  ,  $\delta_0 = 0.0$  ,  $\delta_2 = -0.01$  ,  $\mu = 0.04$  ,  $\beta_s f = 0.002$  ,  $\beta_r = 0.6489$  ;  $a_2$  = planar response amplitude;  $a_{1n}$  ,  $a_{2n}$  = nonplanar response amplitudes; (—) stable, (---) unstable with at least one eigenvalue being positive.

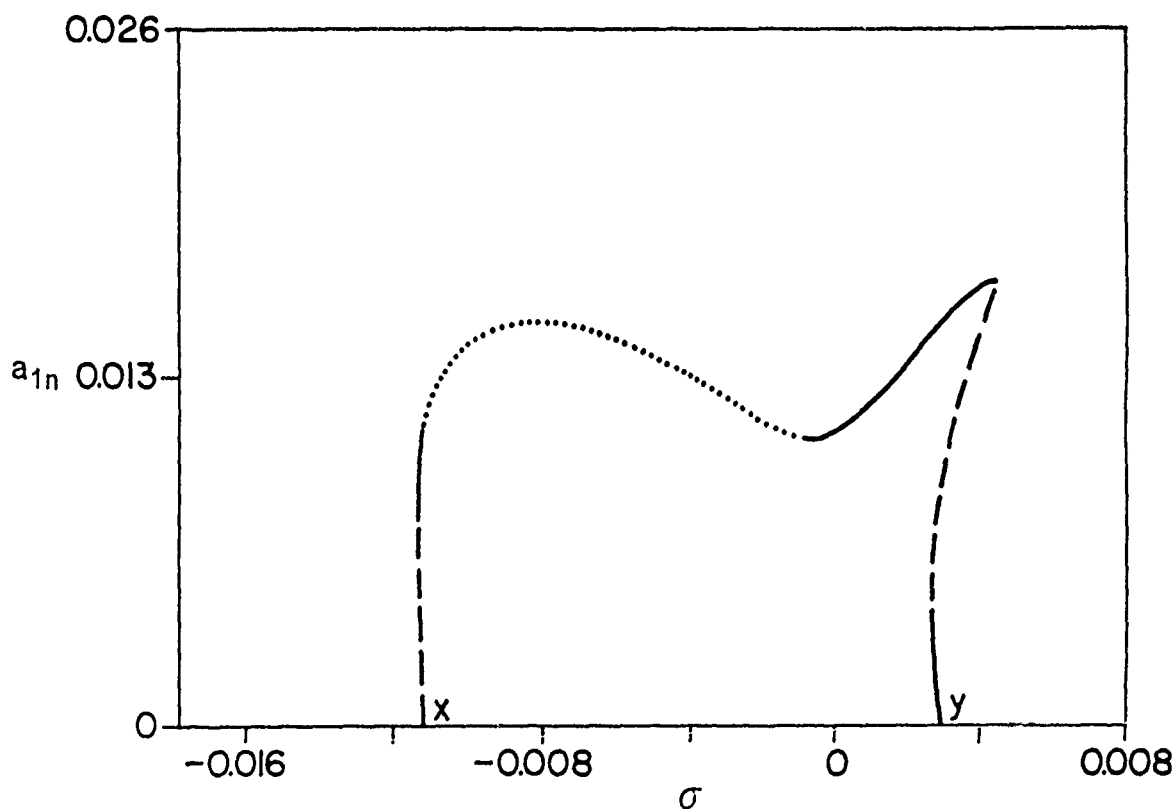
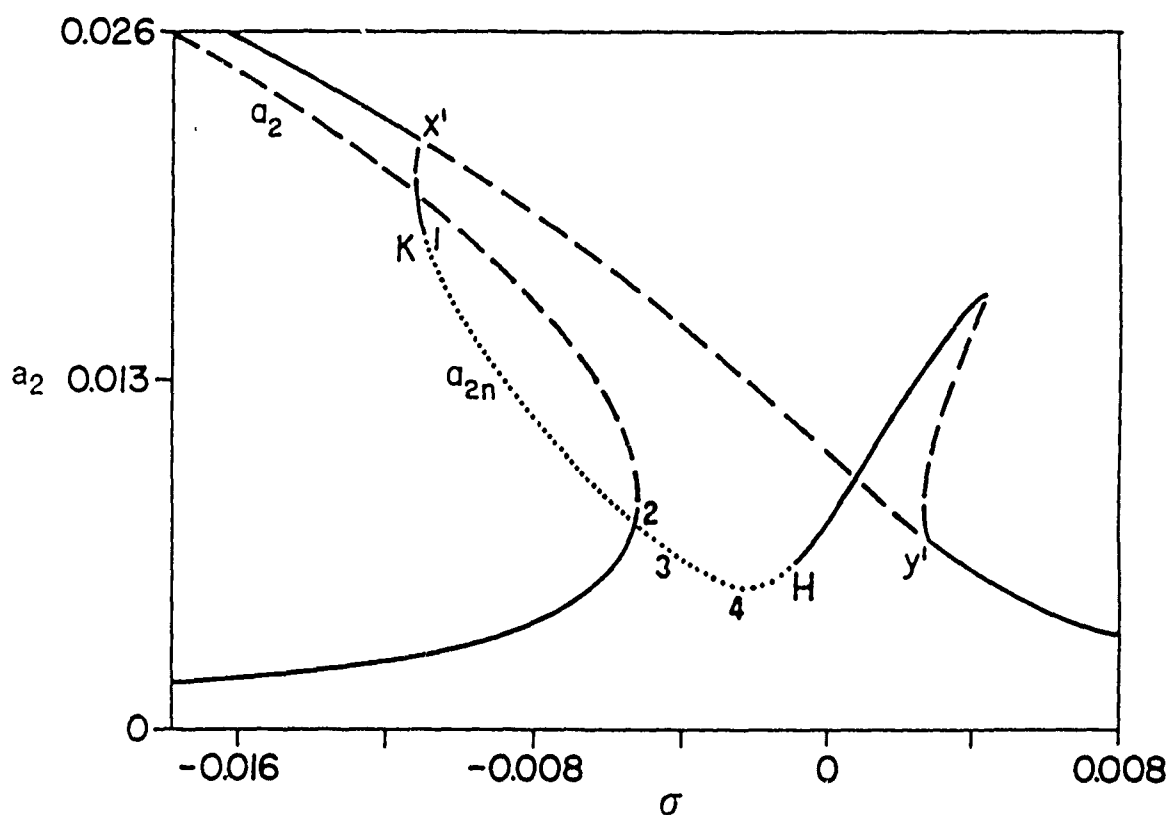


Figure 3. Response curves of the second mode for a beam with an aspect ratio  $b/h \approx 1.0$  : mode (2,2) ,  $\omega_{12} = \omega_{22}$  ,  $\delta_0 = 0.0$  ,  $\delta_2 = 0.002$  ,  $\mu = 0.04$  ,  $\beta_s f = 0.00006$  ,  $\beta_v = 0.6489$  ;  $a_2$  = planar response amplitudes;  $a_{1n}$  ,  $a_{2n}$  = nonplanar response amplitudes; (—) stable, (---) unstable with at least one eigenvalue being positive, (....) unstable with the real part of a complex conjugate pair of eigenvalues being positive; (a) response curves of  $w(s,t)$ , (b) response curves of  $v(s,t)$ .

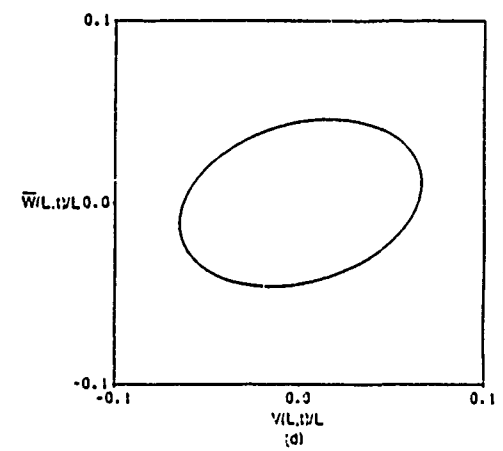
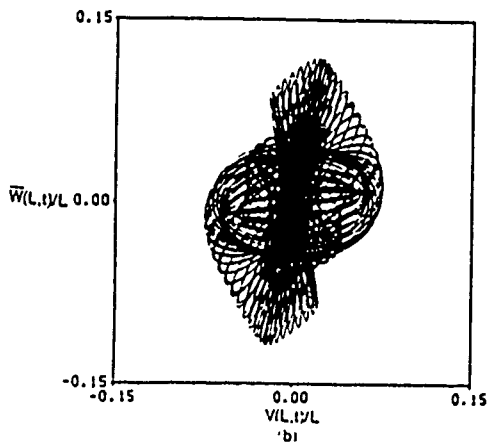
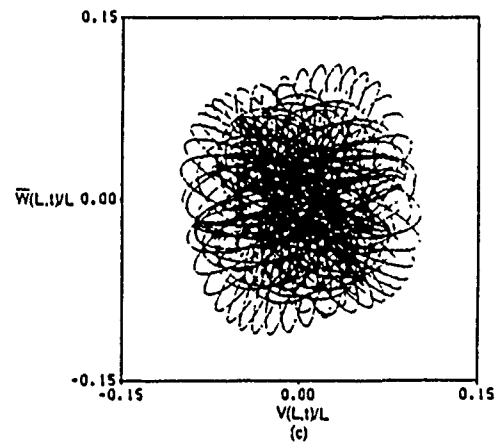
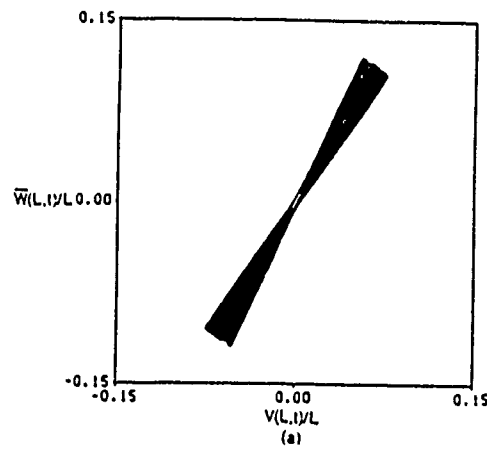


Figure 4. Path of the tip-end of the beam for the case of an amplitude- and phase-modulated motion :  $b/h \approx 1.0$  , mode (2,2) ,  $\omega_{12} = \omega_{22}$  ,  $\delta_0 = 0.0$  ,  $\delta_2 = 0.002$  ,  $\mu = 0.04$  ,  $\beta_1 f = 0.00006$  ,  $\beta_1 = 0.6489$  ,  $\varepsilon = 3$  , (a)  $\sigma = -0.01117$  , (b)  $\sigma = -0.005231$  , (c)  $\sigma = -0.005131$  , (d)  $\sigma = 0$  (steady whirling motion).

**EFFECTS OF ROTATING FRAME TURBULENCE (RFT) ON  
HELICOPTER BODY RESPONSE**

J.V.R. Prasad, D.P. Schrage, J.Riaz  
School of Aerospace Engineering  
Georgia Institute of Technology  
Atlanta, Georgia 30332

and

G.H. Gaonkar, R. Madhavan  
Department of Mechanical Engineering  
Florida Atlantic University  
Boca Raton, FL 33431

The abstract of a paper submitted for possible presentation at the Third Technical Workshop and Aeroelastic Stability Modeling of Rotorcraft Systems, March 12-14, Duke University, Durham, North Carolina.



## Abstract

Rotating frame turbulence, or RFT, refers to the actual turbulence experienced by the blades, and requires noneulerian description and sampling of measurements. Its characteristics are strikingly different from those of conventional models based on eulerian or space-fixed description, and these differences increase with decreasing advance ratio and altitude. Therefore, RFT effects on gust sensitivity of rotorcraft and tilt rotors are appreciable during low-altitude and low-speed operations. Typical examples include NOE maneuvers, light-house and offshore oil-platform missions and ship landing of rotorcraft. The tilt rotor "chugging" problem, which is basically a fore-to-aft low-frequency acceleration of the rigid body mode coupling with the rotor torque mode, is another example. That chugging occurs at relatively low speeds and aggravates during descent shows that RFT effects should be included in the treatment of this problem.

In axial flight, though the RFT and space-fixed turbulence are stationary, the RFT spectral density shows large peaks at integer multiples of the rotor speed (1P, 2P, etc.) and transfer of energy essentially from the low-frequency region ( $\leq 1P$ ) to the high frequency ( $> 1P$ ). Figure 1 shows the spectral density  $S(f)$  of the vertical turbulence velocity at 0.7R blade station on the basis of the Dryden model. The results refer to  $L/R=4$ , very low altitude conditions at which turbulence scale length  $L$  is comparable to the rotor radius  $R$ . They are presented as  $f*S(f)$  versus  $\ln f$ , which gives a better picture of the spectral density variation or transfer of energy in the low-frequency region. It is noteworthy that the area under the curve,  $\int f*S(f)d(\ln f)$ , gives the variance, as in the conventional  $S(f)$  versus  $f$  presentation shown in the upper-left inset figure. The upper-right inset figure refers to the autocovariance function  $R(\tau)$ . Since the area under the spectral density curve is the same in both the space-fixed and rotating frame description, the transfer of energy from the low-frequency region to the high-frequency region is balanced by the occurrence of peaks. The RFT effects of transfer of energy and the occurrence of peaks cannot be predicted in the space-fixed description of turbulence and severely affect the helicopter gust response statistics of standard deviation, threshold crossing and peak distribution. In forward flight, the differences in characteristics are much more fundamental in that the RFT becomes periodically nonstationary or cyclostationary although the space-fixed turbulence remains stationary. Concerning the RFT's stochastic structure and its

effects on helicopter body response, this paper addresses the following topics: 1) Instantaneous or frequency-time spectrum of RFT, 2) Finite impulse response (FIR) filter for RFT, and 3) Application of FIR filter to generate the helicopter body response to RFT, including comparisons with a conventional approach in which response statistics are computed directly.

### Instantaneous Spectrum

The frequency-time or instantaneous spectrum  $S_w(f,t)$  provides a means of describing both the energy transfer with respect to frequency  $f$  and the periodically varying nonstationarity (cyclostationarity) with respect to  $t$ . Here the subscript  $w$  refers to the vertical turbulence velocity, the only component included in this investigation. Moreover, the instantaneous spectrum  $S_w(f,t)$  shows the distribution of energy in the  $(f,t)$  plane and is therefore real. By comparison, the conventional double-frequency spectrum is a complex quantity involving a real part (co-spectrum) and an imaginary part (quad spectrum) and has a much diminishing physical meaning. For atypical low-speed (advance ratio  $\mu=0.05$ ) and low-altitude ( $L/R=1$ ) condition, Figures 2 and 3, respectively, show the covariance function  $R(t,\tau)$  and the instantaneous spectral density function  $S_w(f,t)$ . It is highly instructive that both of these figures clearly show the velocities. It is this cyclostationarity that has significant bearing on the development of shaping filters (driven by white noise) and the treatment of helicopter body sensitivity to turbulence.

### Finite Impulse Response (FIR) Filters

In axial flight the RFT is stationary. Therefore, the design of shaping filter is straightforward, but algebraically cumbersome due to peaks at integer multiples of the rotor frequency (see Figure 1). However, in forward flight, the RFT is nonstationary although its nonstationarity varies periodically, as shown in Figures 2 and 3. Therefore, the shaping filter system has periodically varying coefficients, and its design is by no means trivial. The FIR filter is an intrinsically stable digital filter that exploits the linearity of the problem as well as the cyclostationarity of RFT. Calculation of the FIR filter coefficients involves the following steps:

- a) select the spectral density function of the turbulence for which a sample function is to be created;
- b) obtain the frequency response of the filter using the spectral density function of step (a);
- c) transform the frequency response into impulse response by a direct use of the inverse Discrete Fourier Transforms;
- d) window the impulse response to the desired filter length;
- e) use the impulse sequence obtained in step (d) as the filter coefficients;
- f) calculate the inner product of the filter coefficients obtained in step (e) and a sequence of random numbers to arrive at the sample function of the turbulence.

Basically, the coefficients of the FIR filter are calculated at each instant in time with respect to the instantaneous power spectrum  $S_w(f,t)$ . Because the RFT is periodically nonstationary, an FIR filter designed using this approximation will have periodic coefficients as well. Conceptually, this amounts to approximating the nonstationary behavior of the RFT with small time intervals of stationary behavior.

### Body Response to RFT

An attractive feature of the filter approach is the feasibility of generating the response sample functions to RFT excitations and the subsequent evaluation of response statistics by 'ensemble' averaging. Therefore, this approach can be directly implemented on current flight simulation programs such as GENHEL. Figure 4 shows a response sample function of the UH-60A Black Hawk helicopter body normal acceleration response to turbulence in hover using the GENHEL flight simulation program. The dominant RFT effects are clearly seen, and, as expected, these effects increase with decreasing values of turbulence scale length.

### Conclusions

Major findings of this investigation:

1. The instantaneous or frequency-time spectrum of RFT provides a feasible approach to modeling RFT to predict both the cyclostationarity (periodically varying nonstationarity) and transfer of energy from the low-frequency ( $\leq 1P$ ) to the high-frequency ( $> 1P$ ) region.

2. The FIR filter approach modified to treat the cyclostationarity RFT can be directly implemented in conventional flight simulation programs. Since it generates response sample functions that are subsequently 'ensemble' averaged, this approach can be used to verify analytical computed response statistics. Preliminary results offer considerable promise.
3. RFT effects are appreciable on helicopter body response. This finding has a significant bearing on ride quality investigations and future development of ride quality specifications in the presence of turbulence.

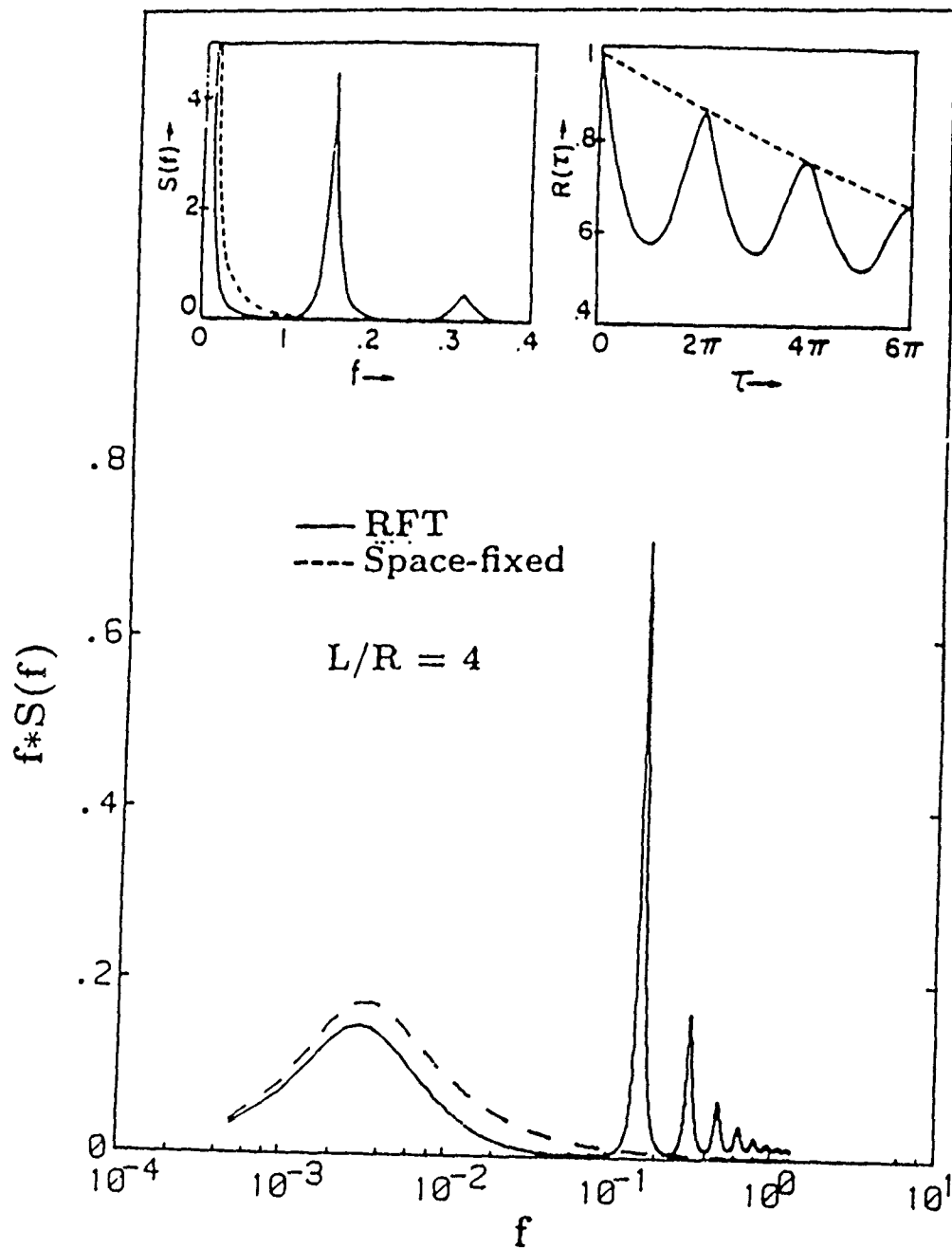
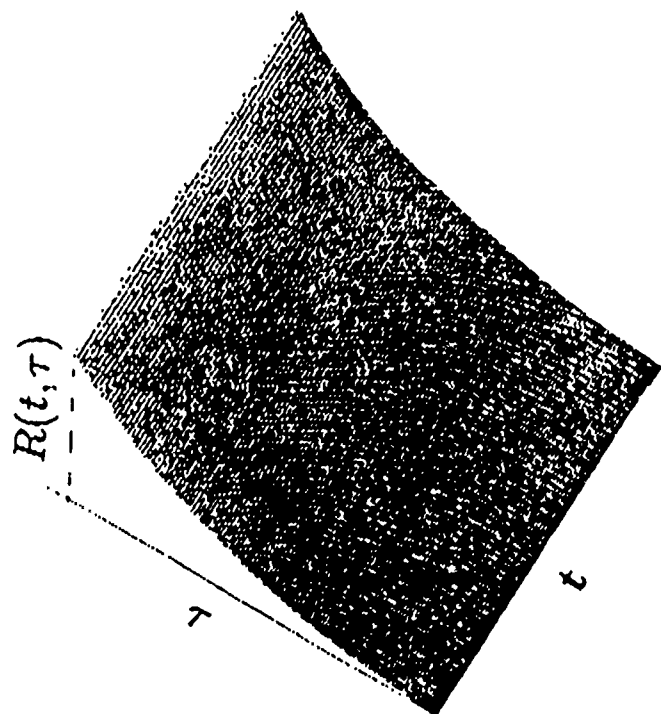


Figure 1. RFT Effects on Space-fixed Dryden Model for the Vertical turbulence at 0.7R blade station.

$\mu=0.05, L/R=1$



Neglecting RFT Effects (Schematic)

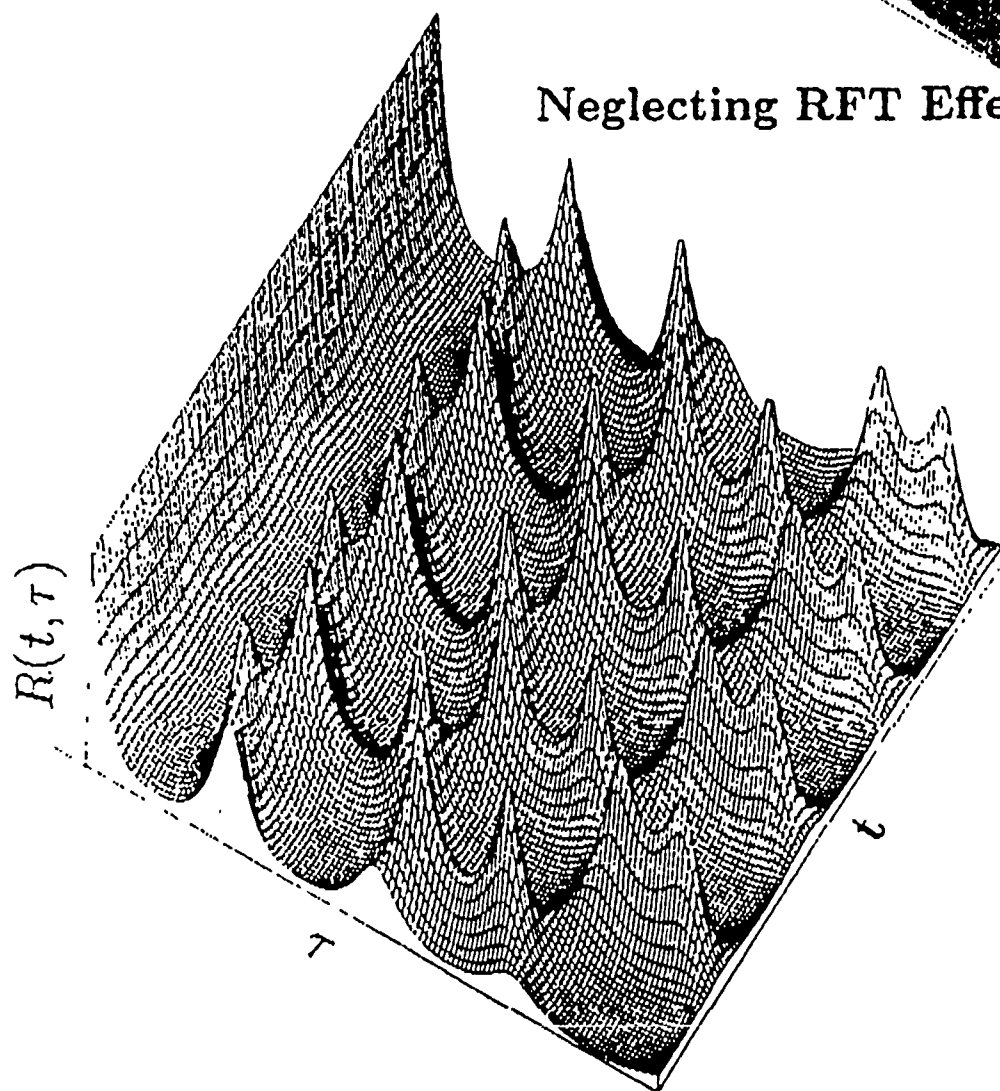


Figure 2 RFT Covariance and its cyclostationarity

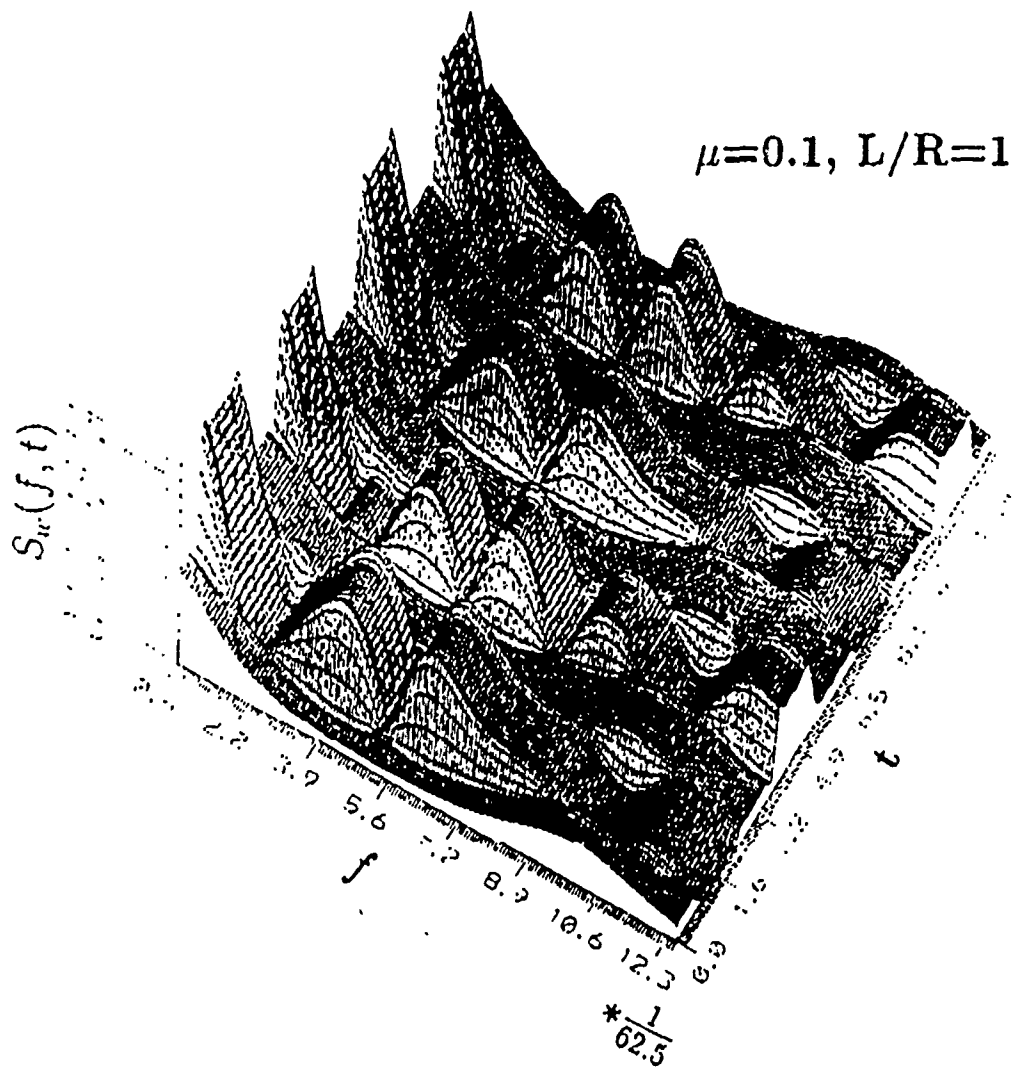
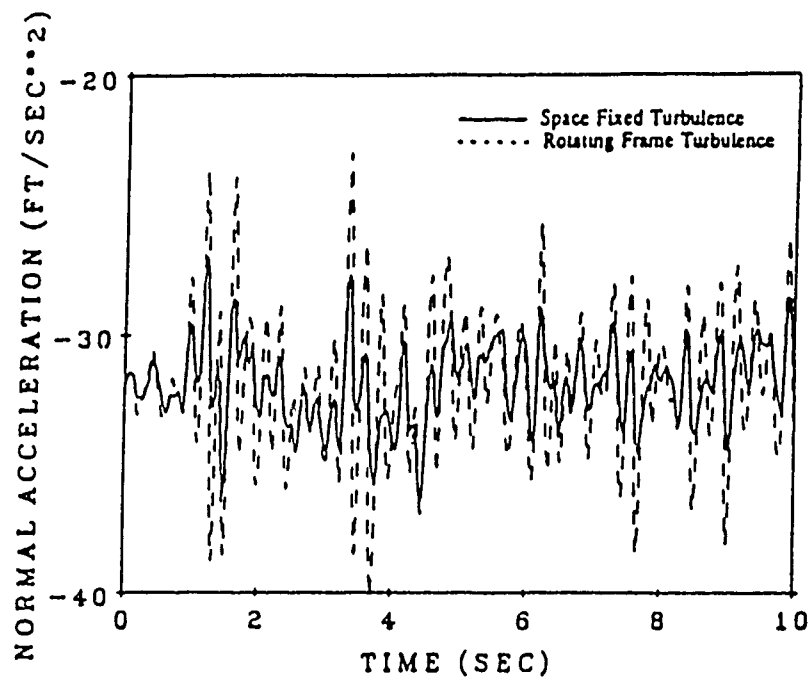


Figure 3 Instantaneous or Frequency-Time Spectra of RFT



Effect of Turbulence on the Black Hawk Helicopter  
Normal Acceleration Response for  $L/R = 1$ .

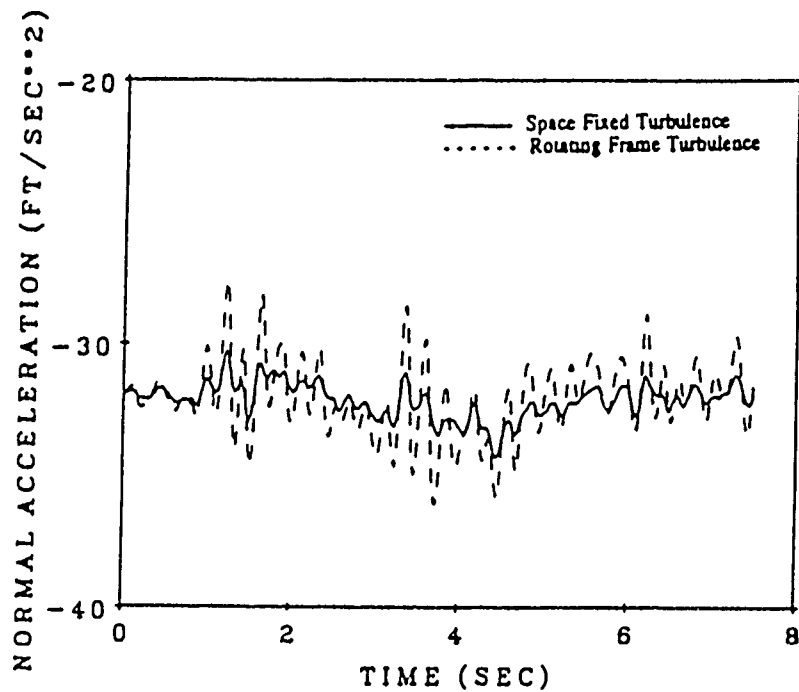


Figure 4. Effect of Turbulence on the Black Hawk Helicopter  
Normal Acceleration Response for  $L/R = 10$ .



# DYNAMICS OF ROTOR BLADES IN CURVED STEADY MANEUVER

W.C. Hassenpflug and M.R.M. Crespo da Silva

Dept. of Mechanical Engrg., Aeronautical Engrg. and Mechanics

Rensselaer Polytechnic Institute; Troy, New York 12180-3590

## ABSTRACT

The dynamics of a rotor blade in a maneuvering flight condition is addressed in this paper. For simplicity, a uniform rigid rotor blade, with small chord and a simple flap and lag spring connection at an offset hinge is considered. The aerodynamic forces are modelled by quasi-steady aerodynamic theory. The equations were derived with the aid of the symbolic manipulation package MACSYMA and a number of fortran programs were developed. The analysis of the infinitesimally small perturbations about a trimmed steady state solution in a curved maneuvering flight is investigated by Floquet theory. The characteristic multipliers associated with the perturbed motion, and stability boundaries in the two-parameter space of flap and lag spring stiffness, are found for several flight parameters.

## INTRODUCTION

To date, the analysis of the stability of the motion of helicopter rotor blades has literally been restricted to two flight conditions, namely hover and constant velocity forward flight, e.g., [1-5]. A set of differential equations of motion governing the dynamics of a rotor blade, including hub acceleration, was recently presented in [6]. However, to the authors' knowledge, no comprehensive analysis dealing with the effect of maneuvers on the blade's response is available. This work addresses this void in the literature. To assess the influence of maneuvers of a helicopter on the stability of the rotorblade motion, the simplest possible case is considered first. This is a level turn in steady flight with constant speed along the hub's trajectory, resulting in a constant acceleration of the hub. For steady flight, the homogeneous differential equations of the infinitesimal motion about a steady state solution have periodic coefficients and, thus, stability of the motion can be assessed by making use of well known methods such as Floquet theory.

## EQUATIONS OF MOTION

The model considered in the analysis consists of a rigid rotor blade with length  $R$  and hinge offset  $e$ . Fig. 1 shows the generalized coordinates  $\beta$  and  $\zeta$  and feathering pitch angle  $\theta$  used in the analysis. The hub is assumed to be moving with constant speed along a horizontal circular trajectory of radius  $R_0$ , with bank angle  $\Phi$  and pitch angle  $\Theta$ . For simplicity, the rotor disk force vector is assumed normal to the hub. A single lead-lag linear spring with stiffness  $K_\zeta$  and a single flap linear spring with stiffness  $K_\beta$  is considered. Adding up all the relative linear and angular velocities and transforming to blade coordinate axes, the absolute velocity of a point on the blade and thus, the kinetic energy of the blade is found. Similarly, from coordinate transformations, the angle between blade chord and relative air velocity is found, from which the generalized aerodynamic forces  $Q_\beta$  and  $Q_\zeta$  are obtained.

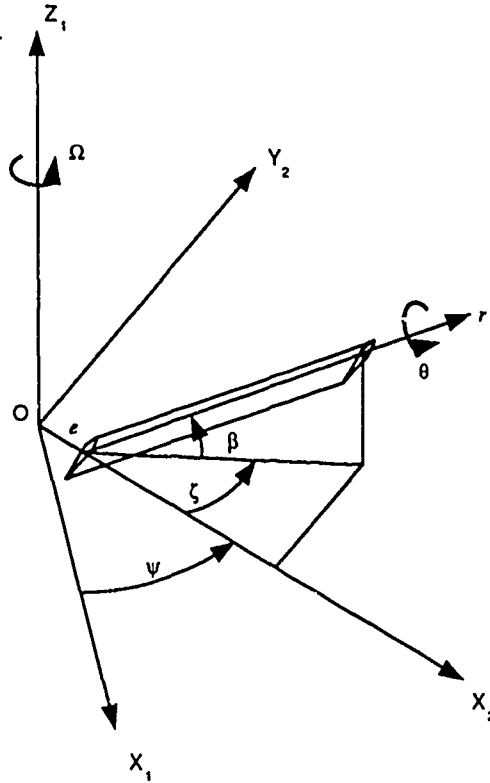


Figure 1. Rotor blade coordinate systems

The differential equations of motion are obtained from Lagrange's equations as

$$\begin{aligned} \frac{d}{dt} \frac{\partial T}{\partial \dot{\beta}} - \frac{\partial T}{\partial \beta} + K_{\beta} (\beta - \beta_{pc}) &= Q_{\beta} \\ \frac{d}{dt} \frac{\partial T}{\partial \dot{\zeta}} - \frac{\partial T}{\partial \zeta} + K_{\zeta} (\zeta - \zeta_{pl}) &= Q_{\zeta} \end{aligned} \quad (1)$$

producing two non-linear equations which are written in vector form as

$$\underline{f}(\ddot{\beta}, \dot{\beta}, \beta, \ddot{\zeta}, \dot{\zeta}, \zeta, \theta) = \underline{0} \quad (2)$$

and the constraint equation

$$\theta(\psi) = \theta_0 + \theta_c \cos(\psi) + \theta_s \sin(\psi) \quad (3)$$

## TRIM

The rotordisk forces, obtained from aerodynamic forces on the blade, are written in normalized form as

$$\begin{aligned} C_T &= \frac{1}{2\pi} \int_0^{2\pi} f_T(\dot{\beta}, \beta, \dot{\zeta}, \zeta, \theta) d\psi \\ C_H &= \frac{1}{2\pi} \int_0^{2\pi} f_H(\dot{\beta}, \beta, \dot{\zeta}, \zeta, \theta) d\psi \\ C_Y &= \frac{1}{2\pi} \int_0^{2\pi} f_Y(\dot{\beta}, \beta, \dot{\zeta}, \zeta, \theta) d\psi \end{aligned} \quad (4)$$

Equations (4) and the expressions for the functions  $f_T$ ,  $f_H$  and  $f_Y$  were obtained with MACSYMA[7]. They are too lengthy and, due to lack of space, cannot be reproduced here.

A constant helicopter weight is assumed, and the bank angle  $\Phi$  is determined from radial flight path equilibrium. To eliminate the additional parameters of the position of the center of gravity of the fuselage in this study, the moment trim equations are disregarded, and the pitch angle  $\Theta$  is determined from equilibrium with an assumed fuselage drag coefficient. The required thrust coefficient  $C_T$  is then defined. Trim conditions are then

$$C_T : \text{given} ; \quad C_H = 0 ; \quad C_Y = 0 \quad (5)$$

These replace the constraint equation (3) so that  $\theta_0$ ,  $\theta_c$  and  $\theta_s$  become three quantities dependent on  $C_T$ ,  $C_H$  and  $C_Y$ .

## SOLUTION OF THE EQUATIONS AND STABILITY

Defining a vector  $\underline{q}(\psi)$  as  $\underline{q}(\psi) = [\beta(\psi), \zeta(\psi)]^T$ , the solution to the equations of motion is written as  $\underline{q}(\psi) = \underline{q}_p(\psi) + \underline{q}_s(\psi)$ , where  $\underline{q}_p(\psi)$  is the particular (trim) solution, and  $\underline{q}_s(\psi)$  is a small perturbation.

The particular solution is approximated by a finite Fourier series

$$\underline{q}_p = \begin{bmatrix} \beta_0 + \beta_{1c}\cos(\psi) + \beta_{1s}\sin(\psi) + \dots + \beta_{N/2}\cos(N\psi/2) \\ \zeta_0 + \zeta_{1c}\cos(\psi) + \zeta_{1s}\sin(\psi) + \dots + \zeta_{N/2}\cos(N\psi/2) \end{bmatrix} \quad (6)$$

The solution is obtained numerically by introducing the Fourier series for  $\underline{q}_p$  into equations (2) and (4). The resulting  $2N+3$  non-linear algebraic equations for the  $2N+3$  coefficients  $\beta_0, \dots, \beta_{N/2}, \zeta_0, \dots, \zeta_{N/2}, \theta_0, \theta_c$ , and  $\theta_s$  are solved numerically by Newton-Raphson's method using exact analytical expressions for derivatives in order to ensure good convergence.

The differential equations of motion for the infinitesimally small disturbance  $\underline{q}_s(\psi)$  are obtained by linearizing the non-linear equation (2) about its particular solution  $\underline{q}_p(\psi)$ . The linearized equations are of the form

$$M(\underline{q}_p) \ddot{\underline{q}}_s + C(\underline{q}_p) \dot{\underline{q}}_s + K(\underline{q}_p) \underline{q}_s = \underline{0} \quad (7)$$

where  $M = \frac{\partial f}{\partial \ddot{q}}$ ,  $C = \frac{\partial f}{\partial \dot{q}}$  and  $K = \frac{\partial f}{\partial q}$ . This is a set of two linear differential equations with periodic coefficients determined by the particular solution  $q_p(\psi)$  and by the periodic pilot's input  $\theta(\psi)$ .

Converting the above equation into a system of four equations written in state variable form as  $\dot{\underline{x}} = A(q_p)\underline{x}$ , where  $\underline{x} = [\beta, \dot{\beta}, \zeta, \dot{\zeta}]^T$ , Floquet theory is then used to obtain the characteristic multipliers associated with the linearized equations, and to determine the influence of a number of system parameters in the stability of the response. An eigenvalue routine is used to determine the four complex characteristic multipliers  $z_i$ , ( $i=1, \dots, 4$ ), from which four complex characteristic exponents  $s_i = \log z_i / (2\pi)$  can be generated. To find the stability boundary in the parameter plane, these are regarded as functions of the parameters  $(K_\beta, K_\zeta)$ . Taking the smallest  $u = \text{Real}(\log z_i)$  for a chosen point in the parameter plane  $(K_\beta, K_\zeta)$ , the particular solution  $\underline{x}_p(\psi)$  and the scalar quantity  $u(K_\beta, K_\zeta)$  are calculated. To find the stability boundary  $u(K_\beta, K_\zeta) = 0$  in the parameter plane, we start with the solution at some point, then construct the gradient  $\text{grad}(u) = \left[ \frac{\partial u}{\partial K_\beta}, \frac{\partial u}{\partial K_\zeta} \right]^T$  by computing the solution at small increments  $\partial K_\beta, \partial K_\zeta$ . A finite step  $\Delta K = \sqrt{\Delta K_\beta^2 + \Delta K_\zeta^2}$  is then used to "march" in the parameter plane along the gradient line to find one point on the boundary. From this point on we proceeded in chosen steps  $\Delta K$  along the tangent direction, normal to the gradient direction (either to the right or left of the gradient line), of the boundary  $u(K_\beta, K_\zeta) = 0$ . A final Newton-Raphson iteration at the end of each step is used to obtain an accurate solution along the gradient line.

Due to lack of space here, results will be shown at the presentation of this work.

### ACKNOWLEDGMENTS

This research was supported, in part, by the U.S. Army Research Office through the Rotorcraft Technology Center at Rensselaer Polytechnic Institute under contract number DAAL03-88-C-0004, Dr. Gary Anderson, Contract Monitor.

### REFERENCES

1. Crespo da Silva, M.R.M. and Hodges, D.H., Nonlinear Flexure and Torsion of Rotating Beams, With Application to Helicopter Rotor Blades – II. Response and Stability Results. *Vertica*, 10, pp. 171-186, 1986.
2. Peters, D.A., Flap-Lag Stability of Helicopter Rotor Blades in Forward Flight, *Journal of the American Helicopter Society*, 1, pp. 2-13, 1975.
3. Bramwell, A.R.S., Helicopter Dynamics. Edward Arnold 1976.
4. Johnson, W., Helicopter Theory. Princeton 1980.
5. Prouty, R.W., Helicopter Performance, Stability, and Control. PWS Engineering, 1986.
6. Johnson, W., A Complete Analytical Model of Rotorcraft Aerodynamics and Dynamics. NASA TM 81182, 1980.
7. Symbolics, MACSYMA User's Guide. Symbolics, Inc., 1987.

# **Intelligent Rotor Blade Actuation Methodology**

Ron Barrett†  
Inderjit Chopra††

Center for Rotorcraft Education and Research  
Department of Aerospace Engineering  
University of Maryland  
College Park, Maryland 20742

Abstract for proposed paper to be presented at the  
Dynamics and Aeroelasticity Stability Modeling of Rotorcraft Systems  
Technical Workshop  
March 12-14, 1990  
Duke University  
Durham, North Carolina

†Rotorcraft Fellow

††Professor and Chairman Aerospace Engineering Department

Control and vibration reduction through the use of intelligent actuator elements has been shown to be effective on several types of aerospace structures. Applications include vibration suppression in space trusses and dynamic control of camber and twist for gust alleviation and flutter suppression on fixed wing surfaces (1-3). Vibration suppression in rotorcraft could be enhanced through the use of intelligent actuators because current methods of vibration reduction in rotorcraft do not address some of the vibration inducing phenomena that occur in actual helicopters including differences in individual blade tracking and magnitude and locations of dynamic stall (4-6). Because the unsteady bending moments in the rotor blade are several orders of magnitude greater than present intelligent actuators can impart, the direct manipulation of the rotor blade in bending is currently not feasible. However, through blade twist manipulation many types of vibration reduction methods could be employed including suppression of blade vibrational modes, in-flight tracking and dynamic stall reduction through small amplitude pitch oscillations (7,8).

Implementation of dynamic blade twist requires the introduction of torsional forcing to quasi-orthotropic blade structures like uncoupled composite or aluminum blades. Since nearly all composite rotor blades in use today have such characteristics, a method of torsional forcing must be developed. Many types of intelligent actuation devices (including piezoelectric actuators) in production today are incapable of imparting this torsional forcing due to their quasi-isotropic nature. Accordingly, this paper deals with the analytical and experimental development of torsional forcing methodology as it relates to the manipulation of intelligent structures.

To introduce torsional forcing from a quasi-isotropic material, a method of directional attachment was developed. The purpose of the directional attachment is to maximize the equivalent longitudinal stiffness of the piezoelectric crystal while minimizing the effective transverse stiffness (as experienced by the laminate). One type of directional attachment is shown in Figure 1.

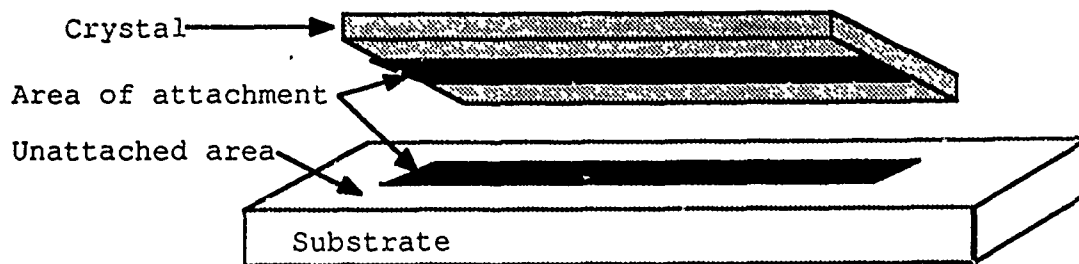


Figure 1 Directional Attachment of Piezoelectric Crystal to Substrate

Two types of test specimens were fabricated to demonstrate this principle. A bending specimen with the arrangement of Figure 2 demonstrated that significant reductions of transverse stiffness could be achieved without corresponding reductions in longitudinal stiffness. The crystals and the attachment direction were oriented longitudinally and transversely for experimentation.

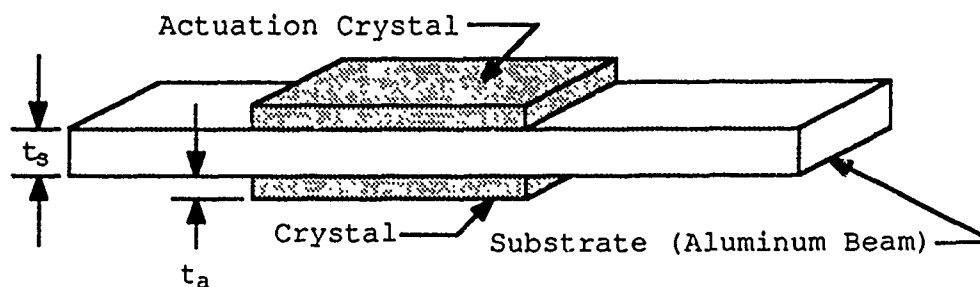


Figure 2 Directional Attachment Specimen Configuration

The other plate test article had crystals at  $\pm 45^\circ$  angles from the longitudinal axis. The crystals produced torsional deflections of the aluminum substrate which further demonstrated that anisotropic behavior could be achieved by directionally attaching two isotropic materials. Piezoelectric crystals were then imbedded in the skin of a Froude scaled rotor blade. From the experiments that followed, the feasibility of using directional attachment to introduce significant torsional deflections of aerodynamic surfaces was demonstrated.

The analytical treatment of piezoelectric crystals in a laminate takes the form of strain-energy relationships. For the static actuation case, the strain energy in a given cross-section is set equal to zero and the laminate strains are solved as can be seen as follows.

$$U = \frac{1}{2} \int_0^1 \left[ [\epsilon_l \kappa_l] \begin{bmatrix} A & B \\ B & D \end{bmatrix}_l + [\epsilon_a \kappa_a] \begin{bmatrix} A & B \\ B & D \end{bmatrix}_a \right] [\epsilon_l] dx \quad (1)$$

Where the subscripts "a" and "l" denote the piezoelectric actuator and laminate and the integration variable "x" is in the longitudinal direction of the laminate. Expanding equation 1 to show the components of the stiffness and actuation matrices gives greater insight to the problem.

$$U = \frac{1}{2} \int_0^1 \left\{ [\epsilon_x^0 \epsilon_y^0 \gamma_{xy}^0 \kappa_x \kappa_y \kappa_{xy}]_l \sum_{k=1}^N \left( \begin{bmatrix} E_{1111} & E_{1122} & E_{1112} \\ E_{1122} & E_{2222} & E_{2212} \\ E_{1112} & E_{2212} & E_{1212} \end{bmatrix} \int_{z_{k-1}}^{z_k} dz \quad \begin{bmatrix} E_{1111} & E_{1122} & E_{1112} \\ E_{1122} & E_{2222} & E_{2212} \\ E_{1112} & E_{2212} & E_{1212} \end{bmatrix} \int_{z_{k-1}}^{z_k} z dz \right) \begin{bmatrix} \epsilon_x^0 \\ \epsilon_y^0 \\ \gamma_{xy}^0 \\ \kappa_x \\ \kappa_y \\ \kappa_{xy} \end{bmatrix}_l \right. \\ \left. + [\epsilon_x^0 \epsilon_y^0 \gamma_{xy}^0 \kappa_x \kappa_y \kappa_{xy}]_a \sum_{k=1}^N \left( \begin{bmatrix} E_{1111} & E_{1122} & E_{1112} \\ E_{1122} & E_{2222} & E_{2212} \\ E_{1112} & E_{2212} & E_{1212} \end{bmatrix} \int_{z_{k-1}}^{z_k} dz \quad \begin{bmatrix} E_{1111} & E_{1122} & E_{1112} \\ E_{1122} & E_{2222} & E_{2212} \\ E_{1112} & E_{2212} & E_{1212} \end{bmatrix} \int_{z_{k-1}}^{z_k} z dz \right) \begin{bmatrix} \epsilon_x^0 \\ \epsilon_y^0 \\ \gamma_{xy}^0 \\ \kappa_x \\ \kappa_y \\ \kappa_{xy} \end{bmatrix}_a \right\} dl \quad (2)$$

For piezoelectric crystals, the number of actuation strains reduce to only  $\epsilon_x$  and  $\epsilon_y$  as the other types of strain actuation including shear and bending are negligible. It should be noted that one inherent characteristic of piezoelectric crystals is that the amount of transverse strain is usually lower than the amount of longitudinal strain (9). Assuming completely isotropic behavior of the substrate and the actuator as well as the same Poisson's ratios, the solution of the beam-bending case is seen for the configuration of Figure 2.



$$K \left[ \frac{E_s t_s^3}{12} + 2E_a \left( \frac{t_s^2 t_a}{4} + \frac{t_s t_a^2}{2} + \frac{t_a^3}{3} \right) \right] = \epsilon_a E_a \left( \frac{t_s t_a}{2} + t_a^2 \right) \quad (3)$$

Predictions of the beam performance followed closely to the predicted performance of equation 3. The modeling of the directional attachment requires closer attention to the boundary conditions on each segment of the crystal and finite bond thickness also affects the amount of directionality that the crystal can impart to the structure. With greater crystal aspect ratios, the directionality increases due to the transverse shear lag that the attachment area encounters.

Future work on intelligent structures for rotorcraft will incorporate more involved lamination schemes for the integration of the actuators into the rotor blade structure. The Froude scaled rotor blade that was constructed for this investigation demonstrated significant torsional deflections for the purposes of some types of vibration control. However, the Froude scaled blade used non-conducting composite plies around the crystals (fiberglass and epoxy). This facilitated greater transfer of the crystal actuation shear strains due to the extremely thin bond line (1-2 mil between crystal surface and fibers). Since many types of composites are good conductors (graphite and boron), an insulation layer must be present between the crystal and the laminate to prevent shorting of the crystal [10]. For directionally attached crystals, the insulation layer may induce unacceptably high amounts of shear lag and cause the structures to have low amounts of deflection. Further investigations of directionally attached crystals in Froude scaled rotor blades will determine these characteristics.

## References

- [1] Crawley, E. F., D. J. Warkentin and K. B. Lazarus, "Feasibility Analysis of Piezoelectric Devices," Space Systems Laboratory, Massachusetts Institute of Technology, Cambridge, Massachusetts, Report MIT-SSL #5-88, January, 1988.
  
- [2] Hanagud, S., M. W. Obal and M. Meyyappa, "Electronic Damping Techniques and Active Vibration Control," AIAA paper 85-0752, presented at the 26th Structures, Structural Dynamics and Materials Conference, April, 1985.
  
- [3] Crawley, E. F., J. DeLuis, N. W. Hagwood, and E. H. Anderson, "Development of Piezoelectric Technology for Applications in Control of Intelligent Structures," paper presented at the American Control Conference, June, 1988.
  
- [4] Nguyen, K. and I. Chopra, "Application of Higher Harmonic Control to Rotors Operating at High Speed and Maneuvering Flight," American Helicopter Society 45th Annual Forum, Boston, Massachusetts, May 1989.
  
- [5] Polychroniadis, M. and M. Achache, "Higher Harmonic Control: Flight Tests of an Experimental System on SA 349 Research Gazelle," American Helicopter Society 42nd Annual National Forum, Washington, D. C., June 1986.
  
- [6] Shaw, J. "Higher Harmonic Blade Pitch Control: A System for Helicopter Vibration Control," Ph.D. Theses, Massachusetts Institute of Technology, 1980.
  
- [7] Leishman, J. G., and T. S. Beddoes, "A Generalised Model for Unsteady Aerodynamic Behaviour and Dynamic Stall Using the Indicial Method," American Helicopter Society 42nd Annual National Forum, Washington, D. C., June 1986.

[8] Leishman, J. G., "Validation of Approximate Indicial Aerodynamic Functions for Two-Dimensional Subsonic Flow," *Journal of Aircraft*, Volume 25, (19), October 1988.

[9] Crawley, E. F. and J. deLuis, "Use of Piezoelectric Actuators as Elements of Intelligent Structures," paper presented at the AIAA/ASME/ASCE/AHS 27th Structures, Structural Dynamics and Materials Conference, San Antonio, Texas, May 19-21, 1986.

[10] Crawley, E. F., K. B. Lazarus and D. J. Warkentin, "Embedded Actuation and Processing in Intelligent Materials," paper presented at the ARO/AHS/RPI 2nd International Workshop on Composite Materials and Structures for Rotorcraft September 14 and 15, 1989.

ARO/Duke University Workshop on Dynamics and Aeroelastic  
Stability Modeling of Rotorcraft Systems

March 12 - 14, 1990

Active Control of Helicopter Ground and Air Resonance

by

G. Reichert

Technical University Braunschweig, Germany

The aeromechanical instability of a helicopter, on the ground or in flight, is caused by coupling between rotor and body degrees of freedom. This instability is commonly denoted air resonance when the helicopter is in flight and ground resonance when the helicopter is on ground. The phenomenon is one of the classical problems of helicopters known since the early days of helicopter history, but still today it is a very actual one, especially for helicopters with hingeless or bearingless rotors which are susceptible to such instabilities.

There is a good basic understanding of the problem and how to avoid the instability in general. But for bearingless rotors it is often very difficult to provide the required damping. Therefore the possibilities of active control in the sense of artificial stabilization of ground or air resonance find increasingly interest. Such an active controller would need sensing and actuating devices, which can operate with a conventional swashplate, and the hardware realization should be no basic problem.

The aim of the paper is to discuss the physical understanding of the phenomenon, for which some modeling aspects seem to be very important. Special consideration will be given to possible control schemes working through the full range of operating conditions of the helicopter which can normally be encountered. Especially stabilization of the air resonance instability has to be seen in direct relation to stability and control augmentation of the whole helicopter. Adverse effects on the flight mechanical modes and thereby on the handling qualities have to be avoided.

# Flap-Lag-Torsional Dynamics of Rotor Blades By a Direct, "Transfer Matrix", Method

Marcelo R. M. Crespo da Silva  
Professor; Department of Mechanical Engineering,  
Aeronautical Engineering and Mechanics  
Rensselaer Polytechnic Institute  
Troy, New York 12180-3590

## Abstract

A direct analysis of the response of a rotor blade is presented without having to replace the full nonlinear equations of motion of the system by a set of equations expanded into polynomial nonlinearities. After the equilibrium solution of the full nonlinear equations is determined, the perturbed motion about the equilibrium is then analyzed. Infinitesimally small motions are considered, and both the eigenfunctions and the eigenvalues associated with linearized motions are determined by a direct method which is based on the properties of the transition matrix associated with such motion.

## Introduction

The investigation of the response of a rotor blade involves the determination of a particular solution to the differential equations of motion and the eigenvalues associated with infinitesimally small motions about such solution. Because of the complexity of the governing differential equations of motion, it is common practice, in the rotorcraft dynamics literature, to first expand such equations, to a pre-determined degree, about the undeformed state of the blade. The resulting equations, which contain polynomial nonlinearities truncated to the desired order, are then used to analyze the aeroelastic response of the blade. One must be careful when working with expanded equations in order to obtain results that are mathematically consistent with the approximating assumptions and which do not produce results that are physically invalid such as those presented in [1] with quadratic equations. As shown in [2-4], the inclusion of cubic nonlinearities is necessary in order to circumvent such inconsistencies.

An analysis of the response of a rotor blade in hover, including the effects of cubic nonlinearities, was presented in [5,6] making use of Galerkin's method with a set of eigenfunctions of a non-rotating beam. The number of Galerkin coefficients is dependent on the number,  $N$ , of eigenfunctions and on the order of truncation of the differential equations of motion. As shown in [6], such number is greatly increased when one increases the truncation order from quadratic to cubic. Also, as shown in [7] for a cantilever with a large tip mass, even the cubic approximation for the equations may yield, in some cases, very inaccurate eigenvalues for the linearized motion.

In the present work, the problem of determining the equilibrium solution and the eigenvalues associated with the perturbed, infinitesimally small, flap-lag-torsional aeroelastic response of a rotor blade in hover is reformulated. The equilibrium state is determined directly by solving the two-point boundary value problem governed by the original, full-nonlinear, equations

of motion. A transfer matrix approach, based on the properties of the transition matrix of the system, is used for determining the eigenfunctions and the eigenvalues associated with the perturbed motion of the system.

## Analysis

The differential equations governing the flexural-flexural-torsional motion of inextensional beams, taking into account all the geometric nonlinearities in the system, were formulated in [2], and in [3] for both extensional and inextensional beams. The system considered here consists of an initially straight and untwisted cantilevered rotor blade of undeformed length  $R$ , pre-cone angle  $\beta$  and collective pitch  $\theta_0$  [5]. The differential equations of motion for the blade were formulated using the approach followed in [3], with the aerodynamic forces modelled as in [5]. For convenience, they are written in terms of orientation angles  $(\theta_z, \theta_y, \theta_x)$ , which are related to the elastic deformations (normalized by  $R$ )  $w(x, t), v(x, t), u(x, t)$  shown in Fig.1, and the elongation  $e_0 = \sqrt{(1 + u')^2 + v'^2 + w'^2} - 1$  as  $v' = (1 + e_0) \cos \theta_y \sin \theta_z, w' = (1 + e_0) \sin \theta_y, 1 + u' = (1 + e_0) \cos \theta_y \cos \theta_z$ . The blade's angle of twist,  $\phi(x, t)$ , is given as  $\phi(x, t) = \theta_x + \int_0^x \theta'_z(\eta, t) \sin \theta_y(\eta, t) d\eta$ . Here, primes denote partial differentiation with respect to the spatial variable  $x$ , which is the distance along the undeformed blade's reference axis, normalized by  $R$ , and dots denote partial differentiation with respect to time, normalized by the rotational angular speed  $\Omega$ . Considering, for simplicity, a homogeneous blade, the normalized differential equations of motion are

$$\begin{aligned} G'_v &\triangleq \left( \frac{A_{\theta_z}}{(1 + e_0) \cos \theta_y \cos \theta_z} + \tan \theta_z \int_1^x f_u dx \right)' = \ddot{v} + 2\dot{u} \cos \beta - 2\dot{w} \sin \beta - v - Q_v \\ G'_w &\triangleq \left( G_v \sin \theta_z \tan \theta_y + \frac{A_{\theta_y}}{(1 + e_0) \cos \theta_y} + \tan \theta_y \cos \theta_z \int_1^x f_u dx \right)' \\ &= \ddot{w} + 2\dot{v} \sin \beta + (x + u)(\sin 2\beta)/2 - w \sin^2 \beta - Q_w \\ A_{\theta_x} &= Q_{\theta_x} \end{aligned} \quad (1)$$

where  $f_u = \ddot{u} - 2\dot{v} \cos \beta + w(\sin 2\beta)/2 - (x + u) \cos^2 \beta - Q_u$ ;  $Q_u, Q_v, Q_w$  and  $Q_{\theta_x}$  are the generalized aerodynamic forces, whose virtual work is  $Q_u \delta u + Q_v \delta v + Q_w \delta w + Q_{\theta_x} \delta \theta_x$ . The expressions for  $A_{\theta_z}, A_{\theta_y}$  and  $A_{\theta_x}$  are obtained as shown in [2,3].

To analyze the motion, Eqs. (1) are written, for convenience, in state variable form as  $y'(x, t) = f(y, \dot{y}, \ddot{y}, \dot{y}', \ddot{y}')$ . The state equations admit the equilibrium solution  $\underline{y} = \underline{y}_e(x)$ . The static equilibrium solution  $\underline{y}_e(x)$  was determined numerically by solving the two-point boundary-value problem governed by the resulting ordinary differential equation  $\underline{y}'_e(x) = f(\underline{y}_e(x))$ . By perturbing the equilibrium solution as  $\underline{y} = \underline{y}_e + \epsilon \underline{y}_s(x, t)$ , expanding the state equations about  $\epsilon = 0$ , and truncating the expansion to  $O(\epsilon)$ , a set of linearized differential equations are obtained. With  $\underline{y}_s(x, t) = \underline{Y}(x) \exp(rt)$ , these equations are of the form  $\underline{Y}'(x) = A(r)\underline{Y}(x)$ . The eigenfunctions  $\underline{Y}(x)$  and complex eigenvalues  $r \triangleq r_r + \sqrt{-1}r_i$  were determined numerically by a transfer matrix method.

Fig. 1 (a and b) show plots of the static equilibrium solution at the blade's tip,  $v_e(1)$ ,  $w_e(1)$  and  $\phi_e(1)$ , and one of the first three eigenvalues associated with the perturbed motion, versus  $\omega_w^*$  — the blade's non-dimensional rotating flap-frequency in vacuum for  $\theta_0 = 0$  [8]. The results shown in these figures are for the four-bladed rotor considered in [6], with non-dimensional rotating lead-lag and torsional frequencies in vacuum, equal to  $\omega_v^* = 1.5$  and  $\omega_\phi^* = 2.5$ , respectively. The values chosen for other parameters of the problem are those used in [6]. The equilibrium solution and the eigenvalues, for  $\theta_0 = 0.5$ , determined in [6] by a Galerkin's procedure with five non-rotating beam modes are also shown in these figures (points marked  $\times$ ) for comparison with the more accurate results determined by the method presented here. Comparison of the results of the two analyses disclose the effect of order truncation when the full nonlinear differential equations of motion of the system are expanded about a state that is not an equilibrium, and replaced by the resulting set of approximate equations with polynomial nonlinearities. These conclusions are consistent with the results presented in [7] for a cantilever with a large tip mass.

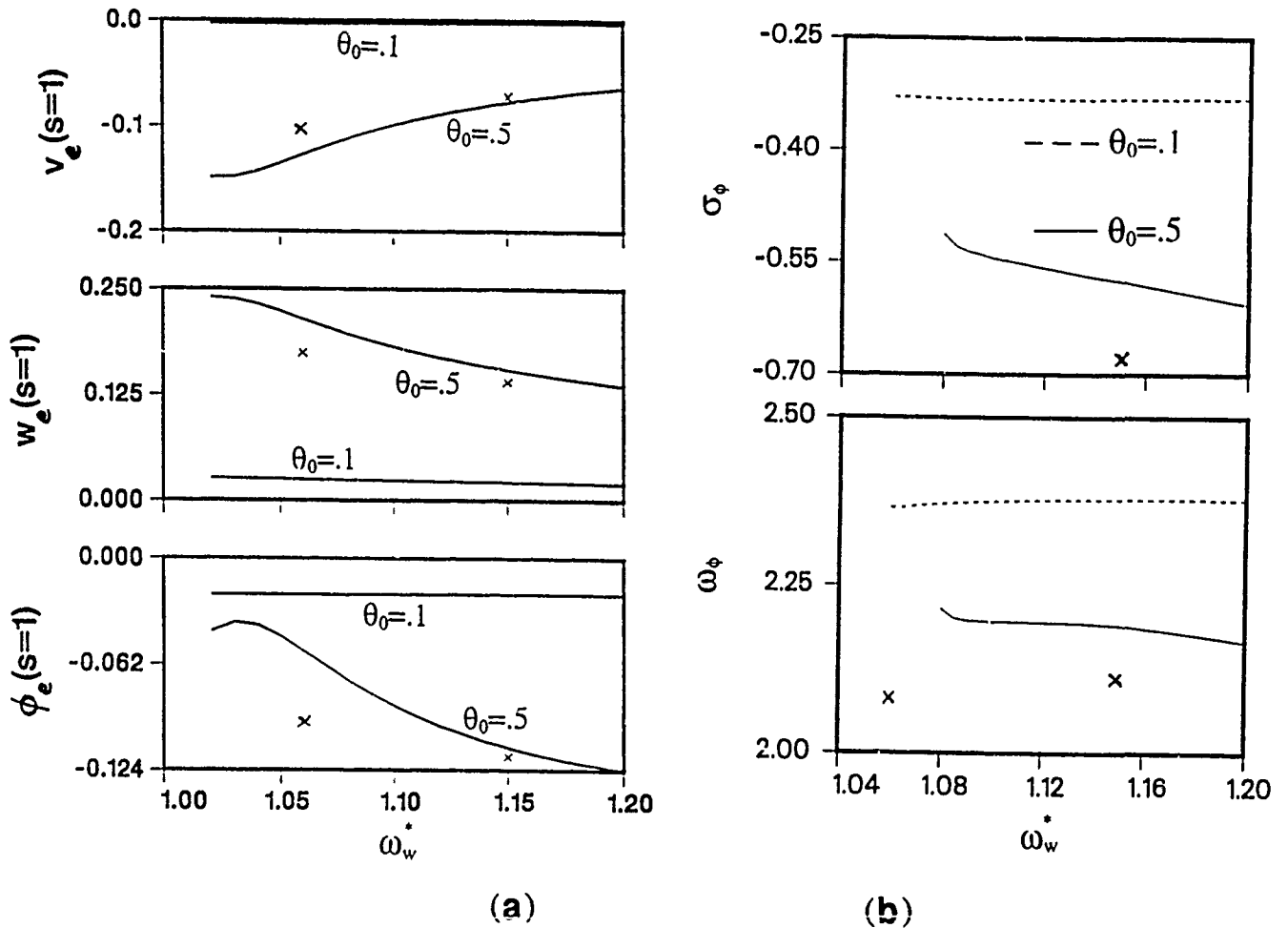


Fig. 1. Static equilibrium ( $v_e, w_e, \phi_e$ ), at blade's tip, and real ( $\sigma_\phi$ ) and imaginary ( $\omega_\phi$ ) parts of an eigenvalue versus  $\omega_w^*$ .

## Acknowledgements

This work was supported by the U. S. Army Research Office and the Aeroflightdynamics Directorate at Ames Research Center under Grant DAAL03-87-K01166. Mr. Clifford Zaretzky provided invaluable assistance with computer programming.

## References

1. Nagaraj, V.T. and Sahu, N., Influence of Transformation Sequence on Nonlinear Bending and Torsion of Rotor Blades. *Vertica*, 11, pp. 649-664, (1987).
2. Crespo da Silva, M. R. M., and Glynn, C. C., Nonlinear Flexural-Flexural-Torsional Dynamics of Inextensional Beams. I: Equations of Motion. *J. Struct. Mech.*, 6, pp. 437 - 448, (1978).
3. Crespo da Silva, M. R. M., Nonlinear Flexural-Flexural-Torsional-Extensional Dynamics of Beams. I: Formulation. *Int. J. Solids and Structures*, 24, pp. 1225-1234, (1988).
4. Hodges, D.H., Crespo da Silva, M.R.M. and Peters, D.A., Nonlinear Effects in the Static and Dynamic Behavior of Beams and Rotor Blades. *Vertica*, 12, pp. 243-256, (1988).
5. Crespo da Silva, M.R.M. and Hodges, D.H., Nonlinear Flexure and Torsion of Rotating Beams, with Application to Helicopter Rotor Blades — I. Formulation. *Vertica*, 10, pp. 151-169, (1986).
6. Crespo da Silva, M.R.M. and Hodges, D.H., Nonlinear Flexure and Torsion of Rotating Beams, with Application to Helicopter Rotor Blades — II. Response and Stability. *Vertica*, 10, pp. 171 - 186, (1986).
7. Crespo da Silva, M. R. M., Zaretzky, C.L. and Hodges, D. H., Flexural-Flexural Dynamics of a Cantilever with a Tip Mass. Submitted for publication, (1989).
8. Hodges, D.H. and Ormiston, R.A., Stability of Elastic Bending and Torsion of Uniform Cantilever Rotor Blades in Hover with Variable Structural Coupling. *NASA Technical Note TN D-8192*, (1976).



## A DIRECT NUMERICAL EVALUATION OF FLOQUET TRANSITION MATRICES FOR PERIODIC SYSTEMS

Der-Ho Wu and S. C. Sinha  
Auburn University, Mechanical Engineering Department  
Auburn, AL 36849

### ABSTRACT

Many problems arising in the dynamics of rotating systems such as the helicopter blades, the rotor bearing systems and the dynamic stability of structures lead to a set of differential equations with periodic coefficients. In general, the equations are nonlinear, however, the stability analyses of all such systems require investigation of linear equations only. In spite of the availability of many techniques, Floquet analysis has served as the main tool in various applications. Floquet analysis is a powerful technique which is easily implemented on a computer and holds most promise in the analysis of large-scale periodic systems. Evaluation of 'Floquet Transition Matrix'(FTM) and eigenanalysis are the two major computational problems encountered in the analysis of periodic systems. Although many techniques have been suggested in the literature, the computation of FTM for large-scale system is still a challenging task. At the present time, the application of a higher order initial-value codes(such as the fourth-order Runge-Kutta or Hamming's Predictor-Corrector) in a 'single pass' scheme is regarded as the most efficient algorithm in the evaluation of FTM. The 'single pass' scheme was suggested about fifteen years ago, but since then not much progress has been made toward the development of new computational techniques.

In this study, a direct numerical evaluation of Floquet Transition Matrix is proposed. The solution of periodic systems is represented in terms of shifted Chebyshev polynomials of first or second kind. The main feature of this technique is that it reduces the original differential problem to a system of linear algebraic equations.

A multidimensional linear periodic system may be represented in the state-space form as

$$\dot{y}(t) = [A(t)] y(t) \quad ; \quad [A(t+T)] = [A(t)] \quad , \quad y(0) = y_0 \quad (1)$$

where  $y(t)$  is  $n$  vectors and  $[A(t)]$  is an  $n \times n$  periodic matrix with period  $T$ .

For a set of Chebyshev polynomials,  $S(t)$  defined over the period  $[0, T]$ , the vectors and matrices appearing in equation (1) may be expanded as

$$y(t) = \sum_{i=0}^{m-1} C_i S_i(t) \quad (2)$$

$$A(t) = \sum_{i=0}^{m-1} D_i S_i(t)$$

and

$$y(0) = y_0 S_0(t) , \quad (3)$$

where  $C_i$  are the unknown vectors,  $y_0$  is the initial vector, and  $D_i$  are known vectors.

Integrating equation (1), utilizing relations in equations (2) and (3), and equating the coefficients of  $S_i$  leads to a set of linear algebraic equations in  $C_i$ , which can be solved by a standard technique.

Once  $C_i$ 's are known, the solution  $y(t)$  can be obtained from equation (2), and the FTM can be directly evaluated.

Several illustrative examples including the stability of Mathieu's equation and column under periodic load are discussed. Potential applications to rotorcraft stability problem are also indicated.

# Lyapunov Exponents for Stochastic Systems with Applications to Helicopter Dynamics

by

N. Sri Namachchivaya and Kurt Heier  
Department of Aeronautical and Astronautical Engineering  
University of Illinois  
Urbana, IL

There are several probabilistic methods which have been presented in the literature for investigating the stability of stochastic dynamical systems. Most investigations have been concerned with stability in moments and almost sure or sample stability. In practice, it is generally most desirable to examine the almost-sure sample stability and the results thus obtained hold true with probability one. It is clear that for first order Itô equations, the region of stability for higher integer moments are included in the regions of stability of lower integer moments and furthermore, all integer moment stability regions are included in the region of sample stability. Recently, an exact relation between conditions for sample stability and conditions of moment stability were established in Kozin and Sugimoto [1] and extended by Arnold [2]. It has been shown by Kozin and Sugimoto [1] that sample stability region in some parameter space is a limit of the regions of the  $p^{\text{th}}$  moment stability as  $p \downarrow 0$ . However, it is difficult to obtain sample stability in such a fashion, since the conditions for the  $p^{\text{th}}$  moment stability is more difficult to obtain for arbitrary  $p$ , in multidimensional multiplicative systems. For this reason, sample stability in this paper is obtained using a very well developed concept of Lyapunov characteristic exponents (see, e.g., Khasminskii [3] and Arnold and Klieman [4]). Furthermore, it is well known that in regions where the system is stable in probability one, the second moments may grow exponentially. It is, therefore, important from the design point of view that the higher order moments decay in some parameter region. To this end, mean square stability conditions are also obtained in this work. The theory developed here is applicable to many engineering systems, however, in this paper attention is focussed on helicopter dynamics.

When a helicopter is in forward flight, even under ideal smooth flow assumption, the blade encounters different flow regions in a period of revolution and the aerodynamic loads along the blade are distributed

nonuniformly. By virtue of this complex but periodic aerodynamic loading, a helicopter rotor blade is a time variant system and is susceptible to severe vibrations. Noteworthy investigations of rotor dynamics in forward flight have been made by Stammers [5], Peters [6], Friedman [7], et al. Stammers paper discussed the nature of flapping torsion flutter and dealt with the presence of periodic coefficients in the equations of motion. It was shown that forward flight can have a significant stabilizing influence on flutter and that, as tip speed increases, flutter occurs predominantly at half-integer frequencies. Peters [6] considered the problem of flap-lag stability in forward flight. It was shown that periodic coefficients were important for flap-lag stability even at low advance ratios. It was also concluded that the variation in rotor trim and in-flow with forward speed had a significant effect on blade stability.

In the service life of a helicopter, numerous encounters with thunderstorm and clear air turbulence can be expected. Because of the very nature that the lift is generated by blade rotation, some level of self-created turbulence is also unavoidable. Thus, to make the analysis realistic, random turbulence in the atmosphere is included in many recent investigations, and considerable progress has been made towards understanding mean square flap-lag stability. The inquiry into the effects of atmospheric turbulence on the stability of a rotor blade was initiated by Lin, Fujimori, and Ariaratnam [8]. Here, the stability of uncoupled flap motion in the presence of random turbulence was investigated for the operating condition of hover and forward flight.

The coupled flap-lag equations of motion for forward flight previously derived by Peters [6] were generalized by Prussing and Lin [9] to include random turbulence in the airspeed components of the blade. Here, a mean square stability analysis was performed only for the case of hover with vertical turbulence. It was shown that vertical turbulence appears to increase the stability of the coupled flap-lag motion for realistic rms turbulence velocities.

In this work, almost sure stability for coupled flap-lag motion is examined using the well developed concept of Lyapunov exponents. To this end, the equations of motion derived by Prussing and Lin [9] are used, i.e.,

$$\begin{bmatrix} \ddot{\delta\beta} \\ \ddot{\delta\zeta} \end{bmatrix} + [C] \begin{bmatrix} \dot{\delta\beta} \\ \dot{\delta\zeta} \end{bmatrix} + [K] \begin{bmatrix} \delta\beta \\ \delta\zeta \end{bmatrix} = \begin{bmatrix} F_1 \\ F_2 \end{bmatrix}$$

where

$$C_{ij} = \bar{C}_{ij} + \xi C_{ij}^{\xi} + \eta C_{ij}^{\eta} + \nu C_{ij}^{\nu}$$

$$K_{ij} = \bar{K}_{ij} + \xi K_{ij}^{\xi} + \eta K_{ij}^{\eta} + \nu K_{ij}^{\nu}$$

$$F_i = \xi F_i^{\xi} + \eta F_i^{\eta} + \nu F_i^{\nu}, \quad i = 1, 2, j = 1, 2.$$

The variables  $\beta$  and  $\zeta$  are the blade flap and lead-lag angles, respectively, and  $\xi$ ,  $\eta$  and  $\nu$  are the non-dimensional lateral, longitudinal, and vertical random turbulence components of the air flow relative to the blade. The matrices  $C$  and  $K$  consist of deterministic ( $\bar{C}_{ij}$ ,  $\bar{K}_{ij}$ ) and stochastic components and the inhomogeneous forcing terms  $F_1$  and  $F_2$  are also functions of the random turbulence components. This analysis is an extension of the recent work reported by Sri Namachchivaya and Prussing [10] on the almost sure stability of decoupled flap motion.

As the first step in the analysis, a set of approximate Ito equations are derived using both deterministic and extended stochastic averaging methods. The effect of turbulence is greater near the critical points of the dynamical system. In the vicinity of such critical points, extended stochastic averaging yields a set of 2-D reduced Ito equations as

$$da = m_a(a, \phi, \mu, \lambda) dt + \sigma_{ij}^a(a, \mu, \lambda) dw_{aj}$$

$$d\phi = m_{\phi}(a, \phi, \mu, \lambda) dt + \sigma_{ij}^{\phi}(a, \phi, \mu, \lambda) dw_{\phi j}$$

where  $m_a$ ,  $m_{\phi}$  are the drift coefficients and  $\sigma_{ij}^a$  and  $\sigma_{ij}^{\phi}$  are the diffusion coefficients of the associated Fokker-Planck equation, and  $W_{aj}$ ,  $W_{\phi j}$  are Wiener processes of unit intensity. It is worth pointing out that  $a$  and  $\phi$  processes are coupled and the rate of growth of the amplitude process depends on the evaluation of the  $\phi$  process on a unit circle. The Lyapunov exponent  $\hat{\lambda}$  defined as

$$\hat{\lambda} = \lim_{t \rightarrow \infty} \frac{1}{t} \ln ||x(t; x_0, t_0)||, \quad x = \{\delta\beta, \dot{\delta\beta}\}$$

is calculated for the above  $\text{It}\hat{o}$  equations using the approach given by Khasminskii [3], and Sri Namachchivaya and Prussing [10]. The dynamical system is said to be almost sure stable (stable with probability 1) if  $\lambda < 0$ .

Consider an  $n$ -degree of freedom system, which represents many physical problems including the flap-lag motion, i.e.

$$\ddot{x}_i + 2\alpha_i \dot{x}_i + \Omega_i^2 x_i = \varepsilon^{1/2} A_{ij} x_j \xi(t) + \varepsilon \mu B_{ij} x_j \sin \nu t, \quad i, j = 1, 2, \dots, n$$

where  $A_{ij}$  and  $B_{ij}$  are elements of constant matrices. In this equation, we shall assume that the 1<sup>st</sup> mode (lead-lag) has small damping compared to the rest of the modes. The maximal Lyapunov exponent  $\lambda$  can be calculated as

$$\hat{\lambda} = -\rho + \frac{\mu}{2} \left\{ \frac{I_{1-i\Delta}(\bar{\mu})}{I_{-i\Delta}(\bar{\mu})} + \frac{I_{1+i\Delta}(\bar{\mu})}{I_{i\Delta}(\bar{\mu})} \right\}, \quad \rho = \frac{2\alpha_1}{\omega_0} - \frac{1}{2} k_{11}^2 + \sum_{j=1}^n \frac{k_{1j} k_{j1}}{4\kappa_j} \hat{S}(\Omega_{ij}^+)$$

where  $I_{1-i\Delta}(\bar{\mu})$  represents the Bessel function of imaginary arguments, and imaginary order,

$$\bar{\mu} = \frac{\mu P_{11}}{2D}, \quad \bar{\Delta} = \left\{ \lambda + k_{11}^2 \psi(1) - \sum_{j=2}^n \frac{k_{1j} k_{j1}}{4\kappa_j} [\hat{\psi}(\Omega_{ij}^+) - \hat{\psi}(\Omega_{ij})] \right\} / D$$

$$D = \frac{1}{2} + [k_{11}^2 (2S(0) + S(1))], \quad \kappa_j = \omega_j / \omega_0, \quad \nu = \omega_0 (1 - \varepsilon \lambda)$$

$$P_{ij} = A_{ij} / \omega_0^2, \quad k_{ij} = B_{ij} / \omega_0^2$$

$S(\cdot)$  and  $\psi(\cdot)$  are cosine and sine spectrums of the stochastic excitation  $\xi(t)$ , and  $\lambda$  is the detuning parameter.

## REFERENCES

1. F. Kozin and Sugimoto, 1977. Proceedings of the Conference on Stochastic Differential Equations and Applications, ed: J. David Mason, Academic Press, New York. Relations between sample and moment stability for linear stochastic differential equations.
2. L. Arnold, 1984. SIAM J. of Applied Mathematics, Vol. 44, No. 4, pp. 793-802. A formula connecting sample and moment stability of linear stochastic systems.
3. R. Z. Khasminskii, 1967. Theory of Probability Applications, Vol. 12, pp. 144-147. Necessary and sufficient conditions for the asymptotic stability of linear stochastic systems.
4. L. Arnold and W. Kliemann, 1983. Probabilistic Analysis and Related Topics, Vol. 3, ed: A. Bharucha-Reid, Academic Press, New York, Qualitative theory of stochastic systems.
5. C. W. Stammers, 1970. The Aeronautical Quarterly, February. The flutter of a helicopter rotor blade in forward flight.
6. D. A. Peters, 1975. J. of American Helicopter Society, Vol. 20, No. 4, pp. 2-13. Flap-lag stability of helicopter rotor blades in forward flight.
7. P. Friedman, 1973. J. of American Helicopter Society, Vol. 18, No. 4, pp. 13-23. Some conclusions regarding the aeroelastic stability of hingeless helicopter blades in hover and in forward flight.
8. Y. K. Lin, Y. Fujimori and S. T. Ariaratnam, 1979. AIAA Journal, Vol. 17, No. 6, pp. 545-552. Rotor blade stability in turbulent flows, Part II.
9. J. E. Prussing and Y. K. Lin, 1982. J. of American Helicopter Society, Vol. 27, No. 2, pp. 51-57. Rotor blade flap-lag stability in turbulent flows.
10. N. Sri Namachchivaya and J. E. Prussing, J. of Sound and Vibration (submitted for publication). Almost-sure asymptotic stability of rotor blade flapping motion in forward flight in turbulent flow.

**Recent Efforts in Integrated Aerodynamic Load/Dynamic Optimization  
of Helicopter Rotor Blade**

**by**

**Aditi Chattopadhyay  
Research Scientist  
Analytical Services & Materials, Inc.  
Hampton, Virginia 23666**

**and**

**Yihwan Danny Chiu  
Research Engineer  
Lockheed Engineering & Sciences Company  
Hampton, Virginia 23666**

**Proposed Abstract for  
Third Technival Workshop on Dynamics and Aeroelastic Modeling  
of Rotorcraft Systems  
Duke University, Durham, NC  
March 12 - 14, 1990.**



Recent Efforts in Integrated Aerodynamic Load/Dynamic Optimization  
of Helicopter Rotor Blades

by

Aditi Chattopadhyay  
Research Scientist  
Analytical Services & Materials, Inc.  
Hampton, Virginia 23666

and

Yihwan Danny Chiu  
Research Engineer  
Lockheed Engineering & Sciences Company  
Hampton, Virginia 23666

Abstract for  
Third Technival Workshop on Dynamics and Aeroelastic Modeling  
of Rotorcraft Systems  
Duke University, Durham, NC  
March 12 - 14, 1990.

Introduction and Background

Currently at NASA Langley Research Center, there is an effort to integrate various disciplines in the rotor blade design process<sup>1</sup>. An investigation at partially integrating some of

these disciplines is reported in Ref. 2, where the integration of aerodynamic loads effects and the dynamic aspects of blade design was addressed by coupling a comprehensive helicopter analysis code, CAMRAD<sup>3</sup>, the nonlinear optimization algorithm, CONMIN<sup>4</sup>, and an approximate analysis technique. A combination of the blade root 4/rev vertical shear and the blade weight was minimized with constraints on coupled lead-lag and flapping frequencies, blade autorotational inertia and centrifugal stress. The paper demonstrated a significant reduction in the 4/rev vertical shear and blade weight, which were objective functions, along with overall reductions in the amplitudes of the oscillatory vertical airloads both azimuthal and radial. As a byproduct, it was shown that optimization also reduced the total power required by the rotor while maintaining the same  $C_T/\sigma$ ,  $C_T$  being the rotor thrust coefficient and  $\sigma$  the thrust weighted solidity of the blade.

It was of interest to extend the work of Ref. 2 by including other sources of blade vibration that are transmitted to the hub. For a four-blade rotor the other major oscillatory loads are the 3/rev and 5/rev inplane and radial shears, the 3/rev and 5/rev flapping and torsional moments and the 4/rev lagging moment. These are included in the optimization formulation, either in the form of objective functions or as constraints, in the present work. Also, the total thrust of the optimized blade in Ref. 2 was lower than that of the reference blade although the  $C_T/\sigma$  was held constant during optimization. To avoid this loss in the rotor thrust, a constraint is imposed on the total thrust.

### **Problem Statement and Formulation**

Optimization techniques are applied to minimize the vibratory blade loads of a four-blade helicopter in forward flight. This is done by considering all the major sources of vibration (forces and moments) in the rotating frame that are transmitted to the nonrotating hub as 4/rev harmonics of the longitudinal, lateral and vertical forces and the pitch, roll and yaw moments. The objective functions are the 4/rev vertical shear and the 3/rev inplane shear. Constraints are imposed on the 3/rev radial shear, the 3/rev flapping and control moments, the 4/rev lagging moment. Constraints are also imposed on natural frequencies, blade weight, centrifugal stress

and blade autorotational inertia. A constraint is incorporated on the rotor thrust to ensure that the optimum blade performs the same rotor task as the reference blade. Side constraints are also imposed on the design variables to avoid impractical solutions. The bounds are selected from an existing advanced rotor blade model which will be called the 'reference' blade hereafter.

### Blade Model and Design Variables

A linear taper is allowed along the blade planform (Fig.1) and the blade taper ratio,  $\lambda$ , is  $\lambda = c_r / c_t$ , where  $c_r$  is the root chord and  $c_t$  is the tip chord. It is assumed that the blade stiffnesses arise solely from the blade structural component (i.e., the contributions of the nonstructural masses, the skin and honeycomb, etc. are neglected.

The design variables are the blade stiffnesses at the root, the taper ratio, the root chord, the radius of gyration at blade root and the nonstructural weights located spanwise. The blade preassigned properties and the helicopter performance parameters are used from the existing reference blade data. A method called the 'Global Criteria Approach'<sup>5</sup> is used to formulate the multiple objective optimization problem.

### Analysis

The program CAMRAD is used for the blade aerodynamic and dynamic analysis and the program CONMIN is used for the optimization. In addition, approximate analyses of the objective function and constraints involving Taylor series expansions are used to save computational effort. Sensitivity analyses for computing derivatives of the objective function and the constraints are part of the procedure.

The blade is trimmed at each step of design optimization. A wind tunnel trim option, provided in CAMRAD, which consists of trimming the rotor lift and drag, each normalized with respect to  $\sigma$ , and the flapping angle with collective and cyclic pitch and shaft angle is used.

### Results

Optimum designs have been obtained with and without the thrust constraint and the two results are compared. For ease of reference the following notation will be used

Case 1: optimum design with thrust constraint,

### Case 2: optimum design without thrust constraint.

Case 2 signifies a design where the hub shears can be minimized at the expense of reducing the rotor thrust. The remaining constraints are the same for both the cases. Note that this would mean keeping the blade thrust weighted solidity fixed during optimization.

Some typical results obtained are presented in Figs. 2 - 4. Fig. 2 presents a comparison of the 4/rev vertical and the 3/rev inplane shears, which are the objective functions. The reductions are larger in Case 2 due to the fact that the rotor has much lower thrust, however, the optimum blade in Case 1 also has lower values of these shears. It was of interest to investigate whether optimization causes any changes in the blade section airloads. Therefore, the normal and inplane components of the total aerodynamic forces on the section, the lift  $L$  and the drag  $D$ , resolved with respect to the hub plane and denoted by  $F_z$  and  $F_x$  respectively, are plotted. Fig. 3 presents the azimuthal distribution of  $F_z$  at a radial station of  $y/R = 0.99$ . The figure indicates that optimization does not change the magnitude of  $F_z$  in case 1, but reduces its amplitude significantly in Case 2. Fig. 4 presents a comparison of the rotor power coefficient,  $C_p$ , normalized with respect to solidity  $\sigma$ , for the reference and the optimum blades. Even without any consideration of the rotor power, i.e., the power not included in the optimization formulation, the optimum blades in case 1 does not suffer any increase in the total power and in case 2 the power requirement reduces significantly.

The final work will contain more details of the optimized blade. For example a complete history of the constraints (flapping, lagging, control moments, etc.) will be studied. More results will be included to demonstrate the effect of reducing the 4/rev vertical and the 3/rev inplane shears on the blade section airloads. Since a comparison of Cases 1 and 2 indicate a trade-off between reductions in the harmonics of the loads and maintenance of a certain thrust level, results are being obtained with several other thrust conditions to establish a pattern which would be of interest to a blade designer. Additional results ascertaining the effect of such optimization on blade performance will also be obtained.

### References

1. Adelman, Howard M. and Mantay, Wayne R., "An Initiative in Multidisciplinary Optimization of Rotorcraft," NASA TM-101523, AVSCOM TM 88-B-016, October, 1988.
2. Chattopadhyay, Aditi, Walsh, Joanne L. and Riley, Michael F., "Integrated Aerodynamic/Dynamic Optimization of Helicopter Blades," Proc. AIAA/ASME/ASCE/AHS 30th Structures, Structural Dynamics and Materials Conference, Mobile, Alabama, April 3-5, 1989. AIAA Paper No. 89-1269. Also available as NASA TM-101553, February, 1989.
3. Johnson, W., "A Comprehensive Analytical Model of Rotorcraft Aerodynamics and Dynamics," Part II: User's Manual, NASA TM 81183, June 1980.
4. Vanderplaats, G. N., "CONMIN - A Fortran Program for Constrained Function Minimization," User's Manual, NASA TMX-62282, August 1973.
5. Rao, S. S., "Multiobjective Optimization in Structural Design with Uncertain Parameters and Stochastic Processes," AIAA Journal, Vol. 22, No. 11, November 1984.

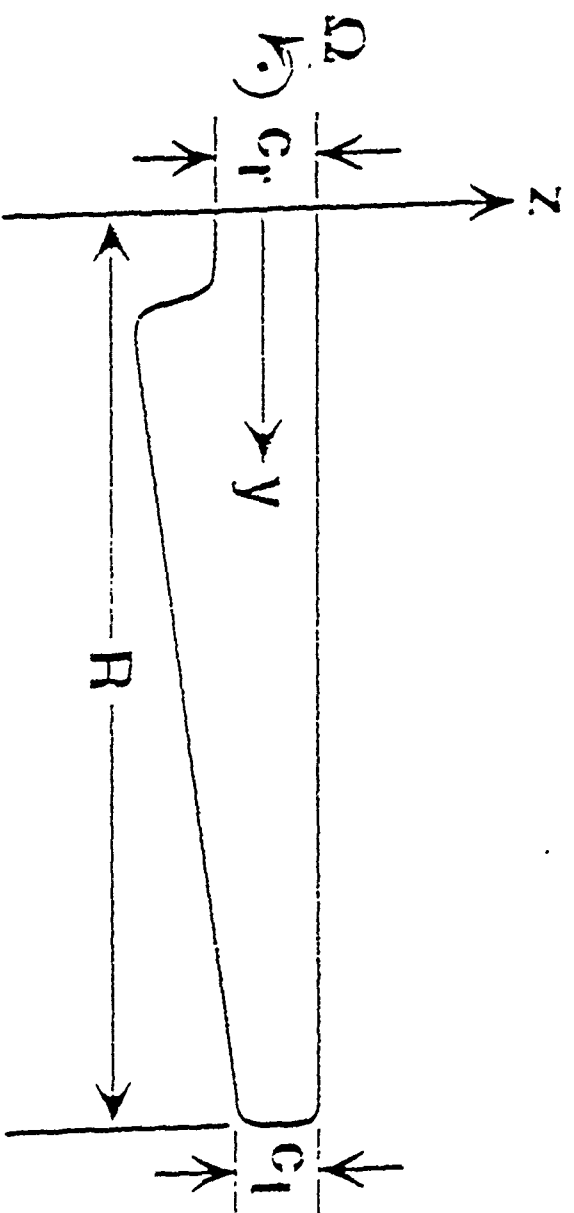


Fig. 1 Rotor blade model

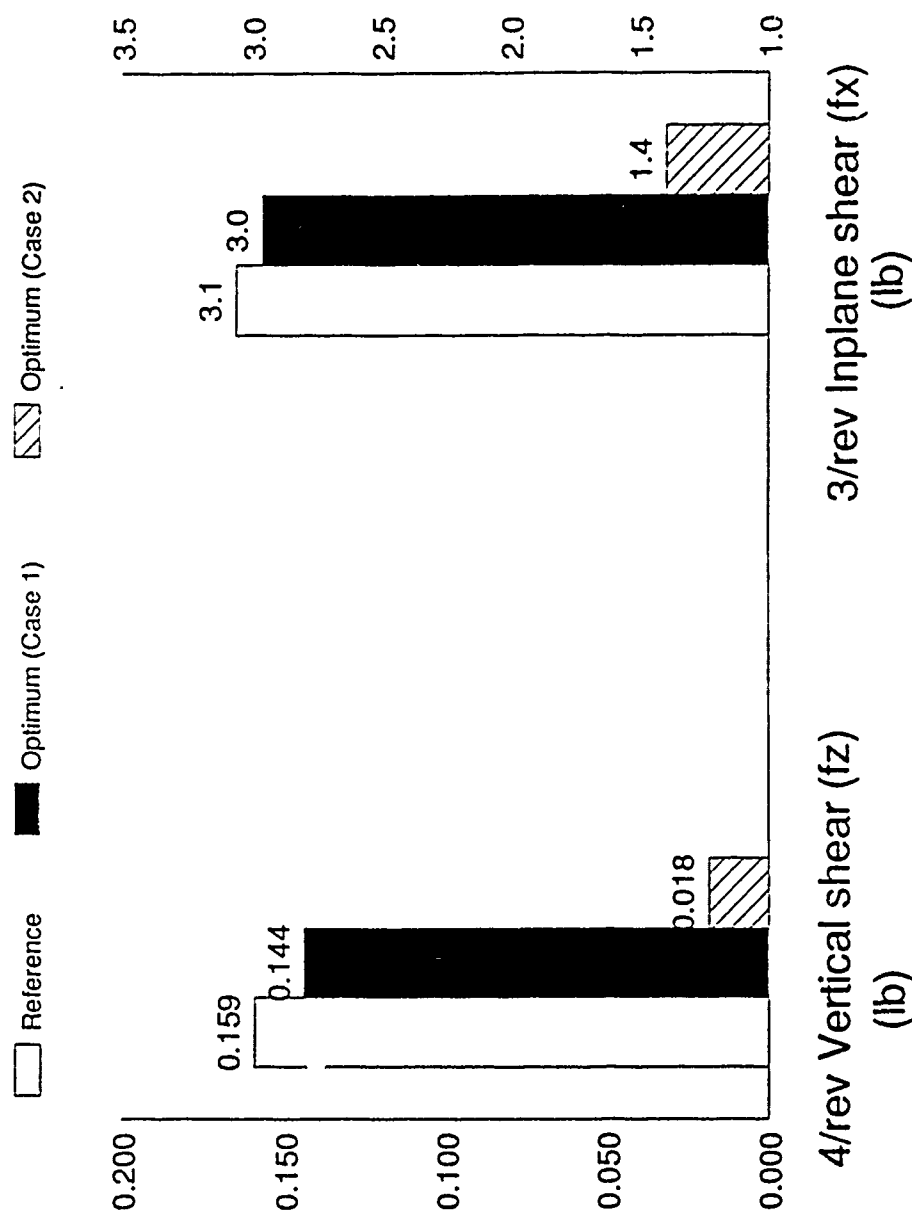


Fig. 2. Comparison of objective functions

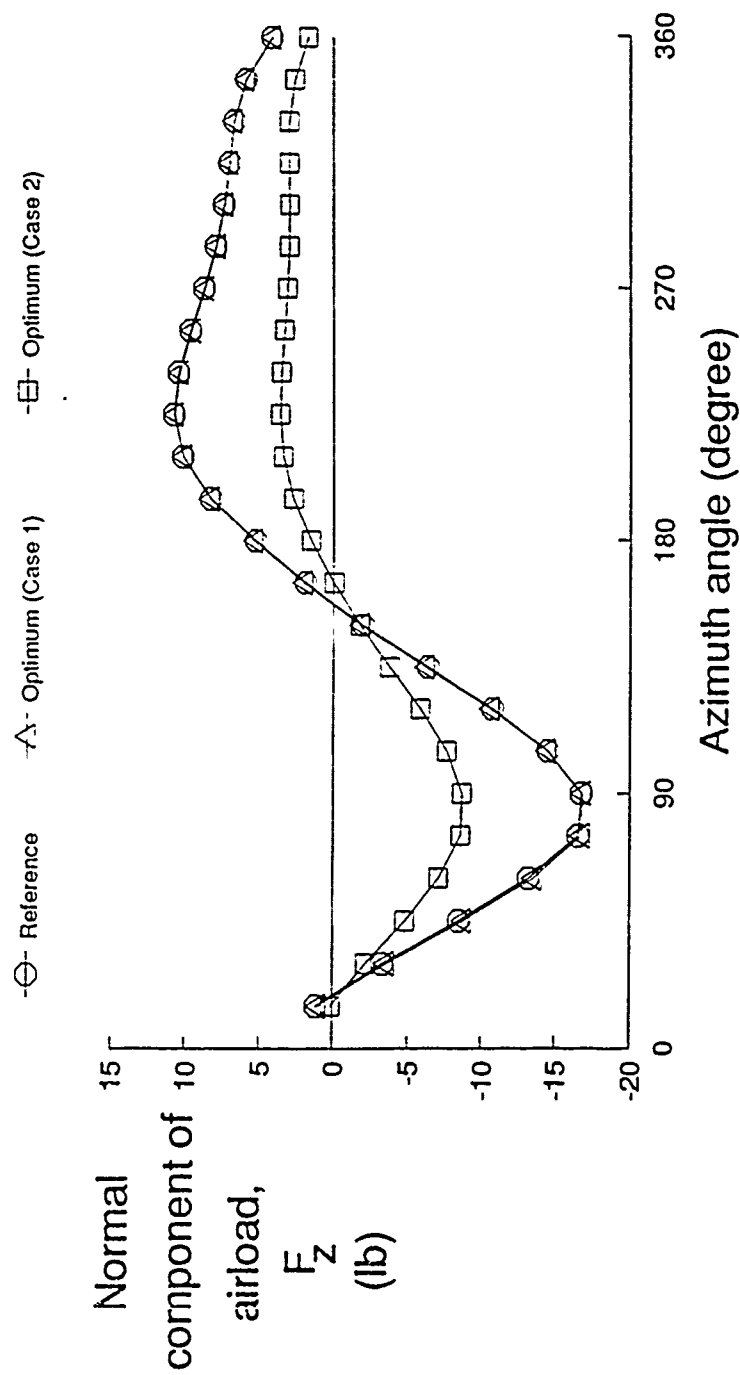


Fig.3 Azimuthal distributions of normal airload component

$y/R = 0.99$ ,  $\mu = 0.3$ ;

Case 1: with 100% thrust constraint

Case 2: without thrust constraint



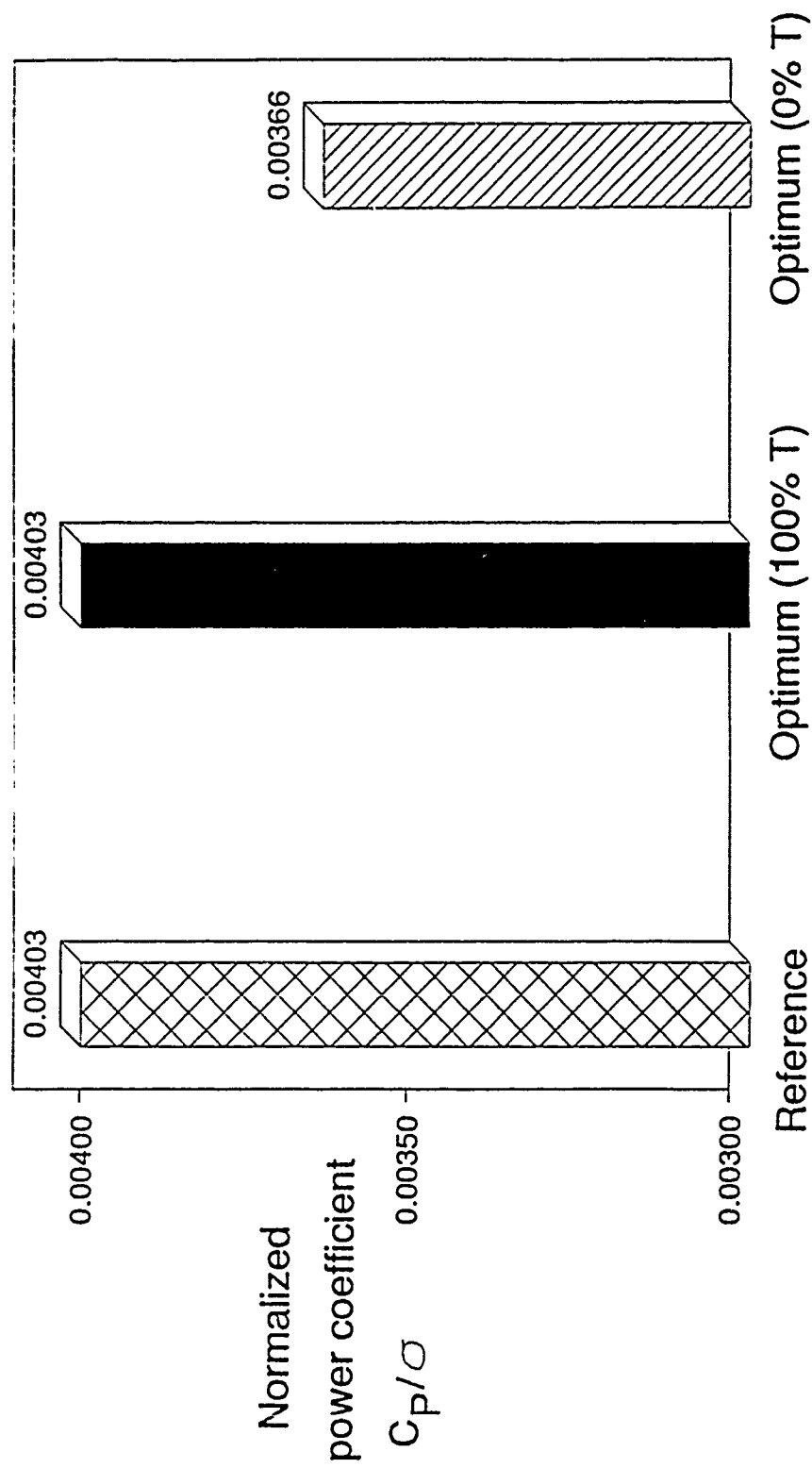


Fig. 4 Comparison of normalized coefficient,  
 $C_p/\sigma$

**RECENT EFFORTS IN INTEGRATED  
AERODYNAMIC LOAD/DYNAMIC OPTIMIZATION OF  
HELICOPTER ROTOR BLADES**

**Aditi Chattopadhyay  
Analytical Services and Materials, Inc.**

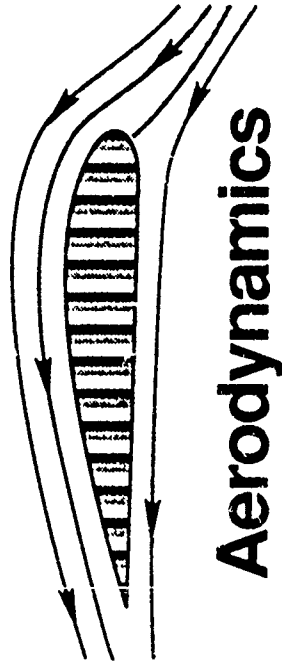
**and**

**Y. Danny Chiu  
Lockheed Engineering and Sciences Co.  
Hampton, Virginia**

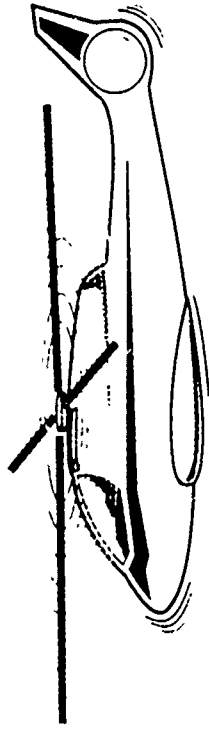
**The Third Workshop on Dynamics and Aeroelastic  
Stability Modeling of Rotorcraft Systems  
Duke University, Durham, North Carolina  
March 12-14, 1990.**

# **INTEGRATED ROTORCRAFT OPTIMIZATION**

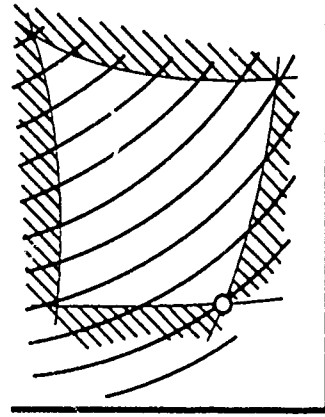
---



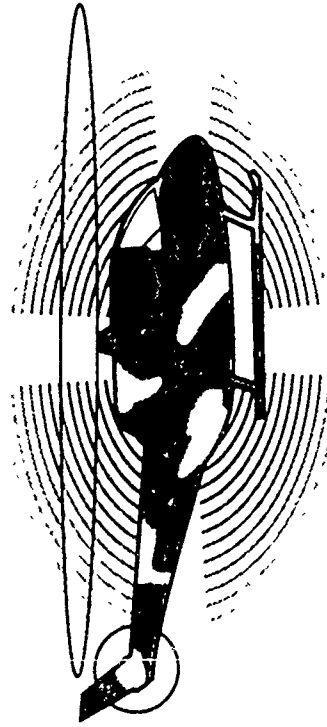
**Aerodynamics**



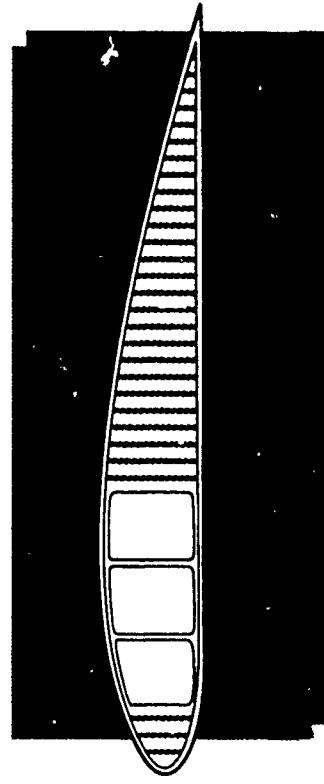
**Dynamics**



**Optimization**



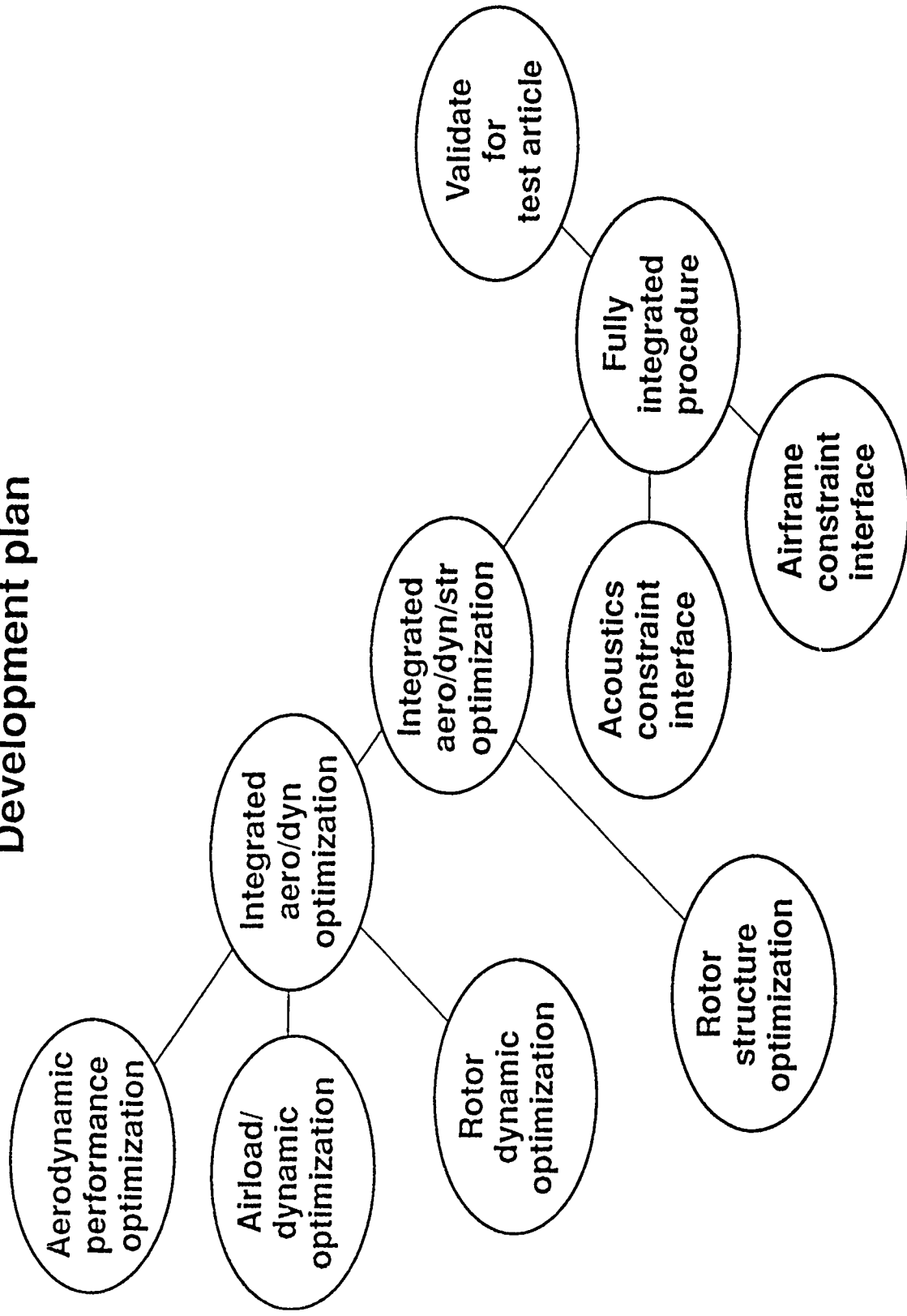
**Acoustics**



**Structures**

# INTEGRATED ROTORCRAFT ANALYSIS

## Development plan



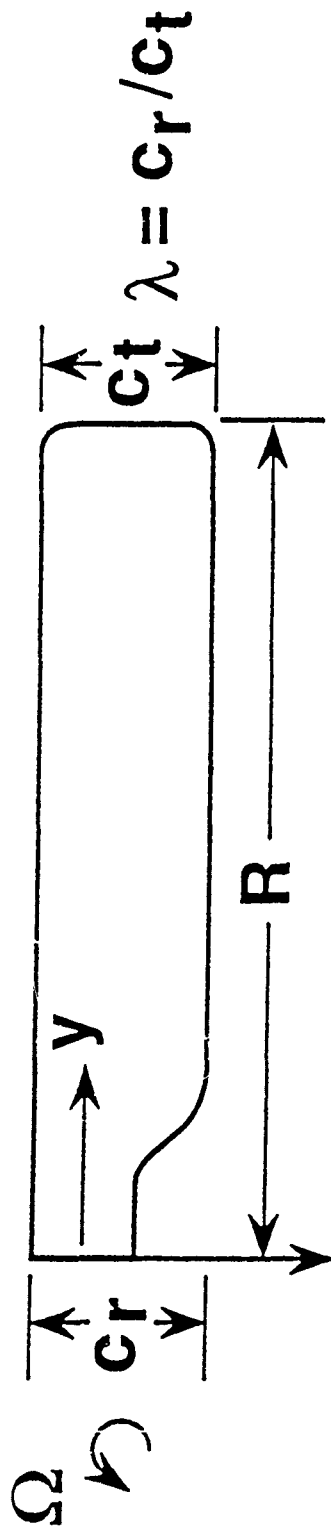
## FOCUS OF CURRENT WORK

- Develop an enhanced integrated aerodynamic load/dynamic optimization procedure to reduce vibration in rotor blades

## KEY CONCEPTS

- Couple aerodynamic loads analysis and dynamic analysis with an optimization procedure
- Integrate airloads that change during optimization with changes in design variables
- Trim the blade at each optimization cycle

## TEST PROBLEM ("Reference Blade")



- Wind tunnel model of advance rotor (GBH type)
- Articulated four-bladed, rigid hub,  $\tau_{max} = -16^\circ$
- Linear twist distribution
- Single airfoil
- Rectangular planform

# OPTIMIZATION PROBLEM

- Objective functions:
  - 4/rev vertical and 3/rev inplane root shears
- Design variables:
  - Stiffness  $El_{xx}$ ,  $El_{zz}$  and  $GJ$  at blade root, root chord, radius of gyration at blade root, taper ratio
- Constraints:
  - 3/rev radial shear
  - 3/rev flapping and torsional and 4/rev lagging moments
  - Frequencies (first four elastic flap/lag)
  - Autorotational inertia
  - Centrifugal stress
  - Blade weight
  - Rotor thrust
  - Bounds on design variables



**FORMULATION OF MULTIPLE OBJECTIVE  
OPTIMIZATION PROBLEM USING  
GLOBAL CRITERIA APPROACH**

- Objective functions:  $F_1(\phi)$  and  $F_2(\phi)$

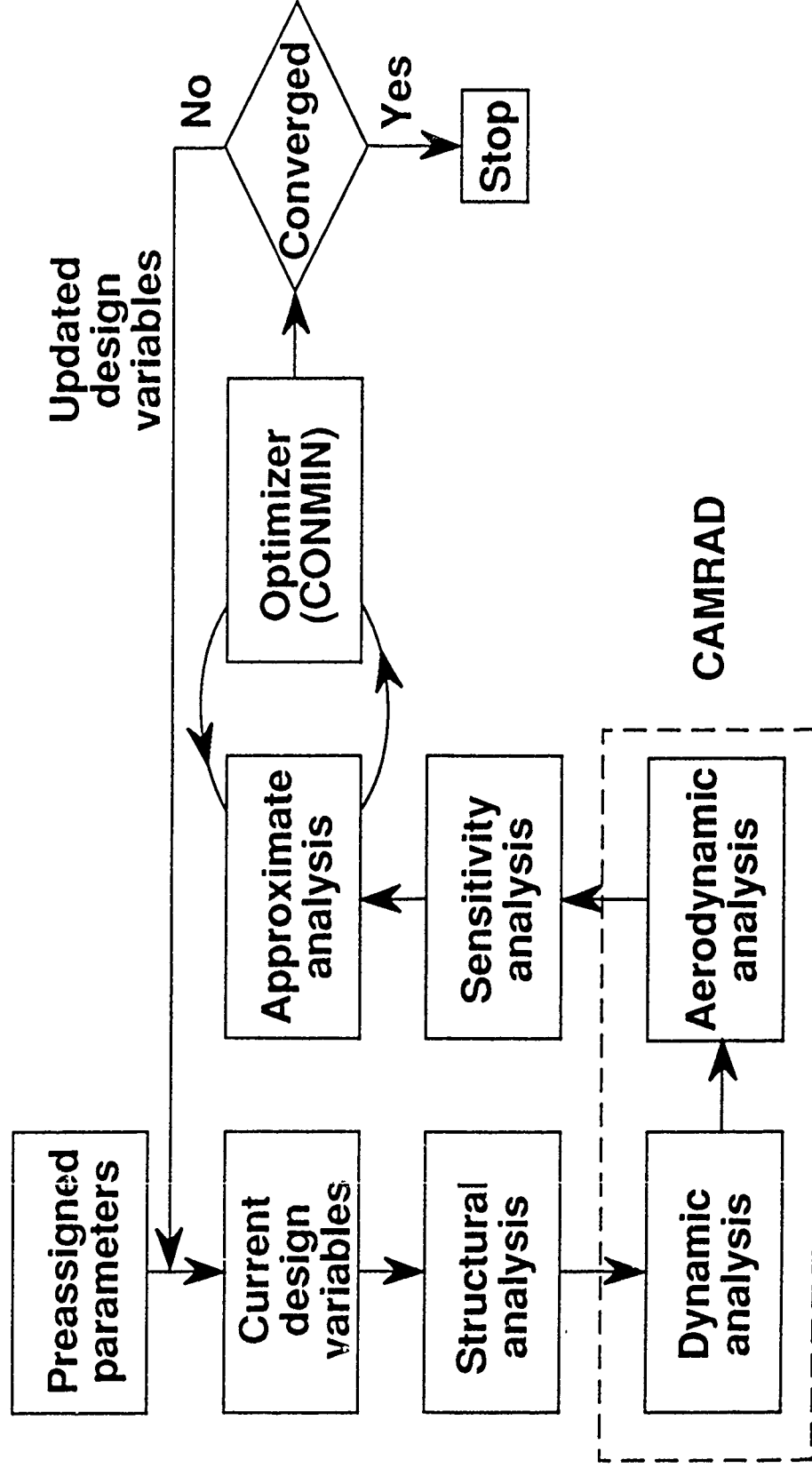
$\phi$  : design variable vector

- Constraints:  $g(\phi) \leq 0$
- Global objective function:

$$F(\phi) = \left[ \left( \frac{F_1(\phi_1) - F_1(\phi_1^*)}{F_1(\phi_1^*)} \right)^2 + \left( \frac{F_2(\phi_2) - F_2(\phi_2^*)}{F_2(\phi_2^*)} \right)^2 \right]^{1/2}$$

subject to  $g(\phi) \leq 0$

# FLOW CHART OF OPTIMIZATION PROCEDURE



# ANALYSIS

- **Structural analysis:**  
Computation of section properties,  
autorotational inertia and centrifugal stress
- **Aerodynamic loads and dynamics  
analysis using CAMRAD**

## Assumptions:

- Uniform inflow
- Yawed flow on rotor
- Unsteady aerodynamics
- No dynamic stall

## **ANALYSIS, CONTINUED**

- **Optimization:**
  - **CONMIN** - based on method of feasible directions
  - **Approximate analysis** - based on linear Taylor series expansion
  - **Sensitivity analysis** - analytical and finite difference

## TRIM CRITERION USED

- Wind tunnel trim option in CAMRAD
- $C_T/\sigma$  ,  $C_X/\sigma$  and flapping angles trimmed using collective and cyclic pitch and shaft angles

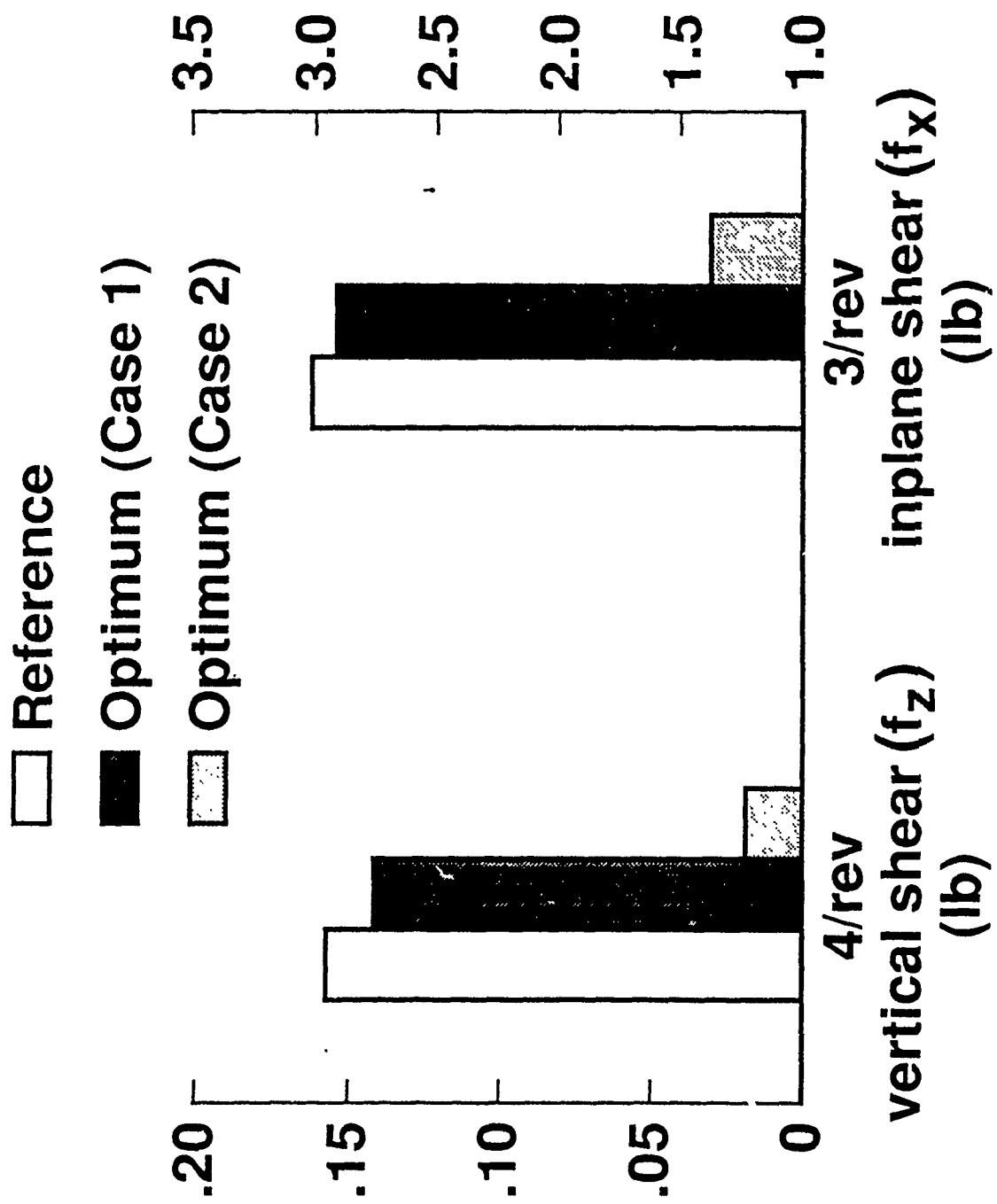
## RESULTS

- Two cases studied
- Case 1: with thrust constraint
  - reference and optimum rotors have same  $C_T$  and  $C_X$  as well as same  $C_T/\sigma$  and  $C_X/\sigma$
- Case 2: without thrust constraint
  - reference and optimum rotors have same  $C_T/\sigma$  and  $C_X/\sigma$

# KEY RESULTS

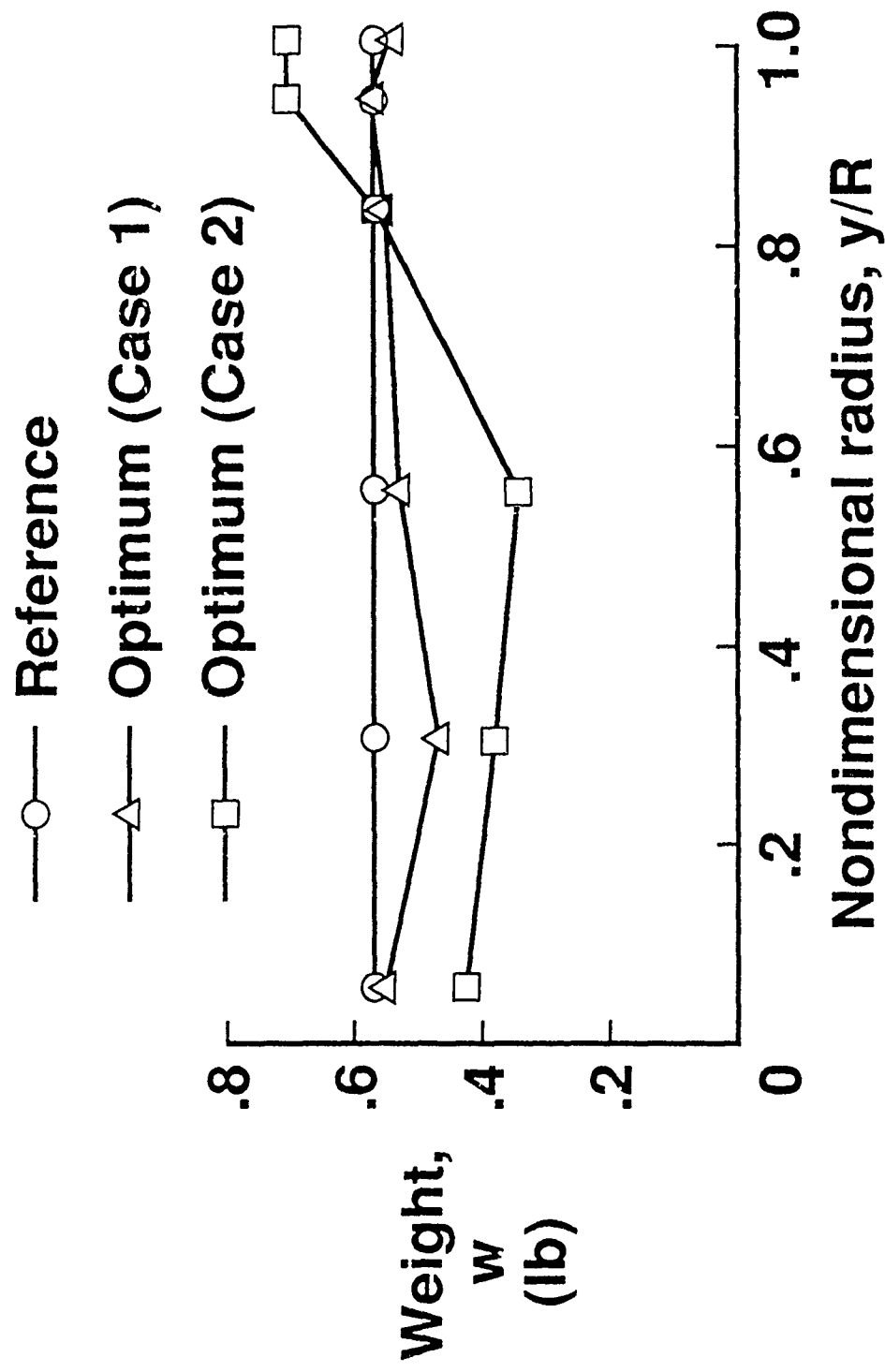
	Reference	Optimum	
		Case 1	Case 2
4/rev vertical shear (lb)	0.16	0.14 (10.9%)	0.016 (89.8%)
3/rev inplane shear (lb)	3.17	3.04 (4.1%)	1.43 (55.0%)
Blade weight (lb)	3.41	3.39 (5.9%)	3.01 (11.7%)
Thrust (lb)	298.7	298.7	158.5 (53.0%)
Solidity	0.122	0.122	0.065 (53.0%)
Taper ratio	1.0	1.0	1.24

# COMPARISON OF OBJECTIVE FUNCTIONS

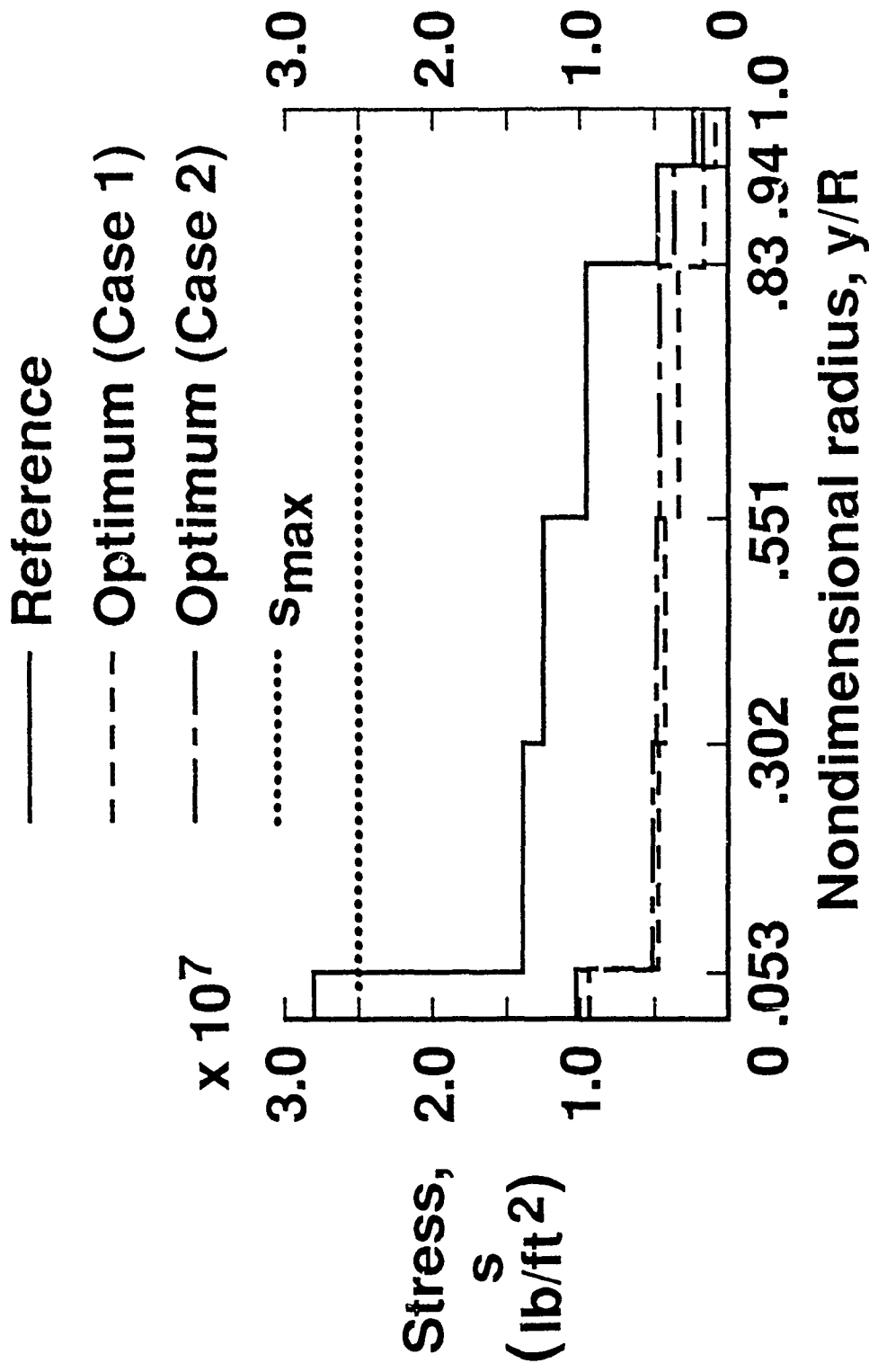




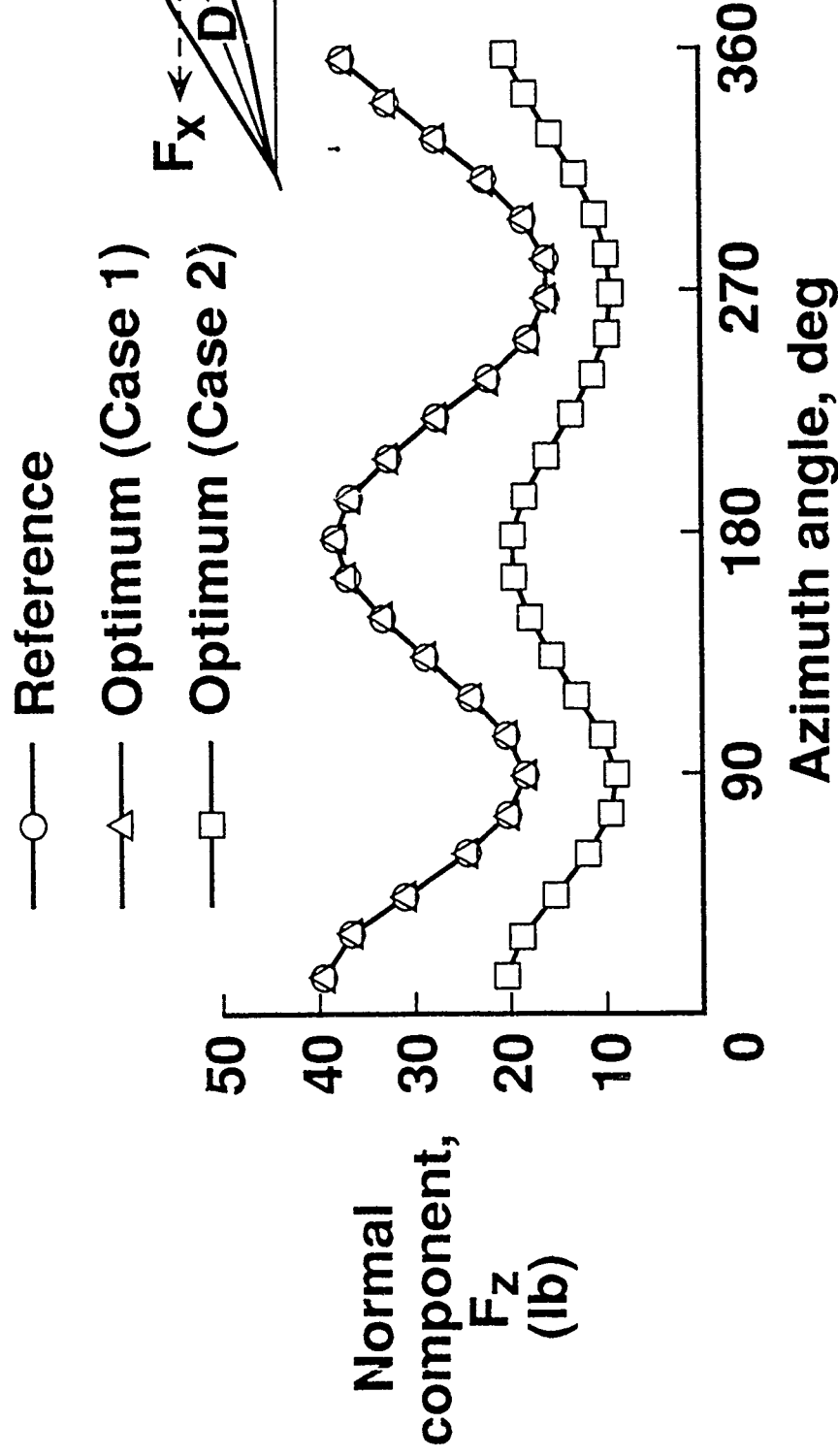
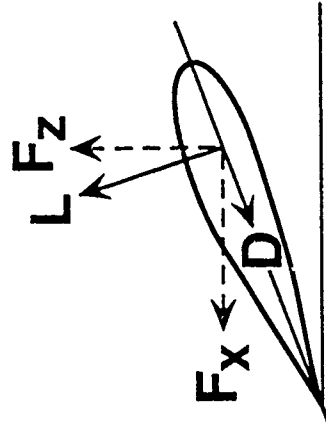
# NONSTRUCTURAL WEIGHT DISTRIBUTIONS



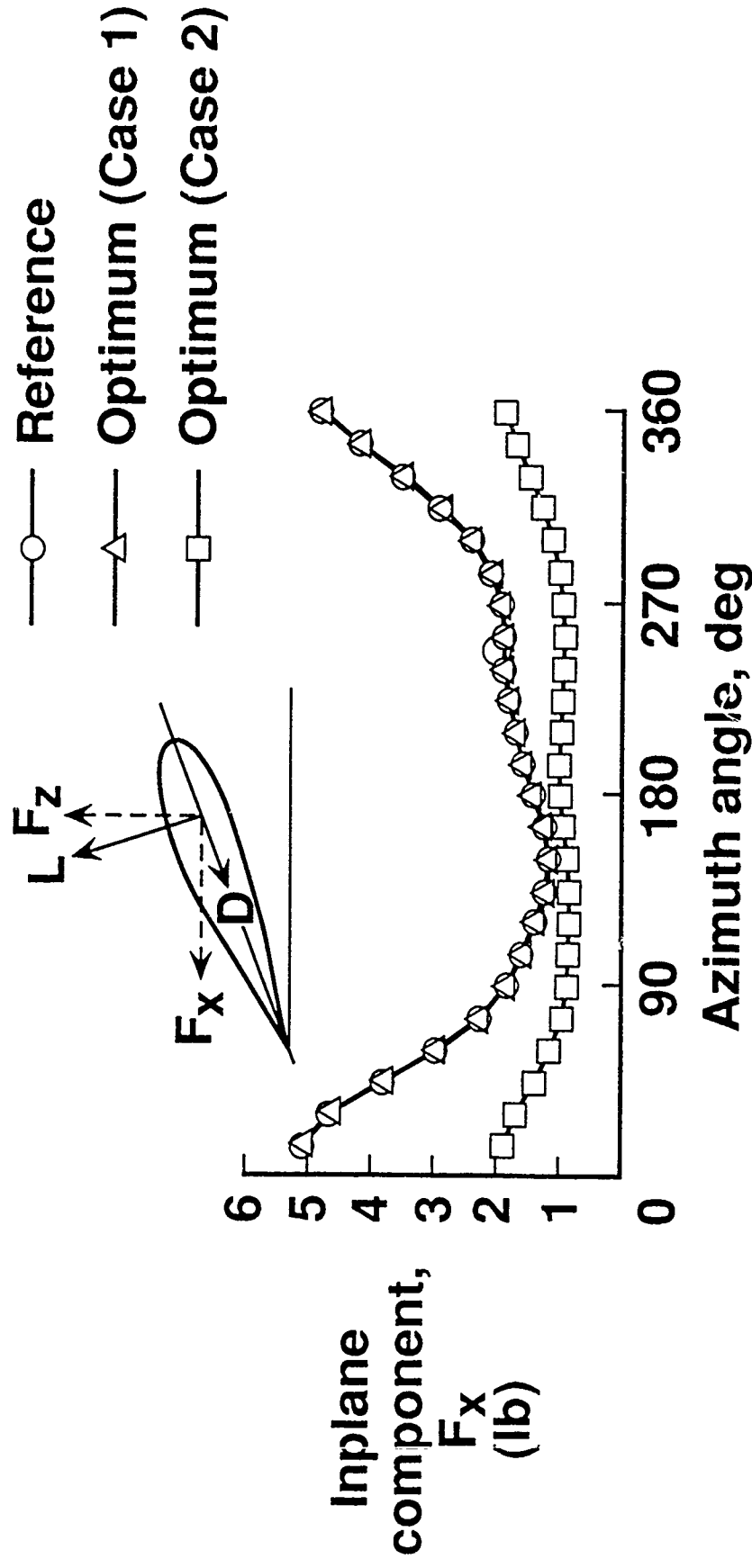
# CENTRIFUGAL STRESS DISTRIBUTIONS



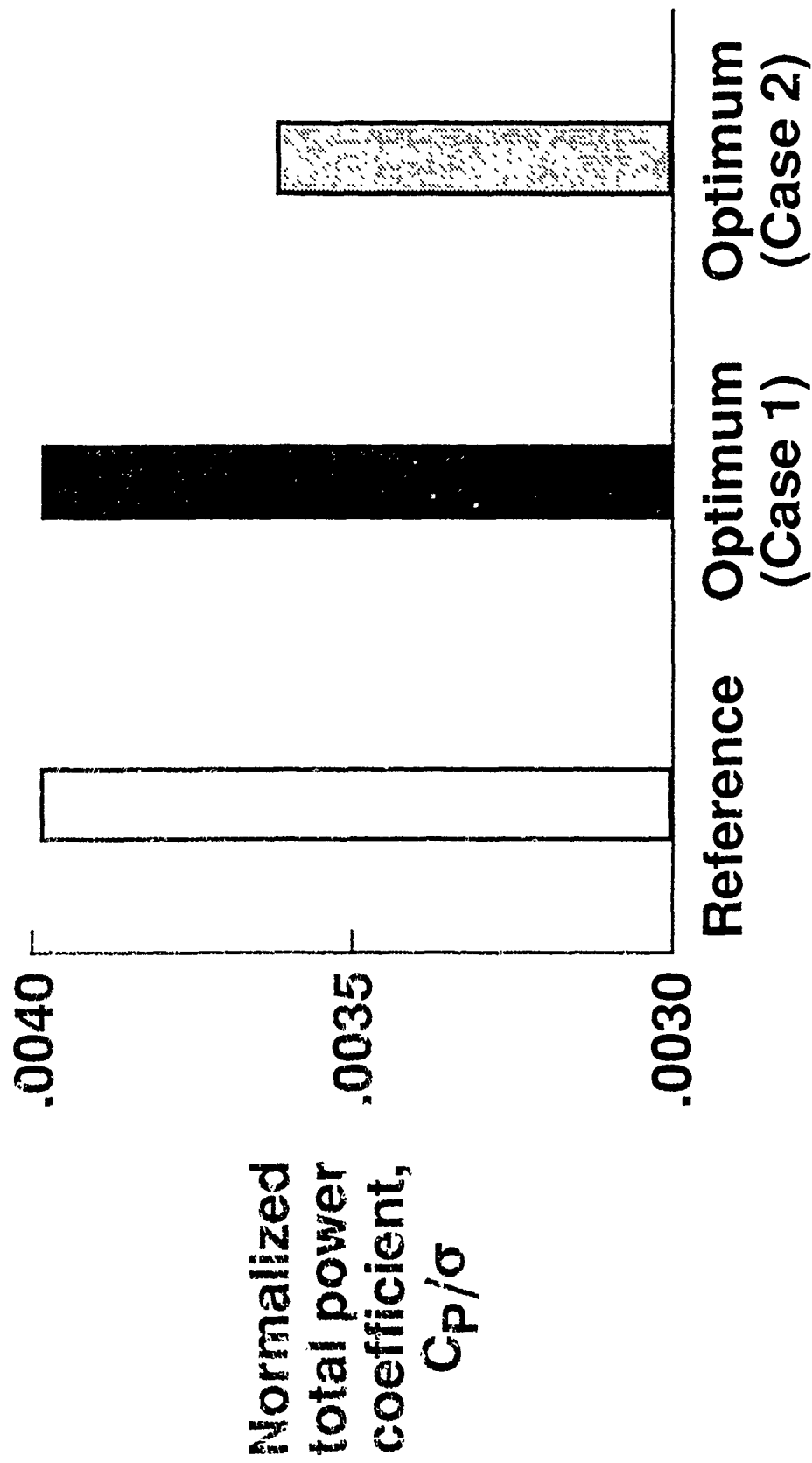
# **AZIMUTHAL DISTRIBUTIONS OF NORMAL COMPONENT OF AIRLOAD, $F_z$** **$y/R = 0.75, \mu = 0.3$**



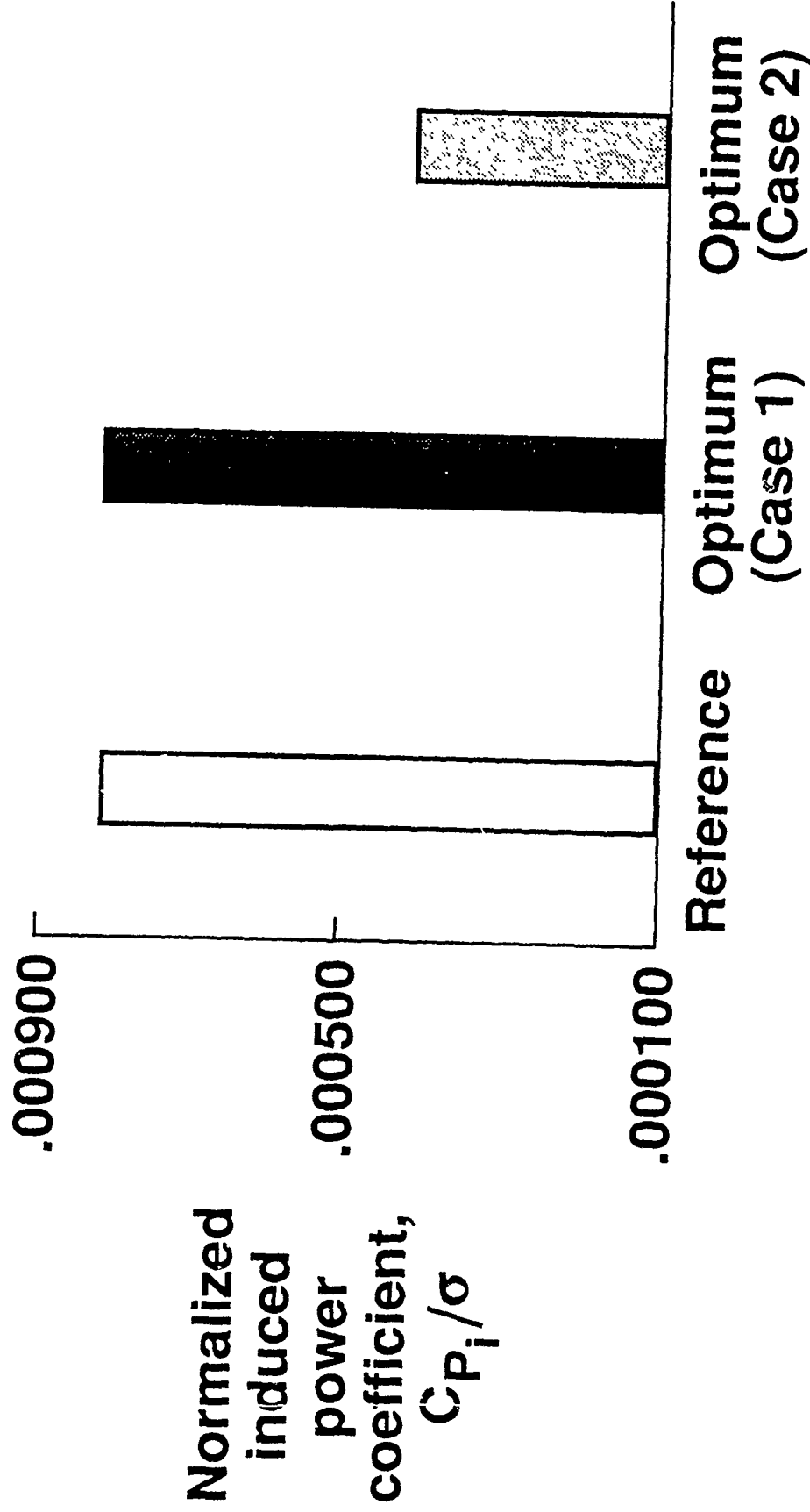
# **AZIMUTHAL DISTRIBUTIONS OF INPLANE COMPONENT OF AIRLOAD, $F_x$** **$y/R = 0.75, \mu = 0.3$**



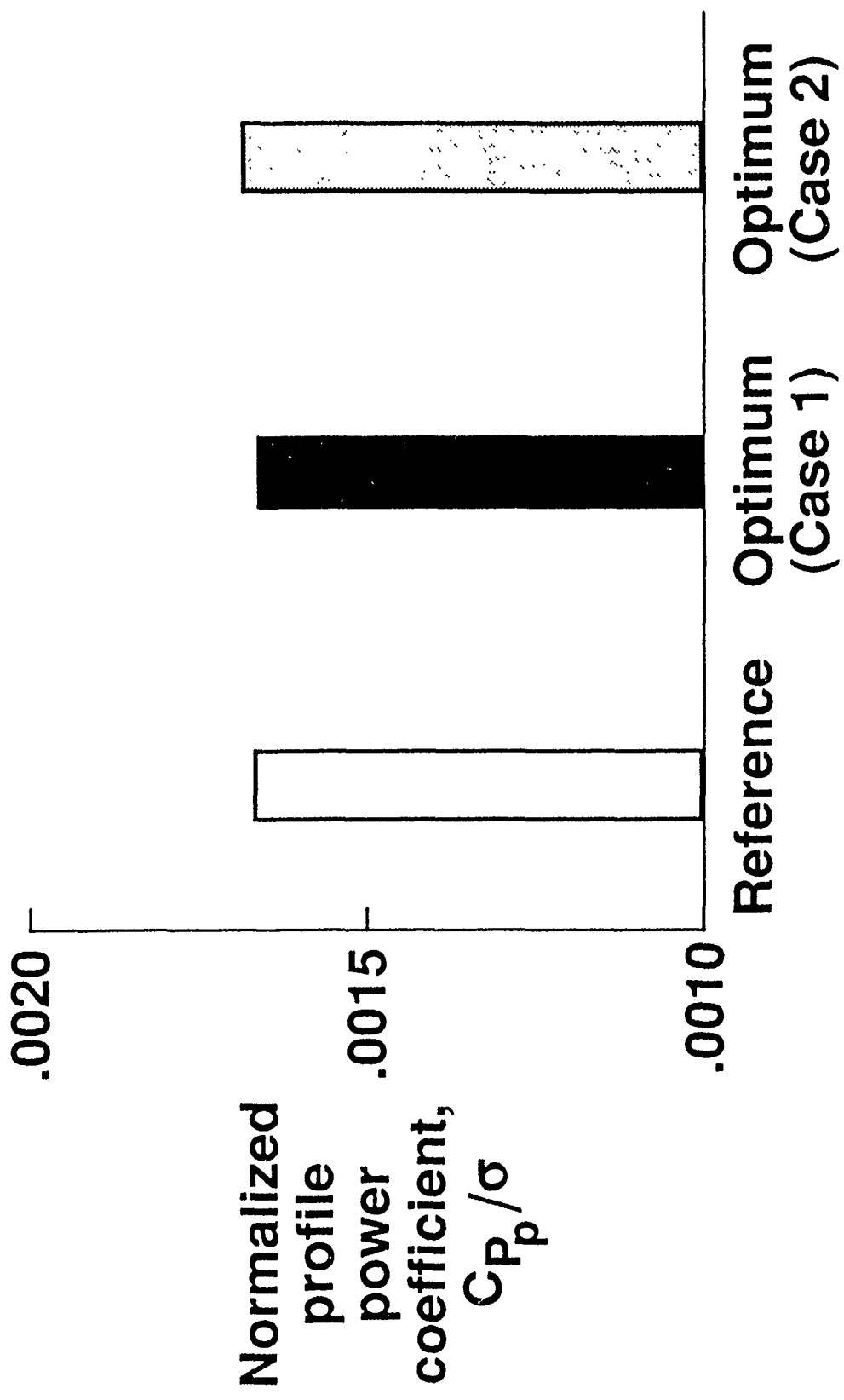
# COMPARISON OF NORMALIZED TOTAL POWER COEFFICIENT



# COMPARISON OF NORMALIZED INDUCED POWER COEFFICIENT

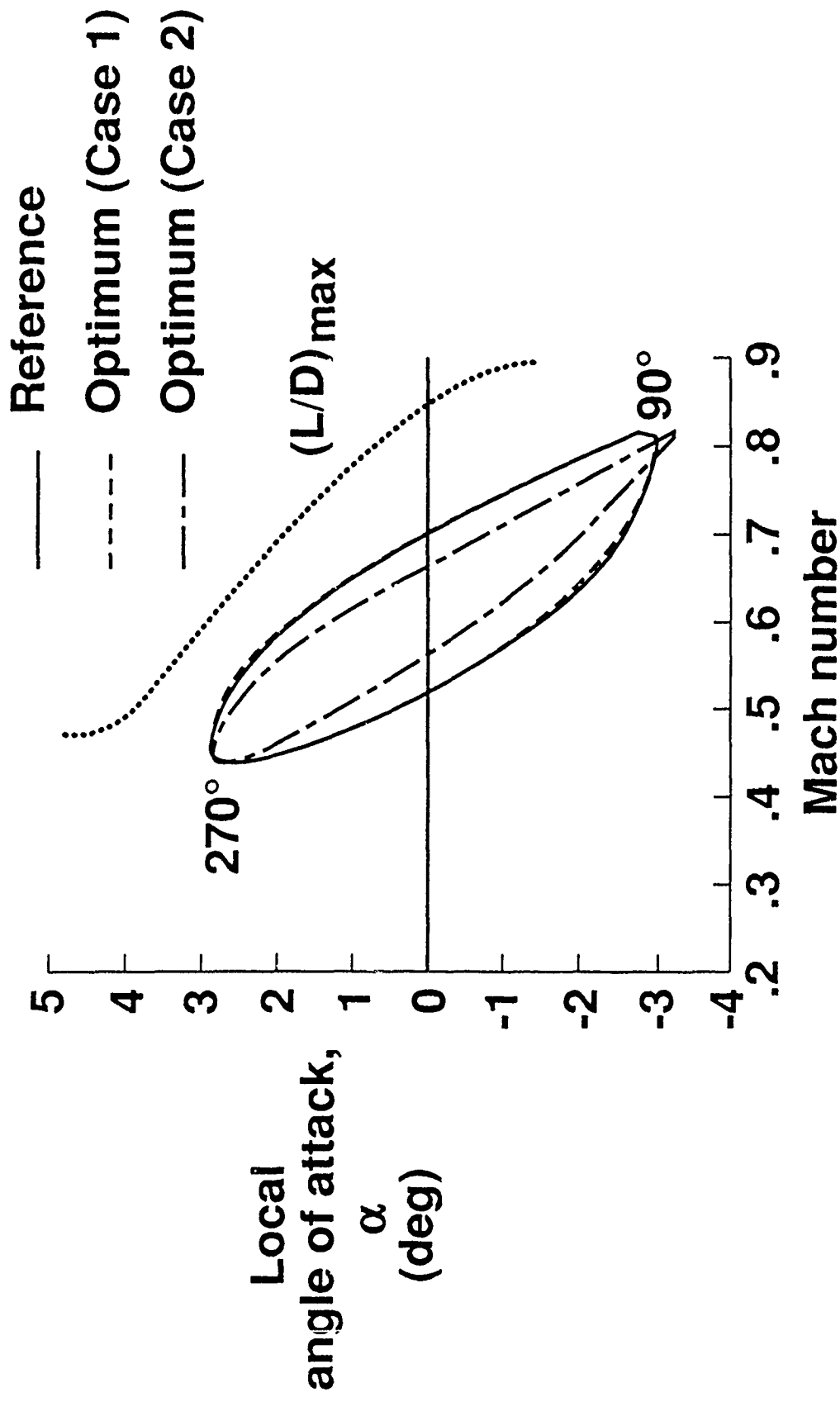


# COMPARISON OF NORMALIZED PROFILE POWER COEFFICIENT



# VARIATION OF LOCAL ANGLE OF ATTACK WITH MACH NUMBER

$y/R = 0.99$





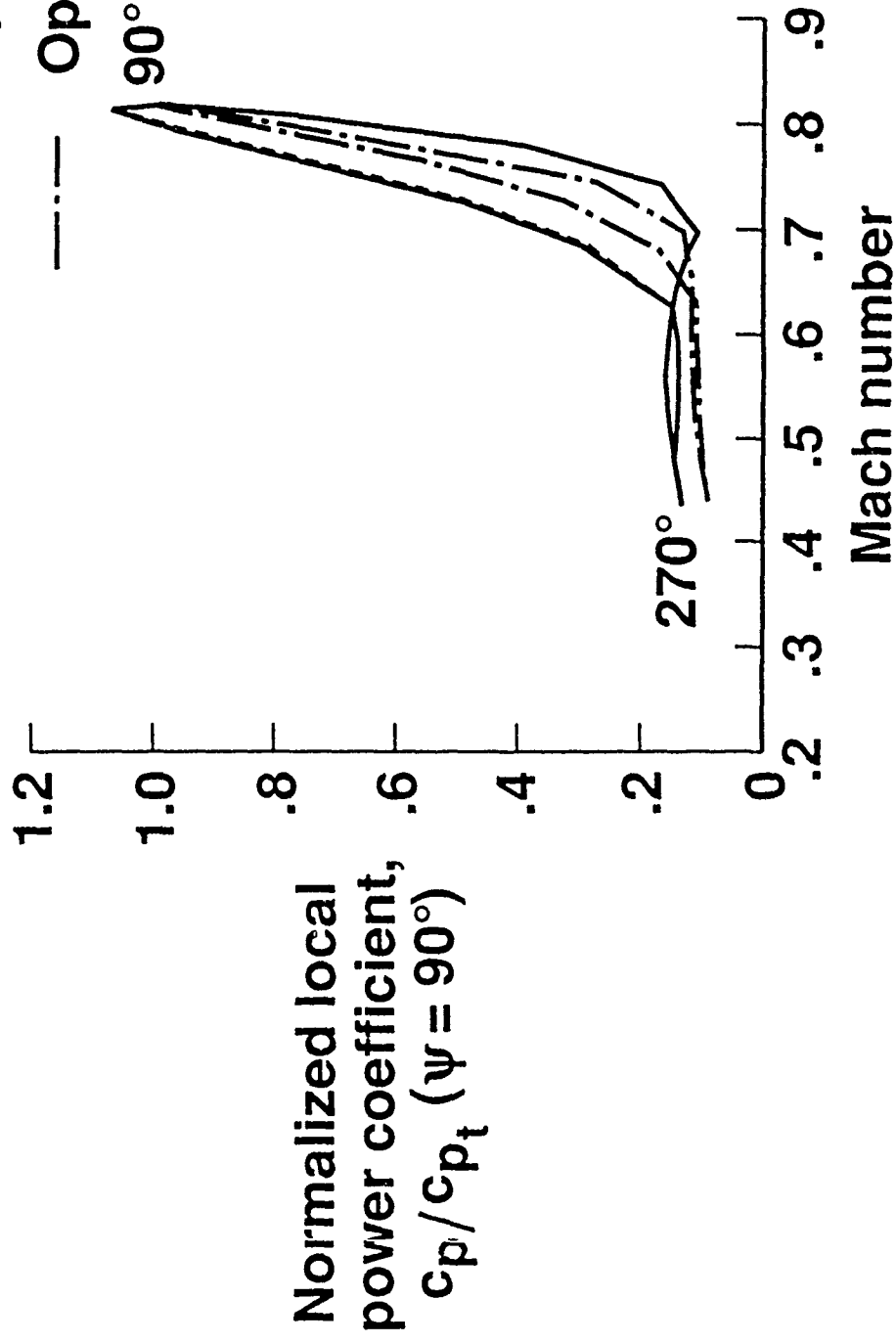
# VARIATION OF LOCAL POWER COEFFICIENT WITH MACH NUMBER

$y/R = 0.99$

— Reference

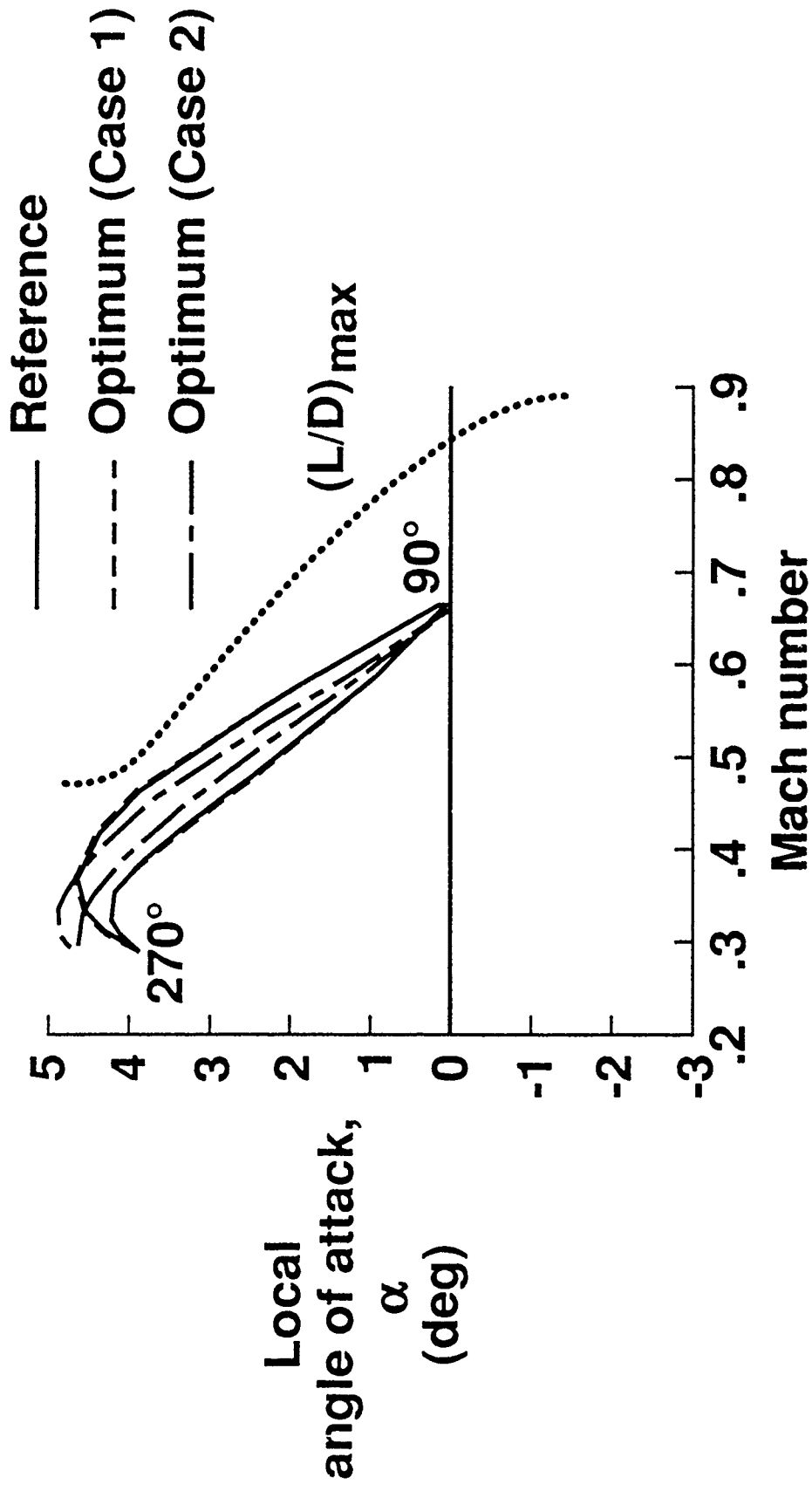
--- Optimum (Case 1)

- · - · - Optimum (Case 2)



# VARIATION OF LOCAL ANGLE OF ATTACK WITH MACH NUMBER

$y/R = 0.75$



# VARIATION OF LOCAL POWER COEFFICIENT WITH MACH NUMBER

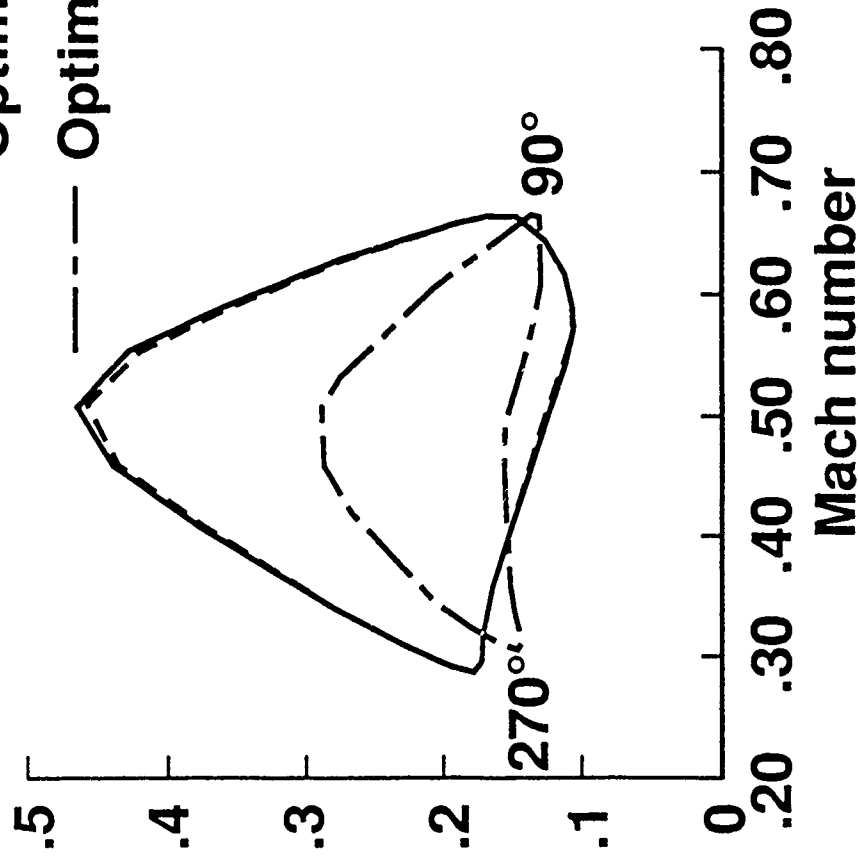
$y/R = 0.750$

— Reference

--- Optimum (Case 1)

--- Optimum (Case 2)

Normalized local  
power coefficient,  
 $c_p / c_{p_t} (\psi = 90^\circ)$



## CONCLUDING REMARKS

- Integrated aerodynamic load/dynamic optimization procedure for rotor blade designs
- Objective functions: 4/rev vertical and 3/rev inplane shears
- Constraints: 3/rev radial shears, 3/rev flapping and torsional moments, 4/rev lagging moment, frequencies, autorotational inertia, centrifugal stress, blade weight and rotor thrust
- CAMRAD, CONNMIN and approximate analysis used
- Global criteria approach used for multiple objective functions

## CONCLUDING REMARKS, CONTINUED

- Optimum designs obtained in 10-15 cycles
- Comparisons made between two cases
  - Case 1: with thrust constraint
  - Case 2: without thrust constraint
- Significant reductions in 4/rev and 3/rev inplane shears for both Cases 1 and 2 without weight penalty
- Other critical shear forces and moments at blade root remained within bounds

## CONCLUDING REMARKS, CONTINUED

- Amplitudes of section normal and inplane forces substantially reduced in Case 2.  
No reduction in Case 1 due to thrust constraint
- Performance criteria, not included in optimum design, virtually unchanged between reference and optimum
- Optimum blade retains same power requirement as the reference blade in Case 1. It has lower power requirement in Case 2

## Application of DYNOPT Optimization Program For Tuning Frequencies of Helicopter Airframe Structures

T. Sreekanta Murthy  
Lockheed Engineering and Sciences company  
Hampton VA 23666

### ABSTRACT

Among the various approaches which are employed in attempts to reduce vibrations in helicopters, the method of airframe structural tuning has begun to receive renewed attention. In the airframe tuning approach, the natural frequencies of the airframe are separated from the frequencies of the rotor-induced loads to avoid resonances and to reduce dynamic responses via appropriate modification of the airframe structure. This approach to the design of airframes has the potential for producing inherently low vibration helicopters. Research work on this approach is relatively new and is contained primarily in references 1 through 5. The cited papers all address the use of local structural modifications aimed at tuning airframe natural frequencies. Several methods have been used in those papers to identify airframe members for modification. Sciarra(1) used a strain energy method; Done and his co-workers (2) and Sobey (3) used the Vincent circle trace of responses as obtained through variation of stiffness in airframe members; Hanson (4) did a comparative study of the above two methods; King (5) used a modal tuning method. Although the term "structural optimization" is used, for the most part the papers do not apply structural optimization in the usual way. Rather the term is used to indicate that any local structural modifications which have been made are the best based on ad hoc considerations such as reduction of responses or strain energy in a member. The use of optimization techniques for airframe structural modifications is rather recent. Indeed, references 6 through 8 describe what are apparently the only published reports on the application of such techniques to simple models of airframes.

As part of the on-going research on helicopter optimization for vibration reduction at LaRC, a study was initiated to develop computational procedures for optimization of practical airframe structures under dynamic constraints. One of the objectives of the study was to develop sensitivity analysis procedures for constraints on the steady-state dynamic response displacement of airframes under rotor-induced loads. Research work in this regard involved development of a solution sequence based on direct matrix abstraction program (DMAP) of MSC/NASTRAN to compute the sensitivity coefficients for the dynamic response constraints. The sensitivity results from the application of the solution sequence to an elastic line model of a helicopter airframe structure are discussed in reference (9). In the research study, a computational procedure based on the nonlinear programming approach of optimization was developed which incorporates the dynamic response sensitivity solution sequence. The procedure has the capability to solve optimization problems with frequency and static constraints in addition to forced response constraints. Implementation of the procedure resulted in a computer code, designated DYNOPT, for optimization of airframes under dynamic constraints. This paper describes the features of the DYNOPT code and demonstrates its application to optimization of the finite element model of a Bell AH-1G helicopter airframe. The results of this study are described and discussed in this paper.

## References

1. Sciarra, J.J., "Use of the Finite Element Damped Forced Response Strain Energy Distribution for Vibration Reduction", Boeing Vertol Company, Report D210-10819-1, U.S. Army Research Office - Durham, Durham, N.C., July 1974.
2. Done, G.T.S. and Hughes, A.D., "Reducing Vibrations by Structural Modification", Vertica, 1976, Vol. 1, pp. 31-38
3. Sobey, A.J., "Improved Helicopter Airframe Response through Structural Change", Ninth European Rotorcraft Forum, Paper No. 59, Sept. 13-15, 1983, Stresa, Italy.
4. Hanson, H.W., "Investigation of Vibration Reduction Through Structural Optimization", Bell Helicopter Textron Report No. USAAVRAD-COM - TR-80-D-13, July, 1980.
5. King, S.P., "The Modal Approach to Structural Modification", The American Helicopter Society, National Specialists' Meeting On Helicopter Vibration "Technology for the Jet Smooth Ride", Vol. 28, No. 2, April, 1983.
6. Done, G.T.S., and Rangacharyulu, M.A.V., "Use of Optimization in Helicopter Vibration Control by Structural Modification", Journal of Sound and Vibration, 1981, 74(4), pp. 507-518.
7. Miura, H. and Chargin, M., "Automated Tuning of Airframe Vibration by Structural Optimization", American Helicopter Society, 42nd Annual Forum, Washington D.C., 1986.
8. Sreekanta Murthy, T., "Optimization of Helicopter Airframe Structures For Vibration Reduction - Considerations, Formulations and Applications", AIAA Aircraft Design, Systems and Operations Meeting, September 7-9, 1988, Atlanta, Georgia.
9. Sreekanta Murthy, T., "Design Sensitivity Analysis of Rotorcraft Airframe Structures For Vibration Reduction", NASA Conference Publication No. 2457, September, 1986.
10. MSC/NASTRAN, "User's Manual Volume I and II", The McNeal-Swendler Corporation, November 1985.
11. Vanderplaatts, G.N., "CONMIN - A FORTRAN Program for Constrained Function Minimization, User's Manual", NASA TMX - 62282, August 1973.
12. Cronkhite, J.D., Berry, V.L., and Brunken, J.E., "A NASTRAN Vibration model of the AH-1G Helicopter Airframe", Volume I and II, Bell Helicopter Report No. 209-099-432, Fort Worth, Texas, June 1974.



Title : Application of DYNOPT Optimization Program For Tuning  
Frequencies of Helicopter Airframe Structures

Author: T. Sreekanta Murthy

Affiliation: Lockheed Engineering and Sciences Company

Mailing Address: M.S. 340  
NASA Langley Research Center  
Hampton VA 23665

Telephone: 804 864 1229

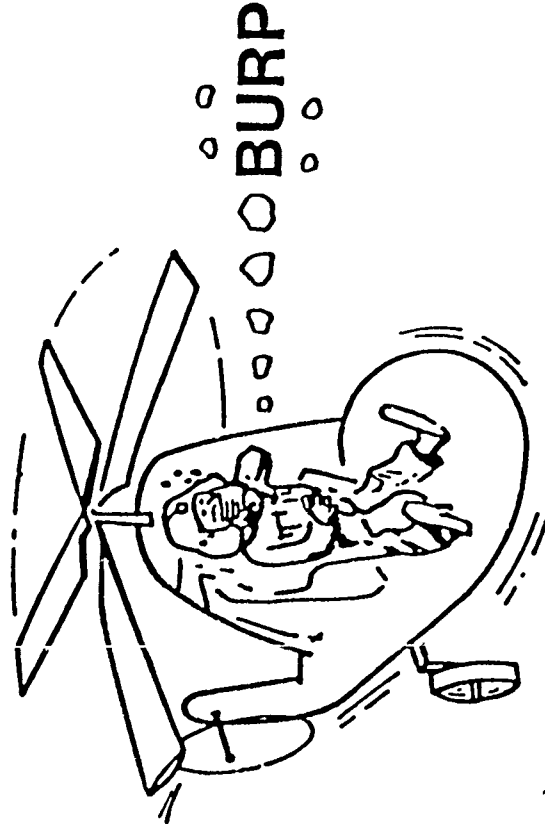
# **Application of DYNOPT Optimization Program For Tuning Frequencies of Helicopter Airframe Structures**

**T. Sreekanta Murthy**  
**Lockheed Engineering and Sciences Company**  
**Hampton Virginia**

**Dynamics And Aeroelastic Stability Modeling of  
Rotorcraft Systems  
Third Workshop**

**Army Research Office and Duke University**  
**Durham North Carolina**  
**March 12-14, 1990**

# THE HELICOPTER VIBRATION PROBLEM



## Problem?

- Pilot discomfort, fatigue, speed limit

## What are the approaches?

- Design low vibration rotor
- Vibration control devices
- ✓ ● Airframe tuning

## How?

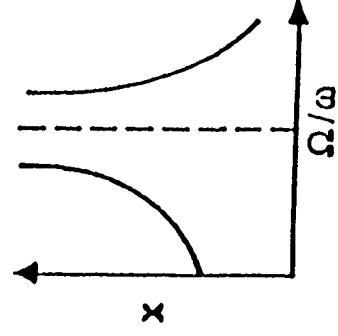
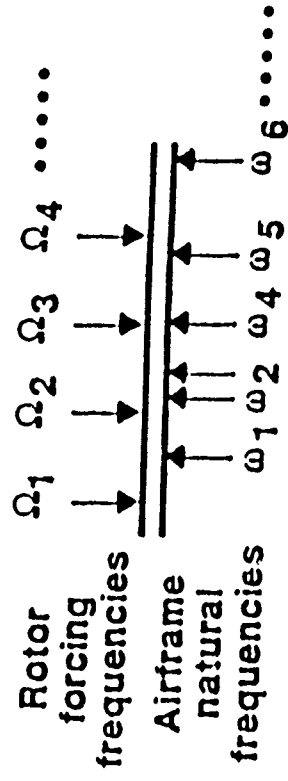
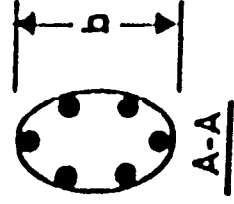
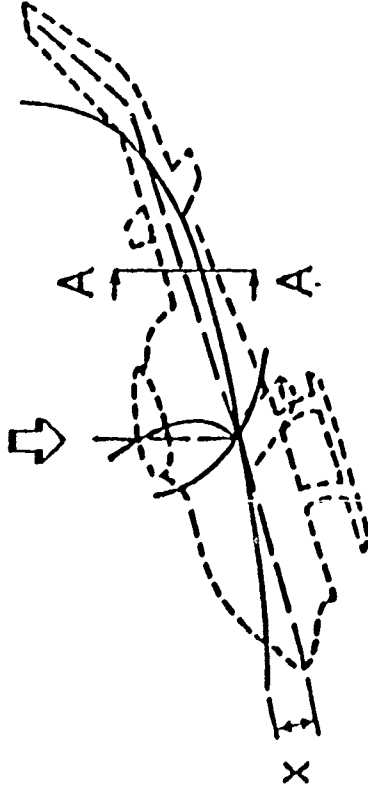
- Intuitive design
- ✓ ● Optimization method

## **OUTLINE**

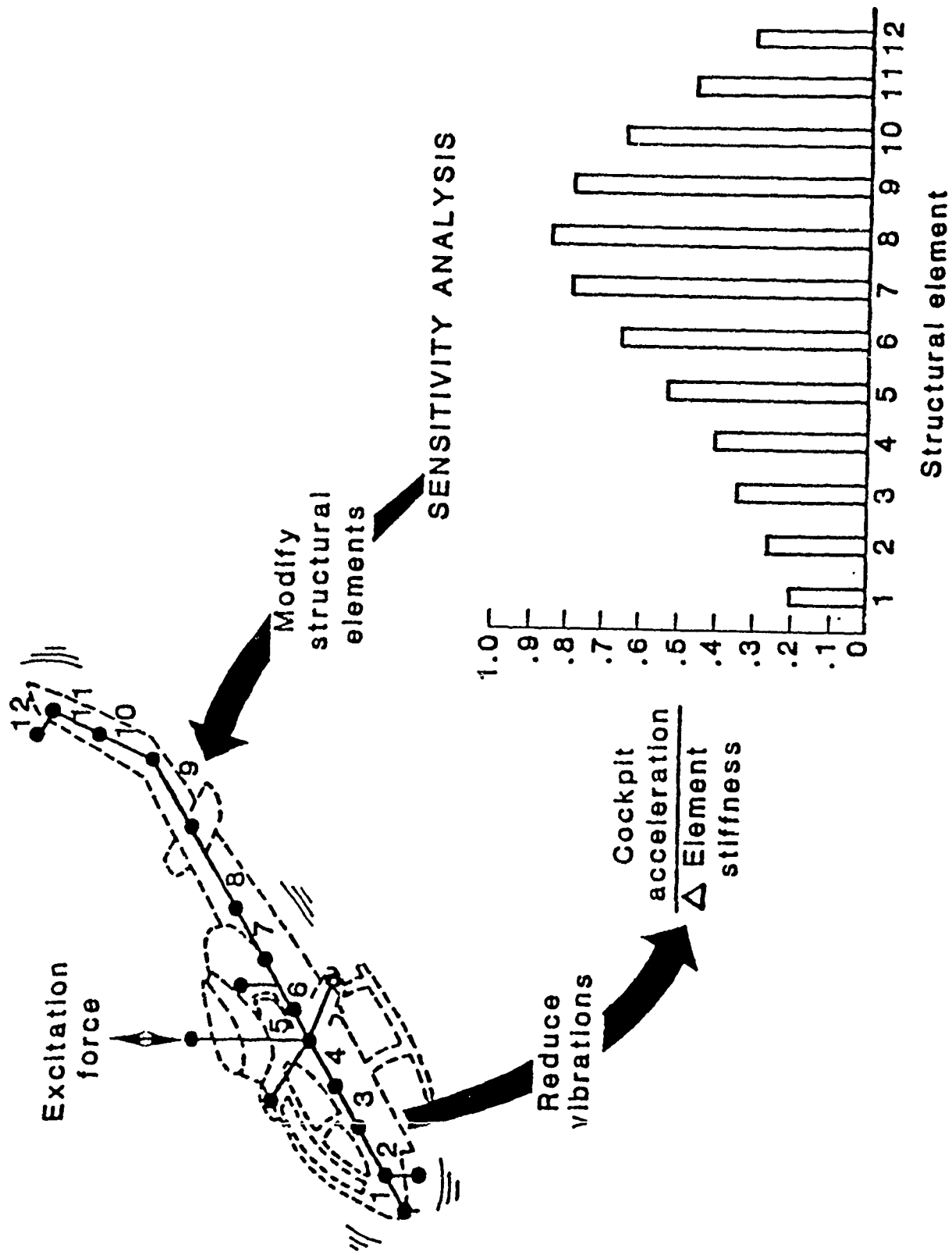
- Optimization methodology for airframe tuning
- Description of DYNOPT optimization program
- Application to Bell AH-1G helicopter airframe
  - Description of airframe structure and FEM
  - Numerical results
- Work-in-progress
- Summary

# AIRFRAME TUNING

Rotor Forces



# HELICOPTER AIRFRAME MODIFICATION TO REDUCE VIBRATIONS



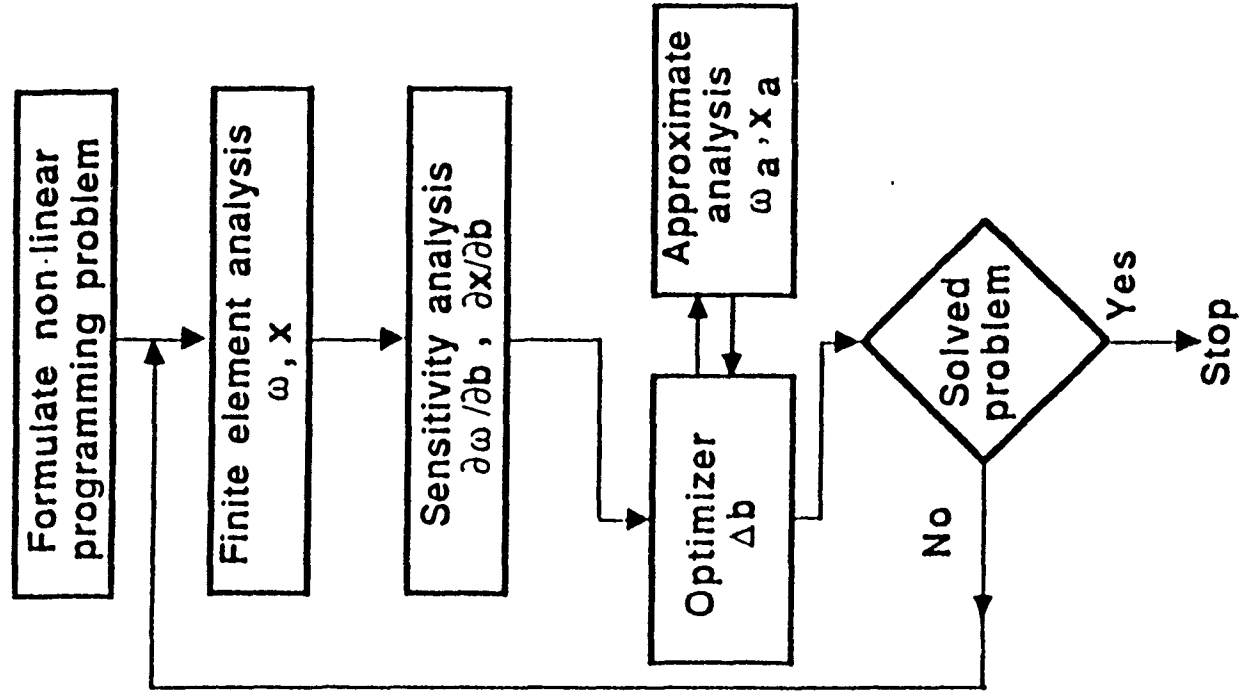
**D Y N O P T**

Program

For

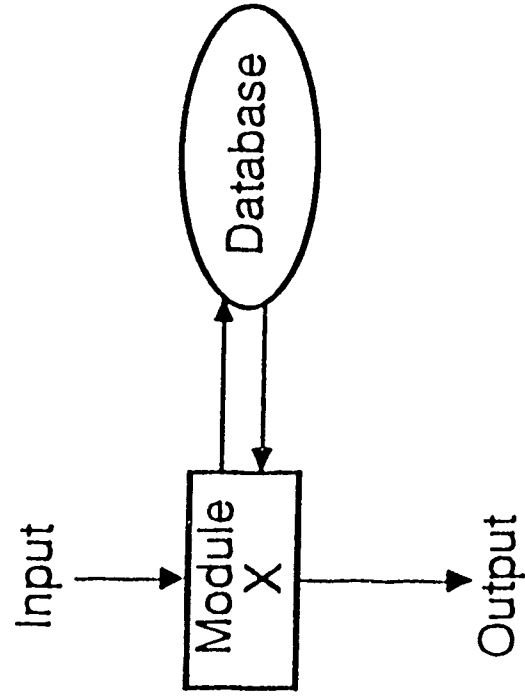
Dynamics Optimization of Structures

# KEY ELEMENTS IN OPTIMIZATION COMPUTATION



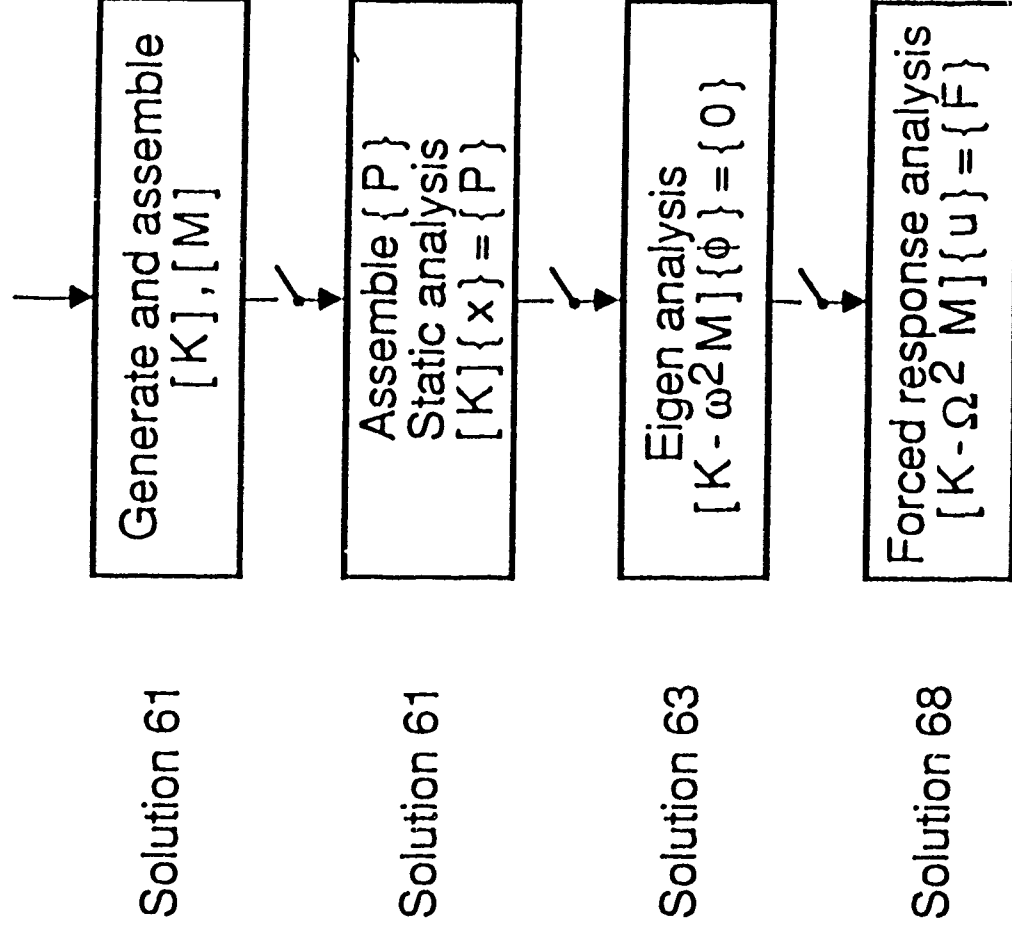


# TYPICAL MODULE



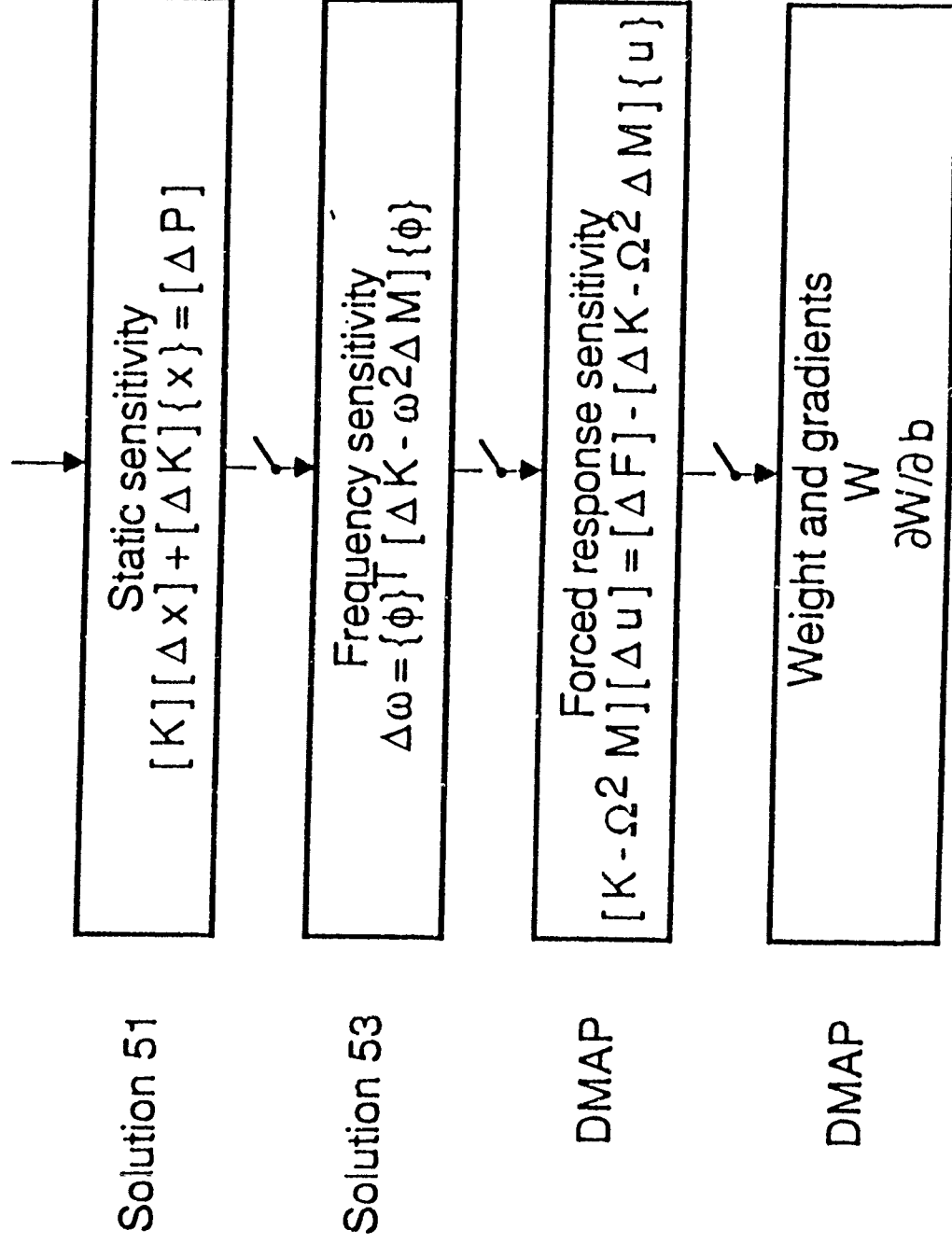
# FINITE ELEMENT ANALYSIS MODULES

(Based on MSC/NASTRAN solution sequence)

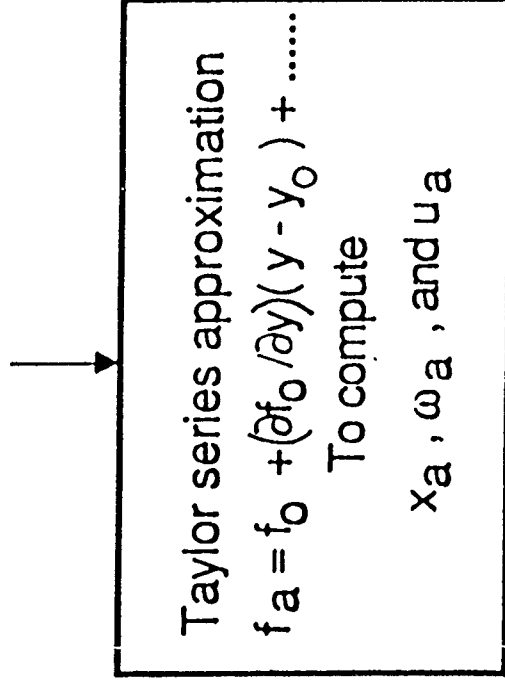


# SENSITIVITY ANALYSIS MODULES

(Based on MSC/NASTRAN solution sequences)



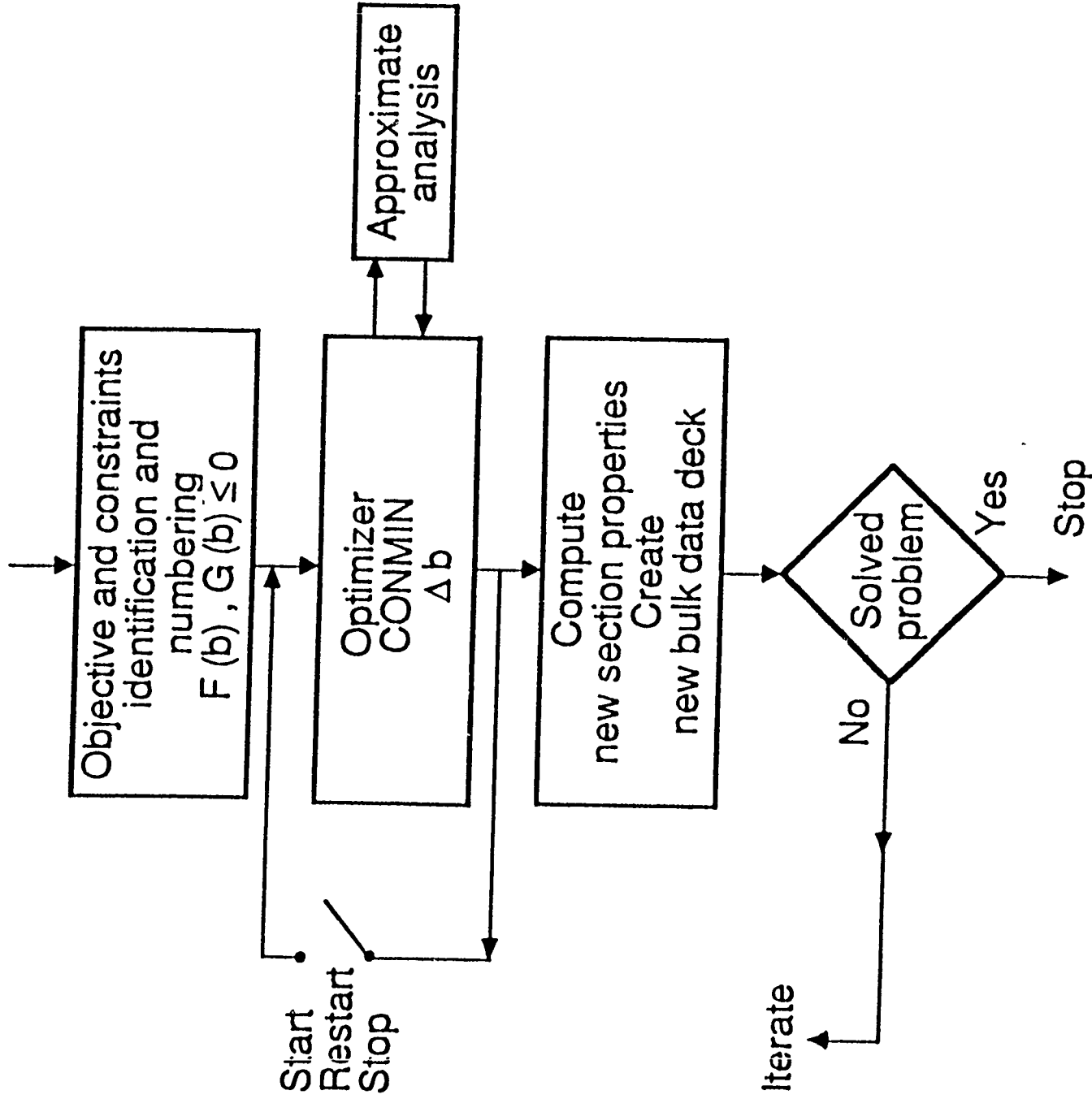
# APPROXIMATE ANALYSIS MODULE



## METHODS

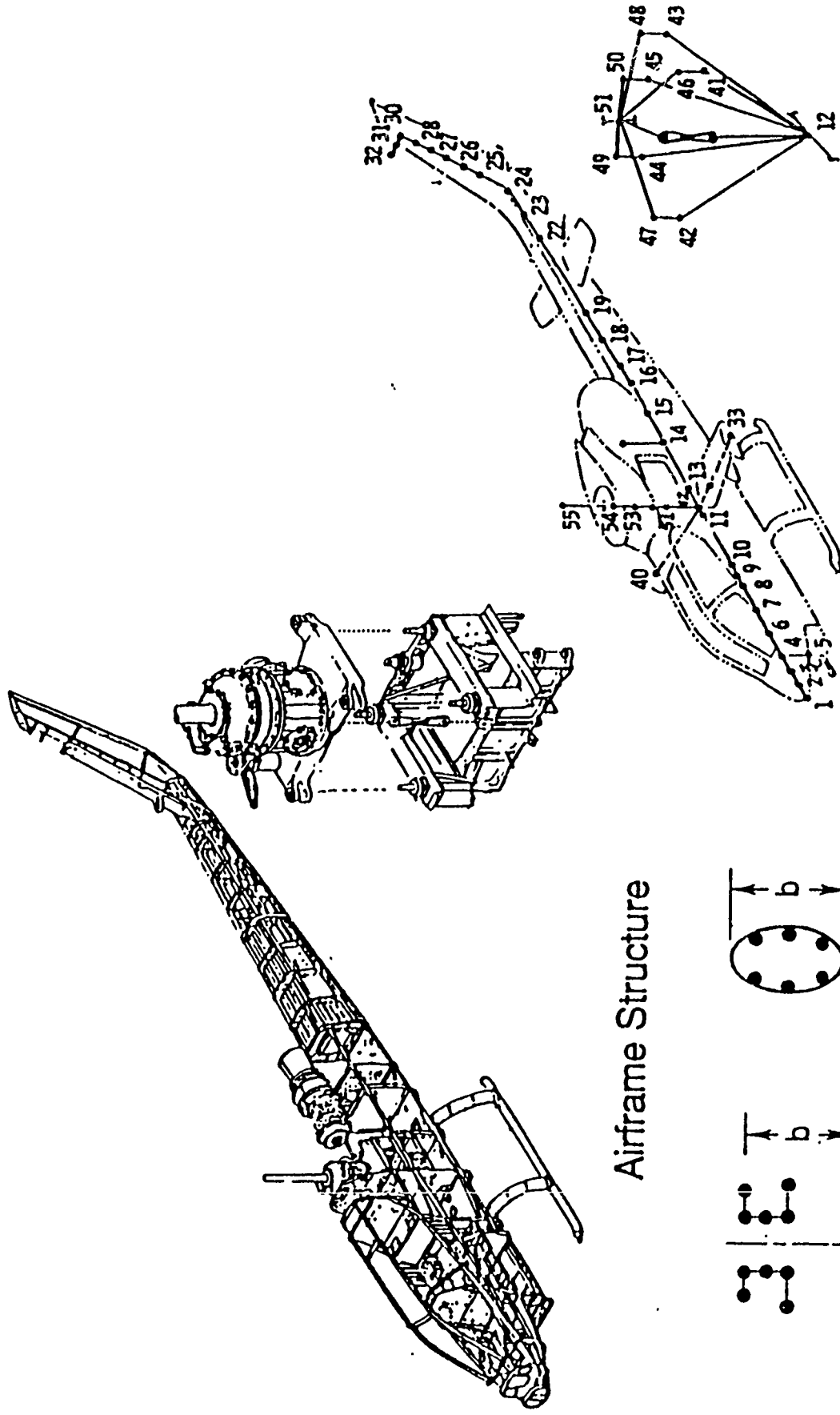
1. Direct  $y \Rightarrow b$
2. Reciprocal  $y \Rightarrow 1/b$
3. Hybrid  $(y - y_o) \Rightarrow (b - b_o) (b/b_o)^\gamma$   
 $\gamma$  integer

# DESIGN CHANGE MODULES



**APPLICATION TO  
BELL AH-1G  
HELICOPTER AIRFRAME**

# AIRFRAME STRUCTURE AND FINITE ELEMENT MODEL






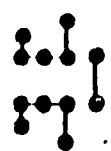
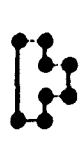



Airframe Structure

Design variables

Elastic Line ("Stick") Model

# DESIGN VARIABLES FOR OPTIMIZATION

(Depth of cross-section b)

SECTION	$\alpha$	$\beta$
	0.2	2.45
	0.35	2.4
	0.2	2.5
	0.2	2.25
	0.4	2.1
	0.34	2.34
	0.0	2.18
	0.2	2.2

Normalized design variable

$$K = \Delta b/b$$

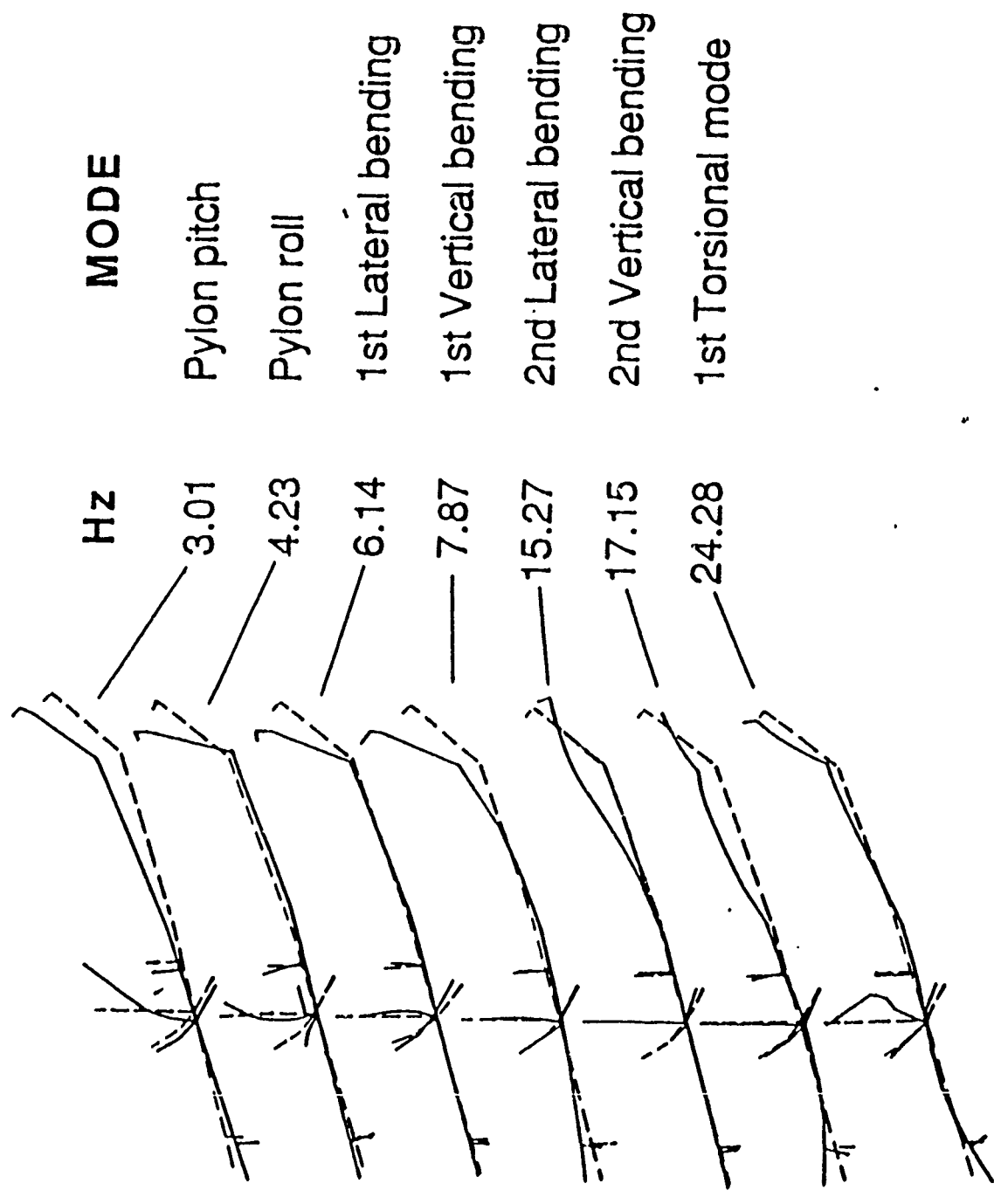
$$\text{Area } A_N = A_0 K^\alpha$$

$$\text{M.I. } I_N = I_0 K^\beta$$

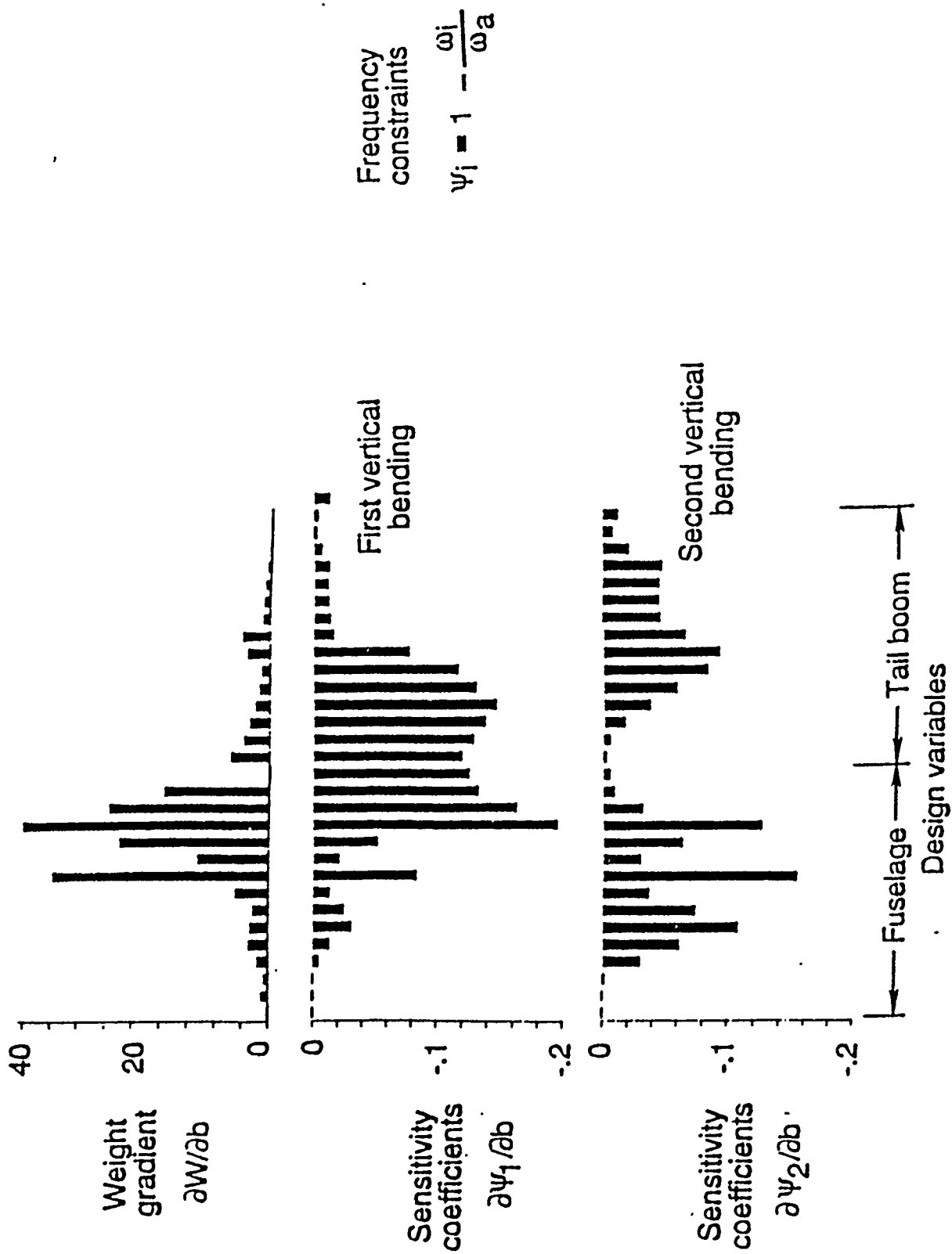


# NATURAL FREQUENCIES AND MODE SHAPES

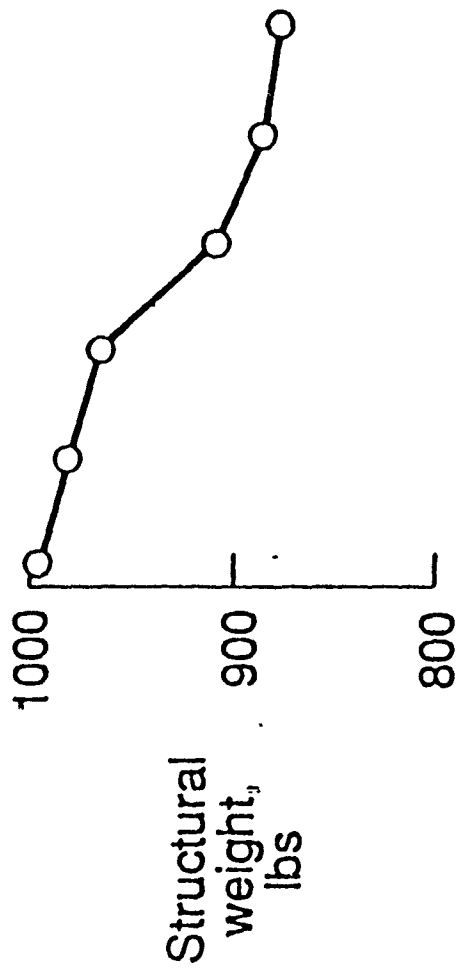
(Elastic line model)



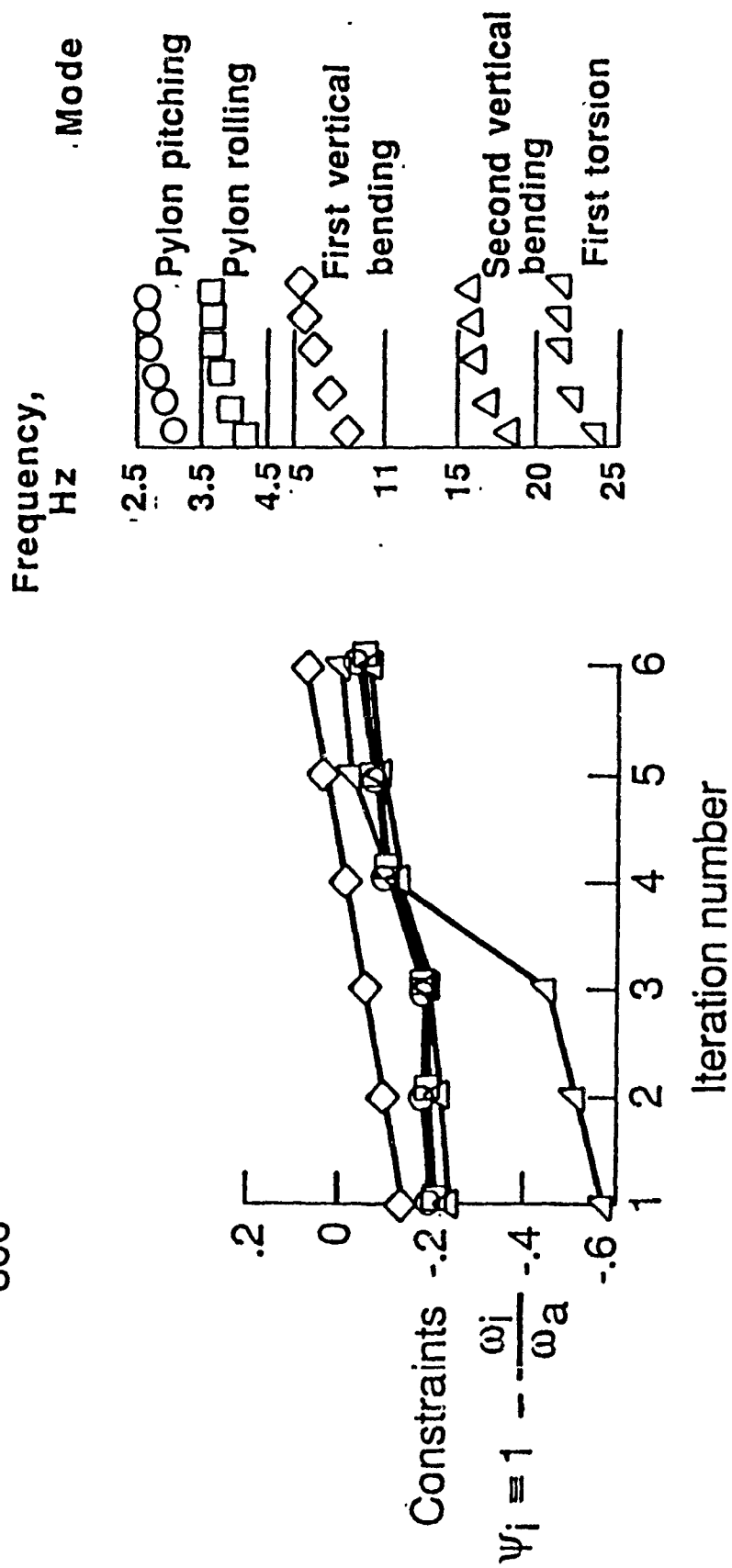
# SENSITIVITY RESULTS



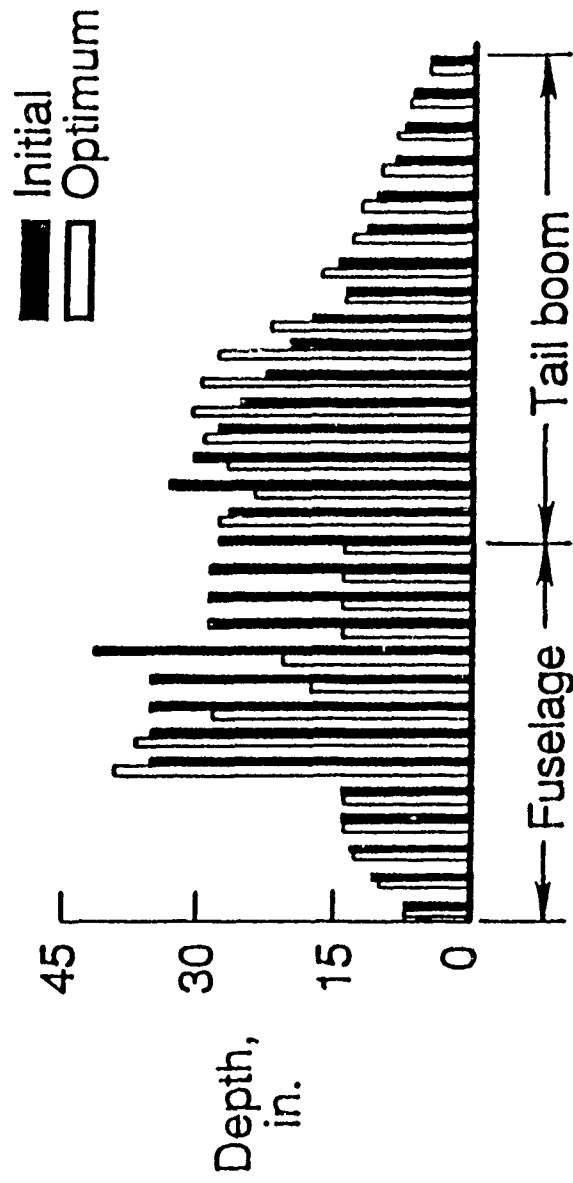
# OPTIMIZATION RESULTS



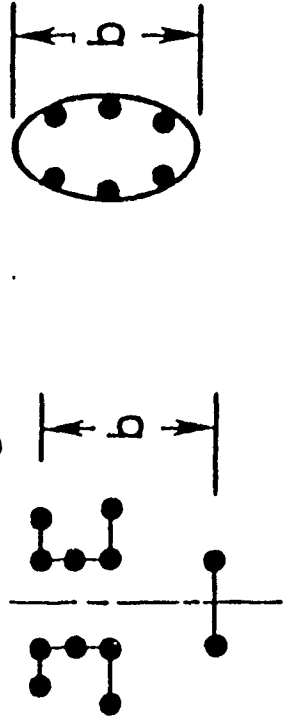
Airframe weight reduced by 100 lbs



# COMPARISON OF INITIAL AND OPTIMUM DESIGNS

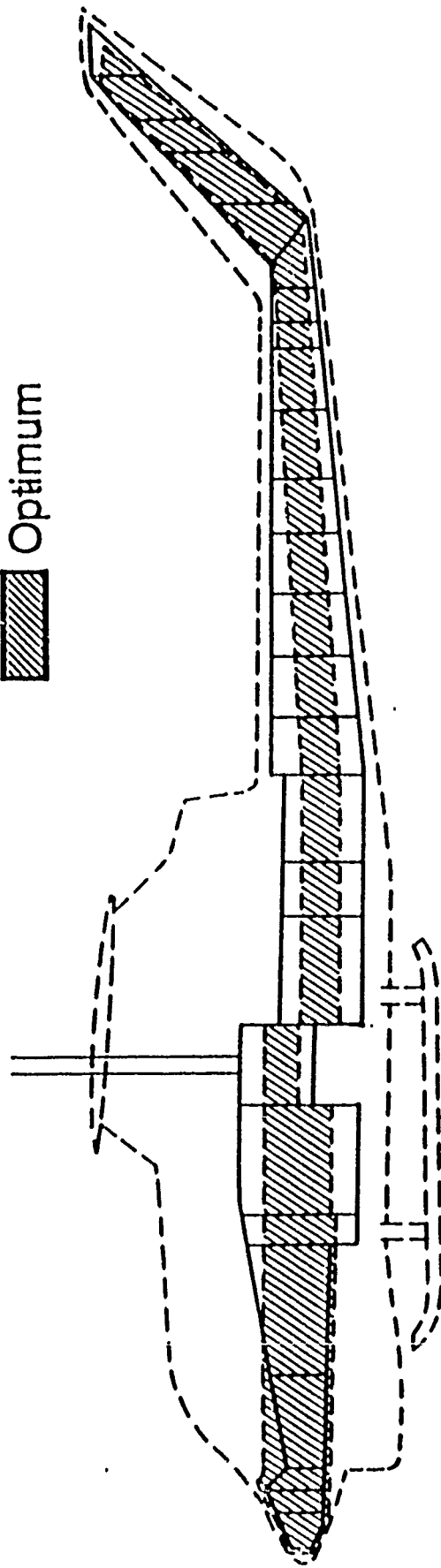


Design variables



# INITIAL AND OPTIMIZED SHAPE OF PRIMARY STRUCTURE

Initial  
Optimum

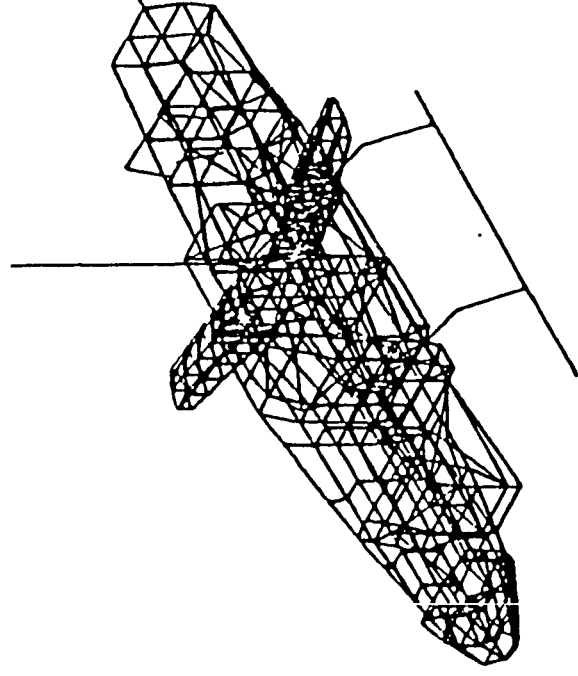


# WORK- IN- PROGRESS

Optimization studies on "built-up" model of AH-1G airframe

- Frequency constraints
- Forced response constraints
- Weight
- Design variables

- Rod, shear panel, beam



490 Grid points  
2953 Structural elements  
241 Analysis degrees-of-freedom

## **SUMMARY**

- Described optimization method for tuning airframes
- Described DYNOPT optimization computer program
- Presented results on optimization of "stick" model of Bell AH-1G helicopter airframe
- Applications to "built-up" model underway

**An Experimental and Analytical Investigation of Dynamic Stall Effects  
on Isolated Rotor Flap-Lag Stability**

Dinesh Barwey                      Gopal H. Gaonkar  
Graduate Student                      Professor  
Florida Atlantic University  
Boca Raton , FL 33431 , (407)-367-3417

Robert A. Ormiston  
Chief , Rotorcraft Dynamics , Aeroflightdynamics Directorate  
Moffet Field , CA 94035 , (415)-694-5835

The abstract of a paper submitted for possible presentation at The Third Technical Workshop on Dynamics and Aeroelastic Stability Modeling of Rotorcraft Systems, March 12-14, 1990, Duke University, Durham, North Carolina



## ABSTRACT

Very little is known about isolated rotor stability under dynamically stalled conditions. This is particularly true of lead-lag modes that are at best weakly damped and for which current methods of predicting damping levels merit considerable refinement. Given the complexity of the flow field of a rotor blade in dynamic stall, it is virtually imperative that analytical results are compared with a comprehensive data base of test results. Accordingly, the present study investigates, both experimentally and analytically, the effects of dynamic stall lift and dynamic stall drag on the flap-lag stability of an isolated hingeless rotor. The emphasis is on the correlation with tests performed on a three-bladed isolated model rotor in the U.S. Army Aeroflightdynamics Directorate's 7 by 10 foot (2.1 by 3.0 m) wind tunnel. The data were collected in two tunnel entries. Model configuration and test procedures were essentially the same for both entries. As shown in Figure 1, the correlation covers a wide range of test conditions for various values of rotor speed ( $\Omega$ ), collective pitch ( $\theta_0$ ), shaft angle ( $\alpha_s$ ), flap-lag structural coupling ratio ( $R$ ) and advance ratio ( $\mu$ ). It includes cases that vary from near zero thrust conditions in hover and forward flight to highly stalled forward flight conditions with advance ratios as high as 0.55 and shaft-tilt angles as high as  $20^\circ$ .

The experimental model closely represents a simple model of a hingeless rotor with rigid blades having spring restrained flap hinges. This intentional simplicity facilitates isolation of dynamic stall aspect the stability problem. The structural details of the analytical model were chosen to correspond as closely as possible to the experimental model. The aerodynamic representation is based on the ONERA unified dynamic stall lift and drag models. The nonlinear equations of blade motions and stall dynamics are perturbed about a periodic orbit or forced response, and the damping values ( $\sigma$ , 1/sec) are evaluated from the Floquet eigenanalysis.

The predictions are based on four theories : 1) *linear theory*, a constant airfoil lift-curve slope and a constant profile drag coefficient, 2) *quasi-steady stall theory*, which is the linear theory refined to include quasi-steady nonlinear lift and nonlinear drag characteristics of the airfoil section, 3) *dynamic stall lift theory*, with quasi-steady drag and 4) complete *dynamic stall theory*, which includes dynamic stall lift and dynamic stall drag. Figure 2 shows the correlation in hover for a collective pitch angle  $\theta_0 = 8^\circ$  (Figure 2a), and in forward flight for  $\theta_0 = 6^\circ$  and  $\alpha_s = 20^\circ$  (Figure 2b). Here, the dynamic stall effects are negligible, as determined from the stall angles based on trim values ( $|\text{angle of attack } \alpha| \leq 12^\circ$ ). Nevertheless, the correlation facilitates an improved appreciation of the dynamic stall effects on lag damping. The predictions cluster into two categories of linear theory vis-a-vis the other three theories. In hover, as seen from Figure 2a, the linear theory is fairly adequate in the prediction of increasing and decreasing trends of damping level, including the reduction in damping level around 400 rpm, where the flap and lag frequencies coalesce. However, the discrepancies between the data and the linear theory consistently increase for  $\Omega > 400$  rpm. By comparison, the remaining three theories provide excellent correlation throughout. To isolate the effects of nonlinear quasi-steady section drag characteristics in substall, additional correlations (not shown) were conducted between the data and the linear theory refined to include nonlinear quasi-steady section drag in substall. It was seen that these substall nonlinear drag characteristics significantly improve the correlation, as is typical of low-Reynolds-number effects of test conditions (in hover, Reynolds number was close to 240,000 at the blade tip). In forward flight, as seen from Figure 2b, the linear theory provides poor correlation by predicting rapidly increasing damping level with increasing advance ratio  $\mu$ , whereas the data show nearly constant or slowly decreasing damping level with increasing  $\mu$ . By comparison, the other theories provide excellent correlation. As in hover, the improvement is primarily due to nonlinear profile drag

effects.

The stalled high-thrust conditions are presented in Figure 3 for the collective pitch angles of  $0^\circ$  and  $3^\circ$ , both for a shaft-tilt angle of  $16^\circ$ . The predictions of linear and quasi-steady stall theories contrast, each providing good correlation for one case and qualitatively inaccurate prediction for the other. For example, the linear theory gives reasonably good correlation only for the case of zero collective pitch angle (Figure 3a). But for the second case of  $3^\circ$  collective pitch angle (Figure 3b), it predicts increasing damping with increasing advance ratio — a qualitatively inaccurate prediction in comparison with the test data. In contrast, quasi-steady stall theory gives good correlation for collective pitch angle  $\theta_0=3^\circ$  (Figure 3b), and qualitatively inaccurate predictions for collective pitch angle  $\theta_0=0^\circ$  (Figure 3a). On the other hand, the dynamic stall lift theory with quasi-steady drag characteristics gives fairly accurate prediction in both cases. In other words, quasi-steady stall theory refined to include dynamic stall lift consistently improves the correlation. Furthermore, inclusion of dynamic stall drag generally provides further quantitative improvement, except for minor degradation in the  $3^\circ$  collective pitch angle case, as seen from Figure 3b.

The preceding correlation covers a very small section of the correlation covering the entire data base of nearly 1200 test points shown in Figure 1. The full presentation with about 20 figures is planned to cover the following topics : dynamic stall lift and dynamic stall drag in Floquet stability analysis, trim analysis and perturbation about a periodic forced response, computational reliability, test procedures, generation of data base and correlation of theory with data to isolate dynamic stall effects. Future research areas uncovered during the correlation, such as possible refinements in the ONERA dynamic stall lift and drag model parameters, are identified as well.

The detailed experimental and analytical investigations lead to the following major findings :

- 1) Conventional Floquet analysis with the ONERA unsteady dynamic stall lift and drag models provides a viable approach for predicting lead-lag mode damping in stalled forward flight conditions.
- 2) For low-advance-ratio cases ( $\mu \leq 0.20$ ), the nonlinear substall drag characteristics of the airfoil section significantly improve the correlation due to low-Reynolds-number effects of the model test data, as investigated earlier on the basis of analytical and experimental results restricted to hovering conditions.
- 3) In comparison with the linear and quasi-steady stall theories, the theory with dynamic stall lift and quasi-steady drag consistently improves the prediction for the entire database.
- 4) Dynamic stall drag generally provides further quantitative improvement. Minor degradation in correlation for some isolated cases as seen in Figure 3b merits further investigation.

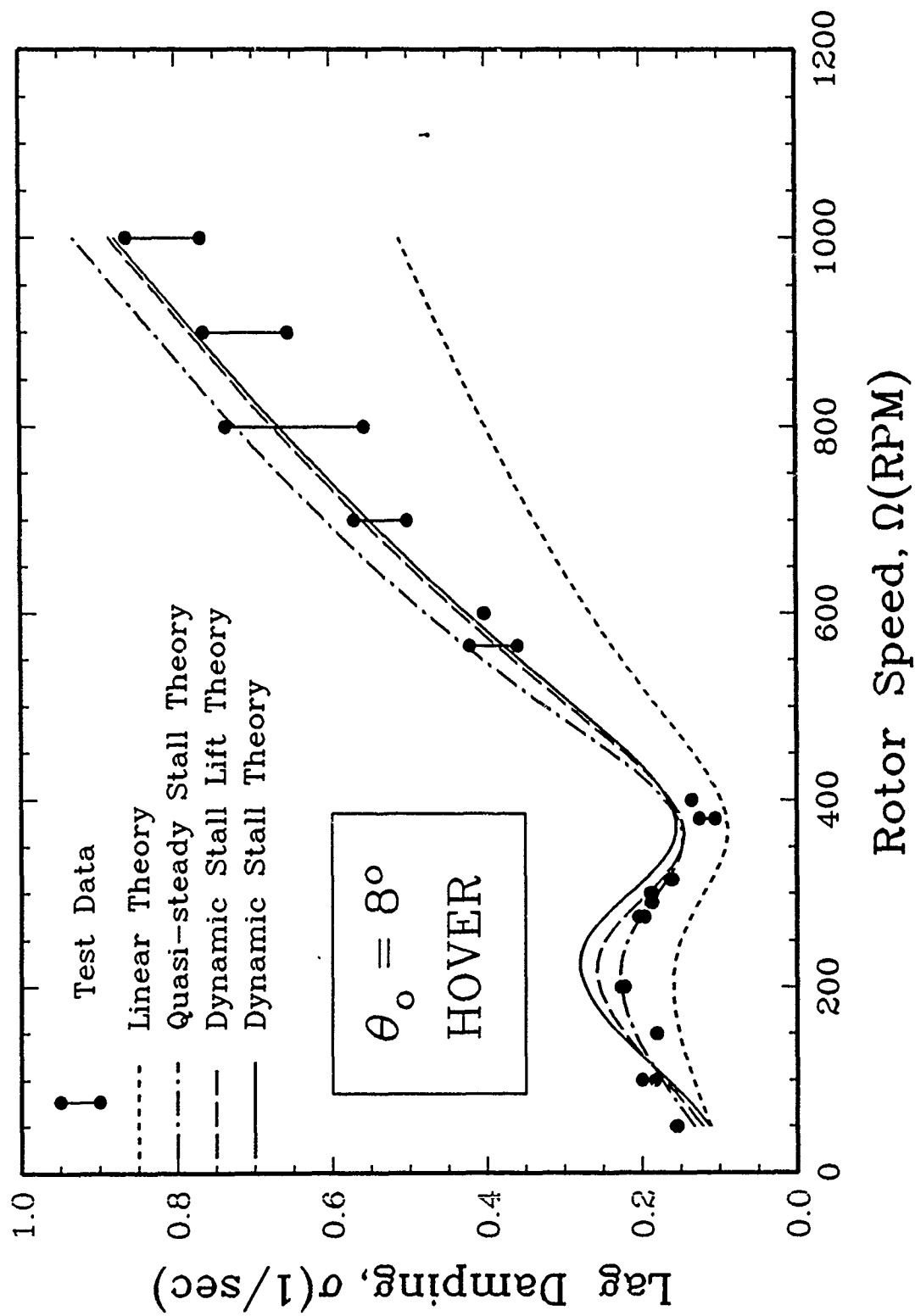
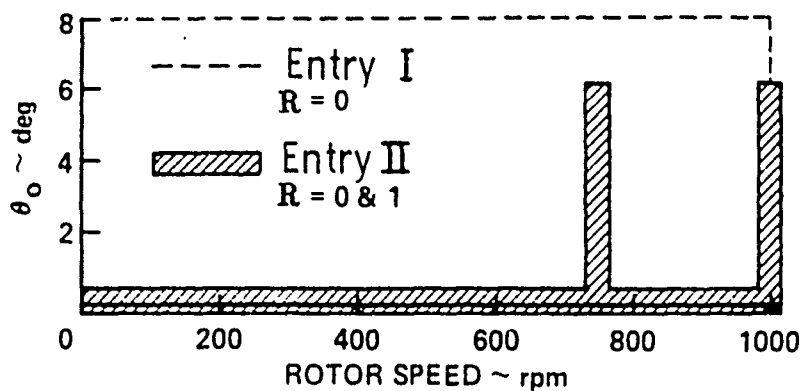
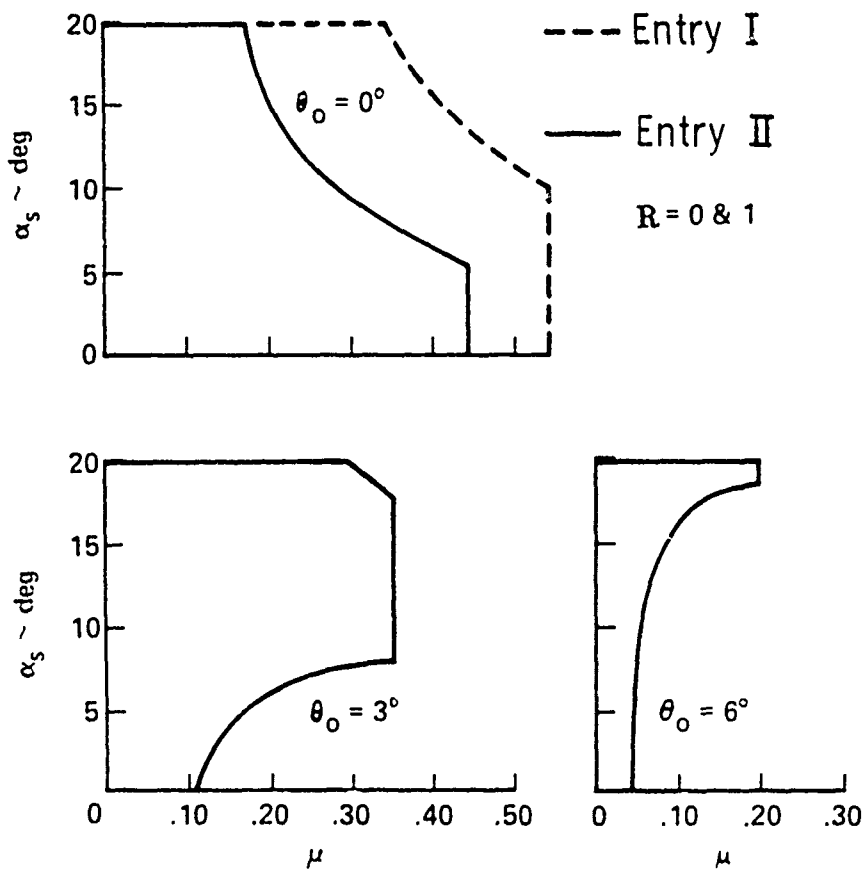


Fig. 2a : Lag Mode Damping Correlation in Hover (  $\theta_o = 8^\circ$  )



(a) Hover tests.



(b) Forward flight tests.

Figure 1: Conditions tested.

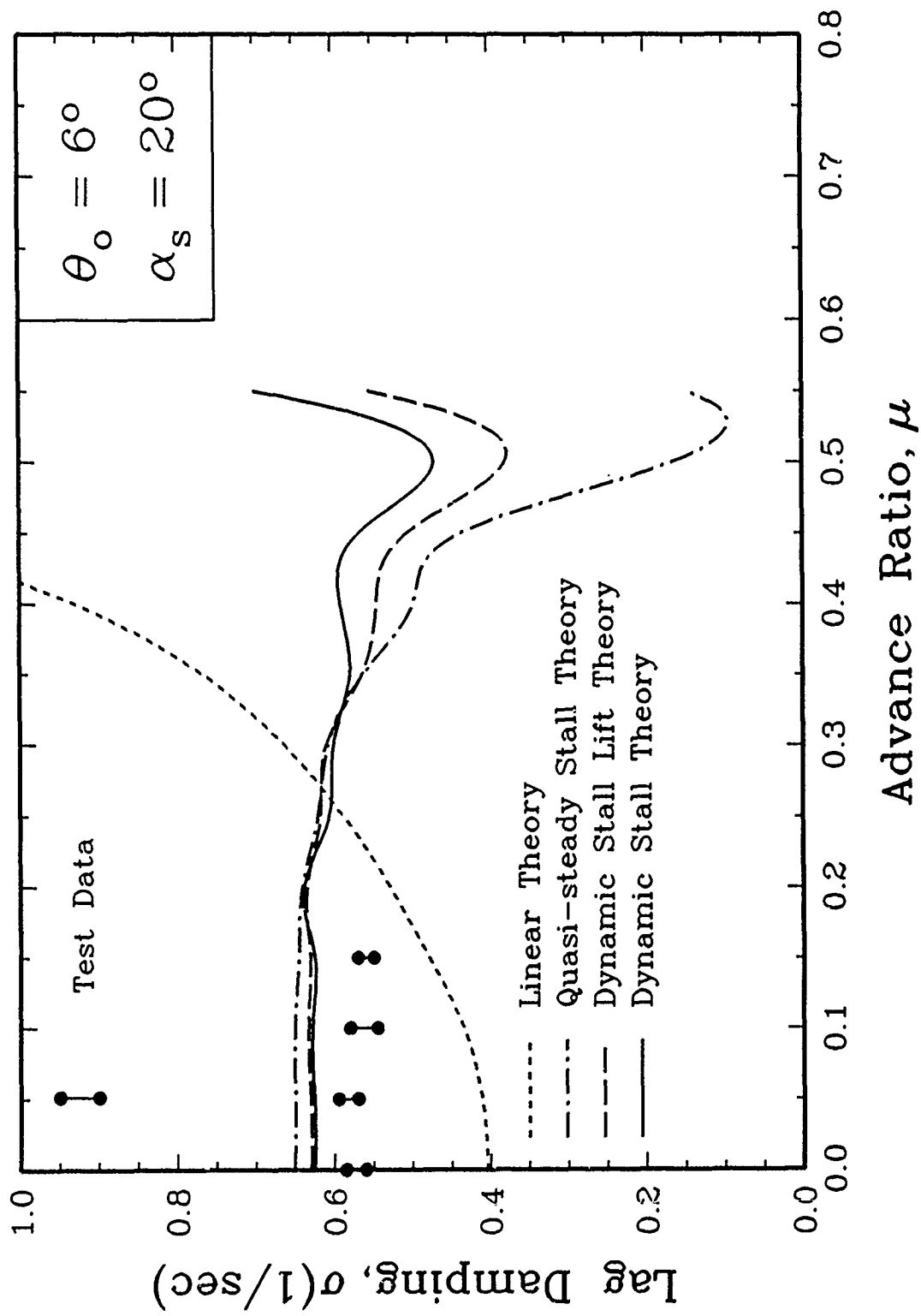


Fig. 2b : Lag Mode Damping Correlation in Forward Flight (  $R = 0$  )

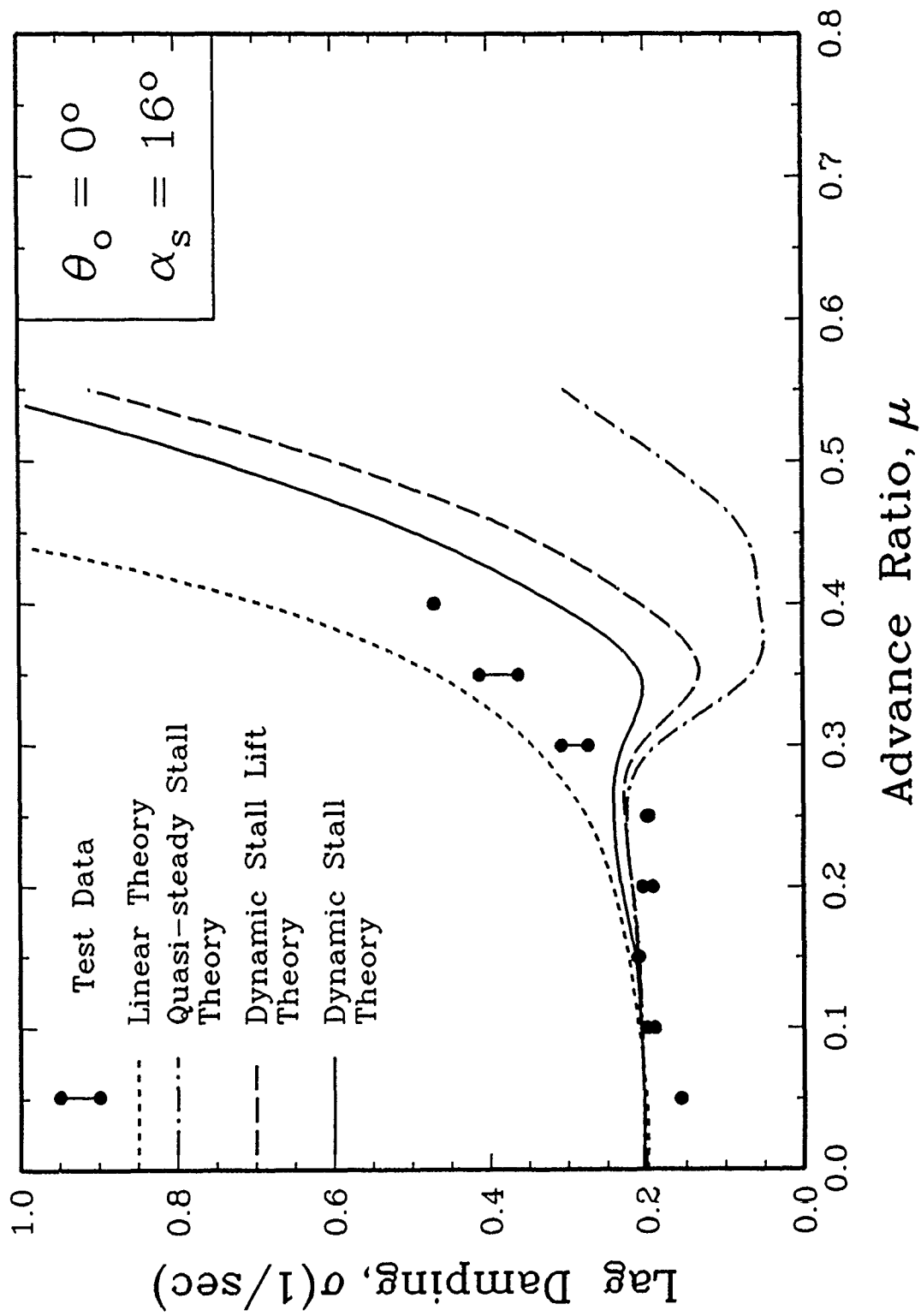


Fig. 3a : Lag Mode Damping Correlation in forward Flight (  $R = 0$  )



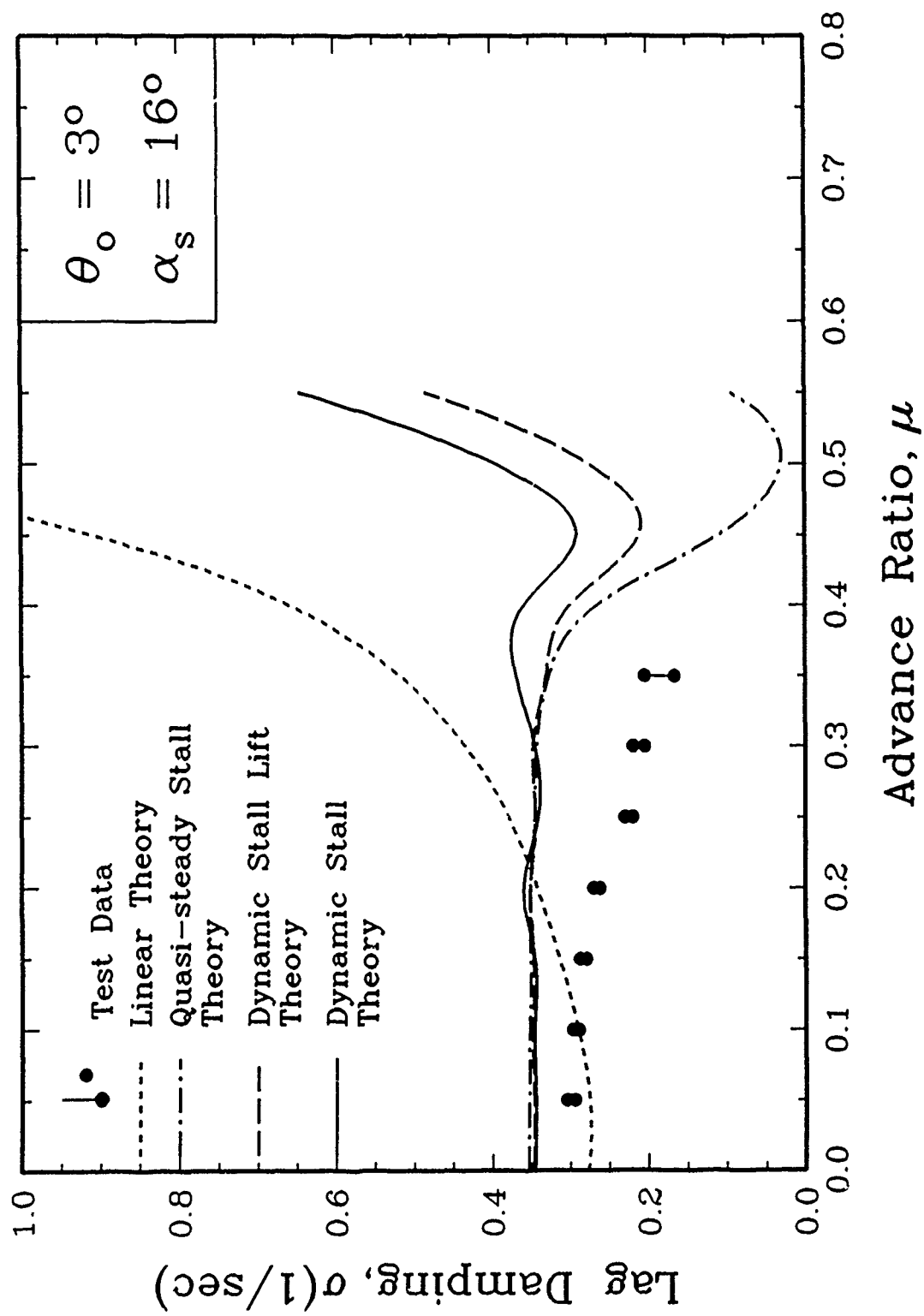


Fig. 3b : Lag Mode Damping Correlation in Forward Flight (  $R = 0$  )

## MEASUREMENTS AND PREDICTIONS CONCERNING ROTOR STABILITY

I. Cafarelli and J.J. Costes

ONERA - BP 72  
92322 CHATILLON Cedex  
France

The necessity to better understand the principal phenomena underlying stability problems in rotors has recently led the ONERA (Office National d'Etudes et de Recherches Aérospatiales) to build a test rotor specifically designed for this purpose.

This rotor is simple enough to permit a physical insight into stability behaviour as a function of various fundamental parameters in both hover and forward flight. It is also expected to yield a data base for validating existing and future predictive codes.

The first series of tests was carried out on an isolated rotor configuration. The blades were hinged in flap and cantilevered in plane. The natural frequency in torsion of each blade was varied so as to create different coupling conditions between the flap and torsion modes. Moreover, the relative importance of other parameters was measured such as rotor speed, collective pitch, rotor tilt, forward speed and  $\delta_z$  coupling.

Three different predictive codes are being studied and validated with respect to these results. Two of these are restricted to hover. They differ in the modeling of the rotor dynamics. Forward flight conditions are predicted using a Floquet mode resolution code.

First results show the sensitivity of the modal coupling to the accurate and detailed modeling of the rotor dynamics.

# **Experimental Investigations of Helicopter Structural Dynamics and the Interaction with Vibration Reduction Systems**

**Manfred Degener**

**DLR - German Aerospace Research Establishment  
Institute for Aeroelasticity  
Bunsenstrasse 10, D-3400 Goettingen, Fed. Rep. Germany**

## *Abstract:*

Vibrations are one of the major problems concerning the performance and ride comfort of helicopters. The vibration behaviour depends both on the rotor induced oscillating loads and on the structural dynamic characteristics of the helicopter itself. Therefore, vibration treatment must take into account both aspects.

The design of modern helicopters is a combination of a light-weight airframe structure and large concentrated masses such as gearbox and engines. This results in complex three-dimensional vibration behaviour with many normal modes lying in the same frequency range as the oscillating rotor loads, which requires a thorough analytical and experimental investigation. In Germany, MBB and DLR have a long cooperation in the field of helicopter structural dynamics. Ground vibration tests have been performed by DLR on the complete MBB helicopter family.

This paper gives a survey of experimental investigations of helicopter structural dynamics. It describes the features of the DLR ground vibration test facility with special emphasis on applications, experiences, and improvements in testing helicopter structures. This relates to realistic boundary conditions during testing, sensor instrumentation, dynamic excitation, and data reduction. An important topic is the correlation of experimental results with the mathematical model. Concepts for correlation, such as orthogonality check and modal assurance criterion, are discussed.

More stringent vibration requirements have caused research organisations and the helicopter industry to develop special vibration reduction systems. The effectiveness of these systems can be strongly influenced by interaction with the structural dynamics of the helicopter. This requires structural tailoring of the airframe to minimize vibration. Experimental results of a recent ground vibration test on a helicopter with and without a vibration reduction system are reviewed to illustrate this effect.

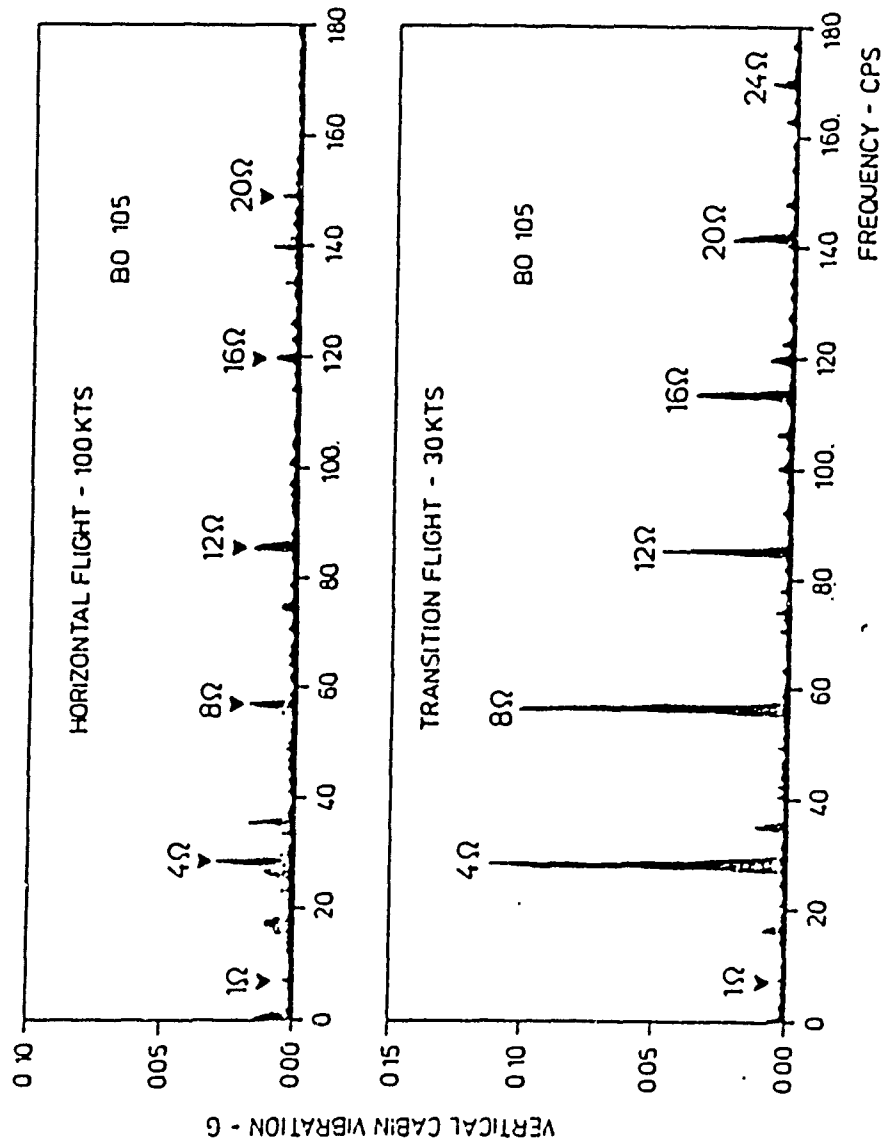
# Experimental Investigations of Helicopter Structural Dynamics and the Interaction with Vibration Reduction Systems

Manfred Degener

Institute for Aeroelasticity  
German Aerospace Research Establishment  
(Deutsche Forschungsanstalt für Luft- und Raumfahrt)  
Bunsenstrasse 10, D-3400 Göttingen, Germany



# Frequency Characteristics of Rotor Excitation



Amplitude Spectrum of the BO 105 Helicopter [1]



# Aspects of Helicopter Structural Dynamics

## *Design Features:*

- light-weight airframe
- large concentrated masses (gearbox, engines)
- combination metallic/composite materials
- vibration reduction systems
- different payload configurations

## *Vibration Characteristics:*

- complex three-dimensional vibration modes
- high modal density
- many local modes
- nonlinearities

## *Requirements for Vibration Analyses:*

- large finite element models
- sophisticated test methods



## Phase Resonance Method

Equations of Motion (physical coordinates):

$$m \ddot{u}(P,t) + d \dot{u}(P,t) + k u(P,t) = f(t)$$

Modal Transformation:

$$u(P,t) = \sum_{i=0}^n \Phi_i(P) q_i(t) = \Phi(P) q(t)$$

Equations of Motion (generalized coordinates):

$$M \ddot{q}(t) + D \dot{q}(t) + K q(t) = \Phi^T f(t)$$

*with*

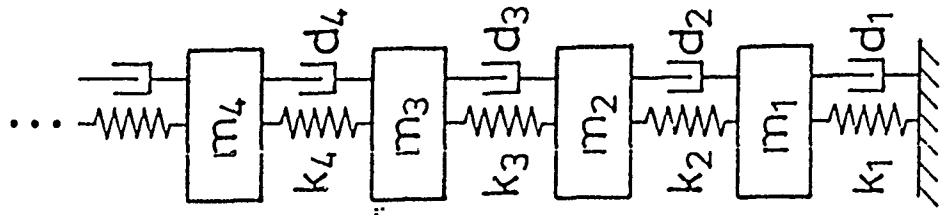
$M = \Phi^T m \Phi$  : generalized mass matrix (diagonal)

$K = \Phi^T k \Phi$  : generalized stiffness matrix (diagonal)

$D = \Phi^T d \Phi$  : generalized damping matrix

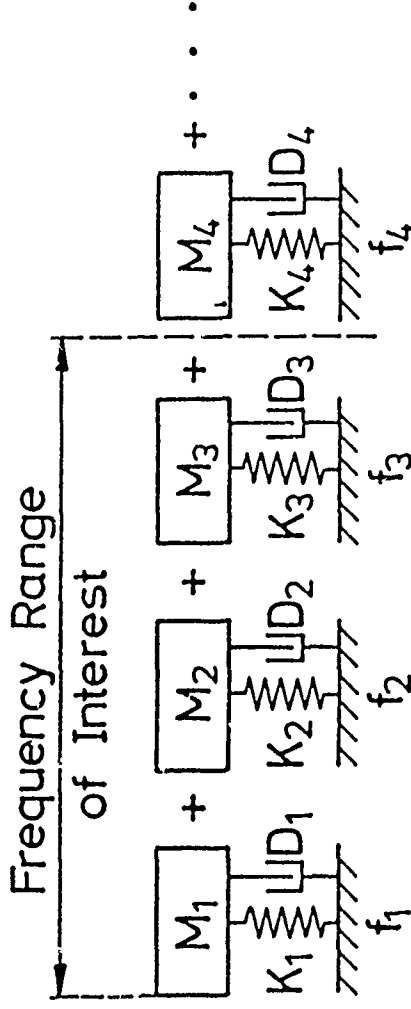


## Principle of Modal Transformation



Physical System

Modal  
Analysis



Modal System



## Phase Resonance Method (cont'd)

Harmonic Excitation:  $f(t) = f_0 \sin \omega t$

Dynamic Response:  $u(t) = u_0 \sin(\omega t + \varphi)$   
 $= u' \sin \omega t + u'' \cos \omega t$

Phase Resonance Criterion:  $\varphi = \pm 90^\circ, u' = 0$

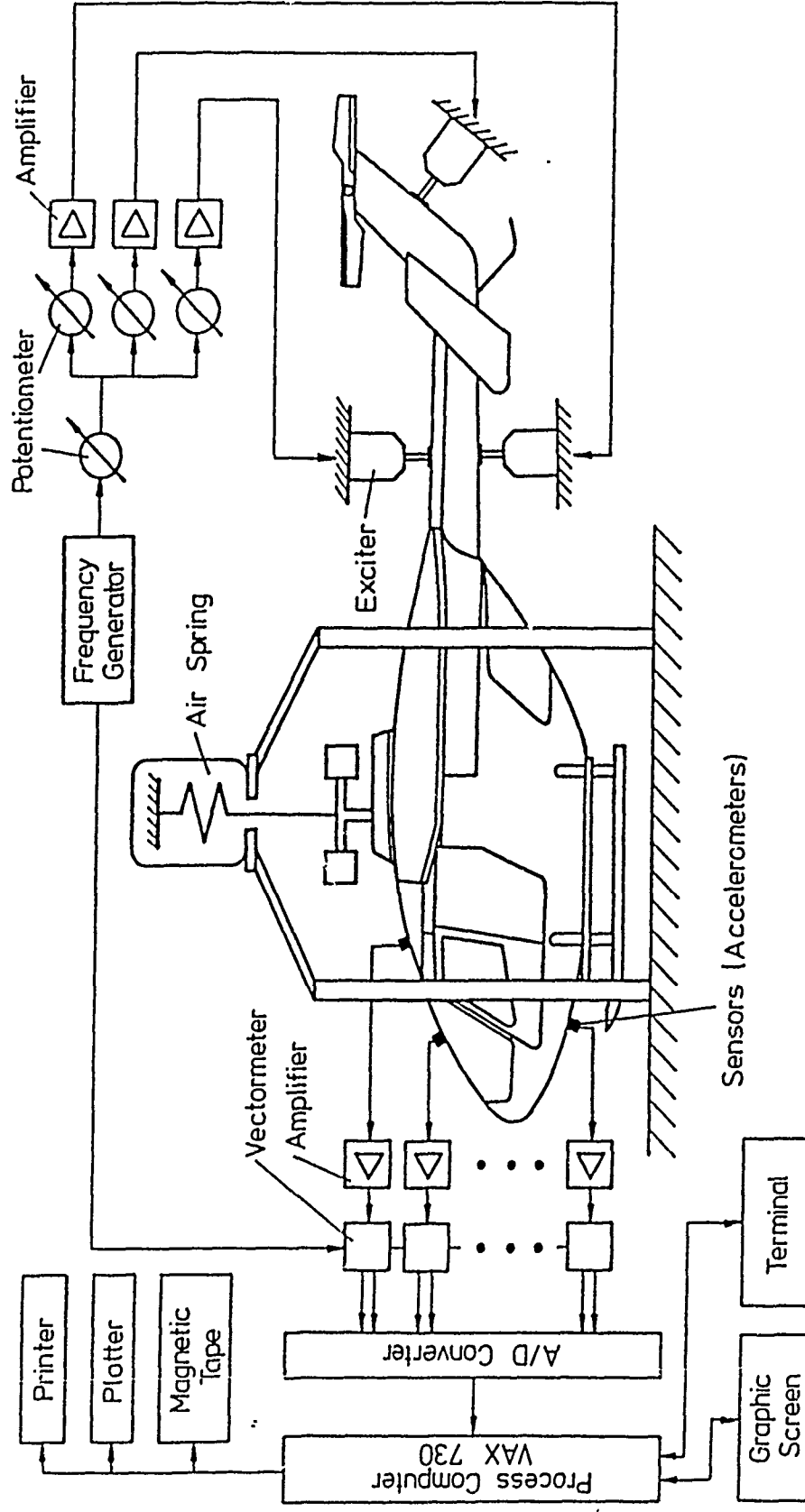
$$\begin{aligned} -\omega d u'' &= f_0 \\ (-\omega^2 m + k) u'' &= 0 \end{aligned}$$

Mode Indicator Function:

$$\text{MIF} = 1 - \frac{\sum |u_i'| |u_i|}{\sum |u_i|^2}$$



# Helicopter Ground Vibration Test Set-up



## DLR Ground Vibration Test Facility

### *Performance:*

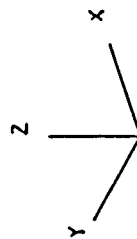
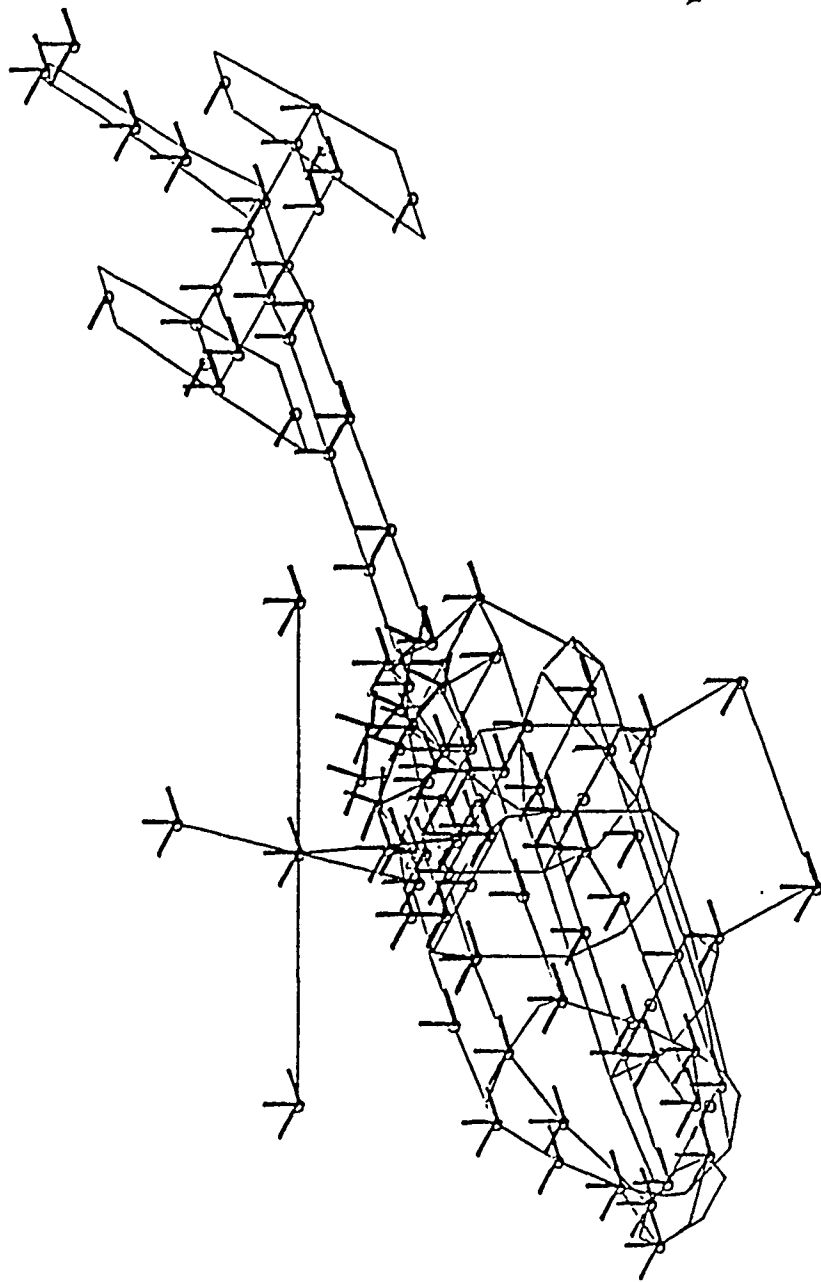
- Vibration testing of aerospace structures
- Modal parameter identification
- Fast identification and isolation of normal modes by MIF's
- Easy and reliable investigation of nonlinearities

### *Features:*

- 512 simultaneous measuring channels  
(accelerometers, amplifiers, and vectormeters)
- 24 electrodynamic exciters
- Computer-controlled online measurement
- Facility designed for large and complex structures
- Mobile equipment (container) for easy transportation



# BO 108 - Measurement Point Plan



# Measurement of Normal Modes

## *Identification of Normal Modes*

- Measurement of MIF's for various exciter configurations

## *Isolation of Normal Modes*

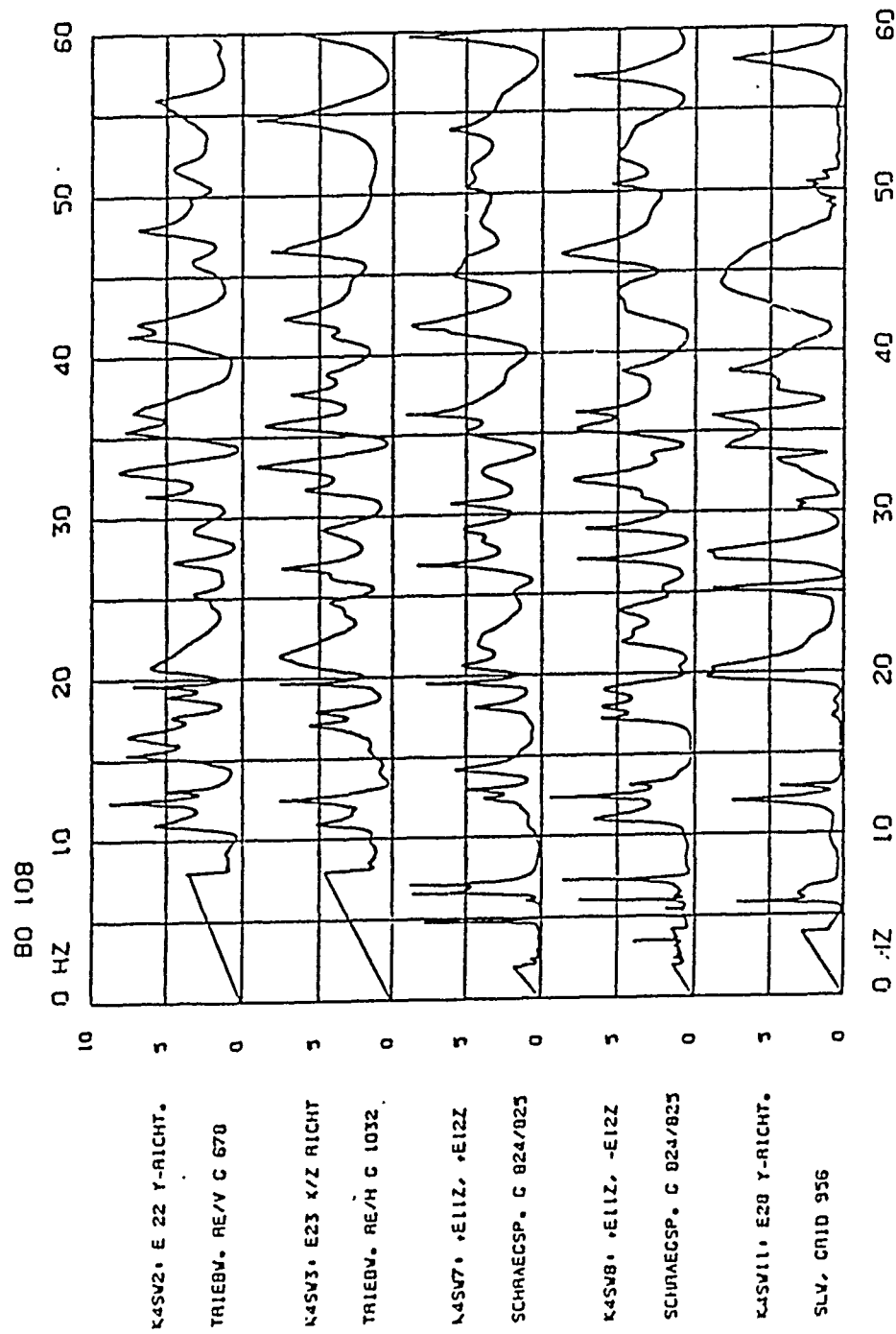
- optimizing MIF-value (  $> 0.9$  )
- frequency adjustment
- variation of exciter forces and locations
- on-line graphic display

## *Measurement of Modal Parameters*

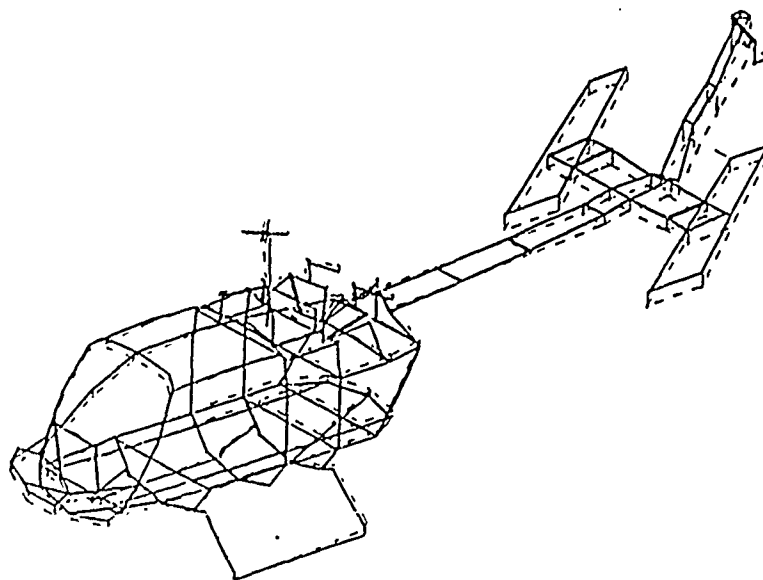
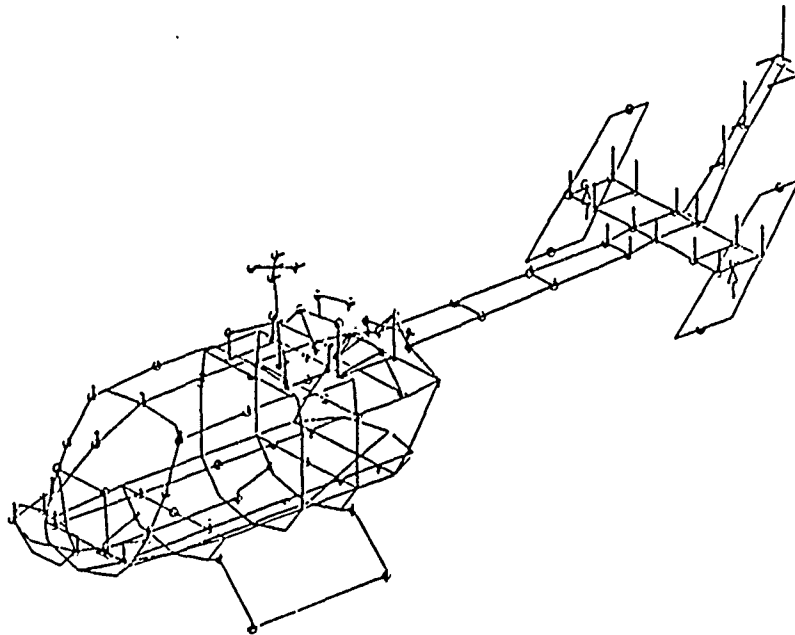
- normal frequency
- normal mode shape
- generalized mass
- damping
- linearity check



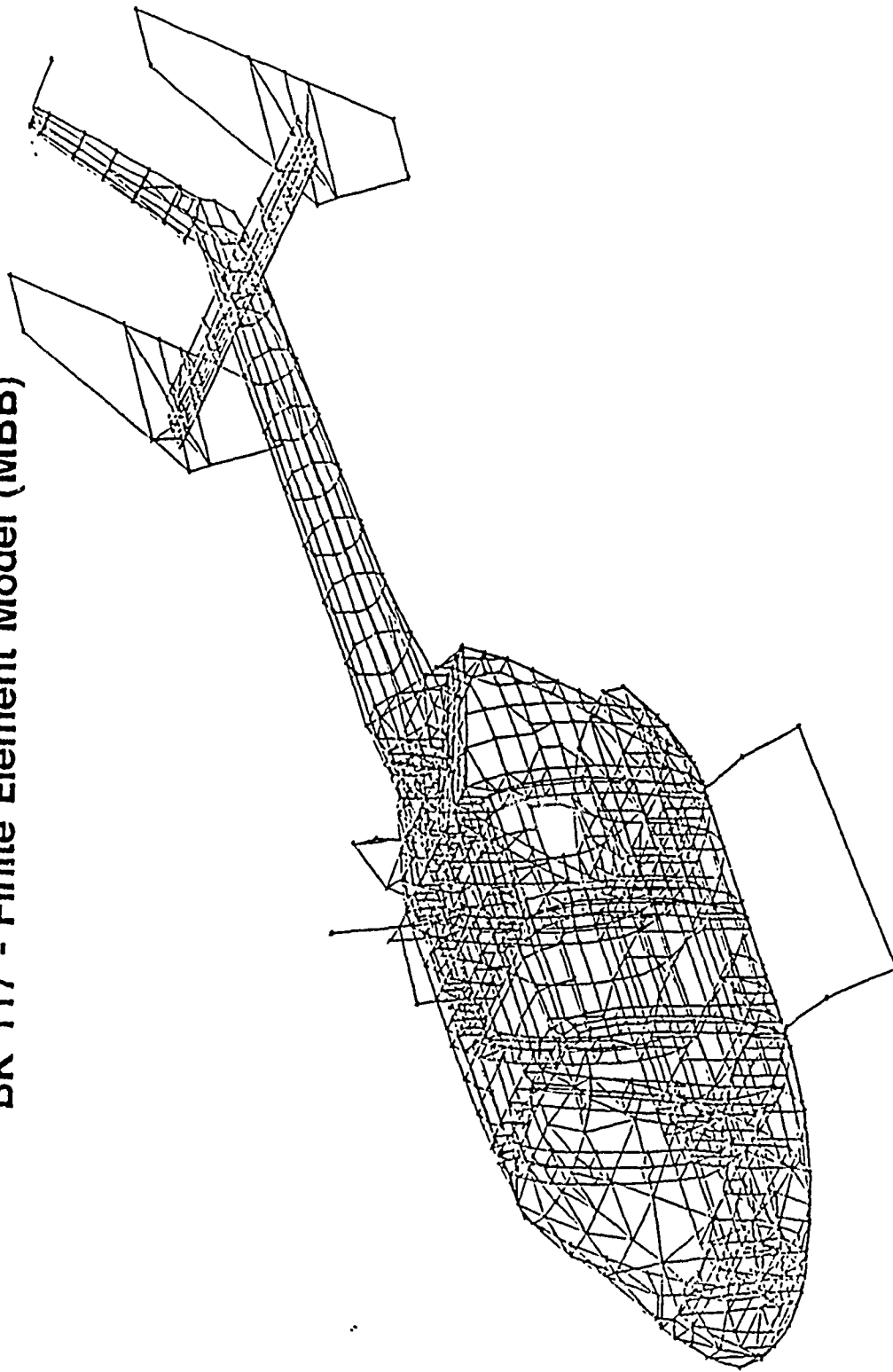
# Identification of Normal Modes by MIF's



# Helicopter Mode Shape



**BK 117 - Finite Element Model (MBB)**



DLR



## Orthogonality Check

Generalized Mass Matrix:

$$\mathbf{M} = \Phi^T \mathbf{m} \Phi$$

Normalized to  $M_{ii} = 1$ :

$$\bar{\mathbf{M}} = \bar{\Phi}^T \mathbf{m} \bar{\Phi}$$

with

$$0 \leq \bar{M}_{ik} \leq 1$$

## Modal Assurance Criterion

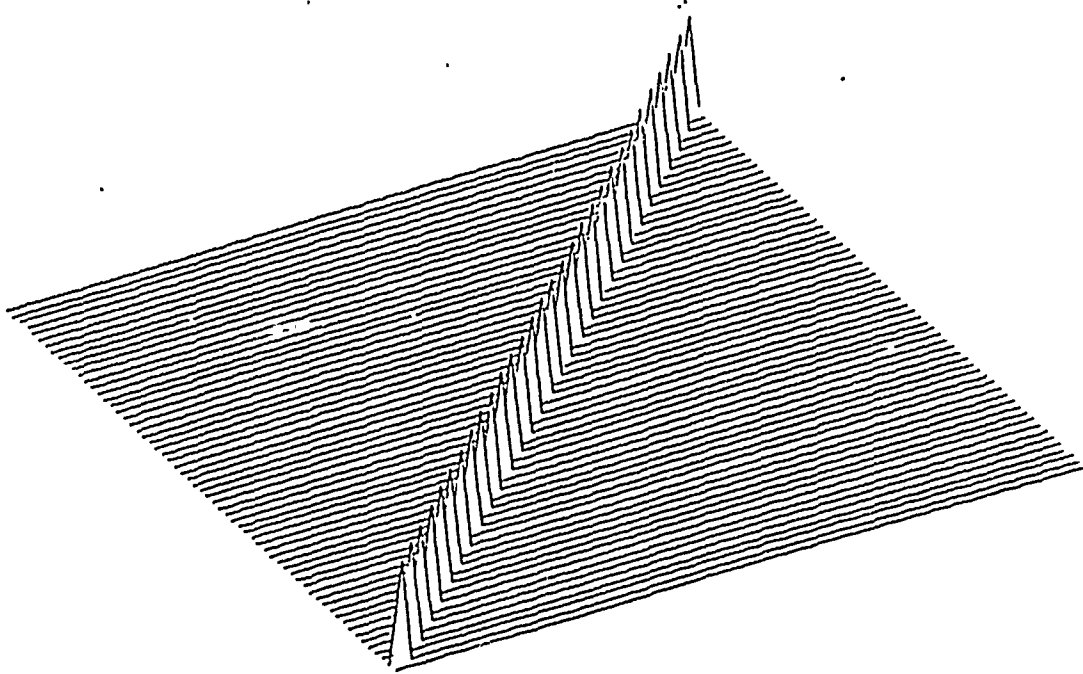
$$\text{MAC}(i,k) = \frac{(\Phi_i^T \Phi_k)^2}{(\Phi_i^T \Phi_i) (\Phi_k^T \Phi_k)}$$

with

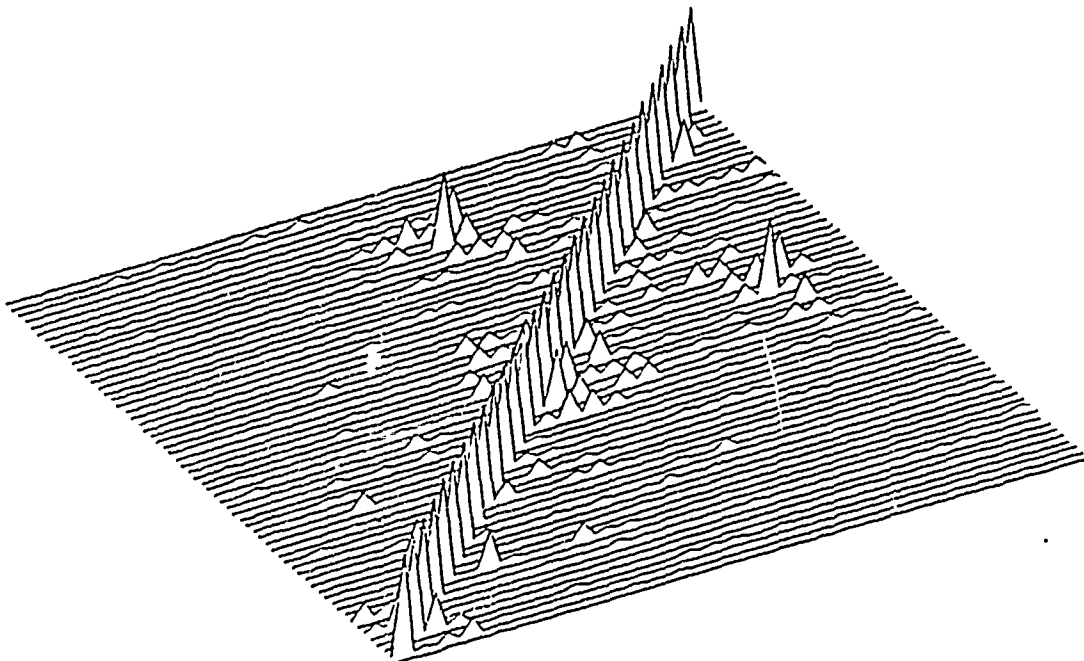
$$0 \leq \text{MAC}(i,k) \leq 1$$



## Orthogonality Check



## Modal Assurance Criterion



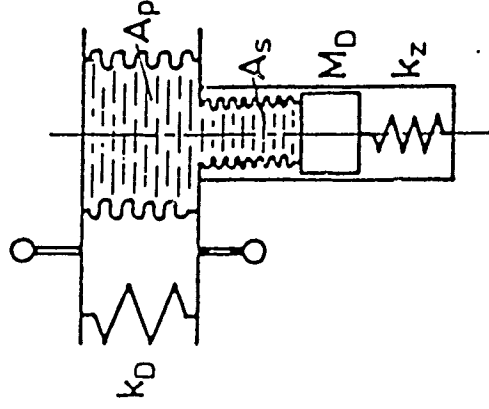
BK 117: FEM mode shapes

## DLR Ground Vibration Tests on MBB Helicopters

Year	Helicopter	Accel.	Config.	Modes
1979/80	BO 105	229	1	29
1981	BK 117 <sup>1</sup>	78	1	18
1988	BO 108	232	3	36
1989	BK 117 <sup>2</sup>	211	4	52
1989	BO 108 <sup>1</sup>	232	1	7
1) with Antiresonance Vibration Isolation System ARIS 2) with Composite Fuselage				

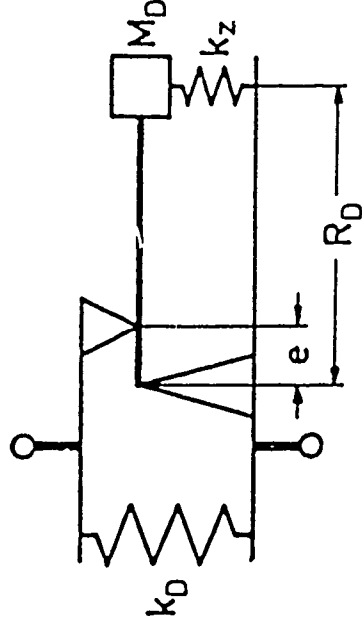


# Antiresonance Vibration Isolation System (ARIS) [3]



$$M_D = \frac{k_D + k_z \left(\frac{A_P}{A_S}\right)^2}{\omega_a^2 \frac{A_P}{A_S} \left(\frac{A_P}{A_S} - 1\right)}$$

Hydraulic System



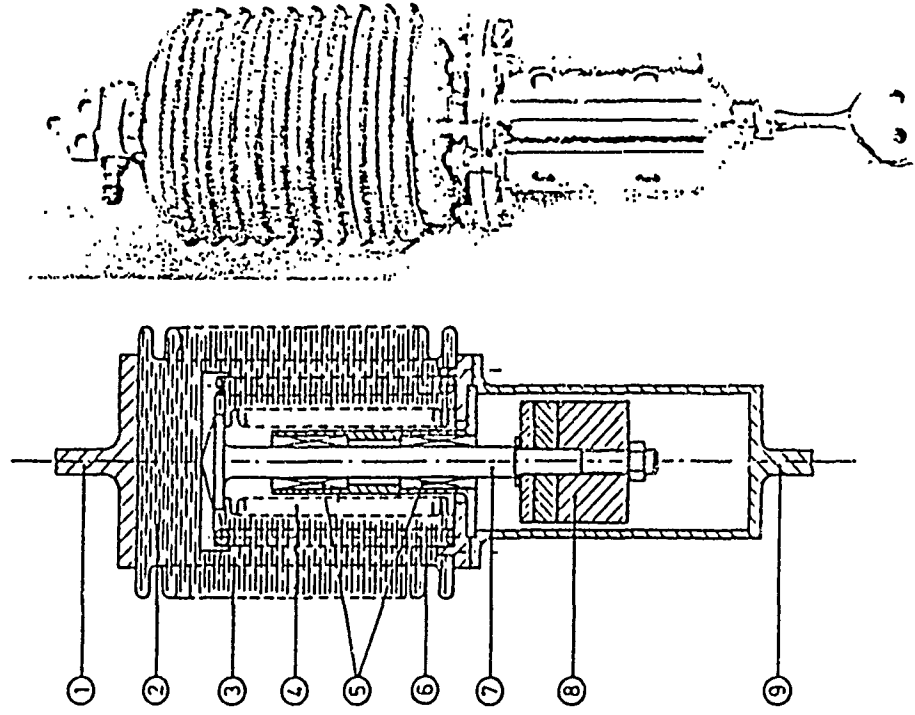
$$M_D = \frac{k_D + k_z \left(\frac{R_D}{e}\right)^2}{\omega_a^2 \frac{R_D}{e} \left(\frac{R_D}{e} - 1\right)}$$

Mechanical System



DLR

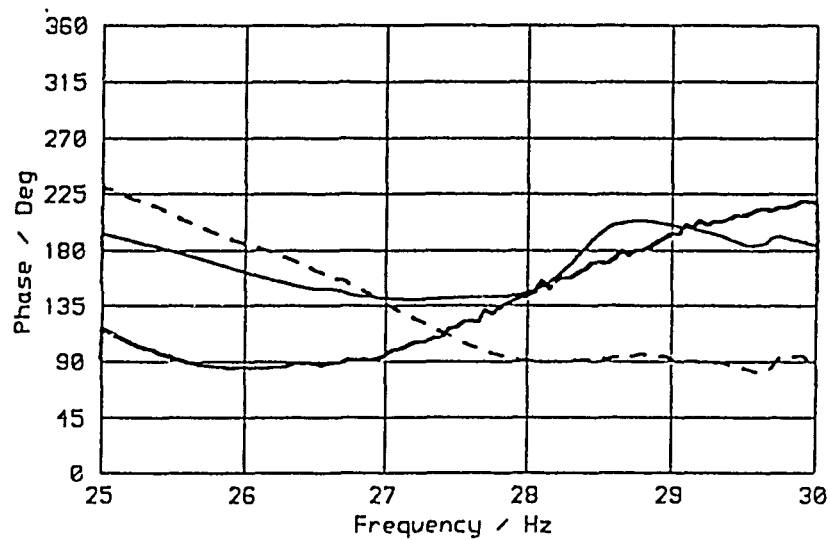
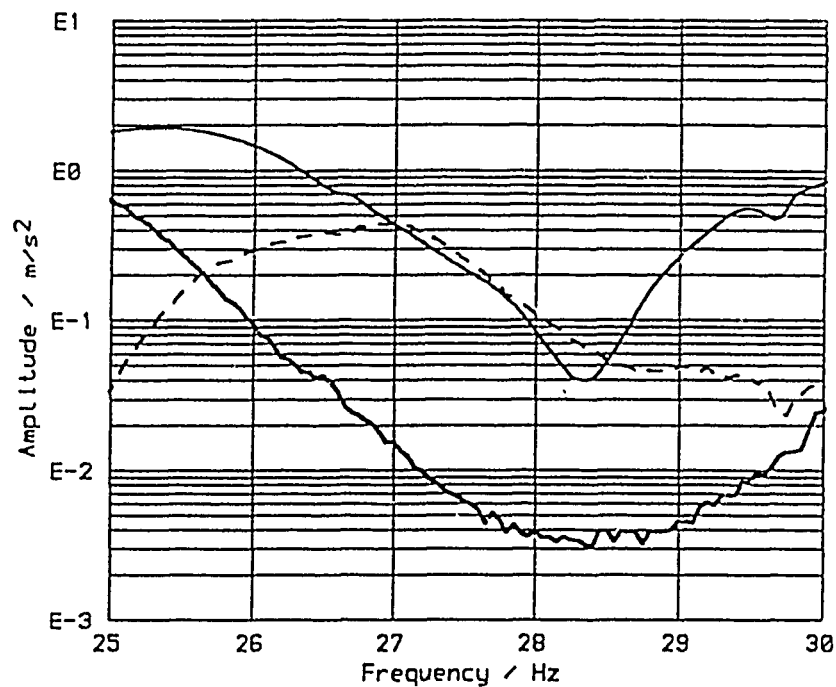
# Antiresonance Vibration Isolation System (ARIS)



1. GEARBOX ATTACHMENT POINT
2. LOW VISCOSITY FLUID
3. THICK-WALLED BELLOWS AND ISOLATOR SPRING
4. THIN-WALLED BELLOWS
5. LINEAR BALL BEARINGS
6. PRE-LOAD SPRING
7. GUIDE SHAFT
8. TUNING MASS
9. FUSELAGE ATTACHMENT POINT

Hydraulic Force Isolator (MBB Design) [3]

# BO 108 - Shake Test Results

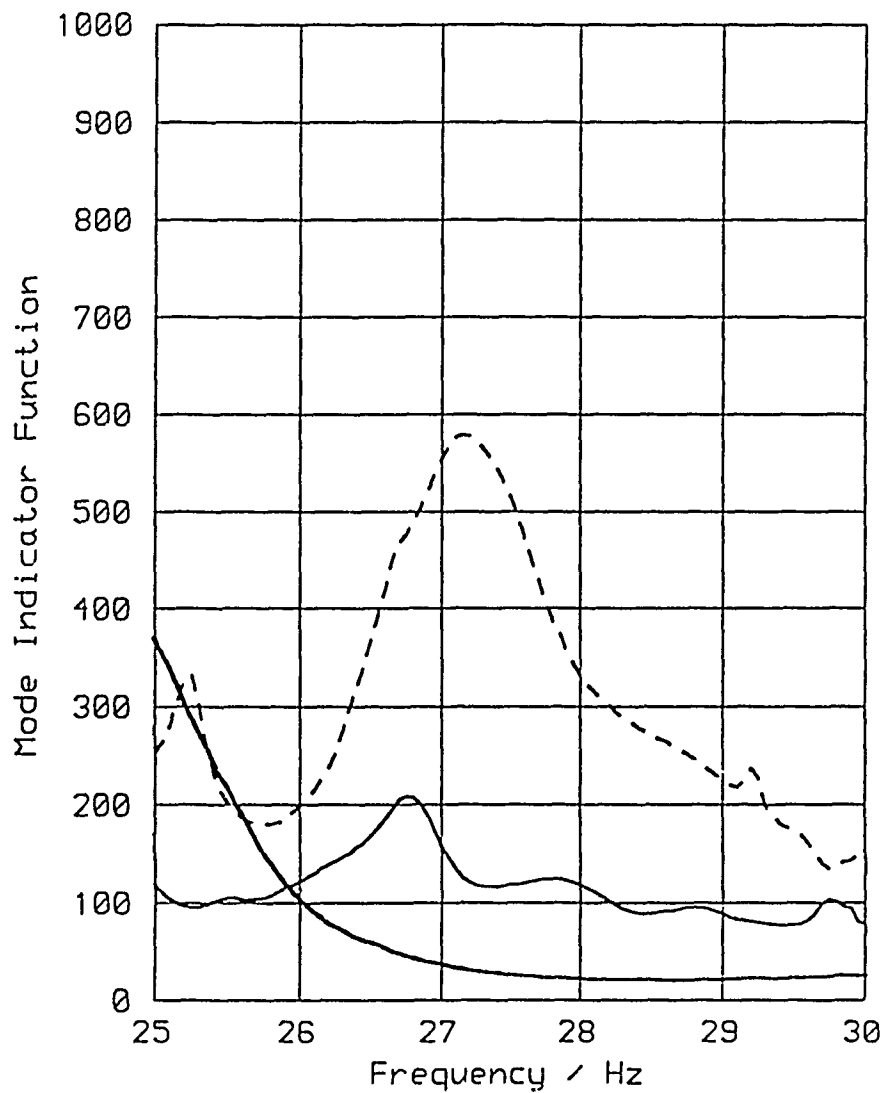


Vertical Vibrations at Pilot's Seat ( $F_z = 400$  N)

- without ARIS, with Rotor Excitation Device (ca. 200 kg)
- - - with ARIS, with Rotor Excitation Device
- with ARIS, without Rotor Excitation Device



## BO 108 - Shake Test Results



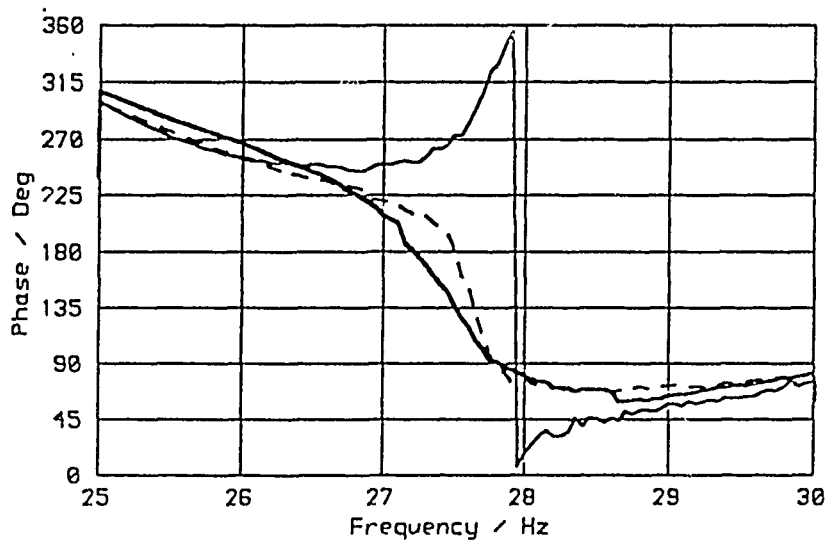
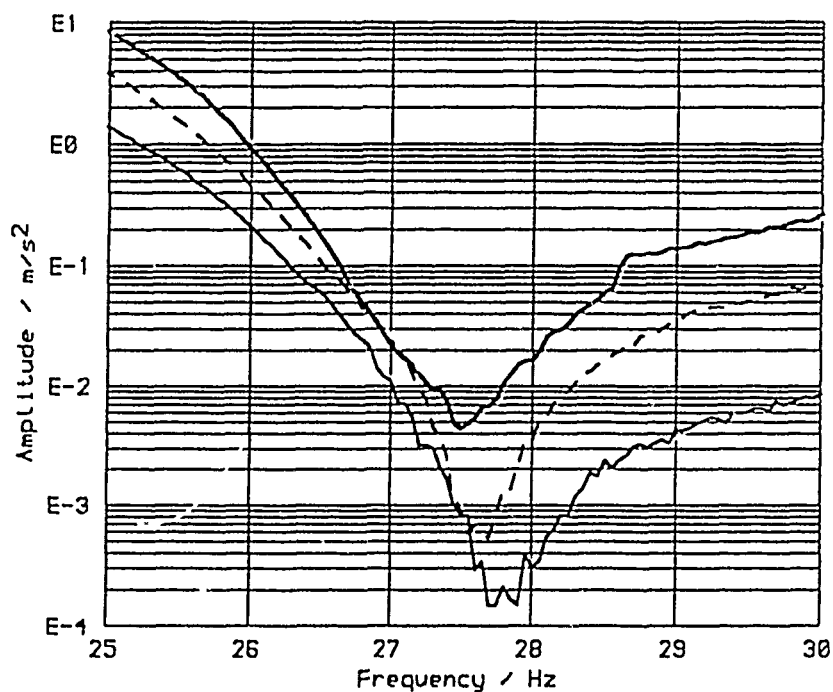
Mode Indicator Function (Vertical Rotor Excitation)

- without ARIS, with Rotor Excitation Device (ca. 200 kg)
- - - with ARIS, with Rotor Excitation Device
- with ARIS, without Rotor Excitation Device



DLR

## BO 108 - Shake Test Results



### Nonlinearity Investigations

— ( $F_z = 560$  N)

--- ( $F_z = 1200$  N)

— ( $F_z = 2000$  N)





## Conclusions

- Helicopter vibrations are influenced by aerodynamic rotor excitation as well as structural dynamic properties
- Advanced analytical and experimental methods are required to evaluate complex helicopter dynamics
- Interaction of structural dynamics with vibration reduction systems requires airframe structural tailoring to minimize vibration levels
- Vibration reduction systems can reduce vibration levels significantly as confirmed by ground and flight tests.



## References

- [1] Reichert, G. Helicopter Vibration Control - A Survey.  
Proc. Sixth European Rotorcraft and Powered  
Lift Aircraft Forum, Bristol, England, Sept. 16-  
19, 1980.
- [2] Stoppel, J. Investigations of Helicopter Structural Dyna-  
Degener, M. mics and a Comparison with Ground Vibration  
Tests.  
J. of the American Helicopter Society, Vol. 27,  
No. 2, pp. 34-42, April 1982.
- [3] Braun, D. Development of Antiresonance Force Isolators  
for Helicopter Vibration Reduction.  
J. of the American Helicopter Society, Vol. 27,  
No. 4, pp. 37-44, October 1982.
- [4] Braun, D. Ground and Flight Tests of a Passive Rotor  
Isolation System for Helicopter Vibration Re-  
duction.  
Proc. Eighth European Rotorcraft Forum, Aix-  
en-Provence, France, Aug. 31 - Sept. 3, 1982.
- [5] v. Tein, V. BO 108 - Technology for New Light Twin He-  
Schick, C. licopters.  
Proc. Fourteenth European Rotorcraft Forum,  
Milan, Italy, Sept. 20-23, 1988.



DLR

# EXPERIMENTAL IDENTIFICATION OF HELICOPTER ROTOR DYNAMICS USING KINEMATIC OBSERVERS: An Abstract

Robert McKillip, Jr.  
Mechanical and Aerospace Engineering Dept.  
Princeton University, Princeton, NJ 08544

Recent investigations using blade-mounted instrumentation has revealed the potential for identification of rotor dynamics as a two step process [1]. Estimation of rotor modal state variables is performed using knowledge of the kinematics of the sensor signal content, and then these estimated state time histories are used to identify the dynamic equation coefficients for a particular linearized mathematical model. Such an approach has the advantage that it decouples the assumed rotor dynamic model structure from the state estimation phase, allowing a wide variety of assumed model forms to be identified from the same set of state estimates. Additional uses for the separated state and parameter estimation scheme include adaptive rotor control applications as well as on-line stability analysis. Fundamental to the technique is the use of blade-mounted accelerometers to provide modal acceleration information to the state observer, taking the place of an assumed dynamic model as is normally used for more conventional instrumentation sets.

A series of hover and forward-flight model rotor experiments will be described that used blade accelerometer data to reconstruct both rotor modal state variables and linear equation parameters. The model tests were conducted at Princeton's Rotorcraft Dynamics Laboratory using a four-foot diameter rotor having the capability for both Individual Blade Control and Higher Harmonic Control [2]. The data processing technique will be detailed, and results of the parameter identification analysis will be compared to linearized theory (see Fig. 1). Examination will be made of the identified model's ability to predict closed-loop blade response experimental data for both hover and forward-flight regimes.

## References

1. McKillip, R. M., Jr., "Kinematic Observers for Active Control of Helicopter Rotor Vibration", Vertica V.12, n.1/2, pp.1-11, 1988.
2. McKillip, R. M., Jr., "Experimental Studies in System Identification of Helicopter Rotor Dynamics", Proc. Fourteenth European Rotorcraft Forum, Milano, Italy, September 1988. To appear in Vertica V.12, n.4, January 1989.

# Parameter Estimation Using Low-Pass Filtered Accelerometers

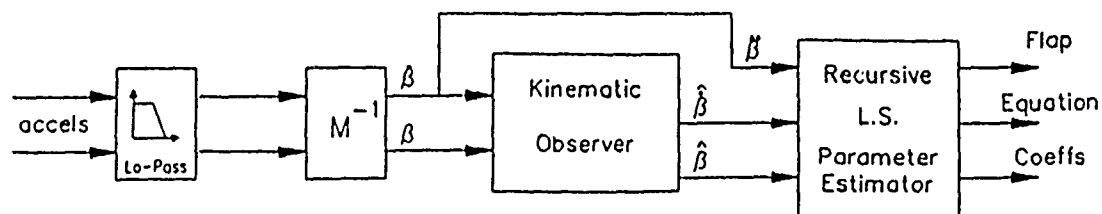


Fig. 1a: Signal Processing Flow Diagram

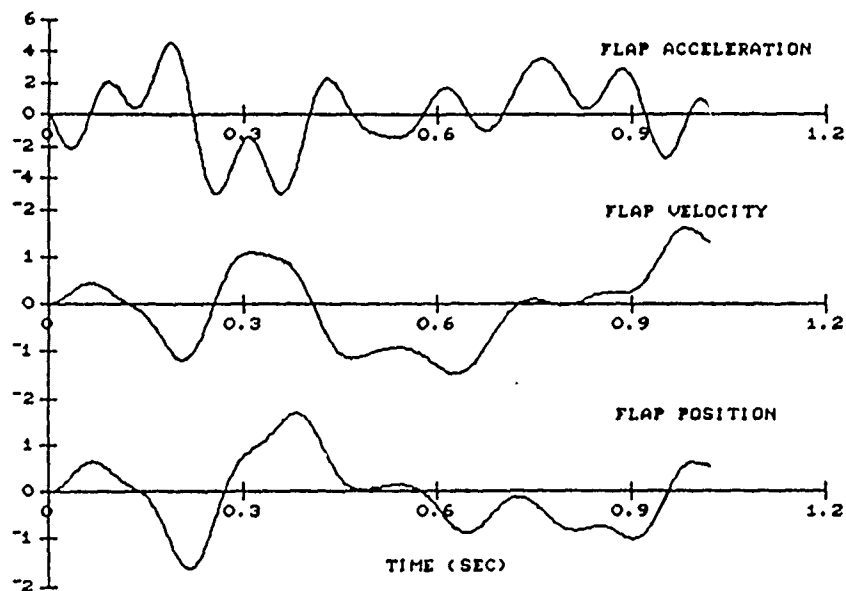


Fig. 1b: Flap Mode State Identification Results

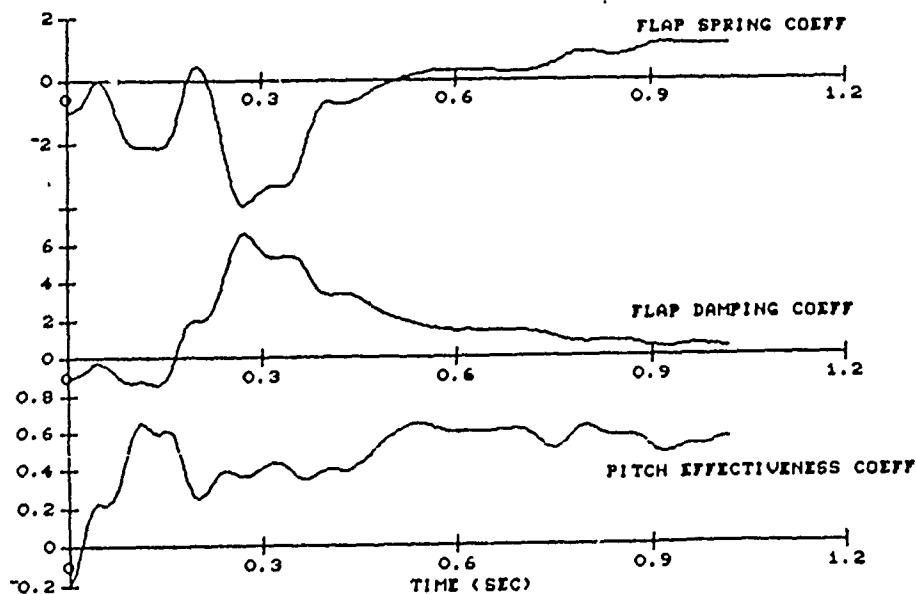


Fig. 1c: Flap Equation Parameter Identification Convergence History

Hover Test Results

## ABSTRACT

### VALIDATION OF ROTOR VIBRATORY AIRLOADS AND APPLICATIONS TO HELICOPTER RESPONSE

Jing G. Yen  
Bell Helicopter Textron, Inc.

The prediction of rotor vibratory airloads and structural loads has been a challenge to rotorcraft engineers. The development of advanced theories and computer codes requires extensive correlations with experimental data. The validation is to demonstrate that the theories do in fact correctly represent the physics of the problem and that the computer code is adequate to be used as a design tool.

Bell Helicopter Textron, Inc., has recently completed, as part of a program to improve rotor wake representations, a major cooperative program with the Army/NASA researchers at Langley Research Center. The program consisted of the testing of a scaled model with pressure instrumented blades. The model was a 0.2 Mach scale of Bell Advanced Light Rotor (ALR). The ALR was a four-bladed bearingless rotor with advanced airfoils. Pressure transducers were installed at five blade spanwise locations. The testing was conducted at the Langley VSTOL wind tunnel in June-July, 1989.

The experimental vibratory airloads (the normal force) are obtained by integrating the individual pressures. The airloads data are presented in time histories as well as harmonic amplitude and phase angles. The data are depicted as functions of the advance ratio and the rotor thrust coefficient. Comparisons of airloads are made between the experimental data and theoretical values. The theoretical values are calculated using three rotor wake models: Drees wake, CAMRAD/Scully free wake, and CAMRAD/Johnson free wake. Computed blade and hub loads for the ALR using the free wake models are correlated with those measured in flight.

Effects of the advance ratio and the rotor thrust coefficient on the vibratory airloads will be discussed. Similarities of the ALR with those reported in the literature will also be addressed. Validation of various rotor wake models in calculating the vibratory airloads and the rotor structural response will be assessed based on the ALR experimental data. Finally, conclusions from this study and recommendations for future work will be made.